Proteomics of Sub-cellular Protein Distribution in Oestrogen and Tamoxifen Stimulated MCF-7 Breast Cancer Cells

Abdulrab Ahmed M Alkhanjaf

A thesis submitted to the University College of London for the degree of Doctoral of Philosophy

July 2016

University College London
UCL

This thesis is dedicated to my parents, wife and children.

DECLARATION

I confirm that all this work is my own work, except where indicated and that I have:

I. Clearly referenced/listed all sources as appropriate.

II. Given the sources of all the pictures, data etc. that are not my own.

III. Not made any use of report(s) or essay(s) by any other student(s), either past or present.

IV. Not sought or used the help of any external professional agencies for the work reported in the thesis.

Signature: . . . . . ***Date:*** . . . . . .

Abstract

Abstract

Hormone receptor positive (HR+) breast cancer represent 70% of all breast tumours. Its oncogenesis is multiple step process thought to be driven by the presence of two transcription factors, the oestrogen receptor (ER) and/or the progesterone receptor (PR). Therefore, the endocrine-targeted therapeutic approach has been focused on both receptors as prognostic markers and therapeutic targets, aiming to alter the oestrogen signalling for patients with ERα-positive disease. The benefits gained from the treatment appear to be limited by developing either de novo or acquired resistance following a period of response to tamoxifen. In the present work, global quantitative proteomics was combined with the analysis of fractions enriched in target subcellular locations (nuclear and cytoplasmic fractions), this has allowed measurement of the changes in total abundance and in the compartmental abundance/distribution between the nucleus and cytoplasm for several thousand proteins differentially expressed in MCF-7cells in response to oestrogen and tamoxifen stimulation in MCF-7 cells.

In the first part of the thesis, we have used a proteomics subcellular spatial razor approach to look at changes in total protein abundance and in protein distribution between the nucleus and cytoplasm following exposure of MCF7 breast cancer cells to oestradiol. The dominant response of MCF7 cells to oestrogen stimulation involves dynamic changes in protein subcellular spatial distribution rather than changes in total protein abundance. Of the 3604 quantitatively monitored proteins, only about 2% show substantial changes in total abundance (>2-fold), whereas about 20% of the proteins show substantial changes in local abundance and/or redistribution of their subcellular location, with up to 16-fold changes in their local concentration in the nucleus or the cytoplasm.

The second part of the thesis focuses on the spatial distribution of proteins in the three sub-proteome fractions (total lysate, nuclear and cytoplasmic fractions) in 4-OHT stimulated MCF-7 cells. Of the 3493 quantitatively monitored proteins, 97 of quantified proteins were detected as a core data set with differential abundance (DA) that was significantly changed in total abundance and/or subcellular location ($P < 0.05$). More than 50% of the proteins show significant changes in local abundance and/or redistribution of their subcellular location, only 19 proteins show substantial changes in the total lysate. Following the rigorous downstream analysis of the pathways significantly overrepresented and GO terms significantly enriched, this analysis showed that protein changes in abundance with 4-OHT across multiple sample types (CNT) were involved in pathways related to metabolism, signal transduction, growth and proliferation, and development. The nuclear response involved upregulation of the proteins participating in the GPCR downstream signalling pathway leading to accumulated response in the cancer pathway by moderately modulating the cell survival (PI3K/AKT) pathway in a circadian rhythm. Furthermore, this was accompanied by substantial changes in the local abundance and /or the redistribution of the metastasis mediating proteins and apoptotic cleavages of cell adhesion proteins.

We propose that dynamic redistribution of the subcellular location of multiple proteins in response to stimuli is a fundamental characteristic of cells and suggest that perturbation of cellular spatial control may be an important feature of cancer.

Table of Contents

List of Tables

List of Figures

List of Supplementary Tables

Abbreviations

4-OHT	Active metabolite of tamoxifen, 4-hydroxytamoxifen
8-OHdG	8-hydroxydeoxyguanosine
AF-1	Activation function-1
AF-2	Activation function-2
AIB1	Amplified in breast cancer 1
AIs	Aromatase inhibitors
ALDOA	Aldolase A
APS	Ammonium persulphate
ATP	Adenosine-5'-triphosphate
BC	Breast cancer
BSA	Bovine serum albumin
cAMP	Cyclic adenosine monophosphate
CDK	cyclin-dependent kinase
CID	Collision induced dissociation
DE	Differentially expressed

DFBS	Dialyzed Foetal Bovine Serum
DMEM	Dulbeco's modified Eagle medium
DMSO	Dimethyl sulphoxide
DNMT	DNA methyltransferases
DTT	Dithiothreitol
E2	Active metabolite of oestrogen, 17β-estradiol
ECM	Extracellular matrix
EDTA	Ethylenediaminetetraacetic acid
EGFR	Epidermal growth factor receptor
ER	**O**estrogen receptor
ERE	Oestrogen Response Element
ERK1	Extracellular signal–regulated kinase 1
ERK2	Extracellular signal–regulated kinase 2
ERT	Human epidermal growth factor receptor 2
ERT	Oestrogen replacement therapy
ESI	Electrospray ionization
ETD	Electron transfer dissociation

ETT	Endocrine targeted therapy
FAK	Focal adhesion kinase
FAOS	Fluorescent-assisted organelle sorting
FBS	Foetal bovine serum
FDR	False discovery rate
FT-ICR	Fourier transform ion cyclotron resonance
GADPH	Glyceraldehyde-3-phosphate dehydrogenase
GLOBOCAN	Global Burden of Cancer
GOBP	Gene Ontology Biological Process
GOCC	Gene Ontology Cellular Component
GOMF	Gene Ontology Molecular Function
GPCR	G-protein coupled receptor
GPR30	G protein-coupled receptor 30
HDAC	Histone deacetylases
HIF-1-α	Hypoxia-inducible factor 1-alpha
HR/AM	High mass resolution and accurate mass
HRT	Hormone replacement therapy

ICGC	International Cancer Genome Consortium
iTRAQ	Isobaric tags for relative and absolute quantitation
KEGG	Kyoto Encyclopaedia of Genes and Genomes
LC	Liquid chromatography
LC-MS/MS	Liquid chromatography–mass spectrometry
LDHA	Lactate dehydrogenase A
LOPIT	Localization of organelle proteins by isotope tagging
m/z	Mass-to-charge ratio
MALDI	Matrix-assisted laser desorption/ionization
MAPK	Mitogen activated protein kinase
MCF-7	Michigan Cancer Foundation – 7 (adenocarcinoma) human breast cancer cell lines
mRNA	Messenger RNA
MS	Mass spectrometry
MS/MS	Tandem mass spectrometry
mtDNA	Mitochondrial DNA
ODC	Ornithine decarboxylase complex

OXPHOS	Oxidative phosphorylation
p53	Protein 53
pACC	Perturbation/accumulation p-value
PBS	Phosphate buffered saline
PC	Pyruvate carboxylase
PCK2	Phosphoenolpyruvate carboxykinase
PI3K	Phosphatidylinositol 3–kinase
PIP3	Phosphatidylinositol (3,4,5)-trisphosphate
pOVR	Over-representation p-value
PPI	Protein-protein interaction
PPP	Pentose phosphate pathway
PTEN	Phosphatase and tensin homology
RAGE	Receptor for advanced glycation end-products
ROS	Reactive oxygen species
SDS	Sodium dodecyl sulfate
SDS-PAGE	Sodium dodecyl sulfate polyacrylamide gel electrophoresis
SERD	Selective oestrogen receptor down-regulator

SERM	Selective oestrogen receptor modulator
SHBG	Sex hormone binding globulin
SILAC	Stable isotope labelling by amino acids in cell culture
SpC	Spectral count
SRC-1	Steroid receptor coactivator-1
TARGET	Therapeutically Applicable Research to Generate Effective Treatments
TBS	Tris-buffered saline
TBST	Tris-buffer saline, 0.1% Tween20
TCA	Tricarboxylic acid
TNBC	Triple negative forms of breast cancer
VDAC	Voltage-dependent anion channels
VEGF	Vascular endothelial growth factor

Acknowledgement

UCL must receive my first grateful acknowledgements; my peers, colleagues, friends and mentors, all priceless contributions to my achievements throughout this programme.

Firstly, I must express my gratitude to my supervisor, Professor Jasminka G. Zimmermann who provided time in her lab, a helping hand and gave me confidence in my ideas throughout this PhD, while also keeping me motivated. Professor Zimmermann has illuminated my journey with the constant encouragement and advice since 2013, and I thank her for her time.

Dr Ann Walker co-advised my PhD and monitored my progress, arranged meetings, and provided invaluable advice and suggestions.

My personal opinion is that Centre for Nephrology is unusual in having the departmental Postgraduate Tutor such Dr Jill Norman. Jill has been a great help in terms of academic progress and the various administrative issues I was to comply with – many thanks to her.

Through a tragic car accident a few years ago, I lost my father. I perused my education as he always inspired me to do so; each degree I obtain, each success I achieve, and each dream I realise are dedicated to him. My mother is the guardian of my life, a wonderful support network of protection and a strong bond of love, my deepest thanks to her.

My wife handled such a great responsibility taking care of our family and supporting me, raising my spirits and guiding me through the lowest points of frustration. She has provided unconditional support, and without her, it would have been impossible to achieve. To our five children, our five stars, I own them an apology for the time I have been absent, but I hope that they will understand, one day, I did this for them as well.

I would like to extend my thanks to members of proteomics group: Mark Crawford (Lab Manager); Gabrilla Pinto; and finally, Benedetta Lombardi (Post doc). Great colleagues and wonderful friends.

Lastly, I will forever thankful to my great country, KSA that invested in me and to my sponsor (Najran University) that facilitated my sponsorship and provided the resources required for this degree and helped me pursue higher education at one of the world's greatest universities, University College of London.

Conferences and Publications

- **Paper (2014):** PINTO, G., **ALHAIEK, A. A. M.**, AMADI, S., QATTAN, A., CRAWFORD, M., RADULOVIC, M. & GODOVAC-ZIMMERMANN, J. 2014. Systematic Nucleo-Cytoplasmic Trafficking of Proteins Following Exposure of MCF-7 Breast Cancer Cells to Estradiol. *Journal of Proteome Research*, 2014 Jan; *13* (2), pp 1112–1127. **DOI:** 10.1021/pr4012359

- **Conference (2014): ALHAIEK, A. A.,** PINTO, G. and GODOVAC-ZIMMERMANN, J, (2014) "Multiple subcellular locations and partitioning of proteins between mitochondria and the nucleus in breast cancer cells". Poster presentaion at 10th Siena conference "From Genome to Proteome: 20 years of proteomics", August 31-September 4th, 2014, Siena, Italy.

- **Paper (2015):** PINTO, G., **ALHAIEK, A. A.** & GODOVAC-ZIMMERMANN, J. 2015. Proteomics Reveals the Importance of the Dynamic Redistribution of the Subcellular Location of Proteins in Breast Cancer Cells. *Expert Rev Proteomics*, 2015 Jan; 12**:**61-74. **DOI:**10.1586/14789450.2015.1002474.

- **Poster (2015): ALHAIEK, A. A.,** PINTO, G. and GODOVAC-ZIMMERMANN, J, (2014) "Multiple subcellular locations and partitioning of proteins between mitochondria and the nucleus in breast cancer cells". Poster presentaion at UCL Division of Medicine Post-Graduate Student Research Day, 9th July 2015, Lodon, UK.

- **Poster (2016): ALKHANJAF, A. A.,** PINTO, G. and GODOVAC-ZIMMERMANN, J, (2016) "Quantitative Global Proteomics Reveals Nucleo-Cytoplasmic Trafficking of Proteins Following Exposure of MCF-7 breast cancer cell to Tamoxifen". Poster presentaion at UCL Division of Medicine Research Retreat, 26th May 2016, Lodon, UK.

- **Paper (2016): ALKHANJAF, A. A.,** PINTO, G., CRAWFORD, M. and GODOVAC-ZIMMERMANN, J, 2016. Moonlighting Proteins in the Spatial Response of MCF-7 Breast Cancer Cells to Tamoxifen. *Oncotarget* (in preparation)

Copyright Permission

Chapter 1 Introduction

1.1 Hallmarks of cancer: an emerging concept of cellular complexity

The growth and death of normal cells are not random processes, they take place at systematically controlled intervals within biological systems; a tumour is a type of growth formed of abnormal cells that are able to commence immortal growth and escape regulatory limitations imposed upon normal cells. In ancient medicine, 3000BC, some cases were described as an abnormal growth of tissue, but classified as idiopathic disorders, with a simple conclusion: "There is no treatment." (American Cancer Society, 2016). Since the mid-20th century, more than 100 types of cancer have been identified (Encyclopædia Britannica Online, 2016). It is now clear that different kinds of tumours have different progression patterns and responses to therapy due to heterogeneity that is neither uncommon among different tumours, nor seldom within individual tumours. For example, in breast cancer, multiple subtypes may exist within the same tissue (intra-tumour heterogeneity) with different patterns of progression, cellular markers and responses to treatment (Brafford and Herlyn, 2005).

In the current era, advanced molecular biology techniques are feasible, and on completion of human genome sequencing and cataloguing cancer mutational genes in the large-scale cancer genome sequencing atlas (TCGA), heterogeneity gives rise to widely dissimilar genetic and phenotypic manifestations among tumour patients. Therefore, inconsistent rates of disease progression and responses to treatment continue to challenge good management in clinical settings and a thorough understanding in research laboratories owing to the natural pathological complexity and poor prognosis of cancer (Brafford and Herlyn, 2005, Patel et al., 2014, Garraway and Lander, 2013).

However, scientists have listed and described numerous genetic mutations that contribute to carcinogenesis from initiation to the metastasis phase; the majority of those genes fall into two categories, oncogenes or tumour suppressor genes (Garraway and Lander, 2013, Macconaill and Garraway, 2010). A gain of function mutations (oncogenes) and a loss of function mutations (tumour suppressor genes) are dynamically chaotic (Andrey, 1989, Calin et al., 2003, Pham and Ichikawa, 2013). Also, abnormal proliferation of tumour cells is associated with accumulative mutations and genetic instability; cells are continuously dividing and accumulating these mutations with each round of cell division, producing proteins to execute numerous functions in a context-dependent manner (Garraway and Lander, 2013, Andrey, 1989, Calin et al., 2003, Pham and Ichikawa, 2013). The growth of cancer is a process known as a carcinogenesis that is neither a single step process nor based on a single cellular event (Foulds, 1958, Vogelstein and Kinzler, 2004). Hence, cancer is a progressive dynamic disorder that evolves gradually to escape the boundaries of the tissue of origin, which ultimately reaches an irreversible phase of metastasis; each stage involves various forms of alterations that result in either a gain of functions (oncogenes) or a loss of functions (tumour-suppressor genes), enabling the progression of malignancy (Hanahan and Weinberg, 2011, Vogelstein and Kinzler, 1993). Malignant tumours are distinguished by six common alterations defined as 'hallmarks' (Figure 1-1): 1] auto-stimulation for growth; 2] immortality and limitless replicative potential; ability to escape growth limitations including 3] growth suppressors or 4] apoptosis; 5] maintained angiogenesis; and 6] the ability to invade (metastasis) both proximal and distant tissues. In addition to the above features, four emerging hallmarks have been added to the pathophysiological manifestations of cancer cells: 1] abnormal metabolism; and, 2] resistance to the immune system; 3] genome instability; and 4] inflamation (Hanahan and Weinberg, 2000, Hanahan and Weinberg, 2011).

It has been widely accepted that tumour cells are driven by genetic instability and metabolic abnormalities; therefore, currently, cancer is known as a genetic and metabolic disorder (Coller, 2014, Hemminki and Hemminki, 2005). Collectively, these hallmarks suggest that neoplastic cells have common themes in their operations and are controlled at different spatial and temporal levels, also, an individual cancer cell is able to manifest self-governing capabilities.

Having said that, the research direction and methods have evolved tremendously to enable the researcher to deeply investigate a very complex disorder aiming towards a better understanding and better overall management, given that the spectra of cancer mutations evolve in a non-linear way within a given type of tumour or different tumours.

Many scholars hold the view that the process from gene to the development of an organism is highly complex and interlinked with complex networks linking hierarchical anatomical system entities and formulating the function or dysfunction of an organism, implying that the lack of knowledge, in many aspects, is related to a reductionist approach to understanding the biology (Figure 1-2) (Grizzi and Chiriva-Internati, 2006, Kitano, 2002, Noble, 2002, Szathmáry et al., 2001).

The rational approach to tackle highly complex biological phenomena, such as cancer, is to develop methods that provide more quantitative information about the dynamicity and plasticity of the nonlinear qualitative multistep cancer progression states (Michor et al., 2004).

How can we adapt and use the advanced high- throughput omics-technologies including genomics, transcriptomics, proteomics and metabolomics to reveal a cancer's enigmatic secrets? Answers can show bias due to the lack of an integrative approach and leaping towards interests that can provide part of a multidimensional image. Having said that, the large scale global research approaches that have been evolving since early genome sequencing may reveal more about the dynamicity and plasticity of various tumours, once they complement one another.

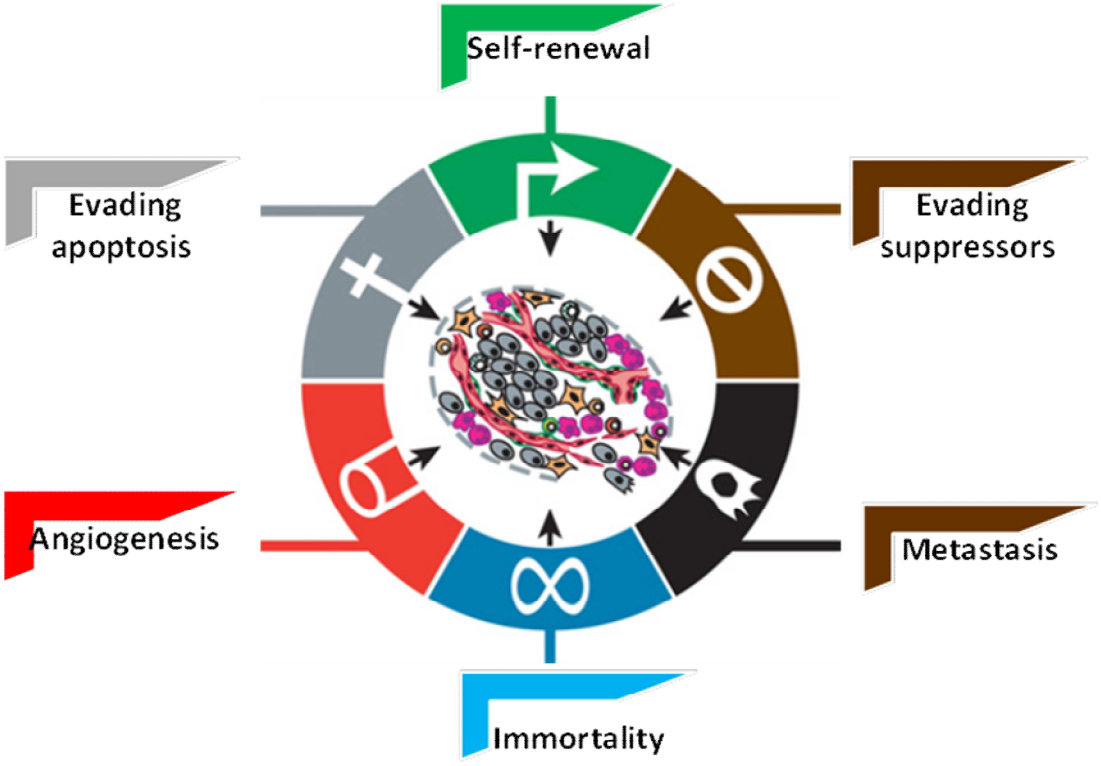

Figure 1-1: The six hallmarks of cancer

This figure shows the six common capability hallmarks shared among cancer types. Adapted from (Hanahan and Weinberg, 2011).

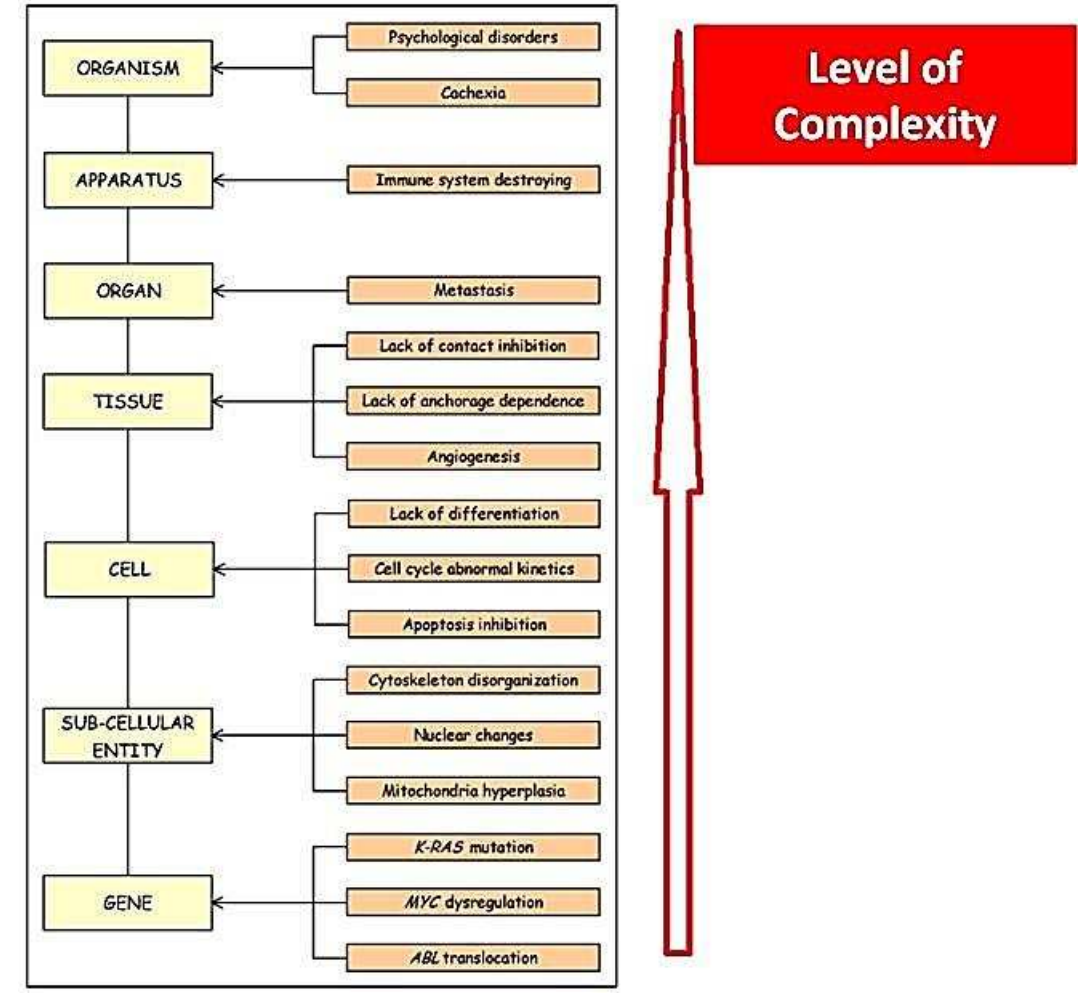

.

Figure 1-2: Hierarchical illustration of human cancer

This figure exemplifies how cancer is a very complex biological system that involves numerous processes at different levels ranging from molecular to environmental. Adapted from (Grizzi and Chiriva-Internati, 2006).

1.2 Increasing incidence, mortality, morbidity and risk factors associated with breast cancer (BC)

The common and dreadful thought that comes to mind upon the diagnosis of a tumour is whether a cure is possible. This fear has its root in the rates of mortality, morbidity and poor prognoses associated with tumours. In the United States, cancer has been reported as the second leading cause of death (Centers for Disease Control and Prevention, 2015). On December 23, 1971 the President Nixon signed the National Cancer Act and declared a 'war on cancer'; this act classified cancer as the most feared disease in the United States, and governmental agencies were then committed to finding a cure within one decade (Hesketh, 2013). Forty years on, although there has been recorded success in distinguishing types and subtypes of tumours, the statistical figures, pathogenesis and tailored treatment/screening (personal) remain a global burden in most types of cancer.

Ferlay et al. (2015) analyse the online global cancer database GLOBOCAN 2012, and estimate the diagnosis of 14.1 million new cancer cases each year and 8.2 million deaths that are associated with various types of cancer with different global distribution patterns. Around 40% of cases were reported in Europe and in the United States, while 60% were diagnosed across developing countries. Among different types of cancer based on an annual statistics, Ferlay et al. (2015) find that, 55% of the global incidence burden is represented over six forms: lung cancer is the most common (1.82 million new cases, 1.6 million deaths), followed by breast and colorectal cancers (1.67 million new cases, 522,000 deaths and 1.36 million, 694,000 deaths respectively), prostate cancer (1.1 million new cases, 307,000 deaths), stomach cancer (951,000 new cases, 723,000 deaths) and lastly, liver cancer (782,000 new cases, 745,000 deaths).

The World Health Organisation in 2011 predicted that there would be 2-fold increase in cancer-associated mortality, from 7.6 million deaths by 2030; however, 70% of the current death figures mainly occur in nations with lower living standards (Jemal et al., 2011).

Based on GLOBOCAN, from 2008 to 2012, the incidence rate of breast cancer elevated sharply to 1.7 million new cases and 522,000 breast cancer related deaths. Although the mortality rate is declining in industrialised countries, the incidence rate is still higher among women in those countries compared to less developed parts of the world (International Agency for Research on Cancer, 2016). The wide variation of incidence rate is in part due to changing lifestyles and accompanying risk factors, as well as reproductive and hormonal variations, while the declining death rate is due to the availability of more effective diagnostic tools and improved strategies in adjuvant treatment (Jemal et al., 2010). Incidence of breast cancer, in light of current statistical information, is not expected to reduce in the near future; thus, the public health burden remains highly topical (Gannon et al., 2013).

1.3 Breast cancer (BC)

The aetiology of breast cancer cannot be linked to a single factor, both genetics and lifestyle/environment are recognised as risk factors that must be considered in terms of aetiological implications; BC is a multifactorial disorder.

1.3.1 Reproductive risk factors associated with breast cancer

Extensive experimental, clinical and epidemiological studies have identified that exposure to ovarian oestradiol (E2) and progesterone hormones, notably oestradiol (E2), is the most significant risk factor in developing breast cancer (Angelopoulos et al., 2004, Bernstein, 2002, Cui et al., 2013, Yue et al., 2010). Epidemiological studies have led to speculation that age at menarche, childbearing and menopause, provides explanations concerning the impact of internal hormonal exposure over a lifetime (Bernstein, 2002). Although age is the most speculated risk factor often used to identify the women at high risk of developing breast cancer (Nelson et al., 2012), it resides among unconvincing evidence.

Women with late menopause at 55 plus years of age, seem to be at high risk, possibly due to long term exposure to internal hormones from menstrual cycles (Colditz and Rosner, 2000). An early onset of the menstrual cycle (early menarche), at 12 years or younger at regular intervals, increases the chance of developing breast cancer fourfold than women with late menarche (Bernstein, 2002). In short, we need to emphasise the specific point that chronic exposure to internal oestrogens may be described as the long term menstrual cycles, i.e. early onset and late cease.

Among other speculative proposals, (Bernstein et al., 1986) believe that child bearing age is considered to be of paramount importance in developing breast cancer whose first pregnancy was at age 30, than those younger than 20 years. The protective effect of early full term pregnancy before the age of 20 has been demonstrated in many epidemiological studies (Albrektsen et al., 2005, MacMahon et al., 1970). A 50% decrease in cancer risk is noted in comparison to late pregnant and nulliparous women (Meier-Abt and Bentires-Alj, 2013). Furthermore, women that breastfeed can form protection against developing breast cancer; 35% lower possibility than non-lactating women (Enger et al., 1997, Enger et al., 1998). Breastfeeding has the greatest effect on the delay and reduction in menstrual cycles; its protective effect is linked to the low level of hormonal exposure during lactation (Bernstein, 2002).

Body weight, at the age of menopause, is associated with breast cancer incidence, since adipose tissue is the main endogenous reservoir of androgens (Lamas et al., 2013, Stephenson and Rose, 2003), and obesity reduces the level of circulating sex hormones binding globulin (SHBG), and subsequently, the level of free oestradiol increases in blood circulation (Key et al., 2011, Moore et al., 1987). Furthermore, Lamas et al. (2013) correlate the enhanced proliferation of oestrogen receptor (ER+) in MCF-7 breast cancer cells to fat intake. Nevertheless, improving lifestyle by controlled body weight with frequent physical exercise, and a reduction in fatty diets could have an impact on reducing the risk of breast cancer (Bernstein, 2002). Oral contraceptives and hormone replacement therapy (HRT) are both considered exogenous sources for circulating hormones; however, risk of developing breast cancer does not appear to be similar among women exposed to these agents. New recommendations for oral contraceptive have helped to reduce the risk (Kumle et al., 2002), but HRT, notably oestrogen replacement therapy (ERT), is not always safe and an individual assessment with a tailored and structured plan prior to prescription, aiming to reduce

postmenopausal symptoms, would provide a more effective benefit and reduce the risk of over-exposure to oestrogen (Hou et al., 2013).

1.3.2 Heterogeneity of breast cancer

All enabling characteristics of cancer hallmarks are shared by most types, including breast cancer. In addition to those hallmarks, breast cancer has inherited enigmatic heterogeneity, which makes the clinical manifestations of the disease unpredictable, and thus can lead to ineffective management (Ellsworth et al., 2010). However, finding an indefinite way to rationally diagnose, treat and provide an accurate prognosis is the ultimate goal of current research, and the current trend of treatment is amenable to be targeted and individualised, i.e. a drug working by design, as opposed to chance.

With regard to the diagnosis and prognosis of breast cancer, pathologists have a crucial role in translating the biological changes associated with breast cancer into useful information that helps in the neoadjuvant/adjuvant treatment or when estimating the probability of recurrence and metastasis. They rely on traditional sets of methods/indicators, such as morphological changes, tumour size and grade, lymph node status, and the immunohistochemistry determination of diagnostic/prognostic markers, such as ER/PR and human epidermal growth factor receptor 2 (HER2) (Kittaneh et al., 2013). However, molecular techniques, in addition to the clinical pathological paradigm, have illustrated the diversity of breast cancer subtypes and justified the inconsistencies in clinical behaviours of same-stage cancers, and therefore, highlighted the importance of a personalised diagnosis/prognosis treatment plan in clinical decision making (Allison, 2012). High throughput technologies such as gene expression microarray, have revealed a distinct breast cancer cellular classification with innate biological characteristics for each subtype that may influence initiation, proliferation, recurrence and thus rationalise personalised treatment

based on an individual biomarker (Eroles et al., 2012). Immunohistochemical expression of receptors has joined gene expression profiling to provide a platform for the current most common subtypes: luminal A, luminal B, HER2, basal and normal forms (Perou et al., 1999, Perou et al., 2000). Each subtype has specific molecular characteristics as shown in Table 1-1 with examples of cell lines, as a research model, representing each subtype (Holliday and Speirs, 2011, Neve et al., 2006, Prat et al., 2010).

Table 1-1: Five common subtypes of breast cancer

Classification	*Immunoprofile	Other characteristics	**Example cell lines
Luminal A	ER^+, $PR^{+/-}$, $HER2^-$	Ki67 low, endocrine responsive, often chemotherapy responsive	MCF-7, T47D, SUM185
Luminal B	ER^+, $PR^{+/-}$, $HER2^+$	Ki67 high, usually endocrine responsive, variable to chemotherapy. $HER2^+$ are Trastusumab responsive	BT474, ZR-75
Basal	ER^-, PR^-, $HER2^-$	$EGFR^+$ and/or cytokeratin $5/6^+$, Ki67 high, endocrine nonresponsive, often chemotherapy responsive	MDA-MB-468, SUM190
Claudin-low	ER^-, PR^-, $HER2^-$	Ki67, E-cadherin, claudin-3, claudinin-4 and claudinin-7 low. Intermediate response to chemotherapy	BT549, MDA-MB-231, Hs578T,
HER2	ER^-, PR^-, $HER2^+$	Ki67 high, Trastusumab responsive, chemotherapy responsive	SKBR3, MDA-MB-453

*Immunohistochemical and molecular characteristics of five subtypes of breast cancer (Holliday and Speirs, 2011).

**Research cell line models for each subtype (Neve et al., 2006, Prat et al., 2010).

1.3.3 Endocrine therapy

Breast cancer subtypes are not yet universally applied to clinical settings, and required further standardisation. However, they have contributed to an understanding that the treatment response is inconsistent and can be linked to an individual molecular marker, therefore, we know today that ER is a therapeutic target for hormone therapy, and that human epidermal growth factor receptor 2 (HER2) is potentially a target protein for Trastuzumab therapy (Bang et al., 2010, Eroles et al., 2012, Lynch et al., 2004, Marty et al., 2005, Pao et al., 2004, Piccart-Gebhart et al., 2005, Van Cutsem et al., 2011). The triple negative forms of breast cancer (TNBC) with no expression of any of these receptors. TNBC still represent the most aggressive subtypes, hence no historical therapeutic targets have been established and adjuvant treatment is restricted to chemotherapy (Perou et al., 2000).

In adjuvant hormonal treatment, women with ER and/or PR positive tumours, irrespective of the stage, show better survival rates in a typical response to the targeted approaches that include ER modulator tamoxifen (Block ER), E2 synthesis inhibition by aromatase inhibitors (AIs), and ER-degrading agent Fulvestrant (Figure 1-3) (Gradishar, 2010). However, a disease free interval would develop a resistant relapsed form (acquired resistance), hence limiting the long term efficacy of endocrine treatment (Ring and Dowsett, 2004). A better understanding of the mechanism of action of both nuclear and cytoplasmic ER would clarify the mechanism underlying this resistance.

There is a significant difference between hormonal replacement therapy (HRT) and endocrine targeted therapy (ETT); the former is prescribed to alleviate postmenopausal symptoms, particularly osteoporosis, and has since been proved to be unsafe for breast cancer patients, while the latter is an antioestrogen approach of treatment targeting the oestrogenic signalling pathways.

In 1896, a link was found between breast cancer and hormones, given that the tumour regression was associated with the deprivation of hormones following oophorectomy (Dixon, 2014). The first synthetic non-steroidal oestrogen that has been shown to have natural anti-tumour characteristics was Diethylstilbestrol (DES), but severe side effects were encountered along with the administration, therefore the Food and Drug Administration (FDA) soon banned its use (Haddow et al., 1944).

In the early 1960s, researchers developed the contraceptive tamoxifen, but this drug has shown that it deprives oestrogen signals that favour cancer development rather than preventing pregnancy (Jordan, 2003); therefore, the FDA licensed tamoxifen in 1973 as an essential antioestrogen treatment (Jordan, 2003), which has been extensively used to date. The endocrine treatment approach can be administered alone in ER-positive patients, or along with other chemotherapeutic agents (Colleoni et al., 2001). Figure 1-3 shows that the main theme of endocrine targeted therapies is to reduce the growth of oestrogen-dependent tumours by inhibiting oestrogen synthesis (aromatase inhibitors, Letrozole) (Buzdar, 2005), antagonising oestrogen binding with ERs by selective modulators (SERMs, tamoxifen) (Shiau et al., 1998), and selective down-regulators (SERDs, Fulvestrant) (Long and Nephew, 2006), which are frequently prescribed to premenopausal and postmenopausal women with breast cancer characterised as ER positive.

It has been found that 5-year adjuvant treatment of tamoxifen reduces the relapse rate in a period extended up to a decade from the day the treatment commences, and enhances the rate of survival to a one third reduction of breast cancer associated mortality (Davies et al., 2011). Moreover, further reduction in both mortality associated breast cancer and recurrence, has been reported with continuing treatment for up to 10 years, rather than a 5-year treatment cycle (Davies et al., 2013).

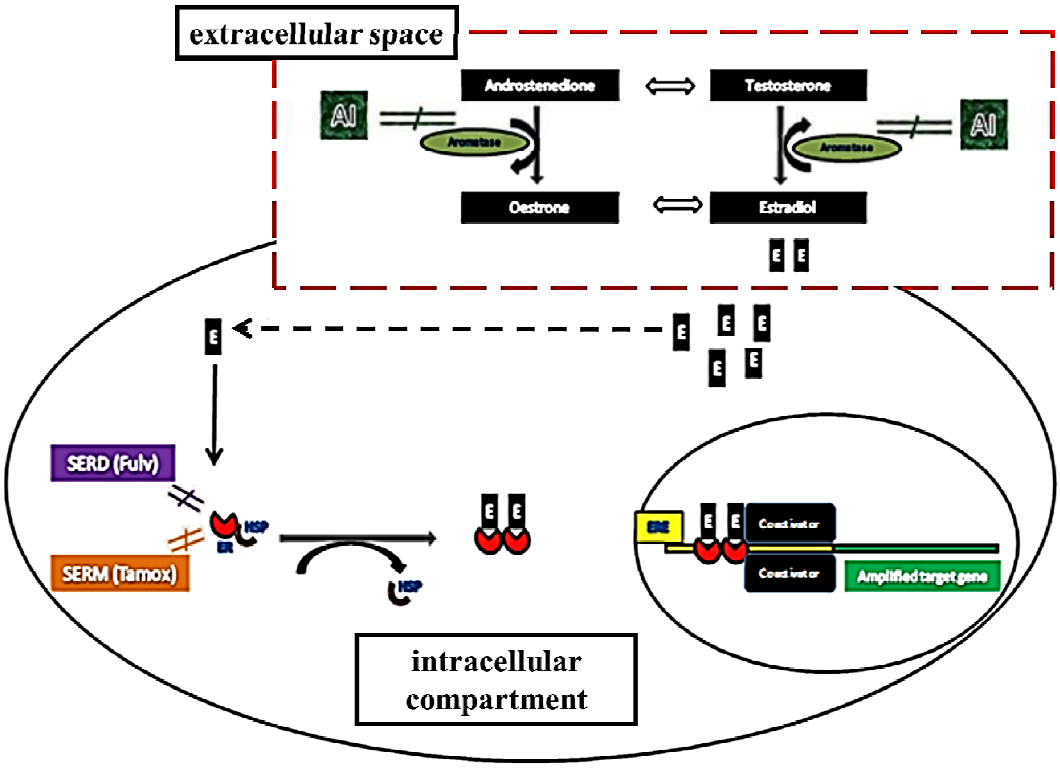

Figure 1-3: Endocrine targeted therapy in ER positive breast cancer

Diagram showing that through the action of the peripheral aromatase, androgens are converted into oestrogen (E), oestrogens are diffused into the intracellular space, bind ER, and activates the ER signalling cascades. For the three groups of the endocrine treatments, three targets are shown in the pathway: aromatase inhibitors targeting oestrogen synthesis, tamoxifen (SERM) modulating ER, and fulvestrant (SERD) downregulating ER. Adapted from (Dixon, 2014).

1.3.4 Mechanisms of endocrine resistance

The complete mechanism underlying the acquired resistance to the endocrine targeted therapeutic approach, remains to be elucidated. It is important to note that we gained incomplete knowledge regarding how signalling transduction pathways and their components affect the rate of cellular survival, proliferation or death; we are still far from determining the exact mechanism by which oestrogen mediated processes in breast cancer are interconnected with such a complex system (Chang, 2012). Therefore, antioestrogen resistance is unlikely to arise due to a single cellular event/mechanism that is not linked to various cellular events that are enigmatic and heterogenic in different breast tumours (Clarke et al., 1990). However, in relation to tamoxifen resistance, there are several mechanisms attributable to developing resistance, some are discussed below. Several molecular characteristics seem to be involved in the balance between agonistic and antagonistic activities that include, but are not limited to: modulation of coregulatory proteins, the crosstalk with growth-factor transduction pathways (Ali and Coombes, 2002, Girault et al., 2003, McDonnell et al., 2002), dysregulation of ER expression, redox regulation, cellular origin and stem cells, and autophagy regulation (Chang, 2012, Seo et al., 2012). These mechanisms reflect the complexity of tumours and impose the need for further studies to uncover the pathological manifestations of breast cancer.

1.3.4.1 Loss of ER expression and function

The main aim of tamoxifen treatment is to deprive tumour cells from oestrogenic mediated signalling via its ability to inhibit E2 binding to ER, then resistance is eventually developed due to a loss of expression of the molecular target ER, in particular *de novo* resistance (Jaiyesimi et al., 1995). Complete loss of ER at progression of the tamoxifen resistance tumours was ruled out in ER positive tumours patients by showing responses to other antioestrogens such as aromatase inhibitors (letrozol) after 5-years of tamoxifen treatment (Goss et al., 2005).

In a study using two heterogeneous ER-positive cell line models (T47D and ZR-75-1), it has been suggested that a switch from ER-positive to ER-negative can result from a repression of the ER transcription gene and lead to an overpopulation of ER negative cells (Fuqua, 1994, Jiang et al., 1992). Epigenetic modifications reportedly play a role in the diminished ER-positive phenotype, inactivation of ER-expression via hypermethylation of CpG islands or histone deacetylation inhibition, subsequently, this can reactivate ERα expression in ER-negative breast cancer cells using inhibitors of histone deacetylases (HDAC) and DNA methyltransferases (DNMT). This model of study assumes that epigenetic modulations may improve the response to antioestrogens by desensitising ER-negative cells (Sharma et al., 2005, Zhou et al., 2007).

Although, antioestrogen resistance can promote relapse or cancer recurrence in the absence of any mutations (Brunner et al., 1997), the loss of ER function can be linked to ER gene mutations, which is a negative feedback loop controlling the level of ER translated proteins, and abnormal splice variants (Fuqua, 1994, Jiang et al., 1992). Since tamoxifen has a partial

agonistic activity, the naturally mutated ERs as seen in patients, have also been shown to influence the agonistic actions of tamoxifen in culture cells (Chang, 2012).

1.3.4.2 Modulation of agonistic and antagonistic activities via coregulatory proteins

Coregulatory proteins are categorised according to the roles they play in modulating the ligand-bound ER transcription into either activators (coactivators) or inhibitors (corepressors). They are involved in the transcription complex at the promotor region of ER target genes (Girault et al., 2006). Level of expression and type of these coregulatory proteins are essential determents of downstream ER transcriptions; agonist or antagonist ligand-bound ER induces the conformation changes of the receptors associated with changes in the recruitment patterns to the coregulatory proteins by ERs (Zajchowski et al., 2000). Tamoxifen has been found to exert agonistic activity via recruiting coactivator SRC-1 with the ER AF-1 domain, demonstrating the balance between agonistic and antagonistic activities of the SERMs that are promotor context-dependent (Webb et al., 1998). Such a demonstration of the partial agonistic activity of tamoxifen implies that the contribution of the coregulatory proteins to induce resistance may take two forms: high expression level of coactivators may terminate the antagonistic activity of tamoxifen, while low levels of regulation may favour the switch to agonistic action of tamoxifen. Eventually this could enhance the commencement of the growth of tumour cells and resistance to treatment (Chang, 2012).

Amplified in breast cancer 1 (AIB1), a synonym to steroid receptor coactivator 3 (SRC-1) and thyroid hormone receptor activator molecule 1 (TRAM-1), has been studied extensively in many breast tumours and cell lines, particularly MCF-7 - the higher level of the expression of this protein that is essential for cellular proliferation (List et al., 2001).

Comparing two groups of patients, tamoxifen treated and those not treated with tamoxifen, it has been reported that in the tamoxifen group, patients demonstrated a high level of expression (AIB1) associated with poor prognosis in terms of survival (Osborne et al., 2003). This led to a conclusion that upregulated AIB1 is associated with tamoxifen agonistic activity, and a possible interaction between upregulated AIB1 with HER2 would develop tamoxifen resistance through enhancing the expression of cyclin D1 and interfering with the subsequent signalling pathways and cell cycle (Chang, 2012). Hence the coregulatory proteins are not limited to interact with ERs and may interact with other types of nuclear receptors (Klinge, 2000, Myers et al., 2005). The exact role and extent of the altered expression of these proteins remains unclear and may play a role in developing resistance for tamoxifen treatment (Chang, 2012).

1.3.4.3 Resistance to endocrine therapy due to regulation of redox status

In the reduction/oxidation cycling process, the resulting reactive oxygen species (ROS), particularly hydroxyl radicals, from the metabolism of tamoxifen by the molecular oxygen CYP450 system leading to aggressive breast cancer progression in response to DNA damage and adduct formation, in particular 8-hydroxydeoxyguanosine (8-OHdG) (Fan and Bolton, 2001, Kryston et al., 2011). Furthermore, hydroxytamoxifen (4-OHT) undergoes further activation by peroxidases that result in a formation of DNA adducts (Pathak et al., 1996), and tamoxifen genotoxic effects are linked to the formation of a metabolite known as E (cis/trans-1,2-diphenyl-1-(4-hydroxyphenyl)-but-1-ene) that shares a similar structure with 4-OHT, but undergoes further metabolism to produce a highly reactive, quinone methide, that can alkylate the DNA (Fan and Bolton, 2001). In general, the cells are undergoing various forms of metabolic reaction associated with ROS produced from mitochondria (Murphy, 2009); to survive the oxidative stress, cells adapt diverse mechanisms against

ROS. Hence, cancer cells are exposed to long term production of ROS during antioestrogen treatment; the cells may adapt protective mechanisms via modulating ROS-mediated dysregulation of a-dependent redox-sensitive signalling pathways (Penney and Roy, 2013), notably, peroxiredoxin proteins. For example, it has been found that Prox5 is highly expressed in breast cancers (Karihtala et al., 2003), and the level of expression involves the modulation of the GATA1 (transcription suppressor) via agonist–bound ER. Therefore, one of the proposed activities is tamoxifen-bound ER, that can prevent the repression of Prox5, and therefore enhance cell survival (Chang, 2012, Seo et al., 2012).

1.3.5 Oestrogen receptor and signalling

In the late 1950s the first isoform of oestrogen biding proteins, ERα, was discovered and characterised by Elwood Jensen (Heldring et al., 2007). The ERα knockout mouse survived and changed a three-decade overview of oestradiol-mediated genomic signalling pathways via ERα, as a sole mediator (Lubahn et al., 1993). The discovery of ERβ several years later (Kuiper et al., 1996), led to more questions, because the survival of the ERα knockout mouse was due to the role of ERβ to sustain the functions missed by the knocked out ERα. With double ERαβ knockouts, mice models were able to survive, but with impaired reproductive systems (Krege et al., 1998). These two forms of ER are neither coded by the same gene nor have the same amino acid sequence. ERα gene is located in chromosome 6 while a gene in chromosome 14 follows the encoding of ERβ. The number of amino acids in each protein subset is inconsistent: 595 and 530 amino acids, respectively. Alternative splicing may produce several isoforms of each subtype with different functions, such as ERα46 (Heldring et al., 2007). Based on current available data, ER effects can be divided into two major categories: nuclear (direct transcription) and extra-nuclear effects (Figure 1-3) (Kampa et al., 2013).

Oestrogens are not only vitally essential to maintain and develop a normal reproductive system, but are involved in a wide range of physiological processes (Harvey, 2009). Among oestrogen metabolites that are produced in the body, 17β-oestradiol (E2), the most potent oestrogen metabolite, has the strongest agonistic effect on ERs (Harvey, 2009). ERs form, with other androgen receptors, a large superfamily of nuclear receptors that can act as DNA binding proteins of transcriptional activities when their matched hormones are diffused into the cytoplasmic matrix (Ruff et al., 2000). Both types of ERs are distributed in different tissues with different ratios including the gastrointestinal tract (ERα/β), lung (ERβ), liver (ERα), breast (ERα/β), urogenital tract (ERα/β) and bone (ERα/β) (Della Torre et al., 2016, Kuiper et al., 1997, Teng et al., 2008). Interestingly, the role of these receptors in carcinogenesis is paradoxical and always thought to be in opposition whereby ERα is a carcinogenic mediator, and ERβ has an anti-proliferative effect (Thomas and Gustafsson, 2011). In the classical role of ERs, 17β-oestradiol (E2) is diffused to the cytoplasm and bound to the cytoplasmic ERs, each ligand-bound receptor undergoes conformational changes and dimerization with other receptors. This is followed by the translocation to complex, with a specific sequence on the promotor region of the target DNA, called ERE (Oestrogen Response Element) (Figure 1-3) (Dixon, 2014, Thomas and Gustafsson, 2011). Actually, the transcription of the target gene is mediated via two transactivation domains of ER, named AF-1 (ligand independent N-termini domain) and AF-2 (ligand binding carboxy termini domain) (Dixon, 2014, Nilsson et al., 2001), full agonistic activities of E_2 require both domains to be active in addition to the recruitment of several coactivator/repressor proteins that are localised on the target gene (Dixon, 2014). Of the coactivators that are specific to ER/PR receptors, are P160 SRC-1 (NCOA-1), SRC-2 (GRIP1/TIF2/NCOA2), and SRC-3 (AIB1) (Tien and Xu, 2012). However, this complex can act directly on the target genes or tethering via other transcriptional factors, which eventually leads to produce

the protein executors of specific functions related to proliferative growth. Nevertheless, unbound ERs remain inactive and anchored in the cytoplasm by the associated heat shock protein (HSP-90), which readily dissociates upon ligand binding. Additionally, growth factors may replace the ligand activation and initiate the downstream phosphorylation and receptor activation (Dixon, 2014).

Indeed, the rhythm of the classical (genomic) pathway is very slow and may last days, in comparison with the non-genomic pathway, which is faster, reversible and initiates a growth cascade via the steroid receptors localised in the plasma membrane of the cytoplasm. In this pathway, the activated enzymatic cascades lead to the activation of the proliferative signalling pathways that ultimately turn on the mitogen activated protein kinase (MAPK) and subsequent cell growth (Silva et al., 2010).

Furthermore, compartmental oestrogen biosynthesis has been reported to take place in mitochondria, in the presence of 3β-hydroxysteroid dehydrogenase and aromatase, moreover, the lipophilic property of exogenous oestrogen enhances its transportation into this organelle (Felty and Roy, 2005). Therefore, analysis of interactions between mitochondria and oestrogen is of no less importance and may play an important role in revealing a new target for treatment and prognosis. An enlargement of the mitochondrial morphology in response to a physiologically significant concentration of E2 (10nM), a dose of choice in our project, has been visualised by electron microscopy in MCF-7 cell line (Vic et al., 1982).

1.4 Mass Spectrometry based proteomics

Finding the links between the proteins and their coding genes is a 'landmark' that should change the direction of life sciences (Domon and Aebersold, 2006). Hence, protein identities and their structures can be used to provide researchers with high resolution images that reflect the real complexity governing living systems; the trend was geared towards developing high throughput platforms to enable researchers to make use of the available resources provided by high throughput genomics and genomic projects.

Advances in genomics and high throughput technologies in the last few years, have provided the basis for developing very rich datasets that are accessible to the scientific communities and have paved the way in gaining a better understanding of the underlying mechanisms of cancer developmental steps. Here, and owing to the maturity in gene sequencing technologies, we can have access to several informative platform datasets, such as: The Cancer Genome Atlas (TCGA), the International Cancer Genome Consortium (ICGC) and Therapeutically Applicable Research to Generate Effective Treatments (TARGET) (Kazma et al., 2012, Nik-Zainal et al., 2012, Pugh et al., 2013, The Cancer Genome Atlas Research, 2008, The Cancer Genome Atlas Research, 2011, Verhaak et al., 2010). It is becoming clearer, that relying on functional genomics (transcriptome level) alone, is not sufficient for the generation of information on the overall signalling pathways governing the biological properties of cancer (Boyd et al., 2008). This is for several reasons: first, gene transcriptions may be up-regulated/downregulated in response to a specific signalling cascade; therefore, when signal transduction pathways are activated at a specific time, it is not easy to predict the real time (temporal change) of activation (Shaulian and Karin, 2002). Second, several studies have proven that the level of protein expressed in cells is not directly proportional to

the gene expression level (Anderson and Seilhamer, 1997, Celis et al., 2000, Gygi et al., 1999, Nishizuka et al., 2003). Thirdly, post-translational modification is a natural process that plays a complex role in protein activation, deactivation or degradation (Boyd et al., 2008). Furthermore, a vast amount of powerful proteomic generated data show considerable instability inside living systems and the spatiotemporal dynamicity appears to be a way of assuring bodily function, organ, cells and organelles relationships (Eckersall and Whitfield, 2011, Kholodenko, 2006, Scott and Pawson, 2009).

In light of these observations and complementary to the genomic approach, proteomics is a reliable branch of research that can provide information about rapid dynamic changes (spatial) in real time (temporal) in cell signalling pathways. It can help in refining cancer subtype classification and in tackling cellular processes involved in tumour malignancy, developing new tumour biomarkers and therapeutic targets (Boyd et al., 2008, Lam et al., 2014).

The proteome encoded by the human genome is much more complex, and this is illustrated by the number of protein coding genes (20-25,000 genes), where each gene can give rise to more than one protein at a time, and each protein is eventually subjected to modifications by different mechanisms and plays out its functions in different spaces at different times, with significant differences in order of magnitude (Anderson and Anderson, 2002, Domon and Aebersold, 2006).

In 1995, a proteomics term was coined to describe a new field of research as a large-scale functional proteome (phenotype) encoded by genome (genotype) in a particular cell line, tissue or organism (Anderson and Seilhamer, 1997, Wasinger et al., 1995, Wilkins et al., 1996). In respect to the complexity of biological systems, mass spectrometry (MS) based proteomics has been widely recognised as an essential method with high sensitivity for functional analysis at the protein level (Aebersold and Mann, 2003). There is a general consensus that the developments in this field are closely tied to the completion of the genome sequencing database and the advances of particular techniques and concepts, most notably, the enhanced separation of peptides by coupling online liquid chromatographic (LC-MS) and the introduction of soft protein/peptide ionisation ESI and MALDI. The latter is recognised by the Nobel Prize of 2002 to Fenn and Tanaka (Fenn et al., 1989, Tanaka, 2003).

Every MS system has the following components (Figure 1-5): the Inlet system, ion source, mass analyser and mass spectrum detector. Based on these components, MS can accomplish several tasks including: ionising the neutral molecules contained in the introduced analytes, providing indirect measurement of the mass by separating ions based on mass to charge (m/z), detecting ions and plotting their m/z verses abundances, and in the tandem MS (MS/MS), the ions of interest are fragmented to provide structural information and peptide sequencing by means of low-energy collision-induced dissociation (CID), high energy collision-induced dissociation, and electron transfer dissociation (ETD).

For secure identification of very small amounts in complex mixtures, resolving power and mass accuracy are two most important parameters used to evaluate the performance of MS to separate and distinguish various constituents of the mixture with accurate mass detection. These two parameters determine the selectivity (resolution) and sensitivity (accuracy) of mass analysers.

It is fundamental to the researcher, when selecting a method of choice, to link the selected approach to the research objectives; therefore, *a priori* knowledge originates from addressing many topical questions. For example, why do we use MS in molecular sciences? Or, how many MS analysers are available and why should we carefully select between them?

The heart of a mass spectrometer is a mass analyser. To understand the importance of this part of a whole MS, the emphasis should lay on two important parameters: high resolution and accuracy of mass spectrometry (Koulman et al., 2009). Hence mass is a fundamentally important piece of information, and to obtain highly accurate mass measurements, the MS analysers have evolved tremendously during recent decades. As of late developed MS analysers is the Orbitrap mass analyser (Eliuk and Makarov, 2015). In the standard MS analysis, ions are generated and their mass to charge ratios is measured (m/z), but not the structure or abundance of ions. Tandem mass spectrometry (MS/MS) led to the identification of structures more feasible by adding further fragmentation step in the analysis. There are two classes of tandem MS experiments: First, tandem in space: making ions, mass selecting ions, fragmentation (dissociation), and measuring products all the time, so that everything is conducted in parallel, but at different physical locations, i.e. all processes are occurring all the time, but separated in space, and ions are transmitted from one place to another, which comprises, for example, triple/tandem quadrupole (QqQ) and Orbitrap hybrid instruments. Secondly, tandem in time: it is *in situ* ionisation which is truly a tandem in time experiment,

where ions generation, mass selection, ions fragmentation, and measure the products all in the same physical space, but the processes are separated in time. Examples of this type of tandem mass spectrometry include, but are not limited to, linear ion traps (LIT) and Fourier transform ion cyclotron resonance (FT-ICR) instruments (Hird et al., 2014).

To meet the growing demands of high performance MS analysers that combine both high mass resolution and accurate mass detection (HR/AM), the Orbitrap was coupled with linear trap mass analysis (Eliuk and Makarov, 2015). This hybridisation in technology has helped to develop hybrid instruments, where they combine transmission and trapping events. Linear ion trapping leads to an enhancement of speed and sensitivity for both LC-MS and tandem LC-MS/MS detection, providing multiple measurements for the parental ions (MS^n) followed by fragmentations of the precursors and the production of spectra for those fragmented ions at high rates suiting the needs of large scale proteomics (Glish and Burinsky, 2008).

Back to 2005, the first commercial release of this hybrid instrument (LTQ-Orbitrap mass spectrometer) was introduced by Thermo Fisher Scientific (former Thermo Electron) (Makarov et al., 2006). Figure 1-4 shows the design of the LTQ-Orbitrap mass analyser.

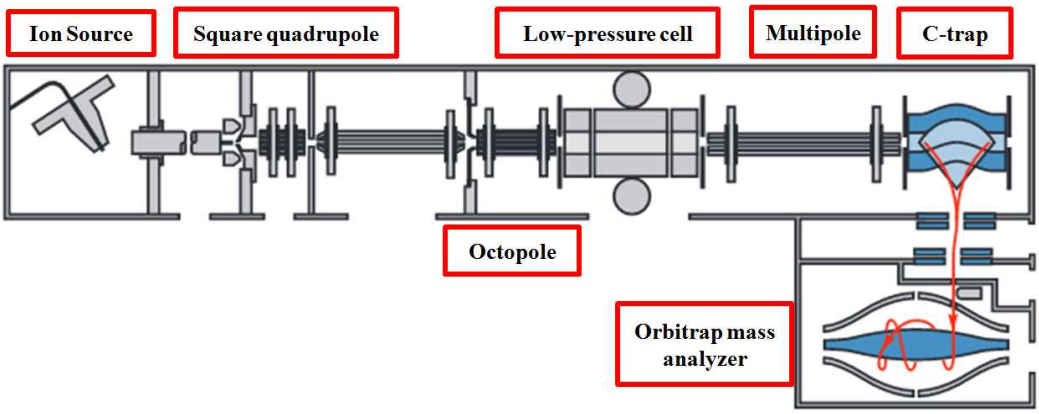

Figure 1-4: Schematic of the LTQ-Orbitrap mass spectrometer.

Hybridisation of the traditional linear ion trap with Orbitrap mass analysers. Adapted from (Eliuk and Makarov, 2015).

The most common types of discovery proteomics fall into three main categories: (1) global proteomics aimed to identify proteins in the sample and the changes in abundance associated with biological perturbations, (2) studying the global post-translational modifications (PTM), and, (3) affinity proteomics to identify proteins that interact with other proteins, nucleic acids or small molecules.

It is now known, as demonstrated by large group proteomics projects such as PROSPECTS (Proteomics Specification in Space and Time), that there are a number of important differences between proteomics and transcriptomics (Lamond et al., 2012). First, proteomics technology is a reliable and truly quantitative branch of research that can provide information about the actual changes in the protein level, considering the life cycle of protein from synthesis through ultimate degradation (post-translational modifications) and relating that to the rapid dynamic changes (spatial) in real time (temporal) in the cell signalling pathways, while transcriptomics is less likely to provide that information. Secondly, the localisation of subcellular proteins, both on a large scale and under endogenous conditions, can be elucidated on large scale proteomics workflows. In sum, proteomics is not a replicate of transcriptomic data, though it can add more unique and accurately obtained information to existing knowledge gained from transcriptomics (Lamond et al., 2012).

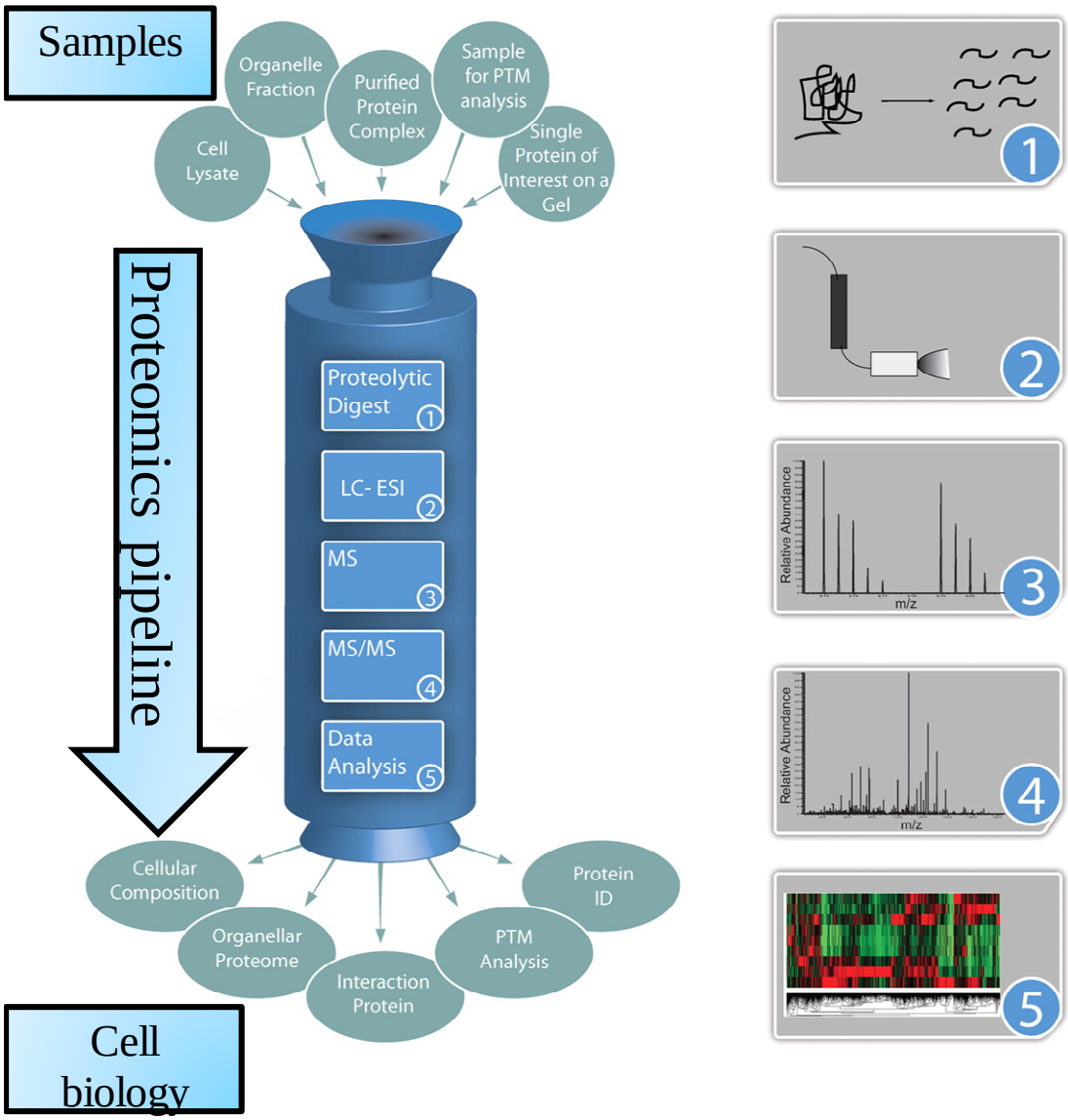

Figure 1-5: MS based proteomics pipeline

Complex sample mixtures of proteins are obtained from cell lysate, tissue or subcellular fractionation. The solubilised proteins in the sample mixture can be subjected to further fractionation using gel electrophoresis before the tryptic digestion of the peptides (1). Molecular species generated from Electrospray liquid eluted techniques (LC-ESI) Liquid is introduced to MS analyser (2,3). The selected parent peptides are fragmented (4) and generated MS/MS spectra are analysed followed by selecting an appropriate downstream bioinformatics application (5). Adapted from (Walther and Mann, 2010).

1.4.1 Quantitative Stable Isotope Labelling by Amino Acids in Cell Culture (SILAC)

Currently, MS provides a powerful analytical technique for the study, characterisation and quantitation of proteins. The high complexity of a proteomics sample poses a significant analytical challenge and places demands on LC-MS workflows. LC-MS experiments can be designed to generate quantitative data by following one of two approaches, either label or label-free. Hence, MS is not a quantitative method *per se*, and protein ID is sufficient for locating the key players in biological pathways; achieving a deeper understanding requires an investigation into the differential regulation of proteins between two cellular states (treated vs. control) (Walther and Mann, 2010).

This has resulted in a growing emphasis on quantitative workflows; alternative methods have been developed to gain accurate absolute or relative quantitation of proteomes on a large scale, such as chemical isobaric (iTRAQ) (Ross et al., 2004) and metabolic labelling (SILAC) of digested peptides (Ong et al., 2002). Although thousands of peptides can be generated from a single run of LC-MS on a complex mixture, biased data can be expected with different runs (replicates) and subsequent protein quantification and identification would be meaningless (Michalski et al., 2011). Therefore, selecting the most suitable and relevant labelling strategy is a current trend in achieving accuracy in abundant measurements (quantity) of identified proteins, allowing an in-depth analysis of the systems biology with a better resolution (Cox and Mann, 2011). SILAC labelling is a method of choice for metabolic labelling of entire proteomes in cell culture, and full incorporation can be achieved with several cell culture doublings in the media containing natural amino acids enriched with stable isotopes, such as ^{13}C and ^{15}N. A shift in mass can be determined by LC-MS/MS (tandem mass spectrometer) in the parent ions (precursors) and the fragmented ions of light

and heavy peptide pairs (light and heavy SILAC) (Ong, 2012). The downstream analysis of the generated LC-MS/MS data can acquire better identification and quantification by integrating bioinformatics software, notably MaxQuant and a peptide search engine (Andromeda) integrated into MaxQuant (Michalski et al., 2011).

1.4.2 Quantitative subcellular proteomics

Protein is not a static component of the cell, and it is a continual challenge facing the biologist to address the impact of a specific treatment on protein localisation and how to measure those changes. Several proteomics approaches have been used to quantitatively to measure the protein abundance/flux in response to biological perturbations. For example, Andersen et al. (2005) used the SILAC labelling to assess the abundance/redistribution between the nucleolus and nucleus of 489 endogenous nucleolar proteins in response to three metabolic inhibitors.

Spatial-based proteomics evolved because the metabolic labelling (SILAC) allowed the comparison of two SILAC ratios between two experiments, i.e., under different stimuli the changes in location from one compartment to another can be quantified; therefore, allowing for the characterisation of dynamic changes in protein subcellular localisation as a result of induced DNA damage of HCT116 cells treated with etoposide (Boisvert et al., 2010).

Many proteomics methods have allowed researchers to study the localisation of proteins into specific organelle and subcellular structural compartments following various sets of enrichment protocols (Andersen et al., 2002, Andersen and Mann, 2006, Dunkley et al., 2004, Sadowski et al., 2006). Collectively, these methods are known as organellar proteomics or subcellular proteomics; hence, these methods are quantitative approaches and differ from the high-throughput proteomics such as protein correlation profiling (Wiese et al., 2007) or the localisation of organelle proteins by isotope tagging (LOPIT) (Dunkley et al., 2004), in two senses. First, they can provide insight into the protein localisation considering the nature of the protein and its redistribution dynamicity to different locations, under biological perturbations, and not exclusively expressed and/or localised to a specific subcellular structure (Gauthier and Lazure, 2008, Hall et al., 2009, Qattan et al., 2010,

Qattan et al., 2012). Second, they can provide the relative and/or absolute measures of the protein abundance at different cellular subsets and physiological states (Baqader et al., 2014, Mulvey et al., 2013, Pinto et al., 2014). It is necessary here to differentiate between the single organelle proteomics and the systematic approach of subcellular proteomics. Although both methods are based a combination of biochemical enrichment protocols and MS-based proteomics, they differ in that the former provides a list of the identified proteins in a specific and isolated organelle, while the latter can provide a quantitative overview of protein distribution/change over multiple compartments in broad biological systems (Drissi et al., 2013, Gauthier and Lazure, 2008).

In general, methods of subcellular fractionation aim to reduce the complexity of the cellular system prior to the proteomics workflow, and enrich the proteome samples with the isolated target organelle(s)/subcellular structures from the rest of cellular compartments. Figure 1-6 shows that the eukaryotic cells are multi-compartmental, and that the purification of specific set(s) of the subcellular structures requires either classical approaches, such as deferential centrifugation (Lee et al., 2010), density gradient centrifugation (de Araujo et al., 2008, Qattan et al., 2010) and differential detergent fractionation (Abdolzade-Bavil et al., 2004, Ramsby et al., 1994), or emerging methods of fractionation, such as free-flow electrophoresis (Zischka et al., 2006), immunoaffinity purification (Ackermann and Berna, 2007) and fluorescent-assisted organelle sorting (FAOS) (Bock et al., 1997, Gauthier and Lazure, 2008). Protein content in the original cell line/tissues are vulnerable to variation during multistep enrichment and fractionation phases; therefore, variability induced by pre-MS steps and the development of a reliable method for quantitative analysis is still considered a challenge (Wasinger et al., 2013). Several methods can be used to roughly characterise the purity of the generated fraction using known localised protein markers, and such markers are less sensitive in detecting contamination than MS/MS (Drissi et al., 2013).

These methods include: enzymatic activity of a particular organelle (Takatalo et al., 2006), immunofluorescence microscopy (Takatalo et al., 2006) and immunoblotting for the presence or absence of a specific known protein (Qattan et al., 2010, Qattan et al., 2012). No one can guarantee quantitative precision based on quantitative mass spectrometry alone; protein concentration in the original sample is vulnerable to variation during multistep enrichment and fractionation phase (Cox and Mann, 2011, Wasinger et al., 2013). Considering the variability induced by pre-MS steps, the development of a reliable method for quantitative analysis remains a challenge (Wasinger et al., 2013). However, continued assessment of the variability introducing methods has led some researchers to produce data with a high degree of accuracy and reproducibility (Mulvey et al., 2013, Pinto et al., 2014, Qattan et al., 2010, Qattan et al., 2012). The dynamics of the subcellular distribution of thousands of proteins in MCF-7, under two different biological perturbations, were investigated in the current project using a high-throughput large scale proteomic quantitative approach (SILAC labelling) taking advantage of the developed subcellular spatial razor model for interpretation (Baqader et al., 2014, Mulvey et al., 2013, Pinto et al., 2014). Figure 1-7 shows the MS-based quantitative proteomics workflow used in this project combining the subcellular proteomics and differential isotope labelling by metabolic incorporation.

The subcellular spatial razor formulation can distinguish between changes in total protein abundance (S_t) and redistribution (S_n/S_c) (Figure 1-8) to/from a target organelle (e.g. the nucleus). For all three of systems analysed with this framework, correlation between changes in total abundance and in subcellular nuclear/cytoplasmic redistribution has been found to be low, i.e., changes in compartmental abundance do not simply mirror changes in total protein abundance (Baqader et al., 2014, Pinto et al., 2014). The orthogonal basis set {S_t, S_c/S_t, S_n/S_t} for the three measured SILAC ratios separates changes in total protein abundance (S_t) from a distribution plane (S_c/S_t, S_n/S_t) that reflects the redistribution of a protein. Conservation of mass (highly reproducible subcellular fractionation and no differential protein losses between stimulated/unstimulated samples during MS sample preparation) requires that the data points lie in 2 quadrants corresponding to N → C or C → N redistribution of the protein. The subcellular spatial razor model assumes that a given protein can be in the nucleus (n) and in the cytoplasm (c) for both unstimulated (u) cells and stimulated (s) cells. The corresponding abundances (Figure 1-8) are $A_{n,u}, A_{n,s}, A_{c,u}, A_{c,s}$. There are three SILAC ratios given by:

$$S_n = A_{n,s}/A_{n,u}, \qquad [1]$$

$$S_c = A_{c,s}/A_{c,u},$$

$$S_t = (A_{n,s} + A_{c,s})/(A_{n,u} + A_{c,u}).$$

The values for the fractions of the protein in the nucleus in unstimulated and stimulated cells, f_u and f_s, are closely related to the SILAC ratios:

$$f_u = A_{n,u}/(A_{n,u} + A_{c,u}) = (S_t - S_c)/(S_n - S_c), \quad [2]$$

$f_s = A_{n,s}/(A_{n,s} + A_{c,s}) = S_n(S_t - S_c)/S_t(S_n - S_c)$. Furthermore, the fractions f_u and f_s are closely related to the parameters used in a three-dimensional orthogonal basis set for the experimental results (see below).

$$S_n/S_t = f_s/f_u, \quad [3]$$

$$S_c/S_t = (1 - f_s)/(1 - f_u)$$

Experimental application of the spatial razor requires fractionating the total cellular proteins (total fraction) into two subcellular fractions such that: nucleus-enriched fraction + nucleus-depleted fraction (cytoplasm) = total fraction and measuring the set of SILAC ratios {S_n, S_c, S_t}. Although formulated here for the nucleus, a spatial razor could also be applied to other subcellular locations through the use of sample triplets such as {mitochondria-enriched, mitochondria-depleted, total-fraction}.

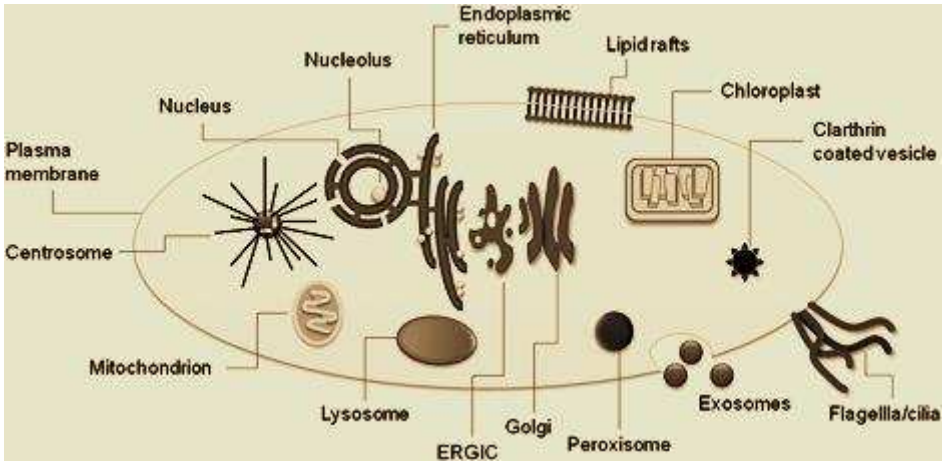

Figure 1-6: Sub-compartmental composition of eukaryotic cell.

Adapted from (Lee et al., 2010).

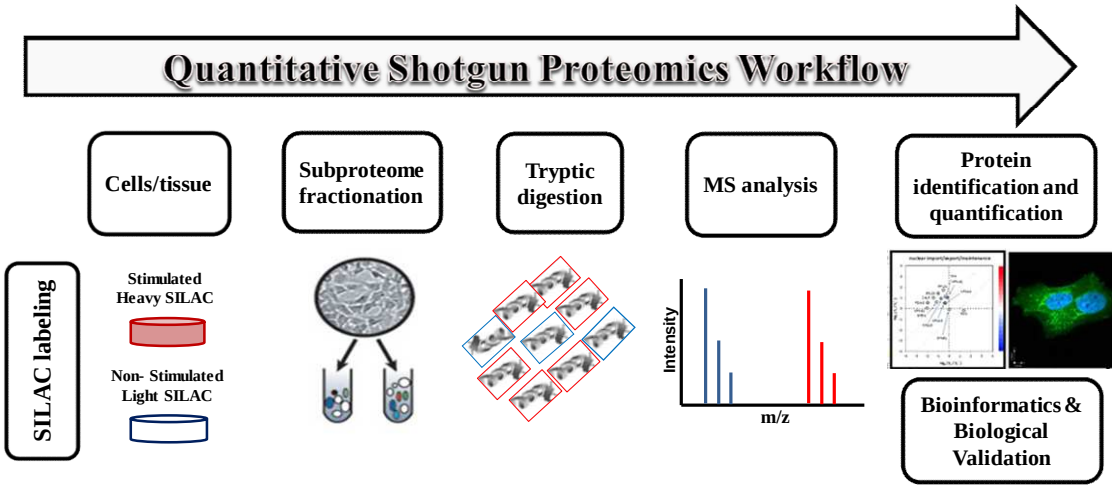

Figure 1-7: Workflow for subcellular analysis with quantitative shotgun proteomics

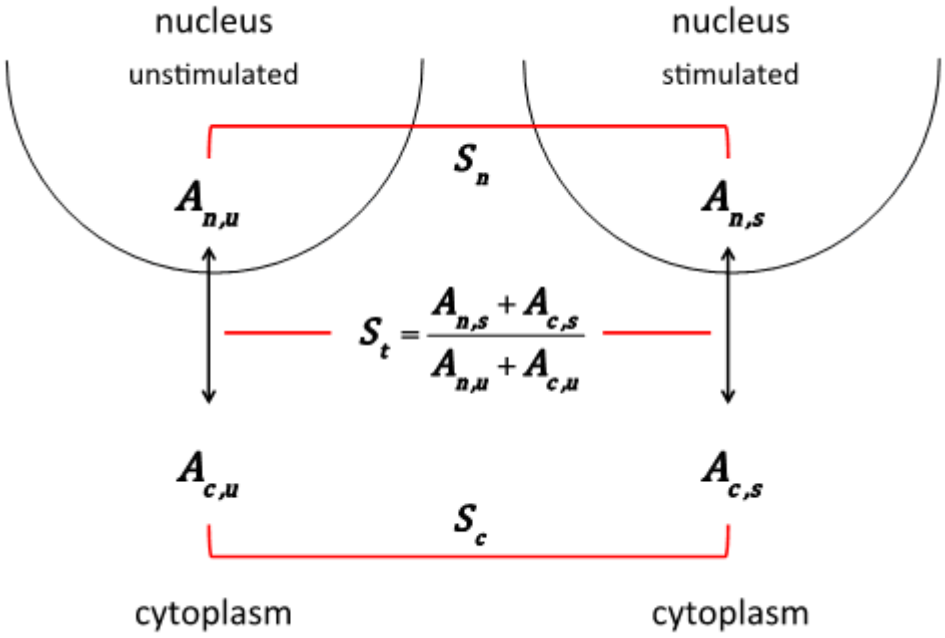

Figure 1-8: Subcellular spatial razor model.

A protein (A) has different abundances in unstimulated (u) or stimulated (s) cells and in the nucleus (n) or in the cytoplasm (c). The ratio of the abundance of the protein between unstimulated/stimulated cells is measured by SILAC isotope ratios for the nucleus (S_n), the cytoplasm (S_c) and for a total cell lysate (S_t).

1.5 Objectives of this project

The nuclear genome is dramatically altered (unstable) in cancer cells, to escape the apoptotic growth restrictions imposed on normal cells while mitochondrion associated metabolism abnormality is considered to be an essential supplier of the new cellular components during cancer proliferation (Hanahan and Weinberg, 2011). Indeed, multiple lines of evidence primarily view cancer as a metabolic disease and more dependent on aerobic glycolysis and/or glutaminolysis to provide new cellular components for the new proliferated populations of cancer cells (Vander Heiden et al., 2009). Further findings suggest that growth response in cancer cells can be mediated by ER in one of two ways: classical genomic pathways that have a very slow onset of action, several hours or days, and cytoplasmic signalling pathways that can occur in seconds. In this manner, oestrogen could rapidly act on mitochondria, consequently, the cross talk between subcellular organelles, nucleus and mitochondria, seem to be channelled through oestrogen-mediated signalling pathways involved in the proliferation (Chen et al., 2009). For these reasons, the overall goal of this project is to use the high throughput proteomics technology combined with the enrichment of subcellular target proteins after SILAC labelling to elucidate the possible relationship between major changes in the compartmental proteins and the cellular response to biological perturbations of oestrogen (E2) and tamoxifen (4-OHT) in the MCF-7 breast cancer cell line.

To that end, the following aims are specifically addressed:

1. To quantify the spatial dynamics of subcellular large scale proteomics of MCF-7 cells under oestrogenic and anti- oestrogenic stimulation.

2. To apply quantitative shotgun SILAC-based global proteomics to reveal changes in protein expression and redistribution between subcellular compartments in response to the biological perturbations E2 and 4-OHT.

3. To validate the spatial razor formulation in estimating whether the changes in protein quantitation are due to changes in the total abundance or re-localisation of proteins between subcellular compartments.

4. To identify major pathways and groups of proteins related to oestrogen-dependent breast cancer and/or drug resistance.

Such quantifications of the dynamical response under biological perturbations will help to gain a better insight into spatial control of breast cancer and elucidate the possible mechanisms underlying the proliferative action of oestrogen and/or the partial proliferative action of tamoxifen that may lead to the acquisition of resistance over time.

Chapter 2 Materials and methods:

2.1 Starting cell culture from frozen cells

The SILAC protein quantisation kit with DMEM was ordered from the Thermo Scientific (Rockford, USA, 89983) and contained all reagents for isotopic labelling including the following: SILAC Dulbecco's Modified Eagle's Medium, 2 × 500mL; 13C6 L-Lysine-2HCl (heavy Lysine), 50mg; L-Lysine-2HCl (light Lysine), 50mg; L-Arginine-HCl (light Arginine), 2 × 50mg; and Dialyzed Foetal Bovine Serum (DFBS), 2 × 50mL (separate dispatching at -20°C). For double labelling, 13C6 15N4 L-Arginine-HCl (heavy Arginine) was ordered separately (89990). Storage, preparation, and SILAC procedure were carried out as per the manufacturer's instructions.

2.1.1 Cell counting

Following the trypsinization of cells, uniform suspension of containing a single cell was obtained by diluting the cells in a suitable volume of medium to ensure that the cells are neither too diluted nor too concentrated. A 1:1 dilution of the cell suspension was prepared in trypan blue solution, 0.4% (Thermo Fisher Scientific, UK) and pipetted up and down several times to ensure a uniform cell suspension, and 10 µl out of the trypan blue-cell suspension was used to charge one chamber of a hemocytometer (Hausser Scientific, Horsham, PA, USA). A trypan blue-cell suspension was transferred to one of the chambers of the hemocytometer and placed carefully on the edge of the cover slip to fill the chamber by capillary action. The phase contrast microscopy visualized the live cells (unstained) and dead cells (blue stained) at 40x magnification. The cells in four corner squares plus the middle square were counted, the total number of cells average overlying 1 mm^2 was doubled, for the dilution with trypan blue, to obtain the number of cells per ml suspension.

2.2 Metabolic labelling (SILAC)

The SILAC protein quantisation kit with DMEM was ordered from the Thermo Scientific, Rockford, USA (89983) and contained all reagents for isotopic labelling including the following: SILAC Dulbecco's Modified Eagle's Medium, 2 × 500mL; 13C6 L-Lysine-2HCl (heavy Lysine), 50mg; L-Lysine-2HCl (light Lysine), 50mg; L-Arginine-HCl (light Arginine), 2 × 50mg; and Dialyzed Foetal Bovine Serum (DFBS), 2 × 50mL (separate dispatching at -20°C). For double labelling, 13C6 15N4 L-Arginine-HCl (heavy Arginine) was ordered separately (89990). Storage, preparation, and SILAC procedure were carried out as per the manufacturer's instructions.

2.2.1 SILAC media preparation

Each SILAC Dulbecco's Modified Eagle's Medium (2 × 500mL) was supplemented with 10% of thawed dialyzed FBS and 1% antibiotic antimycotic (10,000 units penicillin, 10 mg streptomycin, and 25µg Amphotericin B per ml). Heavy amino acids, 13C6 L-Lysine-2HCl, and 13C6 15N4 L-Arginine-HCl were dissolved in one of the DMEM and used later for "heavy" isotope metabolic labelling, while the light amino acids, L-Lysine-2HCl, and L-Arginine-HCl, were dissolved in a medium and used later to adapt cells in the natural amino acids that referred to as "light". Media containing dissolved amino acids were sterile-filtered using a 0.22 µm filter (TPP, Switzerland) and stored at 4 °C.

2.2.2 Adaptation phase

MCF-7 cells were adapted to grow in a DMEM: F12 medium; the cells were then divided into two different populations and seeded into two culture flasks with one containing non-radioactive isotopic labelled heavy amino acids (13C6 L-Lysine-2HCl and 13C6 15N4 L-Arginine-HCl) and the other containing normal essential amino acids (L-Lysine-2HCl and L-Arginine-HCl) in SILAC media. Both cell populations were grown at 37°C in a humidified incubator of 5% CO_2 and were passaged for at least five cell doublings by splitting cells at 70-80% confluence. After passage five, incorporation efficiency of heavy amino acids, (13C6 L-Lysine-2HCl and 13C6 15N4 L-Arginine-HCl) was verified by comparing MS analysis of peptides that were heavy- and light-labelled in gel tryptic digested proteins. After full isotopic incorporation was verified to be fully incorporated (>95%), both cells populations (light and heavy) were expanded to the desired number required for treatment and subsequent fractionation.

2.2.3 Treatment phase

2.2.3.1 E2

After six passages, cells were allowed to reach 70% confluency in both heavy and light SILAC media. To eliminate the hormonal effect of phenol red SILAC growth medium that contained phenol red were aspirated off, flasks were washed with PBS, and media changed into the phenol red free MEM for SILAC (Thermo Scientific, Rockford, USA, 88214) with the same “Heavy” and “Light” amino acids labelling. After 24 h, oestrogen (17 beta-oestradiol, E2, Sigma) was added into the cells grown in a heavy SILAC medium to a final concentration of 10 nM, and the control cells (light SILAC medium) were treated with the 0.1% of vehicle ethanol. Finally, both cell pools (E2 stimulated and control) were re-

incubated at 37°C with 5% CO2 for 48 h further with one more new media replacement at an interval of 24 h calculated from the time of stimulation.

2.2.3.2 4-OHT

In order to deliver the treatment of 1 µM 4-OHT (Sigma-Aldrich, H7904) into the desired number of cells for the subsequent fractionation, the SILAC media were changed into the phenol red free MEM for SILAC supplemented with 10% dialyzed FBS and 1% of antibiotic antimycotic solution and incubated for 24 hours at 37°C in a humidified incubator of 5% CO_2. Both cells populations were subjected to further 24 h (total of 48 h) incubation in a fresh phenol red free MEM for SILAC before delivering the dose of treatment into the heavy labelled cells population. After 48 h, the protein abundance in a heavy cell population was altered by applying a dose of 1 µM 4-OHT for further 24 hours incubation while the media were changed into a fresh phenol red free MEM for SILAC (without treatment) in the light labelled cell population.

2.2.4 Cytotoxicity/proliferation assay

The concentration of 1 µM (10^{-6}M) of 4-OHT was previously used in different laboratories, to name a few. It was selected for complete inhibition of oestrogen-dependent ZR-75-1 cells without influencing the growth of tamoxifen-resistant derivatives (Meijer et al., 2006). This dose has been routinely used because of the absence of toxicity and to effectively counter variations in oestrogen content of different batches of bovine serum (Lykkesfeldt et al., 1984, van Agthoven et al., 2012) and an IC50 concentration of a drug that is required for 50% inhibition of in vitro tamoxifen is 1000 nM (Kijima et al., 2005). Therefore, in this project, the dose of 4-OHT was selected to have a non-cytotoxic (non-lethal dose) effect, but a cytostatic (growth inhibition) effect on MCF-7 cells. Cell survival/cytotoxicity assay was

assessed using cell counting kit-8 reagent (CCK-8) (Dojindo Laboratories, Kumamoto, Japan) with various doses of 4-OHT including choosing a dose of 1 μM (10^{-6}M).

2.2.4.1 Cell preparation and standard curve

To determine the cell number to be used in the viability assay and the cck-8 incubation time specific for the MCF-7 cell line, the number of cells was plotted against the absorbance in order to establish the standard curve. The cells were recovered from the culture flasks and the cell number in the suspension was adjusted to $5x10^5$ cells/ml. The wells of 96-well microplate were prepared with 100 μl of media. Then, 100 μl of $5x10^4$ cells suspended to the first well was added and made triplicate serial dilutions of $2.5x10^4$, $1.25x10^4$ and $6.25x10^3$ in a 96-well plate. However, the last well was reserved for the negative control (blank). This well contained only media (no cells) for measurement of background.

For the first time, the 96-well microplate was incubated for 24-48 h in the CO_2 incubator to determine the optimal growth time for the standard curve. 10 μl of cell counting kit-8 reagent (one tenth of the media containing cells) was added to each well on the 96-well microplate. The plate was placed in a CO_2 incubator to react for 1-4 h, and the colorimetric readings used a microplate reader using a filter for 450 nm at different time point intervals, from 1 to 4 h, to plot the number of cells versus the absorbance and establish the standard curve. The upper portion (80%) of the linear range of the standard curve was used to adjust the number of the cells to be used with the test substance (4-OHT) to assess the cell proliferation and cell toxicity.

2.2.4.2 Cell survival/cytotoxicity assay

A 200 µM stock solution of 4-OHT was prepared in absolute ethanol and stored at -20°C. Cells were plated at density of 12.5×10^3 cells by adding 100 µl in a 96-well plate and incubated for 24 h at 37°C in a humidified incubator of 5% CO_2. Upon confluence, media were changed into DMEM-F12 phenol red-free medium supplemented with 10% charcoal treated FBS and medium was changed every 24 h before 4-OHT stimulation. At 48 h, cells were treated with various concentrations of 4-OHT (0.5, 0.1, 1.5, 2.0 µM) in three replicates for each dose. With each dose, a negative control was plated with the same cell number and treated with an equivalent volume of 0.1% ethanol (maximum 0.1%). After 24 hr from the stimulation time point, 10 µl of cell counting kit-8 (one tenth of the cells plus media) was added to each well including the negative control and blank wells. The plate was placed back in a CO_2 incubator for 3:30 hr. The colorimetric readings were taken on a microplate reader using a filter for 450 nm. To calculate the survival rate (%) was obtained for the samples and the negative control using the following equation:

$$\text{Survial rate } (\%) = \frac{A(\text{sample}) - A(\text{blank})}{A(\text{control}) - A(\text{blank})} * 100$$

2.3 Sample preparation

Differential centrifugation was used to obtain the nuclear, cytoplasmic, and total lysate fractions according to the protocol previously described (Pinto et al., 2014, Qattan et al., 2012). All the subsequent steps were performed at 4°C with all buffers containing protease and phosphatase inhibitors cocktail tablets (Roch,UK). Light- and heavy-labelled cells populations grown as monolayers in T75 flasks were washed in ice-cold phosphate buffer saline (PBS) pH 7.4, for three times, cells were scraped from culture flasks on ice using a plastic cell scraper and collected in 15mL conical centrifuge tubes.

2.3.1 Total lysate

12 $x10^6$ cells were scraped, from heavy and light cells populations in ice cold PBS, and the pellets were collected by cold centrifugation at 300 x g for 5 min. Two pellets were collected and each pellet was dissolved and re-suspended in a cold RIPA lysis buffer (50 mM Tris-HCL at pH 7.5, 300 mM NaCl, 1 % NP40, 0.5 % Sodium deoxycholate, 0.1 % SDS, 1 mM EDTA) and transferred to a pre-chilled 1.5 ml microcentrifuge tube, the mixture was agitated on ice for 15-30 min (vortexed every 5 min) and centrifuged at 300 x g for 5 min (Heraeus Biofuge Pico, Thermo Fisher Scientific, U.K.). The cell debris was pelleted by cold centrifugation at 300 x g for 5 min (Heraeus Biofuge Pico, Thermo Fisher Scientific, U.K.), and the supernatant was collected as total lysate (T).

2.3.2 Nuclear and cytoplasmic fraction

The cells were counted and $12x10^6$ cells from light and heavy cell populations were recovered from the culture flasks in a cold PBS using a manual rubber policeman scraper. The pellets were obtained by cold centrifugation at 300 x g for 10 min (Mistral 3000i Refrigerated Centrifuge, 4312-708 BS 4402 rotor). Each pellet was allowed to stand on ice for 10 min ,in a hypotonic osmotic buffer (10 mM NaCl, 1.5 mM MgCl2, 10 mM Tris-HCl at pH 7.4) which was used to swell the cell membrane of the cells; the supernatant was removed by a subsequent step centrifugation at 300 x g for 10 min (Mistral 3000i Refrigerated Centrifuge, 4312-708 BS 4402 rotor). Each pellet was suspended in ice cold isotonic sucrose (breaking) buffer containing (300 mM sucrose, 1 mM EDTA, Heparin 5 U/mL, 10 mM HEPES, 5 mM MgCl2 at pH 7.4), and the cells were homogenized by 10–25 strokes of the pestle of a tight-fitting Dounce homogenizer (0.05-0.08 clearance). Under phase contract microscope, the suspension was inspected after every 10 strokes and homogenization was continued until about 90% of cells were broken. The obtained lysate that contained the subcellular homogony was subjected to a cold centrifugation at 800 x g for 10 min to separate the crude nuclear pellet (N) from the crude post nuclear cytoplasmic supernatant (C).

To release the nuclear proteins, the nuclear pellet was suspended in a high salt breaking buffer containing (20 mM HEPES at pH 7.9, 700 mM NaCl, 1.5 mM MgCl2, 1 mM EDTA, 10 % glycerol), for 2 h at 4°C on an end-over-end rotator. The supernatant was collected and labelled as nuclear fraction (N).

Both nuclear fraction (N) and post nuclear supernatant (C) were subjected to acetone precipitation by adding four volumes of 80% acetone at -20 °C for 1 hr, and the pellets were precipitated by a further cold centrifugation step at 16000 x g (Heraeus Biofuge Pico, Thermo Fisher Scientific, U.K.) and left to dry. The dried pellets were solubilised in a 1x protein solubilisation buffer (20 mM PIPES at pH 7.3, 300 mM NaCl, 2 % Triton X-100, 0.2 % SDS, 2 % sodium deoxycholate). The protein concentration, in each fraction, was quantified using the BCA protein assay kit (Thermo Scientific Pierce, Rockford, USA) by measuring the absorbance of protein samples at 562nm, see below.

2.3.3 Microplate (BCA) protein assay

Bicinchoninic acid (BCA) protein assay kit (Pierce Biotechnology, US) was used for the colorimetric detection and quantification of total protein. In this method, bicinchoninic acid containing reagent is used to enhance the sensitivity and selectivity of the colorimetric detection of the reduced cuprous cation (Cu+1) by protein in an alkaline medium (the biuret reaction) (Smith et al., 1985). The purple-coloured reaction product of this assay is proportional to the protein concentration in the sample and the absorbance of Albumin Standard (BSA) was diluted over broad working range concentrations (20-2000µg/mL) to obtain a nearly linear curve. In the microplate, BCA working reagent (WR) was added to the standards and unknown samples, mixed, and incubated at 37°C for 30 minutes. The plate was allowed to cool down at RT before the absorbance was measured at λ=562nm.

2.3.4 Assessment of subcellular fractionation by western blotting

Fractionation was evaluated by western blot using protein markers for nuclear and mitochondrial subcellular compartments to assess the protocol's enrichment capacity. Therefore, two constitutively protein markers were selected, VDAC, for mitochondrial localization on the total lysate and cytoplasmic fractions, and Histone H3, for total lysate and nuclear fractions.

Twenty micrograms of each sample (total lysate, cytoplasm, and nuclear fractions) were electrophoretically resolved by 12% SDS-PAGE. The resulting gels were transferred to a PVDF membrane using a Mini trans-blot cell and Powerpac basic power supply (BioRad, Herts, U.K.) at a constant 100 V/350 mA. After 1 h, the blots were blocked with 5% milk-TBS-Tween saline buffer (TBST: 20 mM Tris buffer, 150 mM NaCl, 0.1% Tween-20, pH=7.5) for 2 h at 4°C under slow agitation, followed by a rinse for 5 s in TBST. The membranes were incubated overnight at 4°C with two different primary antibodies: anti-VDAC (ab34726, Abcam, Cambridge, U.K.) and anti-Histone H3 (ab1791, Abcam), at 1:1000 and 1:2500 dilutions, respectively. After washing the membranes with TBST three times (10 min for each washing) under agitation, the membranes were incubated for 1 h with a secondary antibody conjugated to horseradish peroxidase (#7074, Cell Signalling Technology, New England BioLabs, Hitchin, U.K.) at a dilution of 1:1000 for VDAC and 1:5000 for H3. The membranes were washed three times with TBST (10 min for each wash) and with TBS for 5 min, under agitation. Finally, proteins were visualised using chemiluminescence reagents ECL Plus and Hyper Film (GE Healthcare, Bucks, U.K.) and a Xograph imaging system Compact x4 (Xograph Healthcare, Stonehouse, U.K.).

2.4 Sample preparation for mass spectrometry and the "Bottom-up" MS approach

In-gel digestion protocol was introduced in the proteomics investigations to increase the protein coverage and the number of identified proteins, however, it has been used for many years and can be optimized with accumulative experience to the particular objectives of the experiment (Shevchenko et al., 2006).

2.4.1 SDS-PAGE and in-gel digestion

The solubilised protein concentration was measured in the cytoplasmic, nuclear, and total lysate sample types (CNT) obtained from the SILAC labelled (heavy) and unlabelled (light) cell populations. Both labelled and un-labelled protein extracts were mixed in 1:1 ratio for each sample type and the proteins in the complex samples were separated based on their molecular sizes using 4–15% SDS-PAGE (BIO-RAD, UK). The separated protein bands were visualized by silver staining (ProteoSilver Plus, Sigma Aldrich, Poole, U.K.) and the bands were excised (27-30 horizontal slices/lane) from the gel lane starting from the higher molecular weight-separated band (top) to the lower molecular weight separated band (bottom). Each band was cut into 1mm cubs, placed in 96-well plate, and incubated at RT for 10 min in 100 µl ddH_2O.

Silver stain was removed by immersion the bands in 100 µl of a distaining solution (100 mM sodium thiosulfate and 30 mM potassium ferricyanide solutions mixed in a 1:1 (v:v) ratio) at RT for 10 min. After several washes with ddH2O to pull off the rest of destining solution, cycles of dehydration (100% acetonitrile), rehydration (25 mM Ammonium bicarbonate), reduction (10 mM DTT, and alkylation (100 mM Iodoacetamide) for 5 h in the ProGest Investigator Instrument (DigiLab, Genomics Solutions, Cambs, UK). Upon completion of these cycles, Trypsin Gold, Mass Spectrometry Grade (Promega, Madison, USA) in 50 mM

ammonium bicarbonate was added in each well containing dried gel piece and incubated for overnight at 37°C. Next day, 0.1 formic acid was added to stop the trypsinolysis and the elute containing the tryptic digested peptides was collected in MS glass vials, vacuum dried and dissolved in 0.1% formic acid for LC-MS/MS.

2.4.2 Mass spectrometry

LC–MS/MS analysis was performed with an LTQ-Velos mass spectrometer (Thermo Fisher Scientific). Peptide samples were loaded using a nanoACQUITY UPLC (Waters, U.K.) with Symmetry C18 180µm × 20 mm (Waters part number 186006527) trapping column for desalting and then introduced into the mass spectrometer via a Stonearch fused silica capillary column 100µm i.d.; 360µm o.d.; 15 cm length; 5µm C18 particles (Nikkyo Technos CO, Tokyo, Japan part number NTCC 360/100-5-153) and a nanoelectrospray ion source at a flow rate at 0.42µL/min. The mobile phase comprised H_2O with 0.1% formic acid (buffer A) and 100% acetonitrile with 0.1% formic acid (buffer B). The gradient ranged from 5% to 30% buffer B in 95 min followed by 30% to 60% B in 15 min and a step gradient to 85% B for 5 min with a flow of 0.42µL/min, finally a return to the initial conditions of 5%B. The full scan precursor MS spectra (400–1600 *m*/*z*) were acquired in full profile with the Velos-Orbitrap analyzer with a resolution of $r = 60{,}000$. This was followed by data dependent MS/MS fragmentation in centroid mode of the most intense ion from the survey scan using collision induced dissociation (CID) in the linear ion trap: normalized collision energy 35%; activation Q 0.25; electrospray voltage 1.5kV; capillary temperature 200°C; and isolation width 2.00. This MS/MS scan event was repeated for the top 20 peaks in the MS survey scan, the targeted ions were then dynamically excluded for 30s. Singly charged ions were excluded from the MS/MS analysis and Xcalibur software version 2.1.0 SP1 build 1160 (Thermo Fisher Scientific, U.K.) was used for data acquisition.

2.5 Protein identification and quantification

For the samples prepared under the biological perturbation of E2, raw MS files from the three technical replicates for SILAC total, nucleus, and cytoplasm experiments were automatically assembled by MaxQuant (version 1.3.0.5) and visualized by Perseus (version 1.3.0.4) software platforms. A matrix of SILAC ratios with rows corresponding to proteins and columns to different 'samples' or 'conditions' was automatically assembled by MaxQuant software and cross-experiment protein ratios were successfully compared for the quantification of SILAC pairs, identification of individual peptides, and assembly into protein groups (Cox and Mann, 2008, Cox et al., 2009). The derived peak list generated by Quant.exe (the first part of MaxQuant) was searched using the Andromeda search engine against human FASTA files (HUMAN.fasta.gz) obtained from the UNIPROT website: (ftp://ftp.uniprot.org/pub/databases/uniprot/current_release/knowledgebase/proteomes, last modified 5/10/2012.

For the samples prepared under the biological perturbation of 4-OHT, peptides and proteins were identified and quantified using the MaxQuant software package (version 1.5.2.8) with the integrated Andromeda search engine against human FASTA files obtained from the UNIPROT website: (ftp://ftp.uniprot.org/pub/databases/uniprot/current_release/knowledgebase/proteomes, last modified 04-12-2014) and the Perseus (version 1.5.1.6) to statistically visualize the obtained data. The following section describes the settings that were selected, for old version and new version software, for SILAC identification and quantifications.

The processed raw files from the three technical replicates of each SILAC labelled protein fractions (total, nuclear, and cytoplasmic) generated tables containing the MaxQuant parameters, information of the raw file contents, and statistics on the peak detection. The

protein and peptides tables contained the information on the reconstructed proteins from the identified peptides in the processed raw files.

MaxQuant parameters for two-state SILAC included multiplicity of 2 for the labelling with lys0/arg0 as light and lys6/arg10 as heavy proteins. The maximum number of labelled amino acids that a peptide can have is 3, and 2 maximally tolerated missed cleavages, uploaded protein sequences that are digested in silico (human FASTA files) was used in the Andromeda search, carbamidomethyl Cys as a fixed modification, revert decoy mode. Identification parameters included a value of 0.01 as the desired false discovery rate (1% FDR) at the peptide and protein match level, which the minimum peptide length is 6 amino acids. In addition to imposing the desired FDR to consider the protein group identification in the final table, a value of 1 was selected as the minimum required of total peptides, including razor and unique peptides, and a minimal Andromeda score of 0 and 40 for accepting unmodified and modified peptides, respectively. The set of protein quantification parameters were selected at a minimal ratio count of 2, using unique and razor peptides to calculate the protein ratios, and only peptides contained specific modifications (Acetyl protein (N-term) and Oxidation (M)) that were used in addition to unmodified peptides.

2.5.1 Correlation and quantisation of proteins across samples.

2.5.1.1 E2

The MaxQuant software package was used to identify and quantify proteins for 16 analysis sets: (a) each nucleus (N) sample replicate and the union of the three N samples, (b) each cytoplasm (C) sample replicate and the union of the three C samples, (c) each total (T) sample and the union of the three T samples, and, (d) each C&N replicate and the union of the three C&N samples. C&N denotes that for each individual replicate, the MS data for the C and N samples were jointly processed with MaxQuant to estimate changes in total protein abundance. For this data, a correction for enrichment of nuclear proteins in the MS data collection was applied during estimation of total protein abundance. Across all samples, a total of 4386 different proteins were identified by sequenced peptides. Of these, 110 corresponded to 55 proteins with multiple isoforms from the same gene that could not be unambiguously resolved across all replicates of the three sample types and were not further analysed for present purposes.

2.5.1.2 4-OHT

A schematic diagram (Figure 3-13) is showing the number of output datasets that are used in this study and summarized the data sets that were generated by MaxQuant with the identified and quantified proteins from the peptide sequencing MS raw files. Three individual replicates for each sample type cytoplasm (C1, C2, C3), Nucleus (N1, N2, N3), and total lysate (T1, T2, T3) were processed before merging the replicates in the denoted UNION dataset. The three replicates of each fraction were merged and processed in MaxQuant to correlate the distinct protein sequence groups and identify the total number for the union of

consensus protein groups across the union data set for the three replicates of each fraction (C-UNION, N-UNION, T-UNION).

2.5.2 Selection of the most significantly changed proteins and bioinformatics:

Two data sets were obtained as the most significant changes proteins obtained from the merged final dataset of the three sample types (CNT) of the 3493 proteins quantified under 4-OHT stimulation, as follows:

2.5.2.1 The extended significance set (overall response) (Tam-270):

For which proteins were selected as differentially expressed proteins (DE) out of a total of proteins with measured expression in the merged union of each sample type (CNT) (Supplementary Table 7). These were obtained using a threshold of 0.05 for statistical significance adjusted p-value (Sig. B) and ±1 for absolute log2 fold expression change. To reduce the impact of the relaxed selection criteria, applied to obtain the Tam-270 significant set, on the downstream bioinformatics, two stringent criteria were applied using Advaita Bio's iPathwayGuide (http://www.advaitabio.com/ipathwayguide): (1) Scoring the pathways based on the impact analysis as described in (Draghici et al., 2007, Tarca et al., 2009). Two types of evidence (p-value) were combined in a unique global p-value in this type of analysis: i) the over-representation analysis (pOVR) verses ii) the perturbation across the pathway topology that propagated by DE genes/proteins upstream or downstream a given pathway. This p-value is then corrected for multiple comparisons using FDR to ensure that the overall percentage of false positives is below the chosen threshold (<0.05) (Benjamini and Hochberg, 1995). These data were analyzed in the

context of pathways obtained from the Kyoto Encyclopedia of Genes and Genomes (KEGG) database (Release 73.0+/03-16, Mar 15) (Kanehisa and Goto, 2000, Kanehisa et al., 2002). The pathway topologies, comprised of genes and their interactions, are obtained from the KEGG database (Kanehisa and Goto, 2000, Kanehisa et al., 2010, Kanehisa et al., 2012, Kanehisa et al., 2014).

(2) For Gene (GO) annotation enrichment analysis (Ashburner et al., 2002; Gene Ontology Consortium, 2004), iPathwayGuide uses the classical over-representation approach to compute the statistical significance followed by corrected p-value using the elim method proposed by Alexa et al. (Alexa et al., 2006) to remove the genes mapped to a significant GO term from more general (higher level) GO terms. These data were analyzed in the context of gene ontology obtained from the Gene Ontology Consortium database (2014-Sep19) (Ashburner et al., 2000, Gene Ontology Consortium, 2001).

2.5.2.2 Core significance set (reliable/specific response) (Tam-97):

All proteins in the CNT dataset were considered as low confidence proteins if they were identified by only one peptide; therefore, the dataset was filtered by “sort” function to remove the entries for proteins lacking more than one peptide. Overall, only proteins identified by at least two peptides (one unique) were considered in the next step of selection. Hence, some of the remaining proteins were quantified with at least two SILAC ratio counts, and the list of proteins was further reduced by imposing another filtration criterion of a minimum three SILAC ratio counts for the reliable quantification of the identified protein. Based on adjusted P-value below 0.05 (Sig B) and log2 fold changes above 1 or below -1,

both up-regulated and down-regulated proteins were obtained and used for the downstream bioinformatics/validation. Of the 916 proteins selected from the correlation data set (CNT) according to the above mentioned criteria, a set of 97 proteins are showing the most significant changes, the distribution scores of significance over the CNT are shown in figure (Figure 3-16) and summarized in Table (Table 3-4). In this data set, 51 proteins were selected as DE expressed out of a total of 97 proteins with measured expression in the cytoplasmic fraction (S_c), 51 proteins out of 97 in the nuclear fraction (S_n), and 29 proteins out of 97 in the total lysate (St). Using InnateDB database (Breuer et al., 2013, Lynn et al., 2008), these data were analysed in the context of pathways incorporated in InnateDB database from major public databases including KEGG, Reactome, NetPath, INOH, BioCarta, and PID and these data were not restricted to immune relevant databases. Hence, we applied a stringent selection criteria to obtain this list of DE proteins, and we conducted the downstream analysis to obtain the pathways significantly overrepresented and GO terms significantly enriched based on uncorrected p-values.

2.6 Confocal microscopy

2.6.1 Effect of E2 using fluorescence imaging of live cells

MCF-7 cells were grown in DMEM-F12 medium on a 35 mm imaging dish with a glass bottom (WillCo-dish® "Series GWSt-3512", WillCo Wells, Amsterdam, Netherlands). Upon reaching 60% confluence, the cells were washed with PBS and incubated for 48 h with DMEM-F12 phenol red-free medium supplemented with 10% charcoal treated FBS and medium was changed every 24 h before E2 stimulation. At 48 h, cells were divided into two parts, non-stimulated (control) and stimulated with 10 nM E2 for further 24 h. After 24 h post-oestrogen stimulation, cells were washed twice in 1x PBS+ (137 mM NaCl, 2.7 mM KCl, 10 mM Na2HPO4 x 2H2O, 1.8 mM KH2PO4, 1mM CaCl2, 0.5mM MgCl2 x 6H2O at pH 7.4). For mitochondrial labelling, each dish of treated and untreated cells was incubated for 30 min with 20 nM, 100 nM, and 200 nM of MitoTracker Green (M7514 from Life Technology) in PBS+ buffer at 37°C, 5% CO2. Before respective nuclear labelling, cells were washed twice with PBS+ buffer and then incubated with 1 µg/ml Hoechst 33342 nuclear probe (R37605 from Life Technology), in dark at room temperature, for 30 further min. Prior to imaging, each dish was washed three times with PBS+ buffer, each wash followed by incubation for five minutes at 37°C in 5% CO2. After the final wash, HEPES containing phenol red and serum free medium was added to each dish to maintain cells alive during confocal imaging. Mitochondria and nucleus were visualized by Perkin Elmer Ultraview Vox spinning disc confocal microscope equipped with ×63 Plan Apo (NA 1.4) oil immersion objective using fluorescence excitation (Ex) and emission (Em) of (490/516nm) and (353/483nm), respectively.

2.6.2 Effects of 4-OHT using fixed cell fluorescence staining

To observe the changes in the cellular morphology in the treated and non-treated cells, the cellular (nuclear membrane(s), mitochondria, fibres, and nucleoli) and nuclear staining was combined using the Chromeo Red Fluorescent Fixed Cell Staining Kit (Active Motif Europe). Cells were grown to the desired confluence in DMEM-F12 medium on coverslips (#1.5 thickness, 13 mm diameter) inside a 24-well plate. The phenol red containing medium was aspirated off and replaced with a fresh phenol free DMEM/F12 supplemented with 10% charcoal treated FBS for 48 h at 37°C in a humidified incubator of 5% CO2, with the culture medium replaced every 24 h. The control cells were treated with ethanol (vehicle) and the treated cells with 1 µM 4-OHT and incubated further for 24 h at 10 min at 37°/5% CO2. Both control and treated cells were washed with cold PBS and fixed by adding 100% ethanol and the 24-well plate was placed at -20°C for 20 min (manufacturer's instructions). The fixed cells were washed twice with PBS and incubated with 1 µM of diluted cell stain solution in PBS at room temperature (protected from light) for 30 min. The stained cells on the coverslips were mounted on glass slides using MAXflour DAPI Mounting Medium and the coverslips were sealed with nail polish prior to imaging. The images were obtained using Confocal Laser Scanning Module LSM 510 with ×63 oil immersion objective and the DAPI stained nuclei was detected using a standard DAPI filter set (370-410 nm/435-485 nm). To detect the cellular stain in combination with stained nuclei, the fluorescent spectra were separated using a filter set (550-580 nm/590-650 nm).

2.6.3 Immunofluorescence validation

2.6.3.1 Subcellular localization of proteins under E2 stimulation

Cells were grown in DMEM-F12 medium on glass cover slips (#1.5 thickness, 13 mm diameter) and treated as described in the live cell fluorescence microscopy section. Control (no E2 starvation/stimulation), unstimulated, and stimulated cells were then fixed in 4% paraformaldehyde for 10 minutes and permeabilized with a fresh 0.3 % Triton X-100 solution in PBS for 5 min. After blocking with 5% BSA in PBS for 1 hour at room temperature, the stimulated and unstimulated cells were both incubated overnight at 4 °`C with primary Anti-Rabbit antibodies to NQO1 (ab34173, Abcam) and PARK7/DJ1 (ab76008, Abcam) diluted in 1% BSA in PBS according to the manufacturer's specifications. Secondary antibody (green) incubation was performed for 2 h at room temperature in the dark using goat Anti-Rabbit IgG H&L (DyLight 488) antibody (ab96899, abcam) diluted 1/250 in 1% BSA/PBS. Control coverslips were divided into two parts: a control-A labelled coverslip was incubated only with secondary antibody, while the control-B coverslip with both anti-PARK7/DJ1 and secondary antibodies. All coverslips were then stained with 1.43 µM of DAPI (D3571, Invitrogen) and incubated for 5 min at room temperature in the dark. In all procedures, every step was followed by washing with PBS for three times. Finally, cover slips were mounted with the Dako Fluorescent Mounting Medium. The immunofluorescence images were obtained with a Perkin Elmer Ultraview Vox spinning disc confocal microscope equipped with ×63 Plan Apo (NA 1.4) oil immersion objective and nuclei were visualised using Ex of 358 nm and Em of 461 nm.

2.6.3.2 Subcellular localization of proteins under 4-OHT stimulation

MCF-7 cells were seeded on coverslips (#1.5 thickness, 13 mm diameter) inside 24-well plate grown under the same growth condition described in the florescence staining section. The cells were exposed to a dose of 1 µM 4-OHT (stimulated cells) and were vehicle treated (non-stimulated control) for 24 hr prior to fixation and immunolabelling. At room temperature, the cells were fixed on coverslips in 4% (w/v) paraformaldehyde for 10 min, permeabilized with 0.3 % Triton X-100 detergent for 5 min at room temperature, and blocked with 5% BSA in PBS for 1 hour. The stimulated and non-stimulated cells were incubated with with primary Anti-Rabbit antibodies to MTCO2 antibody (ab79393, 5µg/ml) and CASPASE-14 (ab174847, 1/250) overnight at 4°C. Next day, a further 1 h incubation at room temperature was conducted with goat polyclonal secondary antibody to rabbit IgG - H&L (Green DyLight® 488), pre-adsorbed (ab96899) at 1/1000 dilution for primary anti-MTCO2 antibody and 1/250 for primary anti-CASPASE antibody. The unspecific binding was assessed by incubating the cells with only secondary antibody at 1/1000 and 1/250 dilutions for 1 h at room temperature. DAPI (D3571, Invitrogen) (Excitation/Emission (nm) 358/461) was used at 1.43 µM concentration to stain the nuclei of fixed cells for 5 min in dark at room temperature. Prior to imaging with Confocal Laser Scanning Module LSM 510 (×63 oil immersion objective), coverslips were mounted on glass slides using Vectashield antifade mounting medium (Vector Labs, H-1000) and sealed with nail polish.

Chapter 3 Results

3.1 Part-I: Systematic Nucleo-Cytoplasmic Trafficking of Proteins Following Exposure of MCF-7 Breast Cancer Cells to Oestradiol

Despite scientific progress in diagnosis and treatment, breast cancer continues to be one of the main causes of death in women. Excluding hereditary predispositions to the onset of this disease, reproductive aspects, such as early menarche and late menopause or an advanced age at the first pregnancy, or behavioral aspects, such as the increased use of hormone replacement therapy, are factors positively correlated to a higher risk of breast cancer occurrence, and all of these factors involve a more prolonged exposure to sex hormones, primarily estrogens (Colditz, 1998, Henderson and Bernstein, 1991). Extended exposure to exogenous or endogenous damaging agents causes an accumulation of irreversible abnormalities in the genome and epigenome that reprogram the cell to accelerate growth and to inhibit its death. Many investigations at the cellular level have been based on measuring gene expression of breast cancer cells using transcriptomic and molecular biology techniques. There are imperative reasons (Chen and Yates, 2007, Laronga and Drake, 2007) to supplement this research with high quality as well as quantity output proteomics strategies (high throughput) to leverage automation to acquire inside and out comprehension of the miniscule premise of malignancy. These incorporate that protein abundance might be not quite the same as transcript plenitude and that for genetic variation, translation and protein stability might be more determinants for protein abundance than transcript levels (Foss et al., 2011). Additionally, as an extremely complex disease, tumour cells incorporate a very complex protein networks to induce the capacity of tumour progress and that requires continuous fine-tuning to this networks through post-translational alterations, for example, phosphorylation (Shaw and Cantley, 2012) and methylation/acetylation.(Dumitrescu, 2012, Liu et al., 2012). A rising theme is that the proteins are not anchored to one single cellular

location, and therfore, subcellular dispersion of proteins (Henke et al., 2011, Mulvey et al., 2013) and other molecules such as tRNA(Chu and Hopper, 2013) is dynamic and context-dependent and that proteins may have different functional roles at different subcellular locations (He et al., 2012, Sirover, 2012, Tristan et al., 2011). For MCF-7 (Michigan Cancer Foundation–7) cells, no less than 50% and possibly as much as 75 % of proteins have been exhibited to have numerous subcellular locations (Qattan et al., 2010). About 1000 proteins have been appeared to be available in both the nucleus and mitochondria of MCF-7 cells and a large number of these proteins are known to have distinctive functions in the two subcellular locations (Qattan et al., 2012). Massive spatio-temporal distribution of proteins is a process by which cells response to an assortment of factors including environmental stress, cell-cycle signals, development components, and hormone exposure (Sorokin et al., 2007). The importance of nucleo-cytoplasmic trafficking of BRCA1 in hereditary forms of breast cancer (Thompson, 2010) is well-known. Given these emerging themes, the present work presents a high throughput proteomics study of the redistribution of proteins between the nuclear and cytoplasmic compartments of MCF-7 breast cancer cells when exposed to estradiol.

Effects of treatment of estradiol stimulated breast cancer cell line, particularly its active metabolite E2 (17β-estradiol), are extensively researched in order to elucidate the underlying mechanisms of carcinogenesis. The solitary stimulation of E2 persuaded propagation of serum-starved MCF-7 cells, E2 induced mitogenic response which contributed to the MCF-7 straining (Hamelers et al., 2003).). In addition, the stimulation of cells with E2 is evident to induce propagation of MCF-7 cells, as well as to initiate apoptosis in MCF-7:5C cells (Hu et al., 2011). The role of oestrogen as the potent at proliferation stimulation of the receptive cells; it is also openly proliferate the consumption of glucose and indirectly stimulate the rate of glycolysis by direct upregulation of regulating glucose transporter 1 expression

(GLUT1) (Rivenzon-Segal et al., 2003) or of the catalytic activity of glyceraldehyde-3-phosphatedehydrogenase(GAPDH) (Joe and Ramirez, 2001). However, the proteomics technologies have been used to detect the over-expression of fructose-1,6-bisphosphatases FBP2 and FBP1, glycolytic enzymes, and oestrogen-regulated proteins, for example TFRC, TPD52L1, GREB1, TFF1, and PGR in MCF-7 cells stimulated with10 nM E2 (Drabovich et al., 2012).

The intracellular biological influences of E2 are mediated via interaction with ER, particularly, the classical ERαβ receptors (ERs) (Nilsson et al., 2001, Parl, 2000). Upon activation via E2 binding to the ERs, the E2 bound ERs undergo conformational changes leading to the development of the stable receptor dimers and detachment of heat-shock chaperone proteins (Kumar and Chambon, 1988). The ligand-bound ERs modulating the transcriptional activities by recognizing and binding to a specific response sequence (ERE) located at the promotor region of the target genes (Brown and Sharp, 1990). In this manner, activation or suppression of the cellular gene expression regulates wide range of mechanisms through the transcriptional initiation/inhibition of the target genes in the cell-specific and promotional manner (Tora et al., 1989), as well as directly introduce certain cell cycle regulatory genes expression (Cicatiello et al., 1993, Hyder et al., 1995). Moreover, in addition to the transcription influences on the genes, the bound E2 controls ER profusion by significantly reducing the half-life up to three to five hours (Nirmala and Thampan, 1995). Indeed, ER is preferentially ubiquitinated in the presence of E2 and the ER-hormone complex is degraded by a cytoplasmic fraction of the proteasome system (Lonard et al., 2000, Wijayaratne and McDonnell, 2001). Apart from transcriptional activities, ER receptors have other activities in the cytoplasm, mitochondria, and at the plasma membrane suggesting that dynamic subcellular trafficking of ER receptors and other proteins might be essential to

the properties of ER-related functional networks (Echeverria and Picard, 2010, Mavinakere et al., 2012, Renoir, 2012).

Our group has focused on the molecular mechanisms related to the dynamic aspects of protein subcellular dispersion in response to the biological perturbations, therefore, global quantitative proteomics high-throughput technology was consolidated with a model enabling the enrichment of subcellular compartments and estimation of the subcellular proteome changes against total changes (Mulvey et al., 2013). Such methodology has permitted estimation of the changes in total abundance and in the compartmental plenitude/dissemination between the nucleus and cytoplasm for a few thousand proteins DE in E2-stimulated MCF-7 cells. A Corollary improvement of a "subcellular spatial razor" model of the dynamic redistribution of proteins has significantly helped to overcome the difficulties of interpretation of big datasets generated by the combined metabolic labelling of stable isotope amino acids in cell culture (SILAC) and high resolving power of mass spectrometry.

The present results demonstrate that as an outcome of estradiol incitement of MCF-7 cells, massive numbers of proteins redistributed between the nucleus and cytoplasm and that many of those proteins show apparent changes in compartmental abundance than in absolute protein abundance, suggesting that dynamic changes in the subcellular distribution of proteins after E2 stimulation is the fundamental response of MCF-7. Furthermore, spatial and temporal changes in localizations of the compartmental proteins may be regulated predominantly by the ER and other nuclear receptors that are driving the response and responding to the spatially distributed functional networks of proteins. Additionally, the strong perturbation of subcellular spatial regulation may be a crucial feature of breast cancer.

3.1.1 Results

The proteomics subcellular spatial razor experiments described in the following are based on a model which envisages that in response to a cellular perturbation, proteins may show both changes in total cellular abundance and in their subcellular spatial distribution between the nucleus and cytoplasm (Figure 1-8). Experimental measurements of protein abundance ratios (SILAC ratios) between stimulated/unstimulated cells are made on three samples: (1) an unfractionated, total cell lysate (T), (2) a nucleus-enriched sample obtained by subcellular fractionation (N), and (3) the corresponding nucleus-depleted sample (C), which we refer to as the "cytoplasm" in the following. The corresponding SILAC ratios provide measures for each protein of the overall change in total cellular abundance (S_t), or of the localized change in abundance in the nuclear (S_n) or cytoplasmic (S_c) subcellular compartments. A mathematical formulation of the model is given in the introduction (see sction 1.4.2). Stringent purification of organelles (e.g., nucleus) was not attempted in this study as we believe it is not feasible to purify to homogeneity organelles that are subject to dynamic changes in their protein content and that unnecessary protein loss is incurred during such organelle isolation methods. We preferred to use highly enriched fractions rather than highly purified organelles. This is a strategy that has previously been shown to successfully detect nucleo-cytoplasmic trafficking and characterized in detail samples obtained with the present subcellular fractionation protocols (Qattan et al., 2012), including extensive evidence that the nuclear-enriched fraction contains very little if any contamination with other cytoplasmic components such as mitochondria, endoplasmic reticulum, Golgi apparatus, etc. As routine controls for the present preparations, we checked the morphology of stimulated/unstimulated cells using fluorescence imaging to verify the morphological changes associted with stimulation in live cells and checked the purity of the nuclear/cytoplasmic fractions using Western blotting (see below). For each sample type, we measured three replicates. Across all

samples, a total of 4386 different proteins were identified by sequenced peptides. Of these, 110 corresponded to 55 proteins with multiple isoforms from the same gene that could not be unambiguously resolved across all replicates of the three sample types and were not further analysed for present purposes. Supplementary Table 1 contains the full experimental data for the remaining 4276 proteins. For quantitative analysis of the distribution of the subcellular abundance of these proteins, we imposed the conservative limits that at least two different sequenced peptides (1 unique) and at least 3 SILAC ratio counts in a single sample replicate were required. This gave 3604 quantified, reliably identified proteins, with the subcellular distribution shown in Figure 3-3, that were used in the analyses described below.

3.1.1.1 Reproducibility of the sample preparation procedures

As shown in Figure 3-1, the proteins chosen as potential organelle markers (mitochondria: VDAC and nucleus: Histone H3) confirm the enrichment capacity of the preparation procedures. They were observed in the expected subcellular locations: VDAC was detected in the total lysate and cytoplasmic fraction while Histone H3 was observed in both the total lysate and nucleus fractions, respectively, but not in the cytoplasmic (nuclear depleted) fraction. Overall, results of the WB experiment are consistent with highly enriched fractionation rather than highly purified, and that is what we aimed to achieve, in the current stage, to avoid loss of protein during purifications, this is a strategy that has previously been shown to successfully detect nucleo-cytoplasmic trafficking (Mulvey et al., 2013).

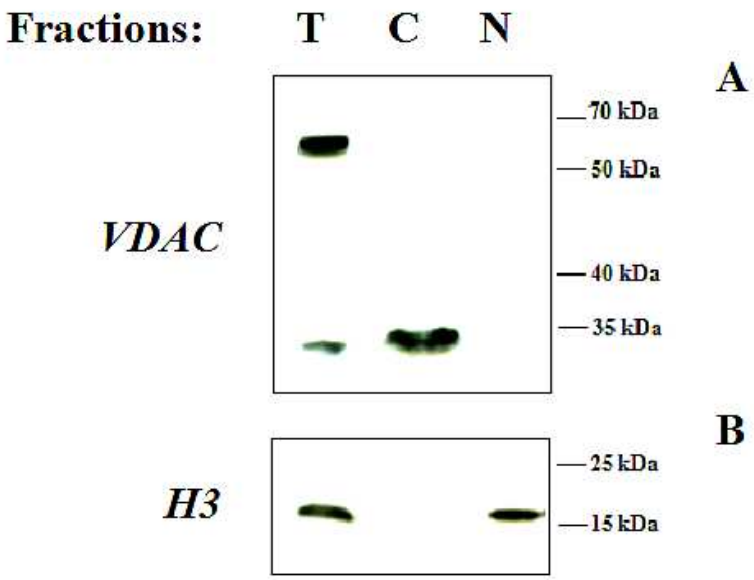

Figure 3-1: Characterization of total lysate (T), cytoplasmic (C), and nuclear (N) fractions of MCF-7 cells.

Immunoblot analysis of the reproducibility of the fractionation procedure using known subcellular markers in the three sample types (TCN). (A) The mitochondrial marker VDAC was found in fractions C and T while the nuclear marker H3 (B) was detected in fractions N and T.

3.1.1.2 Effect of oestradiol on the subcellular morphology

Live cells deprived from E2 (control) had apoptotic activity as visualized by confocal microscope (Figure 3-2.A).Their mitochondria were small and started to disconnect themselves from the perinuclear zone (Figure 3-2.C). After E2 treatment, the majority of nuclei showed absence of apoptotic activity and contained completely dispersed chromatin (Figure 3-2.B), moreover, mitochondrial clustering in a high number around nuclei was observed (Figure 3-2.D). These morphological changes were observed by electron microscope at the physiological relevant concentration of E2 (10 nM) in MCF-7 cells (Vic et al., 1982).

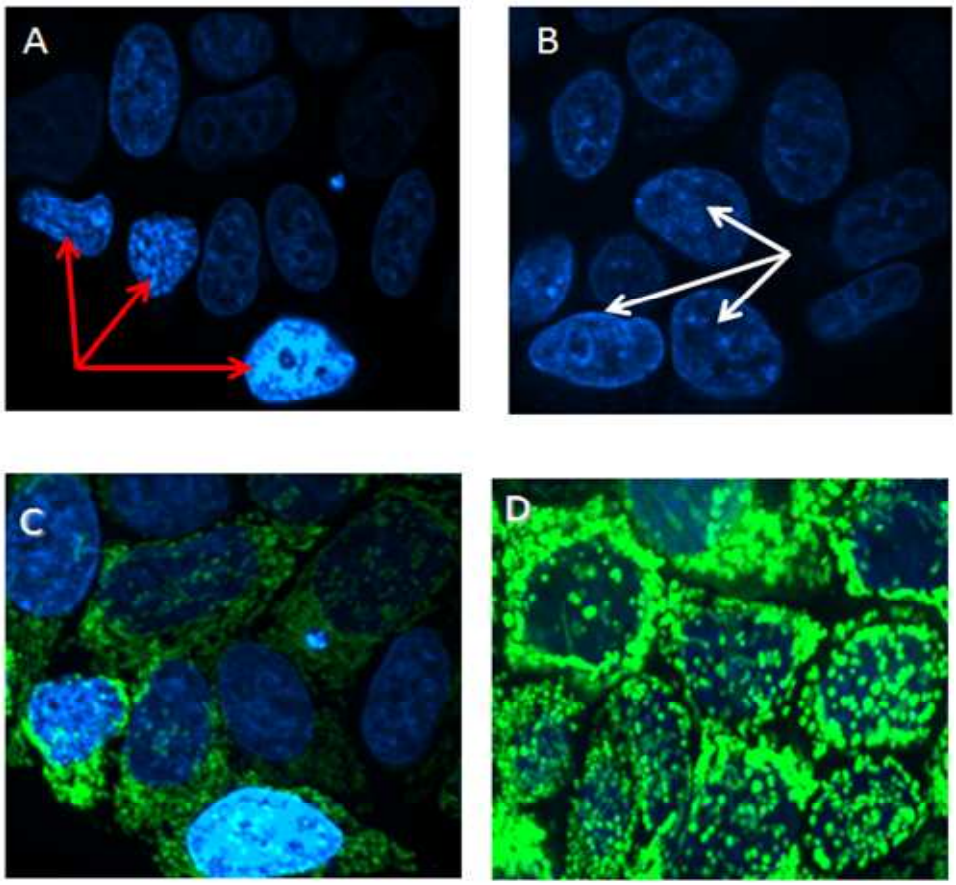

Figure 3-2: Morphological changes in E2-stimulated MCF-7 cells.

Effect of oestradiol (10 nM) on the subcellular morphological changes in live MCF-7 cells stained with 200 nM of MitoTracker Green (mitochondrial fluorophore) and 1 µg/ml Hoechst 33342 (blue nuclear fluorophore) and visualized by fluorescent microscope. (A) Control cells (deprived from E2 for 72 h) with condensed chromatin and fragmented nuclei brighter blue-whitish (red arrows), were reported as apoptotic cells. E2-treated cells (B) uniformly stained blue with evenly distributed chromatin (white arrows), with normal and round nucleus, and were scored as non-apoptotic cells. (C) Control cells (starved from E2 for 72 h) show small size and small number of mitochondria in the perinuclear area compared with E2 treated cells (D) where high number of large and clear mitochondria are clustered in the perinuclear space.

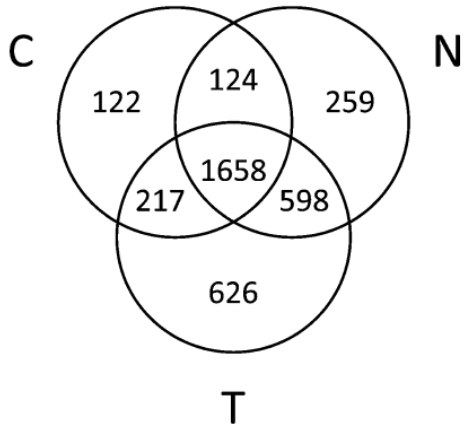

Figure 3-3: Venn diagram of the distribution over sample types for proteins quantified with ≥3 SILAC ratio counts in each sample.

3.1.1.3 Changes in abundance in the nuclear and cytoplasmic compartments

The overall changes in abundance for the proteins are shown in Fig. 3.4. For 2809 total lysate (T) proteins with ≥ 5 SILAC ratio counts across the three replicates (median of 39 counts per protein), only 7 T proteins (0.2%) showed greater than 4-fold increase/decrease in abundance and only 64 T proteins (2.3%) showed greater than 2-fold increase/decrease in abundance in response to estradiol exposure (Figure 3-4A). To check for possible distortion of the distribution profile by lower abundance proteins and/or by variation between replicates, these results were compared with a smaller set of 2197 more abundant proteins for which the lower limit was set to ≥ 3 SILAC ratio counts in all three T replicates (median of 62 counts per protein, (Figure 3-4B). The profile for the distribution of the SILAC ratio S_t for total cellular proteins was hardly changed, which indicates that it is a reliable indicator of total cellular abundance changes.

In the nuclear compartment, very different behaviour was observed (Figure 3-4A). For 1791 nuclear proteins with ≥ 5 SILAC ratio counts across the three replicates (median of 22 counts per protein), only 2 proteins (0.2%) showed greater than 2-fold increase in nuclear abundance. However, 109 proteins (6.1%) showed greater than 4-fold decrease and 560 proteins (31.3%) showed greater than 2-fold decrease in nuclear abundance. For 1064 more abundant nuclear proteins with ≥ 3 SILAC ratio counts in all three N replicates (median of 49 counts per protein), a similar distribution profile for the SILAC ratio S_n for nuclear proteins indicated that lower abundance proteins and/or variation between replicates had little effect on the observed distribution (Figure 3-4B).

For cytoplasmic proteins, largely inverse changes were observed. For 1758 cytoplasmic proteins with ≥ 5 SILAC ratio counts across the three replicates (median of 39 counts per protein), 21 (1.2%)/130 (7.4%) of proteins showed greater than 4-fold/2-fold decreases in cytoplasmic abundance, but 65 (3.7%)/407 (23.2%) of the proteins showed greater than 4-fold/2-fold increases in cytoplasmic abundance. Exclusion of lower abundance proteins by requiring ≥ 3 SILAC ratio counts in all C replicates (median of 54 counts per protein) caused only very modest change in the distribution profile for the SILAC ratio S_c for cytoplasmic protein abundance (Figure 3-4B).

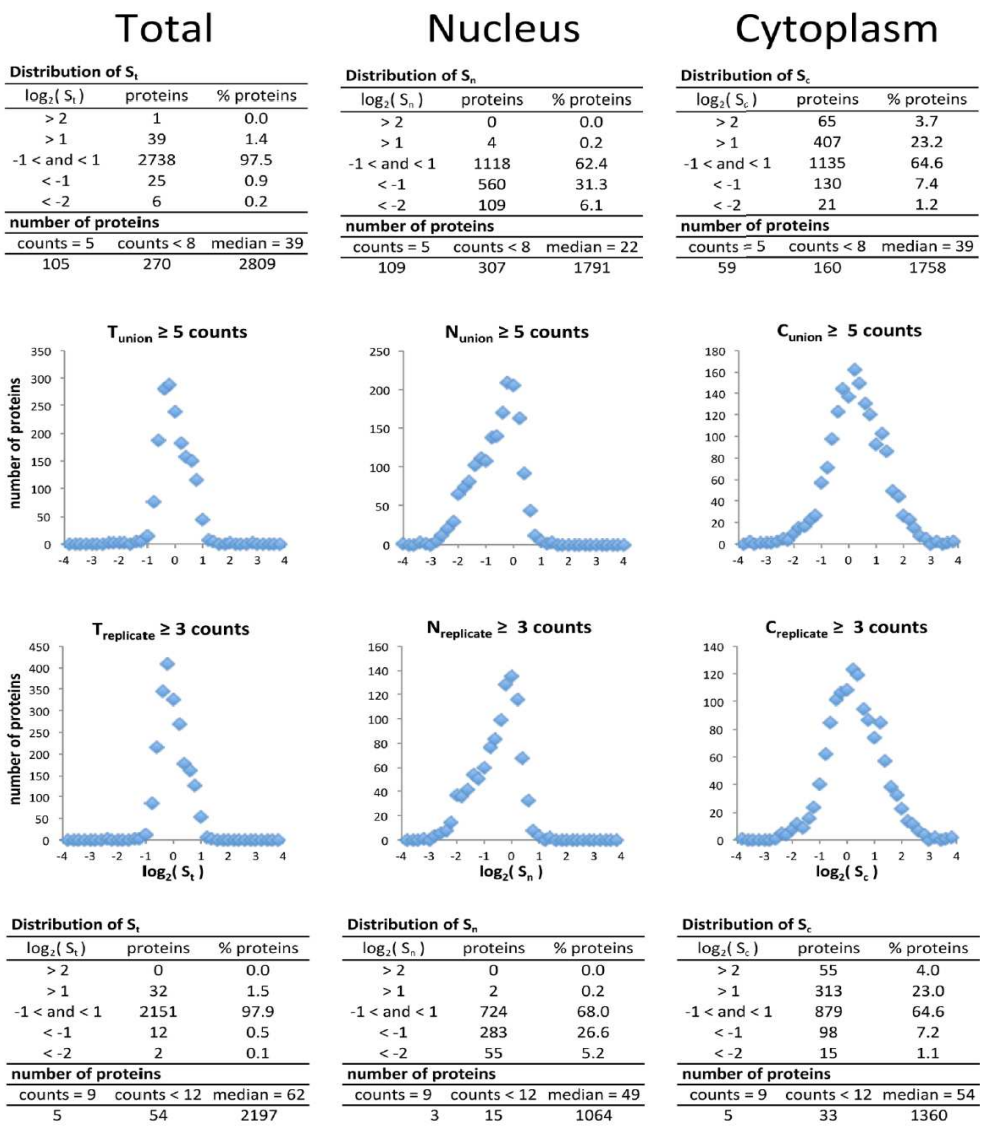

Figure 3-4: Distribution of SILAC ratios for proteins from the total lysate (S_t), nuclear (S_n) and cytoplasmic (S_c) samples.

(A) All proteins with ≥ 5 ratio counts for the union of the three replicates for each sample type. (B) All proteins with ≥ 3 ratio counts for all replicates of each sample type. The inset tables show the number and percentage of proteins that show >4-fold or >2-fold changes in total abundance (S_t), nuclear compartment abundance (S_n) and cytoplasmic compartment abundance (S_c). The tables also show for each distribution the total number of proteins included, the median number of SILAC ratio counts and the number of proteins with smaller numbers of SILAC ratio counts. Figure was designed by JGZ and published in (Pinto et al., 2014).

3.1.1.4 Coupling between total and compartmental changes in abundance

Because the abundance of a protein in the nucleus/cytoplasm can be altered by changes both in total cellular protein abundance and in distribution between the two compartments, the SILAC ratios S_n and S_c do not directly measure redistribution of a protein between the two compartments. If f_s and f_u denote the fraction of a protein in the nucleus in stimulated/unstimulated cells respectively, then $S_n/S_c = f_s(1-f_u)/f_u(1-f_s)$ provides a direct measure for redistribution to/from the nucleus (see section 1.4.2). We directly tested for correlation between total and compartmental changes in abundance by plotting S_n/S_c vs S_t for 724 abundant proteins that had ≥ 3 SILAC ratio counts for all three C, N and T replicates (median of 307 counts per protein, (Figure 3-5A). 424 proteins showed $|\log_2(S_n/S_c)| > 1$ and/or $|\log_2(S_t)| > 1$. However, there was no apparent correlation between overall changes in abundance (S_t) and changes in subcellular distribution (S_n/S_c), that is, the abundance changes in the nuclear and cytoplasmic compartments do not simply mirror changes in total abundance. It should be noted that the distribution profiles for S_t and S_n/S_c show good reproducibility over the three biological replicates (Figure 3-5, B&C), although there is some scatter for major changes in distribution, i.e. $\log_2(S_n/S_c) \lesssim -2$ (see below).

The strong skewing of $\log_2(S_n/S_c)$ to negative values (Figure 3-5C) reflects predominant N ➔ C subcellular redistribution. To further characterize the nature of the redistribution for individual proteins, we used the full 3D model of the subcellular spatial razor. For the 3D space of measured parameters $\{S_n, S_c, S_t\}$, the orthogonal basis set $\{S_c/S_t, S_n/S_t, S_t\}$ separates an axis with changes in total protein abundance (S_t) from a plane (S_c/S_t, S_n/S_t) that depends only on the redistribution of a protein between the nucleus and cytoplasm. Figure 3-6B, shows that in the distribution plane, the data points are constrained by conservation of mass (no differential protein losses between stimulated/unstimulated samples during subcellular fractionation or MS sample preparation) to lie in 2 quadrants that correspond to N ➔ C or N ➔ C redistribution of the protein respectively. Figure 3-6A,C shows typical behaviour for 6 proteins from Figure 3-5A. In the 3D space (Figure 3-6C), the changes in total abundance, perpendicular to the distribution plane, have been color-coded for the average over the 3 replicates. The locations of the data points in the distribution plane (Figure 3-6C) are sensitive to the basal nucleus/cytoplasm distribution of the protein in unstimulated cells. For example, NHP2L1 corresponds to a protein with an abundance distribution strongly skewed to the nucleus. Upon stimulation the nuclear/total abundance is hardly changed ($\log_2(S_n) \sim \log_2(S_t) \sim 0.03$), but the small fraction of the protein in the cytoplasm is increased 6-fold. This might be the behaviour of a protein involved in transmission from the nucleus to the cytoplasm of information about cellular state. Conversely, upon exposure to estradiol the abundance of CASP14 decreased 3-fold, with little or no change in subcellular distribution. ERP29, AGR3 and EZR represent proteins with strong basal distribution to the cytoplasm. ERP29 and AGR3 both show 2-fold increases in total abundance, accompanied by enhanced depletion of the protein in the nucleus. These might be proteins that transmit information about cellular state from the cytoplasm to the nucleus, or this might even reflect negative regulation of their own abundance. EZR shows a moderate decrease in abundance (S_t =

0.71), but this is preferentially in the cytoplasm and leads to a 2-fold increase in the fraction of the protein in the nucleus. Finally, SUB1 (PC4) represents a protein with very little change in total abundance (S_t=1.02), but substantial, coupled changes in abundance in the two compartments (S_n = 1.56, S_c= 0.48). Note that in the 3D space the distribution plane is sensitive to changes in the fractional abundance in both subcellular locations; even where this might, for example, represent an increase/decrease in the nucleus for a trace fraction of the total protein if the protein has a basal abundance strongly skewed to the cytoplasm (see Discussion). There is some scatter between the replicates (Figure 3-6). This together with the inherent precision of the SILAC measurements, especially of the ratios S_n/S_t or S_c/S_t for proteins with basal abundances strongly skewed to one location, can lead to minor apparent violations of conservation of mass and contributes to the scatter in (Figure 3-5C) for $\log_2(S_n/S_c) \lesssim -2$. However, in most cases the overall behaviour of the proteins could be clearly ascertained.

There were appreciable numbers of proteins for which no substantial change in either abundance or subcellular location was detected (bounding box in Figure 3-6A), i.e. the effects of estradiol exposure seem to be selective. Only a handful of proteins showed appreciable changes in total abundance without changes in subcellular distribution (Figure 3-5A). Overall there was very little correlation between changes in total protein abundance and changes in protein abundance in the two subcellular compartments. For some individual proteins, initially counterintuitive results were detectable, e.g. AGR3 increases in total abundance but decreases in abundance in the nucleus (Figure 3-6C).

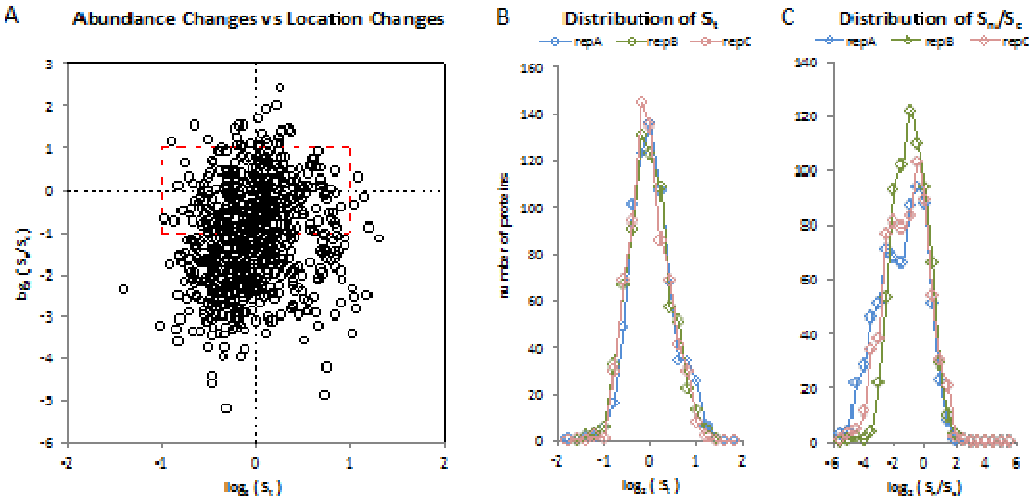

Figure 3-5: Evaluation of the correlation between changes in total abundance and redistribution of abundance between the nucleus and cytoplasm.

(A) Plot of the redistribution parameter (S_n/S_c) vs the changes in total abundance (S_t) for the union over the replicates. The red, dashed bounding box corresponds to 2-fold changes. (B) Distribution of St for the three replicates. (C) Distribution of (S_n/S_c) for the three replicates. Figure was designed by JGZ and published in (Pinto et al., 2014).

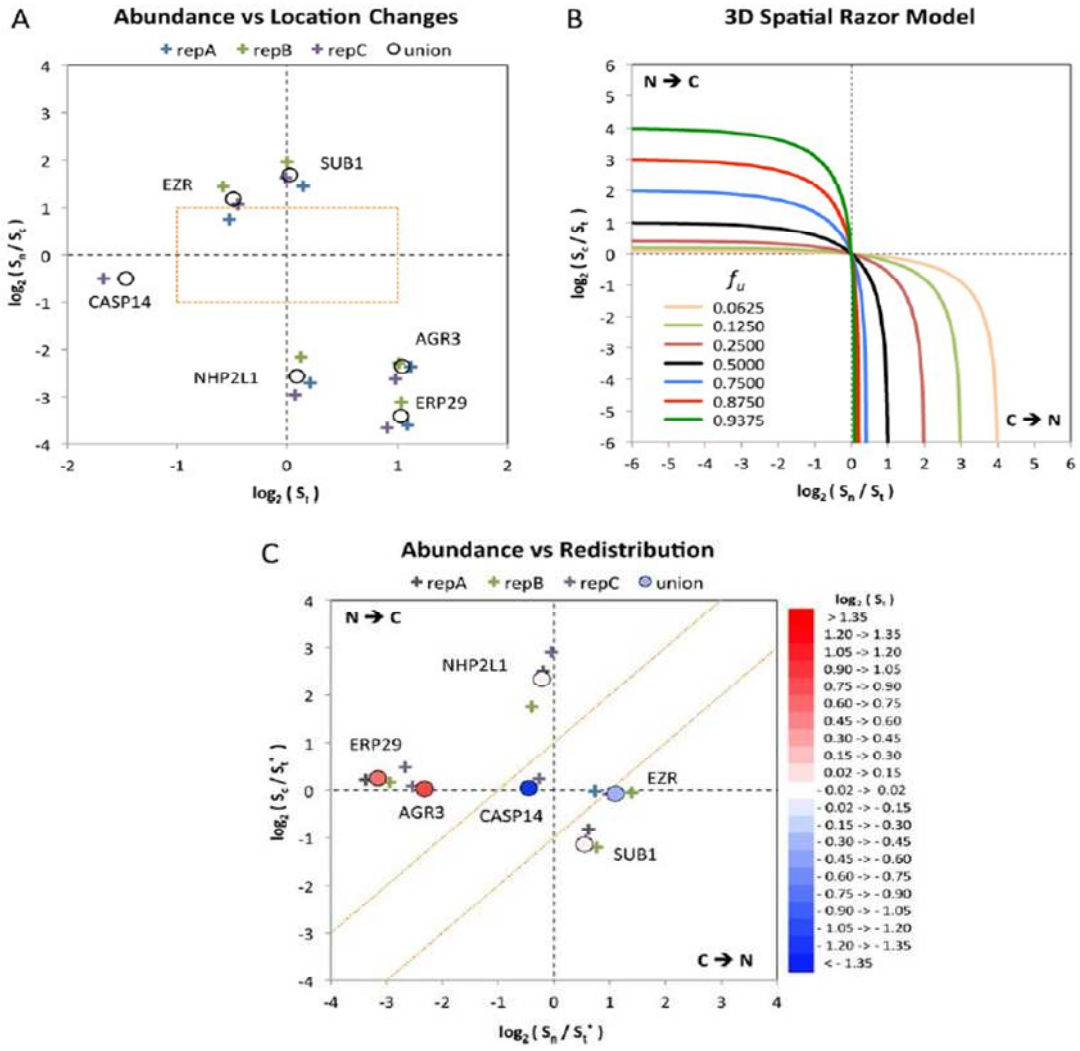

Figure 3-6: Two- and three-dimensional data representations for the subcellular spatial razor.

(A) 2D plot of changes in redistribution between the nucleus and cytoplasm (S_n/S_c) versus total abundance (S_t) for six proteins from Figure 4 showing the experimental scatter. The union is the average over the replicates weighted by the MS intensity recorded for the protein in each replicate. The orange bounding box shows 2-fold changes. (B) For the orthogonal 3D space $\{S_n/S_t, S_c/S_t, S_t\}$, the theoretical distribution plane $\{S_n/S_t, S_c/S_t\}$ for different values of f_u (the fraction of protein in the nucleus in the unstimulated cells) as the fraction of the protein in the nucleus in the stimulated cells (f_s) varies over $0 < f_s < 1$. Conservation of mass restricts the cellular response to two quadrants corresponding to N ➔ C or C ➔ N redistribution of the protein upon stimulation. (C) The six proteins of (A) plotted in the 3D space $\{S_n/S_t, S_c/S_t, S_t\}$. The axis perpendicular to the page is colour coded for changes in total abundance (S_t). The orange bounding lines show 2-fold changes in (S_n/S_c). Figure was designed by JGZ and published in (Pinto et al., 2014).

3.1.1.5 Redistribution of proteins between the nucleus and cytoplasm

We expanded the analysis to proteins that were detected in only one compartment and screened for inadequate MS sampling and/or fractionation artefacts by using the fact that the spatial razor model explicitly includes conservation of mass. This provides a strong framework for screening experimental results for artefacts and obtaining a set of proteins with high confidence changes in compartmental abundance. For example, for proteins present in a single subcellular compartment, changes in abundance in that compartment are necessarily coupled by conservation of mass to changes in total abundance, i.e. $S_n/S_t = 1$ (nucleus) or $S_c/S_t = 1$ (cytoplasm). A similar principle applies to proteins present in both compartments: for ideal sampling and fractionation, joint co-processing of the C and N MS data sets (a C&N data set) should give an apparent change in abundance S_t* such that S_t*/S_t = 1. For the proteins which had at least 3 ratio counts in the appropriate samples and for which the ratio S/S_t could be calculated, all of these ratios showed a Gaussian distribution. Outliers represent proteins for which strict conservation of mass is less reliable due to reduced MS sampling and/or fractionation/extraction artefacts. Of the 3604 proteins in our quantified set, a substantial majority (2597) were detected in more than one sample. However, most such proteins were detected in the CNT subset (1683): only 217/598 proteins were included in the CT/NT subsets and only 160/374 were quantified in both samples. For those single-compartment proteins with good consistency with conservation of mass, the table in Figure 3-7 shows that there were very few proteins with >2-fold changes in abundance. Although the total number of quantified single-compartment proteins is small, the results are consistent with the observation that of 3057 quantified T proteins, only 71 (2.3%) showed >2-fold changes in total abundance.

For the 1363 proteins quantified in all three samples of the CNT data subset, the table in Figure 3-7 shows how the proportion of proteins with appreciable changes in total abundance (S_t), compartmental abundance (S_c, S_n) or redistribution (S_n/S_c) varies with the range of inclusion relative to the center of the Gaussian distribution for S_t^*/S_t. There were no proteins for which the nuclear abundance doubled, only 8 proteins (~1.3%) for which cytoplasmic abundance was halved and only 5 proteins (~1%) for which there was a 2-fold change in total abundance. In contrast, ~14% of cytoplasmic proteins showed doubled abundance and ~30% of nuclear proteins showed halved abundance. About 50% of the proteins showed $|\log_2(S_n/S_c)| > 1$. These percentages were largely independent of the total number of proteins included in the conservation of mass selection range around $S_t^*/S_t = 1$ (Figure 3-7). The behaviour of the individual proteins is shown in Figure 3-7A. Overall, with $|\log_2(S_t^*/S_t)| < 0.5$ the CNT data set included 331 proteins that showed >2-fold change in at least one of the SILAC ratios S_n, S_c, S_t or S_n/S_c. Only 5 proteins showed >2-fold change in S_t and only for CASP14 did the >2-fold decrease in total abundance result in corresponding >2-fold decreases in both the nuclear and cytoplasmic compartments. For the other proteins that showed >2-fold increase/decrease in total abundance (TUFM, AGR3 / BASP1, ACBD3), redistribution resulted in a >2-fold change in only one of the nuclear/cytoplasmic compartments. For 326 proteins there were >2-fold changes in S_n, S_c or S_n/S_c without a >2-fold change in S_t. There were 166 proteins that showed a >2-fold decrease in abundance only in the nucleus, but none that showed a >2-fold increase only in nuclear abundance. There were 83 proteins that showed >2-fold changes in abundance only in the cytoplasm, 77 of which were increased abundance. A >2-fold decrease in abundance in the nucleus coupled with a >2-fold increase in the cytoplasm was detected for 10 proteins. Finally, there were 67 proteins that showed substantial redistribution between the N and C compartments without a 2-fold change in either compartment, e.g. for PSME3, $S_c = 1.83$; $S_n = 0.64$; $S_n/S_c = 0.35$.

To test the robustness of the distribution over the five classes of proteins shown in Figure 3-7A, we extracted a set of 134 proteins for which a 2-fold variation in one or more of S_n, S_c, S_t or S_n/S_c was obtained for at least 2 replicates, with at least 10 SILAC ratio counts in each replicate (Figure 3-7B, median of 549 ratio counts per protein). A summary of the data for these proteins is given in Supplementary Table 2. The distribution over the five classes showed at most modest changes (Figure 3-7A,B) and we therefore take this distribution as characteristic of the response of MCF-7 cells to estradiol. Quantitative data (Supplementary Table 2) show that after E2 stimulation, a marked decrease of compartmental abundance were detected for Protein DJ-1 (PARK7) with a more than 4-fold decrease in the nuclear compartments (S_n= -2.0) and a minor decrease in the cytoplasmic one (S_c= -0.355). In response to E2, PARK7 was significantly redistributed in cytoplasm (N → C). Same reduction in the nuclear level of NQO1 was observed after E2 stimulation (S_n= -2.0) while the cytoplasmic abundance was increased (S_c= 0.89) pointed out the same redistribution (N → C). These relevant proteins, PARK7 and NQO1, were also chosen for MS validation by confocal microscopic analysis. Using immunofluorescence imaging (Figure 3-8), PARK7 was massively reduced in the nucleus in response to E2 while NQO1 was increased in the nucleus of the dividing cells, suggesting a protective role for NQO1 (see discussion). Notable was that in all of the above data subsets, there were very much larger numbers of proteins that showed >2-fold changes in compartmental abundance compared to those with >2-fold changes in total abundance. The functional significance of this data is considered further below and in the discussion. From the proteins in the CT, NT and CNT data sets that showed good consistency with conservation of mass, the 134-set of abundant proteins was used to investigate possible correlations with database/literature information on subcellular location, functional processes, involvement of nuclear import/export proteins, and partitioning of proteins between the nucleus and mitochondria.

Number (%) of proteins with > 2-fold change in compartmental abundance

CT and NT data sets

$\lvert\log_2(S_{c,n}/S_t)\rvert$	total (CT ,NT)	$\log_2(S)$	S_c		S_n		S_n/S_c		S_t (C & N)	
			N	%	N	%	N	%	N	%
< 0.5	56, 169	> 1	1	1.8	1	0.6			2	0.8
< 0.4	45, 145	> 1	0	0	1	0.7			1	0.5
< 0.3	36, 104	> 1	0	0	1	1			1	0.7
< 0.5	56, 169	< -1	3	5.3	2	1.2			0	0.0
< 0.4	45, 145	< -1	2	4.4	2	1.4			0	0.0
< 0.3	36, 104	< -1	1	2.8	0	0			0	0.0

CNT data set

$\lvert\log_2(S_t^*/S_t)\rvert$	total	$\log_2(S)$	S_c		S_n		S_n/S_c		S_t	
			N	%	N	%	N	%	N	%
< 0.5	601	> 1	89	14.8	0	0	11	1.8	2	0.3
< 0.4	493	> 1	70	14.2	0	0	9	1.8	2	0.4
< 0.3	359	> 1	52	14.5	0	0	4	1.1	2	0.5
< 0.5	601	< -1	8	1.3	179	29.7	295	49.1	3	0.5
< 0.4	493	< -1	6	1.2	143	29.0	237	48.1	2	0.4
< 0.3	359	< -1	5	1.4	109	30.3	180	50.1	2	0.5

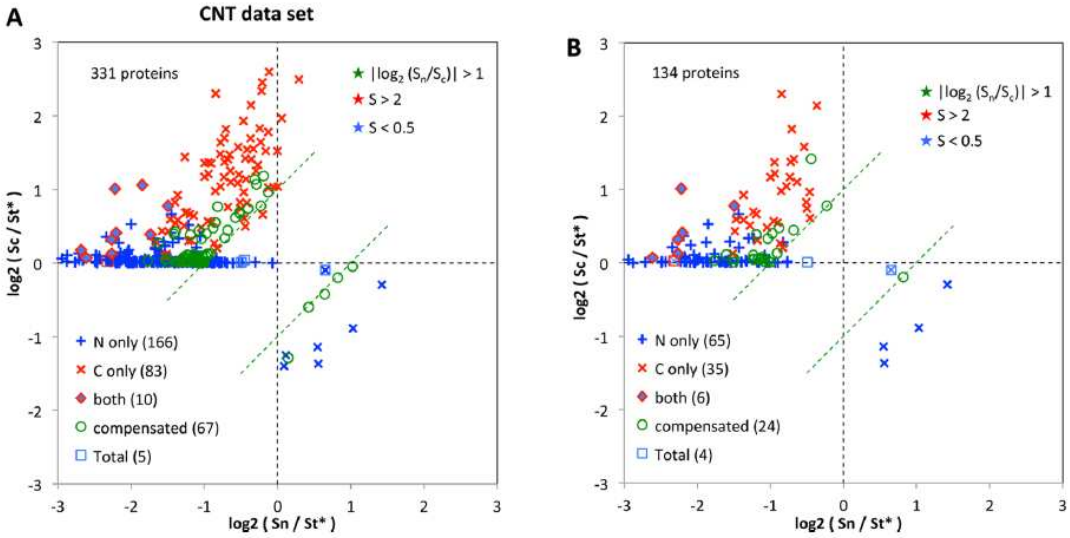

Figure 3-7: Redistribution of proteins.

Table inset. *Top:* number of proteins detected in a single subcellular compartment with >2-fold changes in abundance. *Bottom:* number of proteins detected in both compartments with >2-fold changes in abundance (S_n, S_c or S_t) or in S_n/S_c. The number of proteins included varies with the selection range around S_n/S_t, S_c/S_t or $S_t^*/S_t = 1$ (see text). (A) 3D plot for 331 proteins with $|\log_2(S/S_t)| < 0.5$. (B) 3D plot for 134 proteins with $|\log_2(S/S_t)| \leq 0.5$ that were quantified with ≥ 10 SILAC ratio counts in at least two replicates. The legend (lower left) shows the symbol coding for >2-fold changes only in S_n, only in S_c, in both S_n and S_c, for S_n/S_c only and for S_t. Increases/decreases are color coded (upper right legend). Figure was designed by JGZ and published in (Pinto et al., 2014).

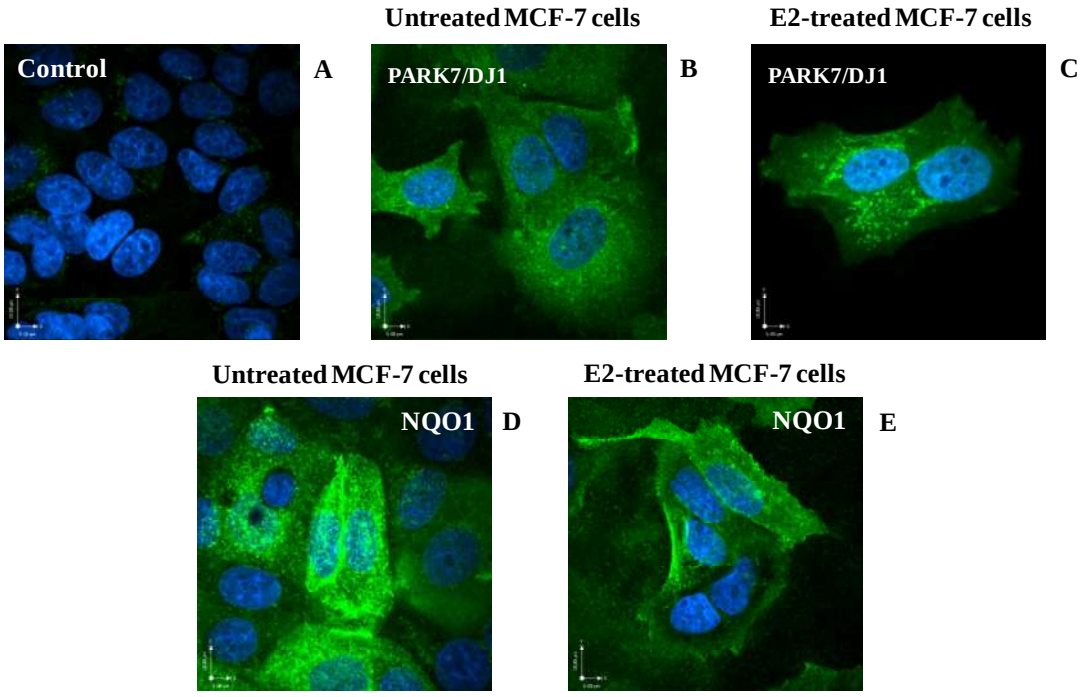

Figure 3-8: Immunofluorescence (IF) of the sub-cellular redistribution of PARK7 and NQO1 proteins in MCF-7 cells.

(A) Goat polyclonal secondary antibody to rabbit IgG - H&L (Green DyLight 488) used as negative control. Oestrogen untreated (B) and treated (C) MCF-7 cells were incubated with primary Anti-Rabbit antibody to PARK7 and goat Anti-Rabbit IgG H&L secondary antibody. Also, untreated (D) and E2-treated (E) MCF-7 cells were incubated with Anti-Rabbit antibody to NQO1 and goat Anti-Rabbit IgG H&L as secondary antibody. DAPI was used to stain the cell nuclei (blue) at a concentration of 1.43µM. Merged images are presented.

3.1.1.6 Subcellular Location Annotation for Proteins with Compartmentalized Abundance Changes

For the 134-set of proteins, we analyzed their current GO CC (cell component) annotation terms. The complete set of 733 annotations to 152 GO CC terms is given in Supplementary Table 2. Table 3-1 shows the distribution of the current annotations over four main top-level cellular locations (nucleus, cytoplasm, plasma membrane, extracellular region), with a further breakdown of cytoplasmic locations. There was no subcellular location annotation for 5 of the 134 proteins. With the vocabulary of Table 3-1, the remaining 129 proteins had an average of 2.7 locations per protein, and a maximum of 6 locations, i.e. many of these proteins are known to have multiple subcellular locations. For example, of the 66 proteins currently annotated to the nucleus, 58 are also annotated to the cytoplasm (Table 3-1). Of the 120 proteins currently annotated to the cytoplasm, 58 are also annotated to the nucleus and 25 to the plasma membrane. This is consistent with the concepts that protein spatial location and organelle composition are dynamic properties that depend on context and that protein function is intimately coupled to subcellular spatial distribution.

On the other hand, we detected 76 proteins in both the cytoplasm and nucleus that have not previously been annotated to nucleus and 14 proteins in both the cytoplasm and nucleus that have not previously been annotated to cytoplasm. These results are consistent with previous studies indicating that current subcellular annotations in the GO CC database underestimate the dispersion of proteins over multiple locations in MCF-7 cells (Qattan et al., 2010, Qattan et al., 2012) and suggest that coupling of cellular function to protein spatial distribution is even more prevalent than is implicit in current subcellular location annotations (see Discussion).

In this context, we recently identified 985 proteins that are present in both the nucleus and mitochondria of MCF-7 cells (Qattan et al., 2012). With the greater number of MS replicates used in the present study, 1069 proteins that were previously detected in mitochondria (Qattan et al., 2012) were detected in the nucleus in the present samples. This included confirmation of the unexpected presence in the nucleus of mitochondrial respiratory chain proteins and of many other metabolically interesting proteins such as pyruvate decarboxylase (PC) and mitochondrial phosphoenolpyruvate carboxykinase (PCK2) (Qattan et al., 2012). At the level of at least 2 peptides and 3 SILAC ratio counts, 829 of these proteins were quantified in both the nucleus and cytoplasm in the present experiments. Following estradiol exposure, N ➔ C redistribution involving >2-fold reduction in nuclear abundance was detected for 249 of these proteins. The 134-set of proteins showing the most reliable changes contained 87 of these proteins, which are included in the functional analysis below. While possible redistribution of these proteins to/from mitochondria will have to be confirmed by additional experiments, this suggests that dynamic subcellular protein distribution may have a major role in communication/coordination between the nucleus and mitochondria.

Table 3-1: Distribution of GO CC annotation for the 134 protein Set

subcellular location	nucleus	plasma membrane	extracellular region	cytoplasm	cytosol	mitochondrion	endoplasmic reticulum	Golgi apparatus	melanosome	peroxisome	endosome	lysosome
nucleus	66	15	4	58	35	10	2	2	5	1	0	0
plasma membrane		27	4	25	15	2	2	3	4	0	2	2
extracellular region			14	12	7	2	6	1	3	0	0	1
cytoplasm				120	75	19	9	6	9	2	4	5
cytosol					75	8	2	4	6	0	4	2
mitochondrion						19	1	1	3	1	0	0
endoplasmic reticulum							9	1	2	0	0	1
Golgi apparatus								6	0	0	2	1
melanosome									9	0	0	0
peroxisome										2	0	0
endosome											4	1
lysosome												5
GO CC ID	GO:0005634	GO:0005886	GO:0005576	GO:0005737	GO:0005829	GO:0005739	GO:0005783	GO:0005794	GO:0042470	GO:0005777	GO:0005768	GO:0005764

3.1.1.7 Functional processes associated with proteins showing compartmentalized abundance changes

For the 134-set of proteins, we used the Reactome software programs (Croft et al., 2011, Milacic et al., 2012) to search for associated functional processes (Table 3-2). Our goal was to test whether the sets of redistributed proteins are likely to have important functional consequences and to obtain a qualitative appraisal of what kinds of processes might be involved rather than to specify exact functions. For example, all 5 proteins involved in glycolysis (a cytoplasmic process), show N ➔ C redistribution involving >2-fold reductions in their nuclear abundance with no appreciable change in their cytoplasmic abundance (Table 3-2). This should not be interpreted as evidence for glycolysis in the nucleus, but rather as an indication for cross-talk between glycolysis and unknown nuclear process(es) that are influenced by estradiol exposure. Similarly, the Reactome p-value can only be moderately indicative since it is normalized to the proportion of all glycolytic proteins and does not assess the significance of redistribution of multiple glycolytic proteins to a "wrong" location differing from the cytoplasm.

With these kinds of caveats in mind, Table 3-2 nonetheless suggests that exposure to estradiol leads to changes in protein distribution that reflect processes over a wide spectrum of functions/subcellular locations. Because of substantial, different skewing in the basal, non-stimulated distribution of the various proteins between the nucleus and the cytoplasm, only some of the redistribution patterns shown for the functions in Table 3-2 are easily interpreted. For example, all 7 subunits of the CCT complex involved in chaperone-assisted protein folding show >2-fold reductions in nuclear abundance, suggesting that this complex might be involvedin protein import/export/folding in the nucleus (see Discussion).

Similarly, all 5 proteins involved in nucleosome assembly show >2-fold increases in cytoplasmic abundance, with very minor changes in their nuclear and total abundance, suggesting this group might reflect signalling to the cytoplasm about a nuclear process. Seven proteasome subunits (see protein degradation in the cytoplasm section of Table 3-2) figure prominently in the functional groups in Table 3-2. Proteasomes occur in both the nucleus and cytoplasm and the distribution pattern includes 4 proteins that show substantial redistribution without 2-fold changes in abundance in either compartment. We suggest that this type of redistribution pattern may reflect balancing of multiple functions between the nucleus and cytoplasm (see Discussion). Other functional groups show more complex redistribution patterns that may reflect wide functional cross-talk that is coupled to basal skewing of abundance over cellular location. This was the case for the plasma membrane functional groups, where it was intriguing to see indications for functions associated with actin-related processes in phagosome formation and for neuronal migration (L1CAM interactions). As with glycolysis, such groupings might reflect cross-talk with nuclear processes. For example, nuclear actin imported via importin-9 supports transcription (Dopie et al., 2012) and myosin isoforms show directed, Ca^{2+}-dependent nuclear import (Dzijak et al., 2012).

Table 3-2: Analysis of Functional Groups with Reactome

Reactome Name	number of proteins	Reactome identifier	proteins in identifier	p-value	distribution (Fig. 6)	gene names
MAJOR CATEGORIES						
Metabolism of mRNA	17	REACT_20605	224	2.0E-10		
Metabolism of proteins	22	REACT_17015	574	1.2E-07		
Gene Expression	27	REACT_71	1031	7.0E-06		
Cell Cycle	16	REACT_115566	478	5.0E-05		
CYTOPLASM						
small molecule metabolism						
Glycolysis	5	REACT_1383	27	9.6E-06	+ + + + +	ALDOA,ENO1,GAPDH,PGK1,ALDOC
Regulation of ornithine decarboxylase (ODC)	8	REACT_13565	50	5.6E-08	o o + + + + + o o	PSMA2,PSMA3,NQO1,PSMA1,PSMB5, PSME1,PSMB6,PSMB7
Vitamins B6 activation to pyridoxal phosphate	2	REACT_25012	3	3.6E-04	o +	PDXK,PNPO
Synthesis and interconversion of nucleotide di- and triphosphates	3	REACT_21330	18	9.3E-04	+ + +	TXN,TXNRD1,GSR
protein translation						
Translation	11	REACT_1014	151	5.3E-06	o x o o x x o x o x x	EIF2S3L,RPS20,EEF2,EIF2S3,RPL12,RPS7, RPS3,RPS3A,RPS16,EIF4H,EIF2S1
3' -UTR-mediated translational regulation	10	REACT_1762	109	2.6E-06	o x o x x o x o x x	EIF2S3L,RPS20,EIF2S3,RPL12,RPS7,RPS3, RPS3A,RPS16,EIF4H,EIF2S1
protein folding						
Cooperation of Prefoldin and TriC/CCT in actin and tubulin folding	8	REACT_17029	27	2.8E-10	+ + + + + + + +	CCT2,TUBB4B,CCT6A,CCT3,CCT4,CCT5, TCP1,CCT7
Association of CCT/TriC with other substrates during biosynthesis	7	REACT_16984	48	4.0E-08	+ + + + + + +	CCT2,CCT6A,CCT3,CCT4,CCT5,TCP1, CCT7
mRNA metabolism						
Regulation of mRNA Stability by Proteins that Bind AU-rich Elements	10	REACT_24994	86	2.6E-08	o o + + + + + o o o	PSMA2,PSMA3,PSMA1,PSMB5,ANP32A, HSPB1,PSME1,HSPA8,PSMB7,PSMB6
Destabilization of mRNA by AUF1 (hnRNP D0)	9	REACT_25325	54	5.3E-09	o o + + + + + o o o	PSMA2,PSMA3,PSMA1,PSMB5,HSPB1, PSME1,HSPA8,PSMB7,PSMB6
Nonsense-Mediated Decay	7	REACT_75886	110	1.9E-04	x x o x x o x	RPS20,RPS3A,RPS16,RPL12,RPS7,RPS3, RBM8A
protein degradation						
Proteasomal clevage of exogenous antigen	7	REACT_111172	44	4.2E-07	+ o o + + o o	PSME1,PSMA2,PSMA3,PSMA1,PSMB5, PSMB7,PSMB6
NUCLEUS						
cell cycle						
Mitotic M-M/G1 phases	10	REACT_21300	266	6.3E-04	+ o o + x + + x o o	TUBB4B,PSMA2,PSMA3,PSMA1,CSNK2B, PSMB5,PSME1,RCC2,PSMB7,PSMB6
Mitotic G1-G1/S phases	8	REACT_21267	133	9.8E-05	o o + + + o x o	PSMA2,PSMA3,PSMA1,PSMB5,PSME1, PSMB6,RBBP4,PSMB7
Nucleosome assembly	5	REACT_22344	45	1.2E-04	x x x x x	NPM1,HIST1H4A,HIST1H2BL,RBBP4, H2BFS
mRNA splicing						
Cleavage at the 3'-Splice Site and Exon Ligation	4	REACT_1331	108	3.1E-02	o o + x	SF3B3,PCBP2,PCBP1,RBM8A
PLASMA MEMBRANE						
receptors and intercellular interactions						
Signaling by Wnt	9	REACT_11045	91	5.7E-07	o o + + + ◈ x o o	PSMA2,PSMA3,PSMA1,PSMB5,PSME1, VPS26A,SNX3,PSMB7,PSMB6
Regulation of actin dynamics for phagocytic cup formation	8	REACT_160086	214	2.3E-03	x x x o + o + x	ACTR3,ARPC5,ARPC3,ACTR2,HSP90AB1,A RPC2,HSP90AA1,ARPC4
Role of myosins in phagosome formation	6	REACT_160090	195	2.0E-02	x x o x o x	ACTR3,ARPC5,ARPC2,ARPC3,ACTR2, ARPC4
L1CAM interactions	4	REACT_22205	107	3.0E-02	+ o x x	TUBB4B,HSPA8,CSNK2B,ITGA2

3.1.1.8 Proteins involved in nuclear import/export

With at least 5 ratio counts in the C, N and T samples, there were 13 quantified proteins (median of 185 ratio counts per protein) in the full data set that have GO annotation corresponding to nuclear import/export/localization/maintenance (Figure 3-9). These proteins showed at most modest changes in total abundance (S_t = 1.19 CALR; 0.65 KPNA2) and essentially no change for RAN or KPNB1. In general, this subgroup of proteins showed a similar pattern to the overall set of quantified proteins, i.e. a trend of N ➔ C redistribution following oestrogen stimulation, with RAN as the only exception. There is little indication for general impairment of nuclear import/export. Indeed, the asymmetric distribution of RAN and karyopherins required for nuclear import is if anything enhanced.

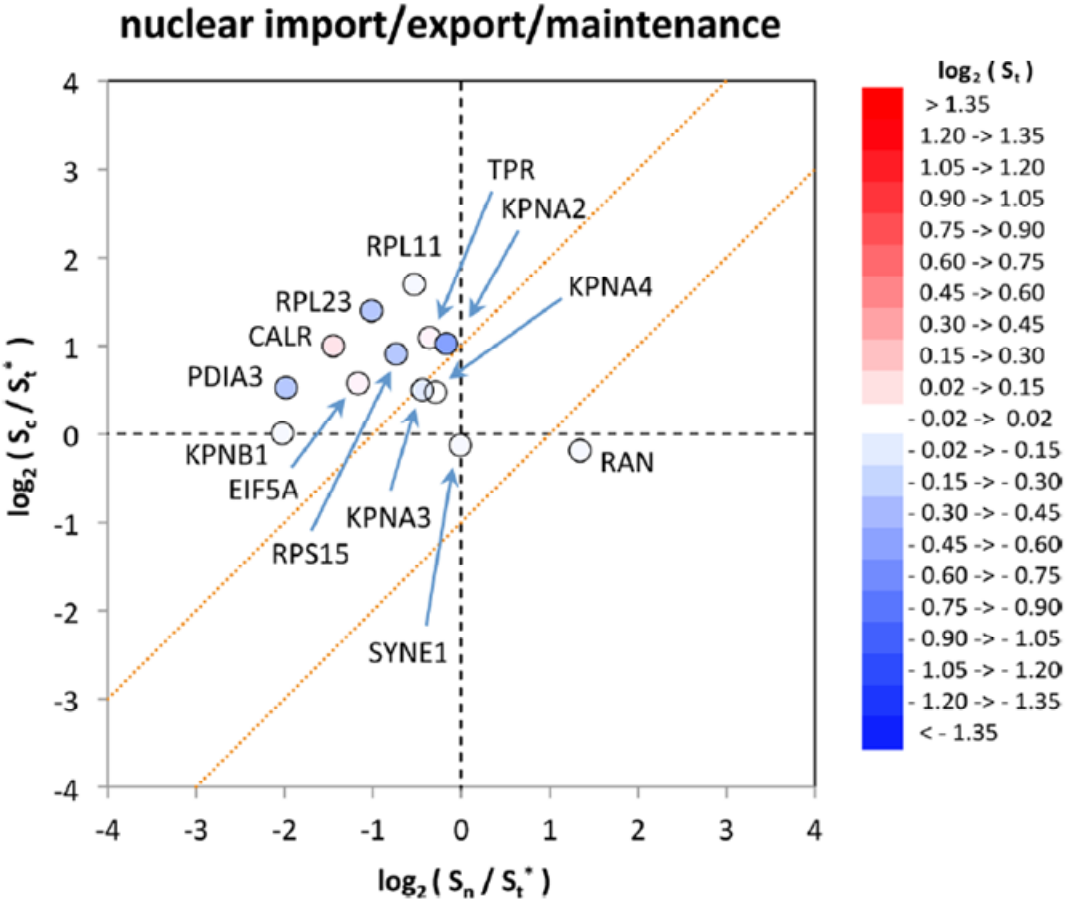

Figure 3-9: Three-dimensional spatial razor plot for proteins with GO annotations corresponding to nuclear import/export/localization/maintenance.

This figure was designed by JGZ and published in (Pinto et al., 2014)

3.2 Part-II: Quantitative Global Proteomics Reveals Nucleo-Cytoplasmic Trafficking of Proteins Following Exposure of MCF-7 breast cancer cell to Tamoxifen

Hormone receptor positive (HR+) breast cancers represent 70% of all breast tumours. Their oncogenesis is a multiple step process thought to be driven by two transcription factors, the ER and/or the progesterone receptor (PR) (Valentina Contrò, 2015). Consequently, the endocrine-targeted therapeutic approach has focused on both receptors as prognostic markers and therapeutic targets (Davies et al., 2011), aiming to alter the oestrogen signalling for patients with ERα-positive disease (Dixon, 2014). The benefits gained from the treatment are limited by development of either *de novo* or acquired resistance following a period of response to tamoxifen. For both types of resistance, the lack of pathological response to tamoxifen is manifested when the tumour cells commence proliferation, challenging the clinical management (Larionov and Miller, 2009) of patients (Larionov and Miller, 2009).

Over the past four decades tamoxifen has been extensively used in neoadjuvant and adjuvant settings for the treatment of hormonal dependent breast cancers by acting as a competitive inhibitor of ER (Dixon, 2014, Shiau et al., 1998, Wakeling, 2000). The ER mediated signalling pathways involve genomic, non-genomic, or mitochondrial pathways that contribute to amplification of the multistep process of tumour development (Bjornstrom and Sjoberg, 2005). It is well established that binding of oestrogen (E2) to ERs leads to subsequent receptor dimerization and recruitment of other coactivators such as SRC-3 and (tethering) transcription factors such as AP-1. This complex acts directly as transcriptional factor by binding to oestrogen responsive elements (EREs) that are located on the promotor regions of the target genes. This initiates transcription of the target genes leading to proliferation, apoptotic inhibition, and uncontrolled growth (Schiff et al., 2005). Full agonistic activity of E2 is achieved via the activation of two transactivation domains known

as activation function 1 (AF-1), regulated by growth factors, and activation function 2 (AF-2), regulated by E2 binding (Wakeling, 2000). Tamoxifen acts as a selective modulator with partial agonistic activity in which the active metabolite of tamoxifen, 4-OHT binds to a ligand binding domain (LDB) of ER. This promotes conformational changes of the ER dimers, leading to recruitment of transcriptional repressors that relocate helix 12 and prevent the coactivator binding and activation of AF-2. Subsequently, the transcriptions of AF-2 dependent genes are downregulated, but partial agonistic activities can be initiated for the AF-1 dependent genes (Schiff et al., 2005). Consequently tamoxifen can inhibit the transcriptional activities of ER in some tissues such as the breast tissue but activate transcriptional cascades in other tissues such as uterus. Therefore, tamoxifen and related compounds show mixed agonist/antagonist properties and are classified as oestrogen selective modulators (ERSM).

In breast tissue tamoxifen acts predominantly as antagonist but there is some evidence that tamoxifen agonistic activities can enhance breast tissue proliferation, thereby leading to limited efficacy and resistance (Gottardis and Jordan, 1988, O'Regan et al., 2006). Furthermore, at the molecular level the active metabolite of tamoxifen, 4-hydroxytamoxifen (OHT), can cause the induction of gene expression related to the the cell cycle, particularly for those genes induced by E2 (Hodges et al., 2003).

Numerous studies have tackled antioestrogen resistance therapy using different approaches. These include various cell line models in culture and/or as xenografts as well as in studies in the clinical adjuvant and/or neoadjuvant settings (Larionov and Miller, 2009). Owing to the complexity and heterogeneity of breast cancer, understanding of the exact mechanisms underlying resistance to tamoxifen remains far from being completely elucidated.

The proposed mechanisms are diverse and consistently indicate that complex cellular mechanisms are involved in the developing resistance. Studies related to the differential metabolism of tamoxifen, mutated/downregulated ER, cross-talk between ER and growth factor transduction pathways, dynamic changes in cell signalling, and cellular responses to oxidative stress have all been carried out with limited success (Chang, 2012, Dixon, 2014). These studies suggest that numerous pathways are intertwined and that more integrative approaches using high-throughput technologies are required to elucidate tamoxifen function, to predict and overcome resistance, and to ultimately lead to better therapeutic interventions.

We have recently developed high-throughput proteomics methods suitable for investigating dynamic aspects of protein subcellular distribution in the response of cells to stimulations (Baqader et al., 2014, Mulvey et al., 2013, Pinto et al., 2014, Pinto et al., 2015, Pinto et al., 2016, Radulovic et al., 2016). This approach, which combines global quantitative proteomics with the analysis of fractions enriched in target subcellular locations, has allowed measurement of the changes in total abundance and in the compartmental abundance/distribution between the nucleus and cytoplasm for several thousand proteins DE in MCF-7 cells in response to oestrogen stimulation. Using stable isotope labelling in cell culture (SILAC) and quantitative high-resolution mass spectrometry analysis demonstrated that oestradiol stimulation of MCF-7 cells results in strong redistribution of massive numbers of proteins between the nucleus and cytoplasm. Many more proteins showed appreciable spatial changes in compartmental abundance than in total protein abundance (Pinto et al., 2014).

We suggested (Pinto et al., 2014, Pinto et al., 2015) that major alterations in the spatio-temporal subcellular distribution of proteins are the dominant response of MCF-7 cells to oestradiol exposure and that a major role of the ER and possibly other nuclear hormone

receptors may be the “polling” of and response to spatially distributed functional networks and that strong perturbation of subcellular spatial regulation may be a crucial feature of breast cancer.

In the present work we apply global, quantitative proteomics analysis of changes in nucleo-cytoplasmic distribution of proteins and of total protein abundance for MCF-7 cells exposed to tamoxifen. Extensive bioinformatics analysis suggests that cellular spatial reorganization is a major component of the molecular basis of tamoxifen function and its use in breast cancer therapy.

3.2.1 Results

We prepared MCF-7 cells according to previously published procedures (Pinto et al., 2014, Qattan et al., 2010, Qattan et al., 2012). Their response to tamoxifen was measured for total change in protein abundance and for compartmental changes in protein abundance in the nuclear and "cytoplasmic" (nucleus-depleted) compartments (Baqader et al., 2014, Jung et al., 2013, Mulvey et al., 2013). Stringent purification of organelles (e.g. nucleus) was not attempted since such organelle isolation procedures can lead to loss of ability to monitor important characteristics of dynamic cellular function (Radulovic et al., 2016, Pinto et al., 2016). We have previously characterized in detail the purity of samples obtained with the present subcellular fractionation protocols (Pinto et al., 2014, Qattan et al., 2010, Qattan et al., 2012, Mulvey et al., 2013, Radulovic et al., 2016). The purity of the nuclear/cytoplasmic fractions used for MS analysis were routinely tested using western blotting as decribed in (section 2.3.4) and shown in (Figure 3-1).

A concentration of 4-OHT (1 μM) was previously characterized as a cytostatic dose for various cell lines and used in different laboratories. It was originally selected for complete inhibition of oestrogen-dependent ZR-75-1 cells without influencing the growth of tamoxifen-resistant derivatives (Meijer et al., 2006). This dose has been routinely used because of the absence of complete toxicity, to effectively counter variations in oestrogen content of different batches of bovine serum (Lykkesfeldt et al., 1984, van Agthoven et al., 2012), and because an IC50 concentration of a drug that is required for 50% inhibition of *in vitro* tamoxifen is 1 μM (Kijima et al., 2005).

Exposure of cells to 1µM 4-OHT for 24 h was used in the present experiments. The dose dependent (0.0-2.0µM) impact of 4-OHT treatment on the survival rate of MCF-7 cells showed that the chosen dose (1µM) was of a cytostatic effect (non-lethal) to MCF-7 cells, whereas a survival rate of less than 50% of the seeded cells was associated with higher doses of 1.5 and 2.0 µM 4-OHT (Figure 3-10A). As a routine control for the present preparations, we checked the morphology of stimulated/unstimulated cells using fluorescence staining with a proprietary dye that can label the nuclear membrane(s), mitochondria, fibers, and nuceleoli in fixed cells. Confocal imaging revealed no remarkable changes in overall cell morphology or in peripheral membranes in the 4-OHT treated MCF-7 cells compared to untreated cells (Figure 3-10B). To further validate the proteomics results and confirm the redistribution of the selected protein(s), immunfluorescence was performed with specific antibodies angainst protein of interest in unstimulated and 4-OHT-stimulated MCF-7 (Figure 3-11Figure 3-12).

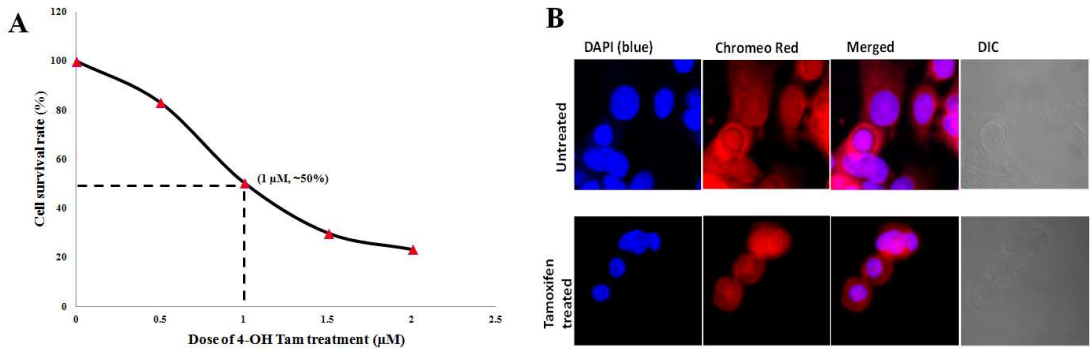

Figure 3-10: Toxicity assay and assessment of morphological changes.

A. Survival rate (%) of MCF-7 cells following stimulation with increasing concentrations of 4-OHT. B. Morphology of MCF-7 cells with/without tamoxifen treatment. The fixed cells were stained DAPI (for nuclei) and counterstained with Chromo Red Fluorescent dye (a proprietary dye) that can label the nuclear membrane(s), mitochondria, fibers, and nucleoli in fixed cells. Merged and DIC (Differential interference contrast) images are presented.

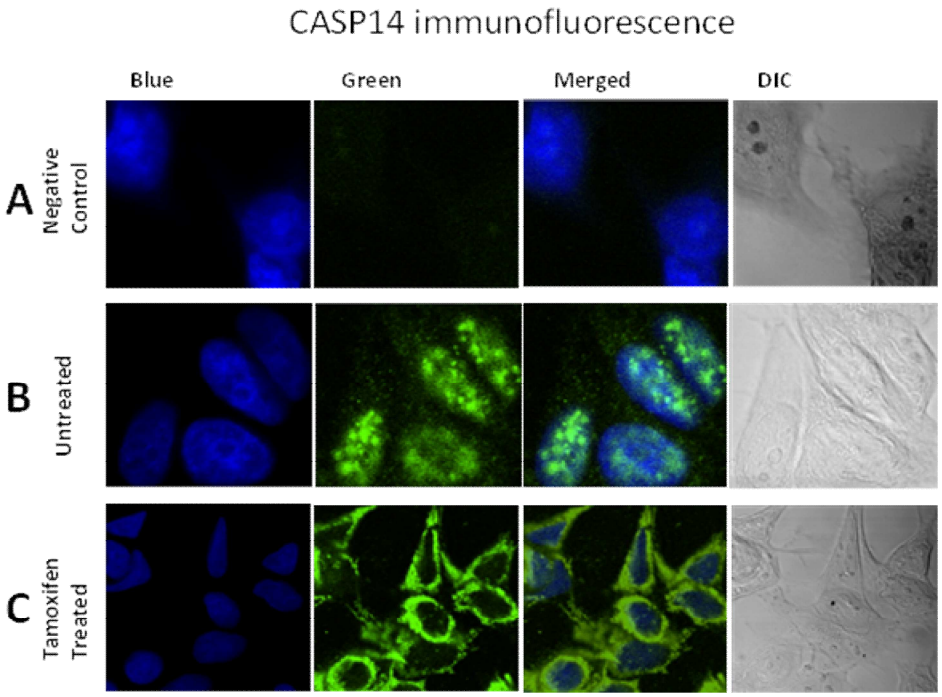

Figure 3-11: Immunofluorescence (IF) of the sub-cellular redistribution of CASPASE-14 protein in MCF-7 cells.

(A) Goat polyclonal secondary antibody to rabbit IgG - H&L (Green DyLight 488) used as negative control. 4-Hydroxytamoxifen untreated **(B)** and treated **(C)** MCF-7 cells were incubated with CASPASE-14 primary Anti-Rabbit antibody and goat Anti-Rabbit IgG H&L secondary antibody. DAPI was used to stain the cell nuclei (blue) at a concentration of 1.43µM. Merged and DIC (Differential interference contrast) images are presented.

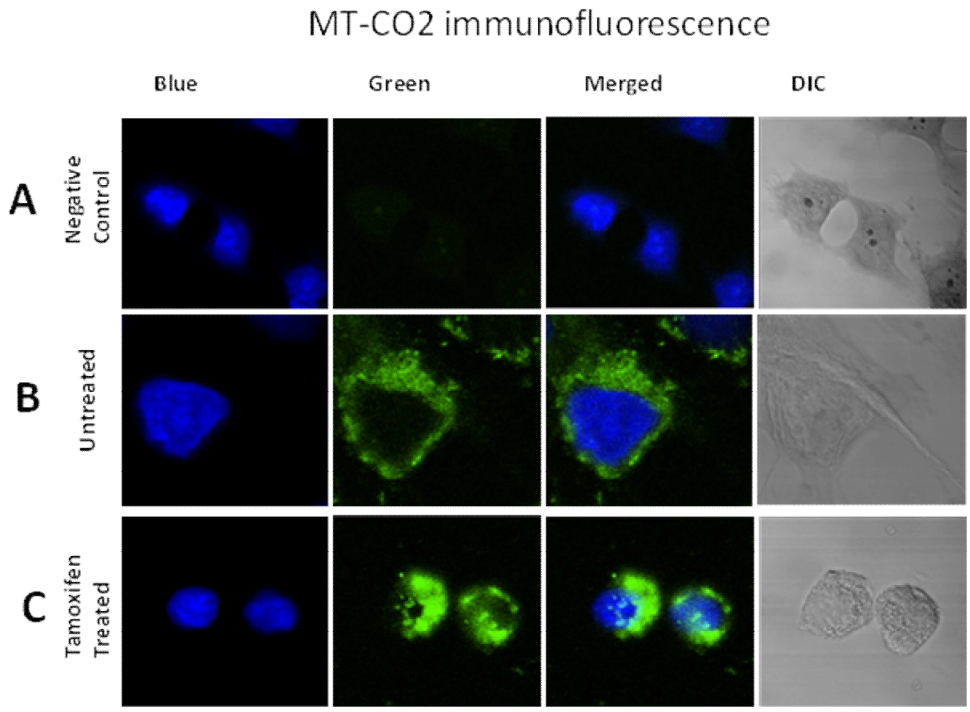

Figure 3-12: Immunofluorescence (IF) of the sub-cellular redistribution of MT-CO2 protein in MCF-7 cells.

(A) Goat polyclonal secondary antibody to rabbit IgG - H&L (Green DyLight 488) used as negative control. 4-Hydroxytamoxifen untreated **(B)** and treated **(C)** MCF-7 cells were incubated with MT-CO2 primary Anti-Rabbit antibody and goat Anti-Rabbit IgG H&L secondary antibody. DAPI was used to stain the cell nuclei (blue) at a concentration of 1.43µM. Merged and DIC (Differential interference contrast) images are presented.

A schematic summary of the experimental workflow, including SILAC labeling, stimulation, and MS quantification, is shown in Figure 3-13. Experimental measurements of protein abundance ratios (SILAC ratios) between stimulated/unstimulated cells were obtained for three samples: (1) an unfractionated, total cell lysate (T), (2) a nucleus-enriched sample obtained by subcellular fractionation (N), and (3) the corresponding nucleus-depleted sample (C), which we refer to as the cytoplasm in the following text. The corresponding SILAC ratios provide measures for each protein of the overall change in total cellular abundance (S_t), or of the localized change in abundance in the nuclear (S_n) or cytoplasmic (S_c) subcellular compartments. Across the three data sets, 2125, 1979, and 3358 proteins were observed in the C, N and T samples respectively (Figure 3-14, Supplementary Table 3-6).

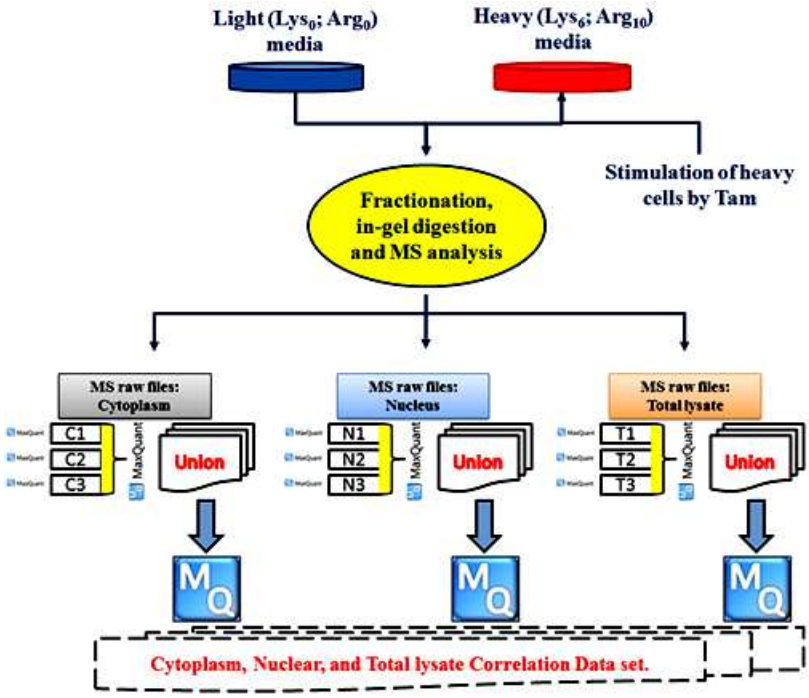

Figure 3-13: Schematic summary of the experimental workflow.

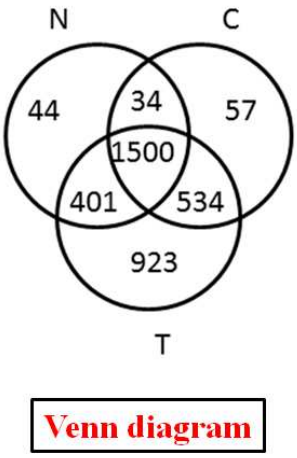

Figure 3-14: Venn diagram showing the number of output data sets and identified proteins in the three sample types (CNT).

The merged final dataset of the three sample types (CNT) of the 3493 proteins quantified with ≥ 1 peptide count and quantified with ≥2 SILAC counts.

3.2.1.1 Changes in abundance for the nuclear and cytoplasmic fraction

For each sample type, we measured three technical replicates (Figure 3-13). The three data sets representing each fraction showed high correlation between the three replicates ($0.85<R^2<0.88$, $0.90<R^2<0.91$, $0.64<R^2<0.85$ for the total lysate, cytoplasmic, fractions, and nuclear fraction, respectively: Figure 3-15).

The overall changes in abundance for the proteins are shown in Table 3-3. The inset tables show the number and percentage of proteins with >4-fold or >2-fold changes in total abundance (S_t), nuclear compartment abundance (S_n), and cytoplasmic compartment abundance (S_c). The table also shows for each distribution the total number of proteins included, the median number of SILAC ratio counts, and the number of proteins with smaller numbers of SILAC ratio counts.

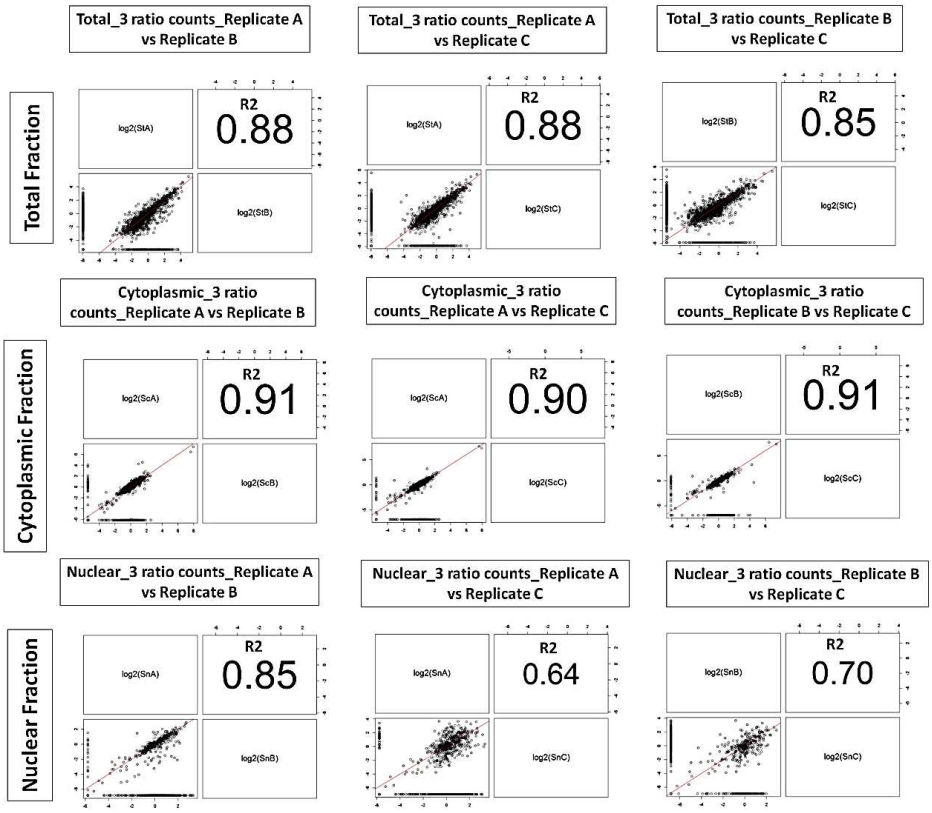

Figure 3-15: Correlation of SILAC ratio between three replicate for the total, cytoplasmic and nucleus.

All the proteins with ≥ 3 ratio counts were included in the calculation of correlation. Outliers mostly correspond to proteins with low numbers of ratio counts. Outliers mostly correspond to proteins with low numbers of ratio counts.

Table 3-3: Distribution of SILAC ratios (5 versus 3) for proteins from the total lysate (S_t), nuclear (S_n), and cytoplasmic (S_c) samples.

(Upper)_All proteins with ≥5 ratio counts for the union of the three replicates for each sample type; (Bottom)_All proteins with ≥3 ratio counts for all replicates of each sample type.

$T_{union} \geq 5$ counts		
$Log_2 (S_t)$	Proteins	% Proteins
>2	146	7.2
>1	367	18.2
-1<and<1	878	43.4
<-1	776	38.4
<-2	200	9.9
Number of proteins		
Counts=5	5≤ and <8	Average SILAC counts=32
188	516	2021

$C_{union} \geq 5$ counts		
$Log_2 (S_c)$	Proteins	% Proteins
>2	13	1.1
>1	116	9.8
-1<and<1	989	83.7
<-1	81	6.8
<-2	33	2.9
Number of proteins		
Counts=5	5≤ and <8	Average SILAC counts=24
95	237	1181

$N_{union} \geq 5$ counts		
$Log_2 (S_n)$	Proteins	% Proteins
>2	25	2.7
>1	176	19.1
-1<and<1	667	72.2
<-1	79	8.6
<-2	43	4.7
Number of proteins		
Counts=5	5≤ and <8	Average SILAC counts=17
95	224	922

$T_{replicate} \geq 3$ counts		
$Log_2 (S_t)$	Proteins	% Proteins
>2	144	9.1
>1	303	19.3
-1<and<1	697	44.4
<-1	571	36.3
<-2	150	9.5
Number of proteins		
Counts=9	9≤ and <12	Average SILAC counts=6
46	164	1571

$C_{replicate} \geq 3$ counts		
$Log_2 (S_t)$	Proteins	% Proteins
>2	11	0.8
>1	151	11.6
-1<and<1	1049	80.6
<-1	102	7.8
<-2	33	2.5
Number of proteins		
Counts=9	9≤ and <12	Average SILAC counts=13
41	121	1302

$N_{replicate} \geq 3$ counts		
$Log_2 (S_n)$	Proteins	% Proteins
>2	34	3.0
>1	224	19.9
-1<and<1	803	71.5
<-1	96	8.5
<-2	45	4.0
Number of proteins		
Counts=9	9≤ and <12	Average SILAC counts=17
40	105	1123

For 2021 total lysate (T) proteins with ≥ 5 SILAC ratio counts across the three replicates (average SILAC counts of 32 counts per protein), 513 proteins (roughly 25%) were upregulated with 146 (7.2 %) and 367 (18.2%) proteins showing greater than 4-fold and 2-fold increase in abundance, respectively (Table 3-3, upper). Differently, a double number of proteins (976 proteins, almost 50%) were downregulated with 150 (9.5 %) and 571 (36.3 %) proteins greater than 4-fold and 2-fold decrease in abundance, respectively. This massive downregulation of total proteins was even supported by a greater number of the downregulated metabolic pathways versus upregulated ones in the total lysate as reported below.

To check for possible distortion of the distribution profile by lower abundance proteins and/or by variation between replicates, these results were compared with a smaller set of 1571 more abundant proteins for which the lower limit was set to ≥ 3 SILAC ratio counts in all three T replicates (average of 6 SILAC counts per protein, Table 3-3, bottom).

A lower number of the nuclear proteins with ≥ 5 SILAC ratio counts across the three replicates (average of 17 SILAC counts per protein) predicted a very different behaviour in nuclear compartment (Table 3-3, upper). For 922 nuclear proteins with ≥ 5 SILAC ratio counts across the three replicates (average of 17 SILAC counts per protein), 176 proteins (19.1%) showed greater than 2-fold increase in nuclear abundance. However, 43 proteins (4.7%) showed greater than 4-fold decrease and 79 proteins (8.6%) showed greater than 2-fold decrease in nuclear abundance. For 1123 more abundant nuclear proteins with ≥ 3 SILAC ratio counts in all three N replicates (average of 17 SILAC counts per protein), a similar distribution profile for the SILAC ratio S_n for nuclear proteins indicated that lower abundance proteins and/or variation between replicates had a little effect on the observed distribution (Table 3-3, bottom).

For 1181 cytoplasm proteins with ≥ 5 SILAC ratio counts across the three replicates (average of 24 SILAC counts per protein), the most of proteins (83.7%) showed less than 2-fold increase/decrease in abundance whereas 116 (9.8%) and 81 proteins (6.8%) reveal a greater than 2-fold increase and decrease in nuclear abundance, respectively. Interestingly, for the cytoplasm, similarly to the nuclear compartment, an equivalent number of proteins as well as the ratios between the decreasing/increasing proteins in abundance were still observed in spite of a lower limit set to ≥ 3 SILAC ratio counts.

3.2.1.2 Changes of proteome after exposure to 4-OHT

In response to 4-OHT treatment, we obtained two significant datasets referred to as extended (overall response) (270-TAM) and the core (specific response) (97-TAM) (see material and method), when applicable, throughout the result and discussion sections. As it is not uncommon to find a uniformed data scale and/or distributions among these two proteomics datasets, these two datasets were obtained from the same quantitative study (Supplementary tables 7 and 8).

Thus, we used the larger list (270-TAM) to increase the power of statistical inference when uploading to iPathwayGuide software to predict the functional proteomics changes. Thus, a total of 94 (31 up and 63 down), 87 (29 up and 58 down), 139 (51 up and 88 down) proteins were selected as DE from C, N, and T samples (Figure 3-16A and C), respectively, and used in the subsequent analysis to tell the biological theme(s) for these proteins. The general response data set (270-TAM) contains proteins that are DE, and lacking more than one peptide and/or more than 2 SILAC counts for identification and quantification, respectively. Our assumption in this project is that to predict the response it is not enough to relay on the change of expression, alone. Therefore, the reliable response data set obtained in this project contains a list of proteins that are: (i) reliably identified (> 1 peptide count), (ii) quantified (≥3 SILAC counts), and have a distribution of significance in the three sample types. Based on these criteria, the reliable list (97-TAM) was selected from the large list (270-TAM). Of the general response data set (270-TAM) proteins selected from the correlation data set (CNT) according to the above mentioned criteria, a set of 97 proteins are showing the most significant changes (Figure 3-16B). The distribution scores of significance over the CNT are summarized in Table 3-4. In this data set, 51 proteins were selected as DE out of a total of 97

proteins with measured expression in the cytoplasmic fraction (C), 51 proteins out of 97 in the nuclear fraction (N), and 29 proteins out of 97 in the total lysate (T).

More than 50% of the proteins show significant changes in local abundance and/or redistribution of their subcellular location (C and N) and only 19 proteins (19% of the entire 97-significant set) show substantial changes in the total lysate (T) (Table 3-4).

Table 3-4: The significance B scores distribution of 97-TAM proteins over the three sample types.

Cytoplasm (Union)	Nuclear (Union)	Total (Union)	Number of proteins
Significance B score distribution			
+ (6); - (18)			24
	+ (10); - (15)		25
		+ (6); - (13)	19
+ (5); - (14)	+ (5); - (14)		19
+ (1); - (4)	+ (1); - (4)	+ (1); - (4)	5
	+ (1); - (1)	+ (1); - (1)	2
+ (4); - (4)		+ (3); - (5)	8

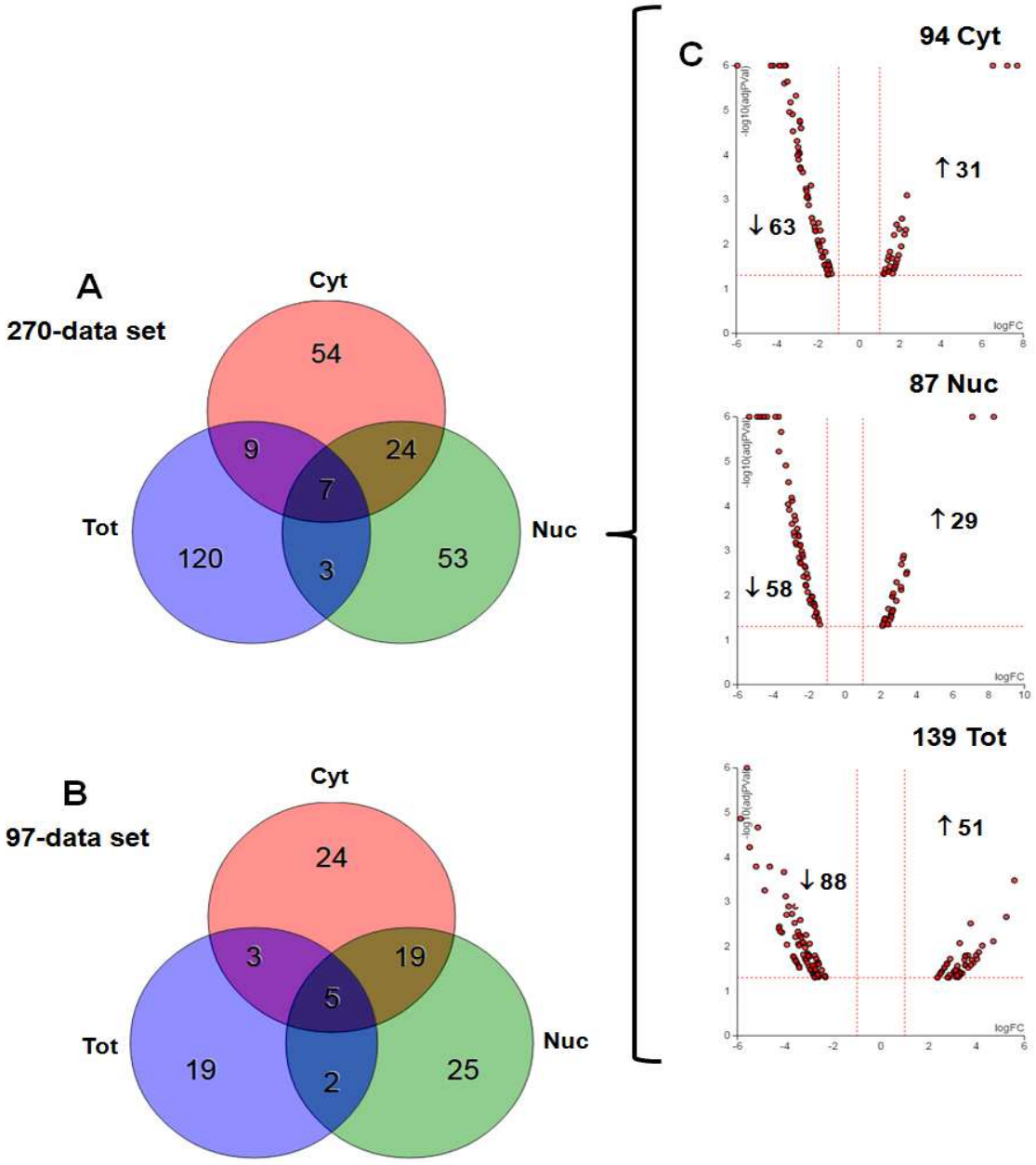

Figure 3-16: Distribution of the significant proteins over the three sample types in 270- and 97-TAM datasets.

Venn diagrams representing the distributions and the intersections over the three sample types for the sets of (A) 270 and (B) 97 significantly changed proteins, unique and/or shared in the CNT set. (C) Volcano plot**:** all 270 are DE proteins and represented in terms of their measured expression change (horizontal) and the significance of their change (vertical). The significance is represented in terms of the negative log of the p-value (i.e., larger number means more significant). The dotted lines represent the threshold used to select the DE genes: ±1 for expression change and 0.05 for significance.

3.2.1.3 Meta-analysis of the functional pathways

In the union of three individual mass spectrometry runs (replicates) of each sample type, there were 1704, 1487, and 2858 proteins with measured expression out of the total identified proteins in the C, N, and T sample types, respectively. These protein list were mapped to the approved gene symbols and reloaded into iPathway Guid software to compute the impact pathway analysis using two types of probability (p-value) :(i) pOVR for the DE proteins in a given pathway and (ii) the perturbation/accumulation p-value (pACC) that computes the perturbation of the given pathway considering not only the enrichment analysis of the DE proteins, but their topological information including direction and type of signals, position, and role in the pathway (more details see materials and methods).

In summary, 94, 78, 1nd 139 proteins (270-TAM) were selected as DE proteins (<0.05 and ±1 log2 FC) out total with measured expression in the C, N, and T sample types, respectively.

In these three sample types (CNT), there were 19 (C), 43 (N), and 28 (T) pathways found to be significantly impacted (Supplementary Table 7). The p-value was corrected for multiple comparison (meta analysis) using FDR (<0.05) for the number of significantly impacted pathways in each sample type (Figure 3-17). The top ranked pathways, in each sample type, were selected after eliminating false positives (5% FDR) (Table 3-5). This analysis showed that protein changes in abundance with 4-OHT across multiple conditions were involved in pathways related to metabolism, signal transduction, growth and proliferation, and development (see Supplementary Table 9).

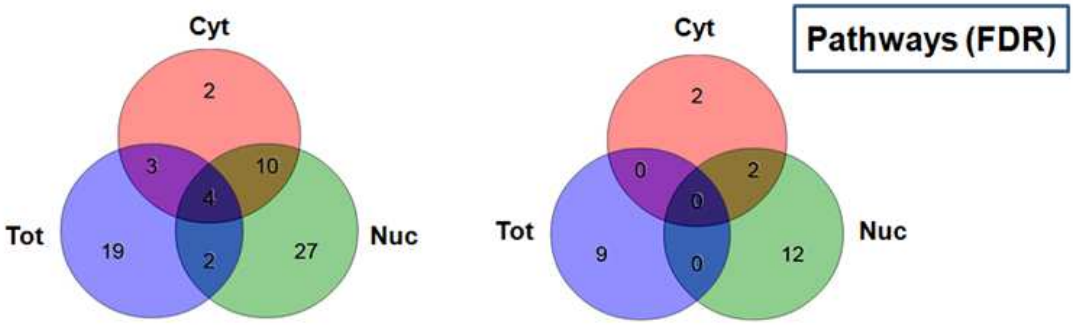

Figure 3-17: Meta analysis Venn diagrams of pathways that are in common or unique across low confidence data set, before and after p-value correction.

TAM-270 data set were filtered as to include the pathways found to be significantly impacted based on corrected p-value (FDR).

In the total lysate experiment (T), five top ranked pathways were identifed as signifcantly impacted and indicate that the significantly changed proteins constitute overrepresntation of metabolic pathways and oxidative phosophorylation (p = 9.1 e^{-05}), and fructose and mannose metabolism (p = 0.005). The protein alterations in the top two pathways were affecting the oxidative phosphorylation. Proteins that were upregulated/downregulated were belonging to the total lysate fraction (T) (Figure 3-18), wherase seven proteins, ALDOA (C), IDH1 (C), LDHA (S_n), MTCO2 (C,N), TKT (N,T), EBP (C), NANS (C,T), all of which were upregulated in the C and/or N fractions with or without change in total aboundance, and seven were downregulated CKMT2 (C), NDUFV3 (N), OAT (N), P4HA1 (C), TST (C,N), NNT (N), and PGLS (C), which were down-regulated in the subcellular fractions (S_n and/or S_c) without change in the total aboundance.

Table 3-5: Top KEGG pathways significantly impacted in the three sample types CNT (TAM-270 data set) and their associated corrected (FDR) p-values.

Cytoplasmic Fraction			
Pathway name	**Pathway Id**	**p-value**	**p-value (FDR)**
Hypertrophic cardiomyopathy (HCM) *	5410	**7.67E-05**	**0.008**
Dilated cardiomyopathy	5414	**3.16E-04**	**0.016**
Cardiac muscle contraction *	4260	**0.001**	**0.036**
Calcium signalling pathway	4020	**0.001**	**0.036**
Adrenergic signalling in cardiomyocytes	4261	**0.003**	0.052
Nuclear Fraction			
Pathway name	**Pathway Id**	**p-value**	**p-value (FDR)**
Circadian entrainment	4713	**6.20E-05**	**0.007**
Dilated cardiomyopathy	5414	**5.59E-04**	**0.016**
Adrenergic signalling in cardiomyocytes	4261	**0.001**	**0.018**
Hypertrophic cardiomyopathy (HCM) *	5410	**0.002**	**0.02**
Pathways in cancer	5200	**0.004**	**0.039**
Total Lysate Fraction			
Pathway name	**Pathway Id**	**p-value**	**p-value (FDR)**
Metabolic pathways *	1100	**9.48E-07**	**9.13E-05**
Oxidative phosphorylation *	190	**2.50E-06**	**9.13E-05**
Non-alcoholic fatty liver disease (NAFLD)	4932	**6.60E-06**	**1.78E-04**
ECM-receptor interaction	4512	**6.37E-05**	**0.001**
Fructose and mannose metabolism *	51	**3.55E-04**	**0.005**

*the p-value corresponding to the pathway was computed using only over-representation analysis.

Based on the statistical selection criteria (significance B <0.05), GSS (glutathione synthetase) was quantified in both C, T samples with significant upregulation in the T sample (S_t= 5.244 and p= 0.002), only. Hence, this protein was not quantified in the nuclear fraction; it was filtered out of the stringent list (97-TAM) showing the distribution of significance in the three sample types based on the selection criteria described in the material and method section.

GSS has a protective role in the cells, among other functions, that is to prevent the oxidative damage by oxidative stress. Notably, the proteins significantly down regulated were related to the oxidative phosphorylation pathway. Moreover, MTCO2 was shown significant increase in the C and N sample and NDUFV3 in N without change in the total abundance associated with either of the two proteins (Figure 3-18A).

The subcellular proteomics (C and N) results shows that the proteins that are related to regulation of the actin cytoskeleton, focal adhesion, adherens junctions were correlated with the overrepresentation of two pathways, in common (Figure 3-17), hypertrophic cardiomyopathy (HCM) -and dilated cardiomyopathy (Table 3-5). Most of the proteins that were affecting these pathways (ATP2A2, DES, DMD, ITGA3, MYBPC3, MYH6, MYL2, MYL3, TNNC1, and GNAS) were downregulated in the subcellular data sets (C and N); the exception was DMD that was decreased in all sample types (CNT) in both pathway and GNAS that was increased in the N sample and affecting the dilated cardiomyopathy (Figure 3-18B).

Furthermore, circadian entailment was significantly impacted (overrepresentation verses total perturbation) in N sample (P = 0.007) suggesting that altered proteins involved in this pathway (CALML3, GNAI2, GNAQ, GNAS, GNB1, GNB2, and CALML5) have a role in

the cell cycle and signal transduction; the distribution of significance of these proteins in the three sample types is shown in Figure 3-18C.

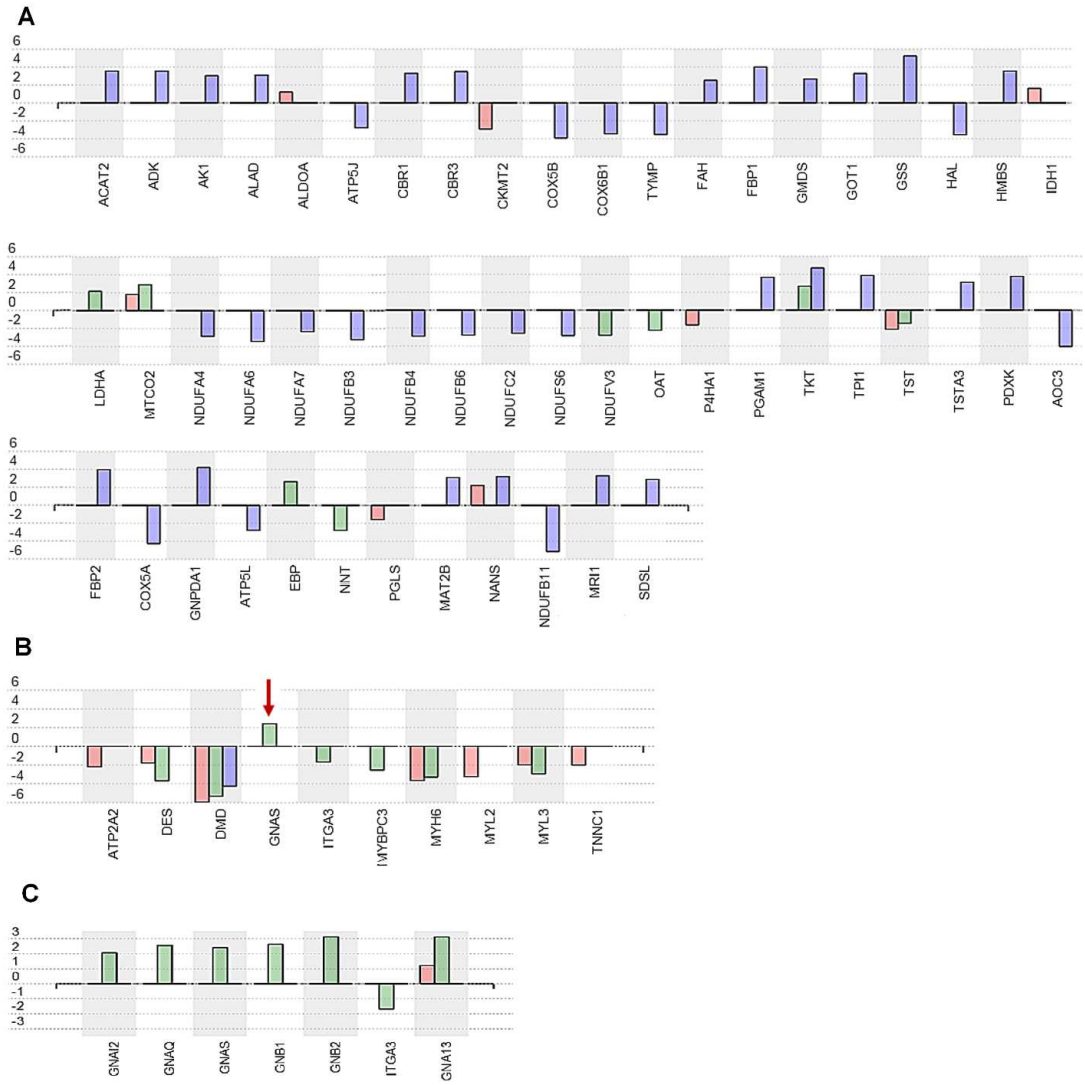

Figure 3-18: Identification of deregulated pathways.

Distribution of up- and down-regulation of total proteins (blue bar), nuclear proteins (green bar) and cytoplasmic proteins (red bar) in Metabolic pathway (A) and in Hypertrophic dilated cardiomyopathy (B) and circadian entailment (C). Note: The arrow indicates the extra protein present only in dilated cardiomyopathy.

A number of proteins show a possible correlation between the cross talk between pathways and the distribution of proteins in the three sample types enriched in our method.

The data shows that there would be a possible cross talk between pathways that related to the spatial distribution of DE proteins rather than overlapping between them. From the analytical results, it was found that the Pathway in cancer (p = 0.039) was significantly impacted in N sample with six Guanine nucleotide-binding proteins (G proteins) and ITGA3, all of which were upregulated in N fraction except ITGA3 was down regulated and GNA13 was significantly upregulated in C and N samples (Figure 3-19). Furthermore, four DE proteins that were identified in the T sample were downregulating ECM-receptor interaction pathway (p = 0.001). The total perturbation (overrepresentation verses total accumulation) was depicted by iPathway software showing down-regulation of integrin alpha 1/beta 1, however, ITGA3 was significantly decreased in the N, but not T or C samples (Figure 6). The crosstalk analysis of signal transduction pathways in breast cancer has identified number of DE genes were overlapped between ECM and Pathways in cancer pathways (Sun et al., 2015).

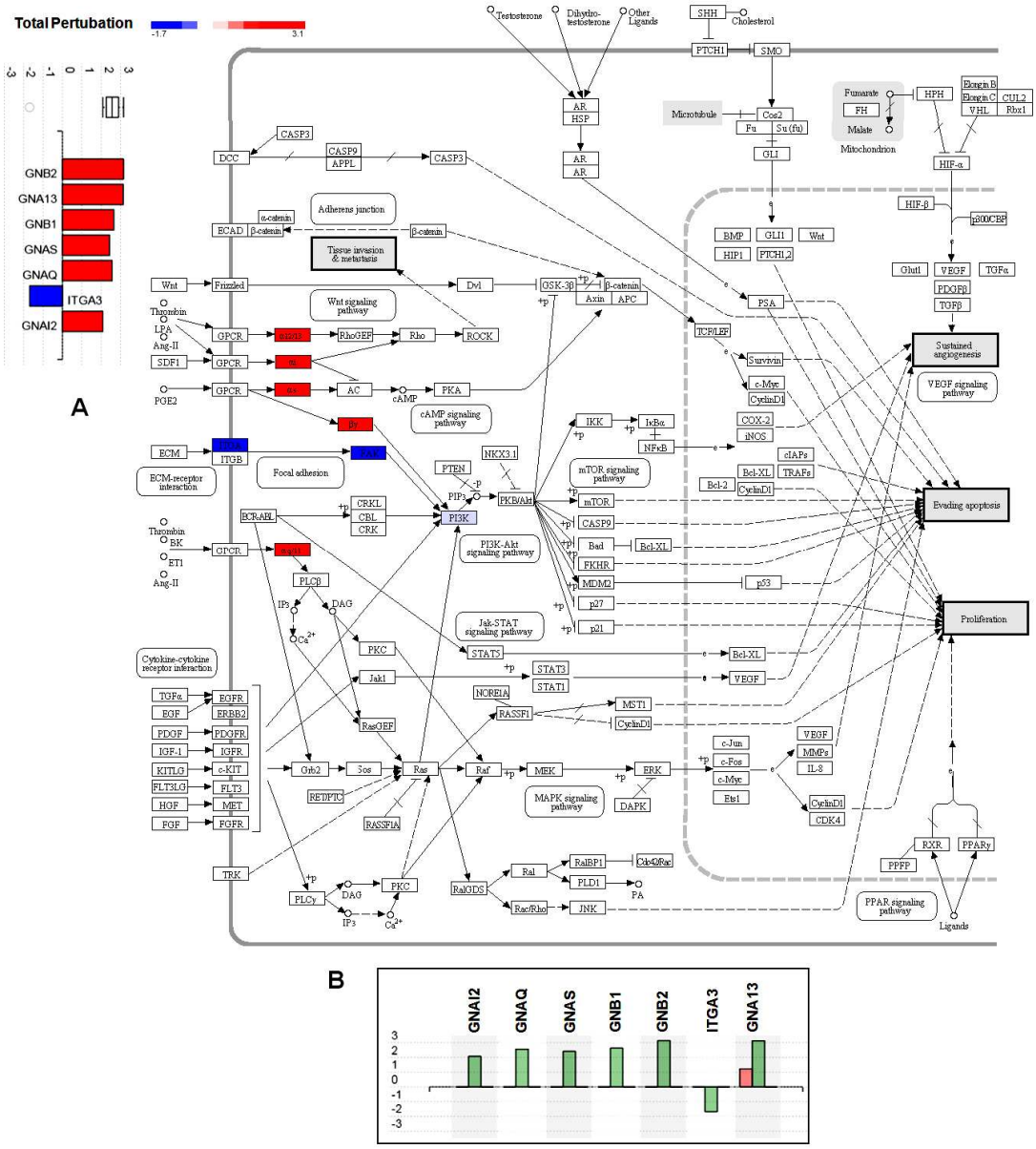

Figure 3-19: Enrichment of Pathways in cancer pathway (KEGG: 05200).

The pathway diagram is overlayed with the computed total perturbation of each gene. The total perturbation accounts both for the gene's measured fold change and for the accumulated perturbation propagated from any upstream genes which is referred to as total accumulation. The legend highlights the different gradients from the highest negative perturbation (dark blue) and, to the highest positive perturbation (dark red). (A) Gene perturbation bar plot: All the genes in Pathways in cancer pathway are ranked based on their absolute perturbation in the N sample. For each gene we represent the signed perturbation with negative values in blue and positive values in red. (B) Distribution of up- and down-regulation of total proteins (blue bar), nuclear proteins (green bar) and cytoplasmic proteins (red bar) in Pathways in cancer pathway.

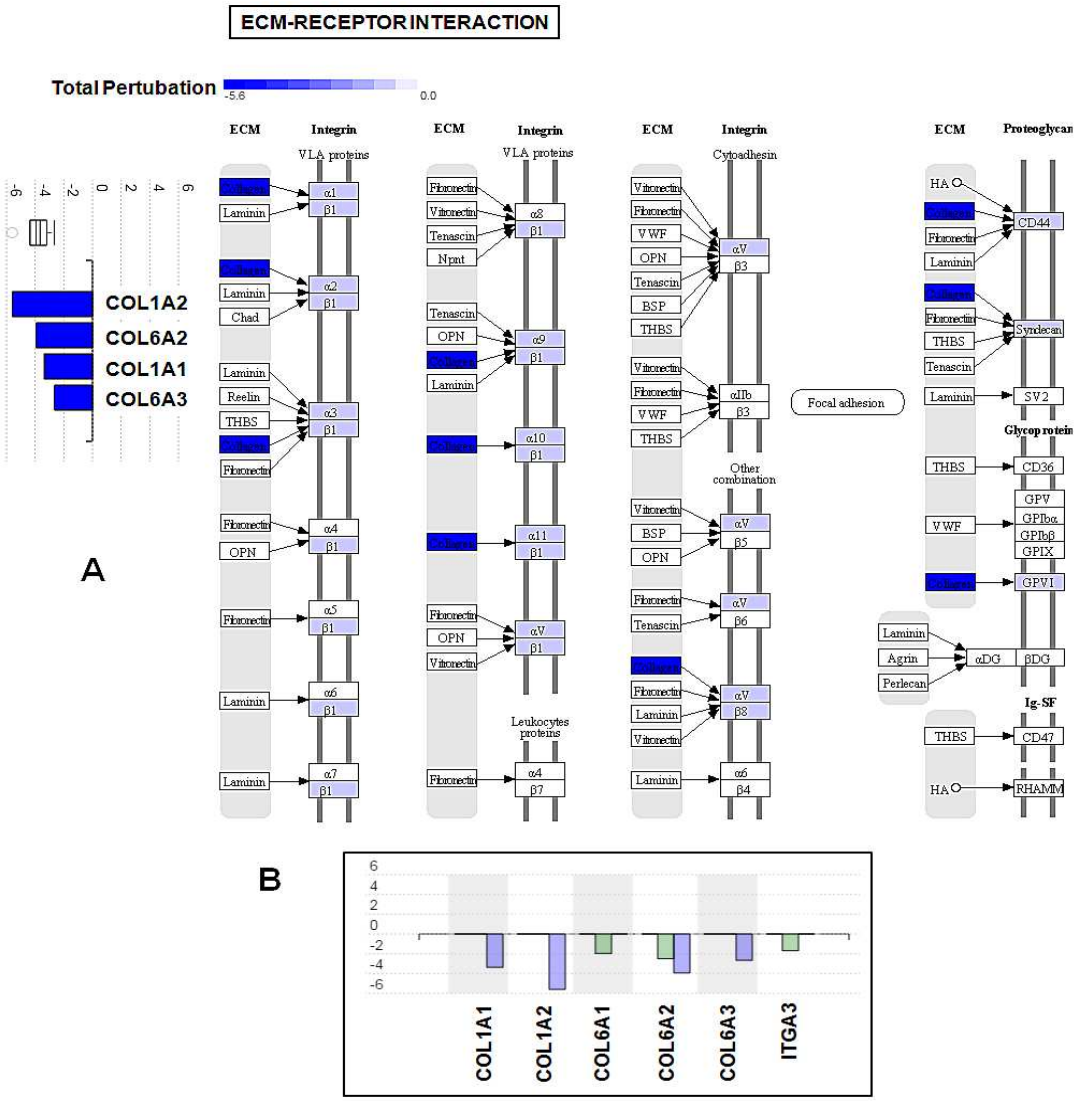

Figure 3-20: Enrichment of ECM-receptor interaction pathway (KEGG: 04512).

The pathway diagram is overlayed with the computed total perturbation of each gene. The total perturbation accounts both for the gene's measured fold change and for the accumulated perturbation propagated from any upstream genes which is referred to as total accumulation. The legend highlights the different gradients from the highest negative perturbation (dark blue) and to the highest positive perturbation (dark red). (A) Gene perturbation bar plot: All the genes in ECM-receptor interaction pathway are ranked based on their absolute perturbation in the T sample. For each gene we represent the signed perturbation with negative values in blue and positive values in red. (B) Distribution of up- and down-regulation of total proteins (blue bar), nuclear proteins (green bar) and cytoplasmic proteins (red bar) in ECM-receptor interaction pathway.

3.2.1.4 GO enrichment analysis

We used the approval gene symbols to upload the proteomics data; therefore, to refer to protein belonging to specific gene, we used the gene expression term in this section, instead of protein expression. In the classical approach of GO annotation, all GO terms considered to be independent; i.e., considering the hierarchical structure of GO terms, the list of genes annotated to a specific term are also annotated to all ancestors in the hierarchy of that term. To overcome this problem, iPathway Guide software uses Elim method that iteratively removes the genes mapped to significant GO terms from more general (higher level) GO terms (Alexa et al., 2006). Figure 3-21A and B show the number of GO terms was reduced in all three samples after imposing Elim correction method compared to the number before correction, thus unnecessary redundancy was removed.

Biological process (BP) annotation of genes by subcellular fractionation (C and N) revealed significant enrichment for a interaction process of myosin located on a thick filament with actin, signal transduction, growth and development, and apoptotic process. Whereas, among the top ranked five BP/MF enriched with the DE genes were related to cellular respiratory system, metabolism, protein synthesis, in the total lysate sample (T), the number of overlapped, top ranked, BP/MF were detected among all fractions that are related to the distribution of significance of the identified DE genes (Figure 3-21A and B). Of these is RAGE receptor binding (4DE/6ALL), (3DE/4ALL), and (4DE/6ALL) in C, N, and T, respectively; three out of four proteins involved in MF were down regulated in all down regulated in all sample types (S100A7, S100A8, and S100A9), whereas S100A13 was upregulated in T sample, only. However, Toll-like receptor 4 binding function was enriched

in the C, T, N (2DE/2ALL), where two proteins were significantly reduced in all sample types (S100A8 and S100A9). The distribution of significance in the proteins that are involved cell growth, apoptotic process, platelet activation, cellular respiration biological processes (BP) in the three sample types are shown in Figure 3-22.

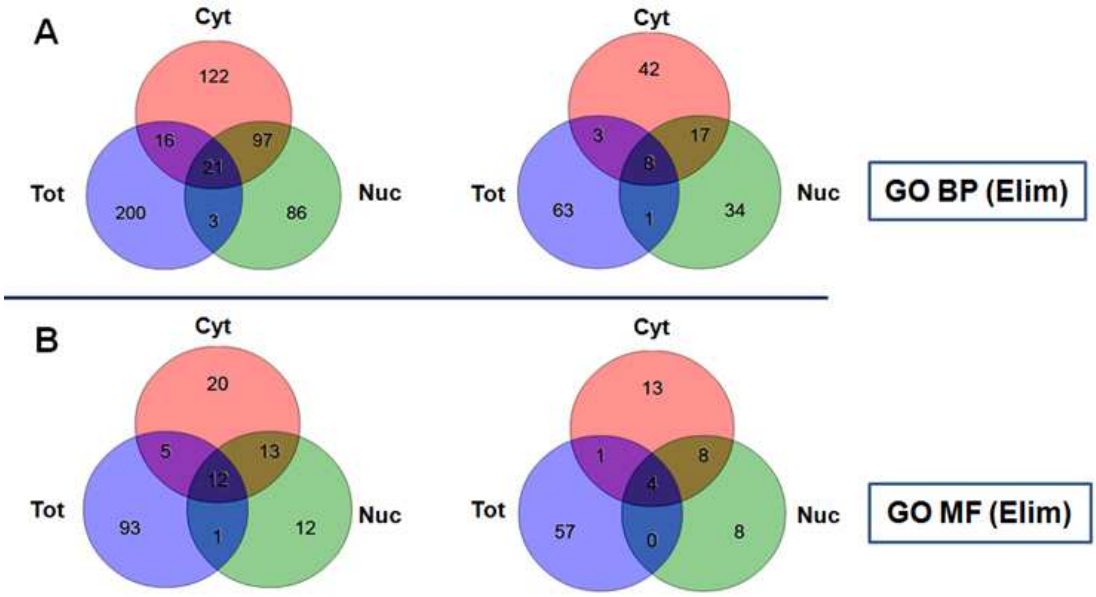

Figure 3-21: Metanalysis venn diagrams of GO terms that are in common or unique across low confidence data set, before and after p-value correction.

TAM-270 data set were filtered as to include the biological process (A) and molecular function (B) GO found to be significantly enriched based on corrected p-value (Elim pruning).

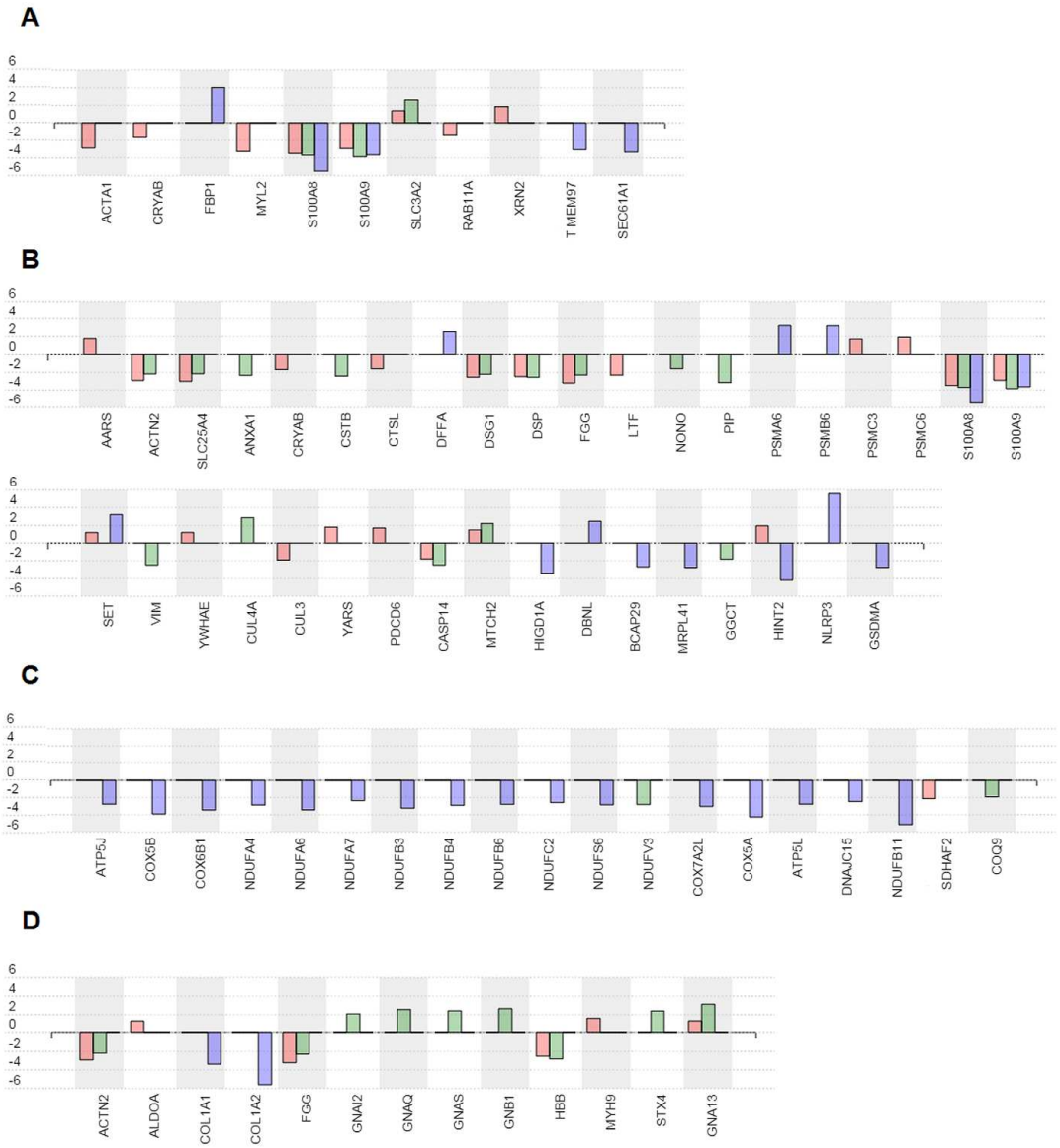

Figure 3-22: Gene ontology enrichment.

All the DE genes that are annotated to (A) cell growth (GO-0016049), (B) apoptotic process (GO-0006915), (C) respiratory electron transport (GO-0022904), and (D) platelet activation (GO 0030168). The distribution of significance in the three sample types is shown as total proteins (blue bar), nuclear proteins (green bar) and cytoplasmic proteins (red bar).

Table 3-6: Top GOBP and MF significantly enriched in the three sample types CNT (TAM-270 data set) and their associated corrected (FDR) p-values (Elim method).

GO:BP	# genes (DE/ALL)	p-value	GO:BP	# genes (DE/ALL)	p-value	GO:BP	# genes (DE/ALL)	p-value
Cytoplasmic Fraction (C)			**Nuclear Fraction (N)**			**Total Lysate (C)**		
muscle filament sliding	**8** / 13	**4.20E-08**	muscle filament sliding	**8 / 15**	**3.20E-07**	mitochondrial electron transport, NADH to ubiquinone	**9** / 34	**8.70E-05**
signal transduction	**38** / 462	**0.004**	sarcomere organization	**4 / 9**	**0.00093**	protein heterotrimerization	**3** / 4	**3.80E-04**
cell growth	**8** / 40	**0.007**	adenylate cyclase-activating G-protein coupled receptor signalling pathway	**4 / 5**	**0.003**	respiratory electron transport chain	**16** / 75	**0.002**
epidermis development	**9** / 26	**0.028**	platelet activation	**9 / 40**	**0.003**	gluconeogenesis	**5** / 28	**0.008**
apoptotic process	**21** / 242	**0.044**	energy reserve metabolic process	**5 / 20**	**0.004**	extracellular matrix disassembly	**4** / 19	**0.01**
GO:MF	**# genes (DE/ALL)**	**p-value**	**GO:MF**	**# genes (DE/ALL)**	**p-value**	**GO:MF**	**# genes (DE/ALL)**	**p-value**
calcium ion binding	**16** / 69	**2.80E-07**	G-protein beta/gamma-subunit complex binding	**4 / 6**	**1.30E-04**	RAGE receptor binding	**4** / 6	**5.30E-05**
structural constituent of muscle	**4** / 10	**0.001**	calcium ion binding	**10 / 54**	**0.00059**	cytochrome-c oxidase activity	**5** / 11	**6.00E-05**
RAGE receptor binding	**3** / 6	**0.003**	RAGE receptor binding	**3 / 4**	**0.00067**	structural constituent of ribosome	**13** / 117	**0.002**
neutral amino acid transmembrane transporter activity	**2** / 2	**0.003**	signal transducer activity	**8 / 42**	**0.002**	Toll-like receptor 4 binding	**2** / 2	**0.002**
Toll-like receptor 4 binding	**2** / 2	**0.003**	Toll-like receptor 4 binding	**2** / 2	**0.003**	fructose 1,6-bisphosphate 1-phosphatase activity	**2** / 2	**0.002**

3.2.1.5 Changes in subcellular compartments abundance and the impact on the functional pathways

For the 97 set of proteins (reliable data set), we carried out an additional pathway analysis, using a public data base (InnateDB) that incorporated Reactome, and we conducted pathway analysis to envisage the possible role/impact of the distribution of proteins on the systematic biological perturbations (Supplementary Table 12). The top pathways of upregulated proteins for the three sample types (CNT) are shown in (Table 3-7) and the highest ranked down regulated pathways are shown in (Table 3-8) with the deregulated proteins enriched in each pathway. Pathways that are related to signal transductions, growth, and development are regulated (up/down) mostly due to changes in the subcellular compartmental proteins (C and N) rather than total changes. The total response (T) as revealed from the top ranked pathways reflects changes in the metabolic processes associated with appreciable change that we observed in the subcellular compartments. In the most of metabolic pathways, total proteins were strongly downregulated, e.g. in TCA cycle and respiratory electron transport, and upregulated for others, e.g. metabolism of carbohydrates.

Among the top ranked downregulated pathways, different distribution in the downregulation of 12 pathways was observed for the cytoplasm (50%), nucleus (less than 10%) and total lysate (more than 40%) (Table 3-8).

The most of proteins associated to metabolic pathways (Table 3-5) were similarly identified by Reactome pathway analysis, which confirmed their subcellular distribution in the detected compartment, *e.g.* ALDOA ($\uparrow S_c$), MTCO2 ($\uparrow S_c$, $\uparrow S_n$), OAT ($\downarrow S_n$), LDHA ($\uparrow S_n$), COX 5A ($\downarrow S_t$), ATP5L ($\downarrow S_t$), NDUFA4 ($\downarrow S_t$), NDUFB6 ($\downarrow S_t$). The same similarity was observed for other proteins, e.g. GNAS ($\uparrow S_n$), GNB1 ($\uparrow S_n$), MYL3 ($\downarrow S_c$, $\downarrow S_n$), ITG3 ($\downarrow S_n$), as some of

these proteins representing a cross talk scenario as depicted from pathway analysis using iPathwayGuid software.

Within the reliable data set (97-TAM) set, interestingly some proteins (20%) were shared between nucleus and cytoplasm (Table 3-4) sowing no changes in the total abundances. Among these proteins, 14 proteins were downregulated and 5 were upregulated for cytoplasm and nucleus compartments (Table 3-4). The distribution calculations (S_n/S_c) and the GOCC (cellular components), of the 19 set of proteins are shows in Table 3-9. This set of proteins showed strong changes in nuclear and cytoplasmic abundance without showing any significant change of total abundance.

Quantitative data show that, after the Tamoxifen stimulation, a marked decrease of compartmental abundance were recorded for CASP14 with a more than 4-fold decrease in the nuclear compartments (S_n -2.488107, p-value 0.000767178) and a more than 2-fold decrease in the cytoplasmic one (S_c -1.787169, p-value 0.008297533). In absence of changes in total abundance, CASP14 was significantly redistributed in cytoplasm (N → C). Otherwise, for MTCO2 protein, a greater 4-fold increase of nuclear abundance (S_n 2.873302, p-value 0.0051) at the expense of cytoplasmic one (S_c 1.819, p-value 0.0036) pointed out an opposite redistribution C → N. These relevant proteins, CASP14 and MT-CO2, were also chosen for MS validation by confocal microscopic analysis (Figure 3-11Figure 3-12).

Table 3-7: Top ranking overrepresented upregulated reactome pathway (TAM-97) (Innate DB).

Condition	Pathway Name	Pathway uploaded gene count	Pathway up-regulated genes count	Pathway up-regulated p-value	Genes (Symbol|Subcellular distribution of significance) UP:Down:No change
Sn	Hemostasis	10	6	0.00184052	ALDOA|Sc:Sn:St; ATP2A2|Sc:Sn:St; GNA13|Sc:Sn:St; GNAS|Sc:Sn:St; GNB1|Sc:Sn:St; GNB2|Sc:Sn:St; HBB|Sc:Sn:St; ITGA3|Sc:Sn:St; SLC3A2|Sc:Sn:St; STX4|Sc:Sn:St;
St	Disease	11	5	0.003473005	ALDOA|Sc:Sn:St; CYB5R3|Sc:Sn:St; GNB1|Sc:Sn:St; PGAM1|Sc:Sn:St; PSMA6|Sc:Sn:St; PSMB6|Sc:Sn:St; PSMC6|Sc:Sn:St; RPLP1|Sc:Sn:St; SLC25A4|Sc:Sn:St; TKT|Sc:Sn:St; TPI1|Sc:Sn:St;
Sn	GPCR downstream signaling	5	4	0.00347368	ANXA1|Sc:Sn:St; GNA13|Sc:Sn:St; GNAS|Sc:Sn:St; GNB1|Sc:Sn:St; GNB2|Sc:Sn:St;
Sn	Integration of energy metabolism	5	4	0.00347368	GNAS|Sc:Sn:St; GNB1|Sc:Sn:St; GNB2|Sc:Sn:St; SLC25A4|Sc:Sn:St; TKT|Sc:Sn:St;
Sn	Platelet activation, signaling and aggregation	5	4	0.00347368	ALDOA|Sc:Sn:St; GNA13|Sc:Sn:St; GNB1|Sc:Sn:St; GNB2|Sc:Sn:St; STX4|Sc:Sn:St;
St	Metabolism of carbohydrates	4	3	0.005725846	ALDOA|Sc:Sn:St; PGAM1|Sc:Sn:St; TKT|Sc:Sn:St; TPI1|Sc:Sn:St;
St	Metabolism	26	7	0.010673624	ALDOA|Sc:Sn:St; ATP5L|Sc:Sn:St; CA2|Sc:Sn:St; COX5A|Sc:Sn:St; COX5B|Sc:Sn:St; CYB5R3|Sc:Sn:St; FAM36A|Sc:Sn:St; GNAS|Sc:Sn:St; GNB1|Sc:Sn:St; GNB2|Sc:Sn:St; HBA2|Sc:Sn:St; HBB|Sc:Sn:St; LDHA|Sc:Sn:St; MT-CO2|Sc:Sn:St; NDUFA4|Sc:Sn:St; NDUFB6|Sc:Sn:St; OAT|Sc:Sn:St; PGAM1|Sc:Sn:St; PSMA6|Sc:Sn:St; PSMB6|Sc:Sn:St; PSMC6|Sc:Sn:St; SLC25A4|Sc:Sn:St; TKT|Sc:Sn:St; TPI1|Sc:Sn:St; TST|Sc:Sn:St; TXNRD1|Sc:Sn:St;
St	Cell Cycle, Mitotic	5	3	0.013346428	PSMA6|Sc:Sn:St; PSMB6|Sc:Sn:St; PSMC6|Sc:Sn:St; SET|Sc:Sn:St; YWHAE|Sc:Sn:St;
Sn	Aquaporin-mediated transport	4	3	0.018559377	GNAS|Sc:Sn:St; GNB1|Sc:Sn:St; GNB2|Sc:Sn:St; RAB11A|Sc:Sn:St;

Table 3-8: Top ranking overrepresented downregulated reactome pathway (TAM-97) (Innate DB)

Condition	Pathway Name	Pathway uploaded gene count	Pathway down-regulated genes count	Pathway down-regulated p-value	Genes (Symbol|Subcellular distribution of significance) UP:Down:No change
St	Respiratory electron transport	7	6	4.54E-05	ATP5L|Sc:Sn:St; COX5A|Sc:Sn:St; COX5B|Sc:Sn:St; FAM36A|Sc:Sn:St; MT-CO2|Sc:Sn:St; NDUFA4|Sc:Sn:St; NDUFB6|Sc:Sn:St
St	The citric acid (TCA) cycle and respiratory electron transport	8	6	1.67E-04	ATP5L|Sc:Sn:St; COX5A|Sc:Sn:St; COX5B|Sc:Sn:St; FAM36A|Sc:Sn:St; LDHA|Sc:Sn:St; MT-CO2|Sc:Sn:St; NDUFA4|Sc:Sn:St; NDUFB6|Sc:Sn:St
Sn	Striated Muscle Contraction	4	4	0.013796563	DES|Sc:Sn:St; MYBPC3|Sc:Sn:St; MYH6|Sc:Sn:St; MYL3|Sc:Sn:St
St	Orphan transporters	4	3	0.014456399	COX5A|Sc:Sn:St; COX5B|Sc:Sn:St; FAM36A|Sc:Sn:St; MT-CO2|Sc:Sn:St
St	SRP-dependent cotranslational protein targeting to membrane	2	2	0.027329193	RPLP1|Sc:Sn:St; SSR4|Sc:Sn:St
St	Translation	2	2	0.027329193	RPLP1|Sc:Sn:St; SSR4|Sc:Sn:St
Sc	Striated Muscle Contraction	4	3	0.034965836	DES|Sc:Sn:St; MYBPC3|Sc:Sn:St; MYH6|Sc:Sn:St; MYL3|Sc:Sn:St
Sc	Apoptotic cleavage of cell adhesion proteins	2	2	0.049689441	DSG1|Sc:Sn:St; DSP|Sc:Sn:St
Sc	Apoptotic cleavage of cellular proteins	2	2	0.049689441	DSG1|Sc:Sn:St; DSP|Sc:Sn:St
Sc	Apoptotic execution phase	2	2	0.049689441	DSG1|Sc:Sn:St; DSP|Sc:Sn:St
Sc	Binding and Uptake of Ligands by Scavenger Receptors	2	2	0.049689441	DSG1|Sc:Sn:St; DSP|Sc:Sn:St
Sc	Scavenging of heme from plasma	2	2	0.049689441	DSG1|Sc:Sn:St; DSP|Sc:Sn:St

Table 3-9: List of 19 proteins showing significant changes in compartmentalized abundance (S_c, S_n), in the absence of significant changes in total fraction.

Gene symbol	GO-Cellular component	S_c Union	S_n Union	$\log(S_n/S_c)$	Distribution
SLC3A2	Nucleus, cytoplasm, plasma membrane, membrane, extracellular vesicular exosome	1.396	2.637	1.241	C→N
MT-CO2*	Mitochondrion, mitochondrial inner membrane, membrane, extracellular vesicular exosome	1.819	2.873	1.054	C→N
MYL3	Cytosol	-1.976	-2.952	-0.977	N→C
SLC25A4	Nucleus, mitochondrion mitochondrial inner and plasma membrane	-3.033	-2.169	0.864	C→N
MYH6	Nucleus, cytoplasm, cytosol	-3.649	-3.297	0.352	C→N
DSP	Nucleus, mitochondrion, cytoskeleton intermediate filament plasma membrane, cell-cell junction extracellular vesicular exosome	-2.494	-2.575	-0.081	N→C
DES	Cytoplasm, cytosol, cytoskeleton	-1.803	-3.688	-1.885	N→C
CASP14*	Nucleus, cytoplasm, extracellular vesicular exosome	-1.787	-2.488	-0.701	N→C
HBB	Extracellular region, cytosol, extracellular vesicular exosome	-2.522	-2.812	-0.291	N→C
HBA2	Extracellular region, cytosol, extracellular vesicular exosome	-2.824	-4.035	-1.211	N→C
DCD	extracellular region, extracellular vesicular exosome	-3.879	-4.513	-0.634	N→C
DSG1	Cytosol, plasma membrane, membrane, cell-cell junction, extracellular vesicular exosome	-2.571	-2.212	0.359	C→N
DSC1	Plasma membrane, membrane, gap junction, extracellular vesicular exosome	-2.594	-2.606	-0.012	N→C
GNA13	Nucleus, plasma membrane, membrane extracellular vesicular exosome	1.221	3.130	1.909	C→N
TST	Extracellular space, mitochondrion, mitochondrial inner membrane, mitochondrial matrix, extracellular vesicular exosome	-2.131	-1.456	0.675	C→N
FUBP1	Nucleus	-1.798	-2.080	-0.282	N→C
LYAR	Nucleus, nucleolus	7.707	7.096	-0.611	N→C
CALML5	extracellular vesicular exosome	-2.752	-2.972	-0.220	N→C
MTCH2	Nucleus, mitochondrion, mitochondrial inner membrane, membrane, extracellular vesicular	1.489	2.220	0.730	C→N

Chapter 4 Discussion

4.1 Part-I: Spatial dynamics in response to oestrogen-stimulated breast cancer cell line (MCF-7)

Overall, the present results indicate that substantial changes in protein abundance in the nuclear/cytoplasmic compartments are observed for about ten times more proteins than those that show large changes in total cellular abundance. To put it plainly, the prevailing outcome of the exposure of MCF-7 cells to E2 shows broad relocation of the labelled subcellular proteins as opposed to alterations in their aggregate abundance. To address this, the following discussion covers three parts corresponding to the three main themes of this work: (1) Assess the suitability and robustness of subcellular spatial razor for examination of this predominant cell response and compare the changes on three consecutive fractions (CNT); (2) To address the relationship between protein subcellular localizations and the reconciliation of cell utilitarian networks, particularly in association with the nuclear hormone receptors; (3) conceivable ramifications related to cancer.

4.1.1 Cellular function and the properties of the spatial razor

The present results show a strong preponderance in the number of proteins with appreciable N → C redistribution following exposure of MCF7 cells to estradiol. It is important to emphasize that this does not imply that the total mass of nuclear proteins is dramatically decreased, and in fact, the present results could still be consistent with an increase in the total mass of nuclear proteins. This is on the grounds that the discrete proteins possess altogether dissimilar cellular abundances and altogether diverse basal skewing between cytoplasm and nucleus. Subjectively, four noteworthy classes of proteins can be recognized in the present results (Figure 3-7). (a) Proteins show observable changes in the total abundance without changes in the subcellular compartmentalization, suggesting minor functional role for these proteins in the cellular response. (b) Proteins for which their reduced levels of expression were predominantly observed in the nucleus, for the majority of this subset there were limited changes in the cytoplasmic fraction (Figure 3-7), i.e. little extents of cytoplasmic proteins located at the nucleus are deported after E2 stimulation. (c) Proteins that are characterized, in this study, with the major increase in the abundance limited to the cytoplasm were associated with minor changes in the nuclear abundance, indicating that nuclear proteins are expelled to the cytoplasm (Figure 3-7). (d) Proteins that exhibit generous changes in abundance in both compartments, just a minority of which (10 of 77, Figure 3-7A) show >2-fold changes in both compartments.

We propose (see below) that proteins in classes (b) and (c) represent messengers that transmit information about cellular state between the nucleus and other subcellular locations, and note that although they involve smaller proportions of proteins, their influence on cellular function can be important due to strong nonlinearities in cellular function.

The last category of proteins in class (d) involves set of proteins that may have importance to check and balance the overall functions states; this property is not necessarily limited to E2 stimulation and may have relevance to the numerous incitements (see below). A noteworthy observation is that spatial razor model has helped the detection of the proteins in classes (b) – (d); these limits of changes are basically imperceptible in estimations of total abundance by proteomics or transcriptomics methods. Furthermore, the preservation of mass test in the spatial razor model gives an exceptionally solid filter to distinguish and recognize the reliable changes in abundance at various subcellular locations, regardless of the fact that minor extents of the total protein abundances are included.

The frame work presented in this study aims to improve and validate proteomics extraction protocols, however, there will be a room for continues improvements in terms of experimental design, subcellular fractions, complete protein extraction, and sample preparation.

In general, the present results and various other late results on the static and dynamic subcellular spatial dissemination of proteins (see below) propose that dynamic spatial proteins relocation is an essential phenomenon that enables the cells to react in response to either internal or external stimuli, and that it ought to be considered in frameworks investigating the system biology.

4.1.2 Protein subcellular distribution and integration of function

There is increasing evidence that substantial proportions of cellular proteins have multiple subcellular locations and may have different functional roles in different locations. This is implicit in available database information where, for example, 36% of human proteins with current GO CC annotation show multiple locations at the level {nucleus, cytoplasm, plasma membrane, and extracellular region}. There are multitudinous researches demonstrating that particular alteration in protein locations is associated with alteration in functional capacities of that protein in response to cellular environment. For instance, many of the proteins required in the glycolysis/gluconeogenesis enzymatic course are known to have distinctive functions in the nucleus (Qattan et al., 2012), incorporating into processes associated with hypoxia, cellular proliferation, and cancer (Luo and Semenza, 2011, Vander Heiden et al., 2010). Furthermore, large scale systematic dynamic changes of the subcellular proteins associated with cell response/capacity is being tracked and recorded. For instance, more than 200 yeast proteins required in an extensive variety of cellular functions display subcellular spatial translocation in response to hypoxia (Henke et al., 2011). The researchers also demonstrated that an assortment of proteins represent changes in the nucleus/cytoplasm dispersion are observed when human fibroblasts (IMR90 cells) are exposed to the cell cycle arrest at the original enactment checkpoint (Mulvey et al., 2013) or to oxidative stress (Baqader et al., 2014). In short, dynamic changes in the subcellular distribution of numerous proteins in response to cellular environment are an increasingly well established phenomenon. It is noteworthy that in these previous studies 2–5% of monitored proteins were found to show appreciable spatial redistribution in response to various stimulations. The roughly 20% of proteins for which such redistribution was detected in the present experiments is so far a striking outlier, which may reflect that MCF7 cells are cancer cells.

There is a clear need for many more global studies of dynamic protein distribution for a variety of cell types and functional contexts.

In current research, the principle question for the more than 230 proteins of sorts (b) and (c) that we recognized (Figure 3-7A) is: do the extents of these proteins in the "wrong" location in respect to their characterized predominant location/functions have a significance alteration to the functional role of the redistributed proteins? This can at last just be answered by further examinations focused on these proteins; yet we note that the idea of moonlighting proteins (Jeffery, 2009) has been has been extensively studied for more than ten years. One of the proteins that has been clearly distinguished as moonlighting protein that have distinctive function at different locations is GADPH. Some of these functions are (a) controlling cell cycle and transcriptional activity (He et al., 2012, Zheng et al., 2003), (b) forming a complex with a hypoxia inducible Siah, an E3-ubiquitin-ligase, causing the translocation of this complex to the nucleus and consequent enhancement of the cellular apoptosis/dysfunction (Hara and Snyder, 2006, Tristan et al., 2011), and (c) interaction with apurinic/apyrimidinic endonuclease (APE1), leading to the DNA repair functions and to a role in maintaining the integrity of the genome (Azam et al., 2008). Many authors have provided the scientific evidences for multifunctional roles of GAPDH in different subcellular locations (Sirover, 2012, Tristan et al., 2011). Other recently elucidated examples of crucial moonlighting proteins are the glycolytic enzymes PKM2 and PFKFB3. Nuclear PKM2 is crucial to the response to hypoxia through participation in transcription complexes with HIFα, (Luo and Semenza, 2011), regulates β-catenin (Yang et al., 2011), and as a a coactivator for Oct4 transcriptional complexes (Lee et al., 2008), may likewise have other nuclear functions. Additionally, nuclear PFKFB3 seems to be essential for cyclin-dependent kinase (CDK) regulated cell cycle and proliferation (Yalcin et al., 2009) and in adjusting

glutamine/glycolysis use over the cell cycle, incorporating into growth of cancer cells (Colombo et al., 2011).

Such moonligting activities are not often feasiable from the presenetly defined protein topology networks, most of those proteins have been distinguished, individually, as case by case. The subcellular spatial razor approach would help to reveal much information and provides a platform for systematic discovery of such proteins. In the present work, an analysis of subcellular proteomics results reveals that many more proteins might be candidates for being moonlighting class in the nucleus that are crucial to specific cellular functions. For example, upon exposure to E2, NQO1 displayed ~ 4-fold reduction in the nucleus and relocalization to the cytoplasmic participation in regulation of the ornithine decarboxylase complex (ODC) and hence participation in polyamine metabolism (Asher et al., 2005). In addition, the influence of ODC on ERα expression (Zhu et al., 2012), suggests potentialy moonlighting roles for this protein.There is some evidence consistent with nuclear "moonlighting" roles for NQO1; it is localized primarily in the cytoplasm, but it has been observed associated with mitotic spindles in the nuclei of a variety of human cells where it has been suggested to possibly play roles in protection against electrophic quinones, aid in the generation of oxidized pyridine nucleotides or shield selected proteins from proteasomal degradation (Siegel et al., 2012). There are many examples of “moonlighting candidates” obtained in the current study such as PARK7 and the 5 enzymes of glycolysis that redistribute to the cytoplasm following estradiol exposure. Furthermore, there were further 60 proteins in the 134-set that Reactome did not place in known functional networks and which might represent “moonlighting” activities.

The present data also suggest that there may be protein complexes and individual proteins that are involved in more general balancing of cellular function. The demonstration that

numerous proteasomal proteins redistribute in response to estradiol and the participation of these proteins in numerous critical functions in both the cytoplasm and nucleus (Table 3-2) suggests that redistribution of proteasomal subunits may represent general mechanisms for balancing different cellular functions at different subcellular locations. Proteasomal degradation of ERα is important to response to estradiol and it may be that the complexity of this (Alarid, 2006, Le Romancer et al., 2011, Nonclercq et al., 2007) reflects subcellular mobility of proteasome components in addition to many other influences. The redistribution of the CCT protein-folding complex between the nucleus/cytoplasm (Table 3-2) may be another such example. Nuclear import and/or activity of some proteins, including nuclear hormone receptors (Echeverria and Picard, 2010, Renoir, 2012), involves chaperone-assisted processes and nucleo-cytoplasmic redistribution of the CCT complex is also observed in the response of primary human fibroblasts to oxidative stress. We also observed redistribution between the nucleus/cytoplasm of numerous chaperones (HSP90B1, HSPA9, HSPB1, HSP90AA1, HSP90AB1, HSPA6, HSPA8, Supplementary Table 2) and HSP90 chaperones are known to play key roles in nucleo-cytoplasmic trafficking of nuclear hormone receptors (Echeverria and Picard, 2010, Renoir, 2012). A similar balancing role may be played by some highly abundant proteins such as the human transcriptional positive coactivator PC4 (mammalian orthologue of yeast SUB1), which has established roles in multiple cellular functions involving stabilization of DNA−protein interactions, chromatin organization, transcriptional activation and repression, DNA elongation, reinitiation and DNA replication and repair (Conesa and Acker, 2010, Das et al., 2006, Malik et al., 1998). This was one of the few proteins to show C ➔ N redistribution (without change in total abundance), a phenomenon that we have previously also observed in the response of primary human fibroblasts to cell cycle arrest at the origin activation checkpoint (Mulvey et al., 2013).

Although not usually discussed as “moonlighters”, nuclear hormone receptors are inveterate subcellular travellers that have a plethora of nuclear, cytoplasmic, plasma membrane and mitochondrial activities associated with their mobility. ERs regulate the expression of numerous nuclear genes (Frasor et al., 2003, Marino et al., 2006). ERs have plasma membrane interactions that involve numerous kinase-dependent signalling pathways (Heldring et al., 2007, Le Romancer et al., 2011, Madak-Erdogan et al., 2008, Renoir, 2012), and there is increasing evidence that these signalling pathways are critical for acquired resistance to therapeutic compounds (Iorns et al., 2008, Yeh et al., 2013). Cooperative organization of nuclear and mitochondrial ERs and their coactivators may have crucial influences on regulation of the mitochondrial respiratory chain (Chen et al., 2009). Many of these activities seem to be directly associated with subcellular mobility of ER and other proteins. For example, efflux of ERα from the nucleus is associated with repression of cell cycle progression and S-phase proliferation in MCF-7 cells (Castoria et al., 2009, Lombardi et al., 2008).

We note that in general nuclear hormone receptors (NHRs) show many of the characteristics that would be expected for proteins with important roles in “polling”, integrating and balancing functions occurring at different subcellular locations. They appear to shuttle between different locations and may have many different localization determinants, e.g. different nuclear import/export sequences and pathways (Echeverria and Picard, 2010, Mavinakere et al., 2012) including ERα (Renoir, 2012). They are often subject to a large variety of post-translational modifications.

In the case of ERα these include phosphorylation, acetylation, ubiquitination, sumoylation, methylation, and palmitoylation in at least 22 sites (Le Romancer et al., 2011). Many of these sites are subject to alternative types of modifications and/or modification by alternative kinases in the case of phosphorylation (Le Romancer et al., 2011). It is possible that such post-translational modifications relay information about functional state between different functions/subcellular locations either directly by "carrier" NHRs or indirectly via the subcellular localization of the proteins executing the modifications. The lifetime of NHRs may also be consistent with continuous "polling" of functional state, e.g. in the absence of oestrogen ERα is very stable, with a half-life of up to 5 days (Nirmala and Thampan, 1995). This drops to 3-5 hours in the presence of estradiol and the receptors are targeted for degradation through a transcription-coupled pathway requiring new protein synthesis (Alarid, 2006, Alarid et al., 1999, Nirmala and Thampan, 1995). In the nucleus NHRs are mobile and characterized by transient interactions with numerous chromatin response elements (Elbi et al., 2004, McNally et al., 2000, Reid et al., 2003). For ERα many of the early response chromatin binding sites are only transiently occupied and may be abortive or result in repression (Stossi et al., 2009), which may reflect the presence of appropriate co-factors in the nucleus. Furthermore, in the nucleus ERα and ERβ have been shown to interact with 498 other proteins, only 70 of which are common to both (Nassa et al., 2011). Of these proteins, 357 were detected in the present experiments: with a minimum of 5 SILAC ratio counts 58 proteins show >2-fold decrease in nuclear abundance and a further 76 show appreciable nucleo-cytoplasmic redistribution ($|\log_2(S_n/S_c)| > 1$). The present results then suggest that the outcome of the "polling" by ERs is likely to be dependent on the nuclear/cytoplasm distribution of numerous other proteins as a function of cellular state. It seems likely that other NHRs fulfill similar "polling" roles, which may include cross-talk between different NHRs (Bolt et al., 2013).

Attempts have been made to use protein-protein interaction (PPI) networks to analyse cellular response to various nuclear hormone receptors. Almost 20% of the proteins involved were connected to chaperone/nuclear import machinery and many have multiple subcellular locations (Echeverria and Picard, 2010), which emphasizes further the importance of dynamic subcellular distribution of proteins. The authors concluded that whole cell analyses only allowed limited inferences and that new high-throughput methodologies that monitor different subcellular locations are needed (Echeverria and Picard, 2010). The proteomics subcellular spatial razor is able to provide the kind of information required.

4.1.3 Possible relationships to breast cancer

Hormone receptor positive breast cancers (luminal subtypes) are the most commonly diagnosed subtypes of breast cancer. The luminal subtypes showed high expression of many proteins that may complex with the receptor pathways and may provide a platform for early detection and differentiation between malignant and benign form of breast cancer (Lam et al., 2014). ERs are groups of proteins of closely related variants (superfamily) integrated in multiple networks with multiple organelles at multiple subcellular locations (Kampa et al., 2013). Interestingly, dynamic shuttling of nuclear ERs between the nucleus and cytoplasm via nuclear import/export can be modulated by agonists/antagonists actions (Kocanova et al., 2010). Accordingly, wide range of observations related to E2 extranuclear ER actions have been reported. Of these, triggering kinases at membrane level (cAMP, cGMP, protein kinases, lipid kinases, and Src kinases with EGFR) and activation of downstream signalling cascades that lead to transcriptional activation (Kim and Bender, 2009).

The present results indicate that in MCF-7 cells estradiol causes much more substantial changes in subcellular protein distribution than have previously been appreciated. Indeed, the dominant response to estradiol appears to be changes in compartmentalized protein abundances rather than in total protein abundance, including numerous proteins that are present in both the nucleus and mitochondria (Qattan et al., 2012). This pattern is consistent with other recent proteomics studies (Baqader et al., 2014, Mulvey et al., 2013, Pinto et al., 2015, Pinto et al., 2016). For 76 proteins involved in central metabolic roles in MCF-7 cells, time-dependent monitoring of total abundance by proteomics single reaction product methods indicated that none had 2-fold changes in total abundance over the first 24 hours of exposure to estradiol (Drabovich et al., 2012). Similarly, study of a tamoxifen resistant MCF-7-derivative cell line also showed only a few proteins with >2-fold changes in total abundance compared to the parent MCF-7 cells (Zhu et al., 2012). Finally, although many proteins showed small changes, only moderate differences in total protein abundance between nontumorigenic MCF10A, MCF-7 and highly invasive MDA-MB-231cells were found (Bateman et al., 2010, Pavlou et al., 2013). Recent work has shown that miRNAs may also play a role in regulation of protein expression and in the initiation and progression of breast cancer (Klinge, 2012), but at the level of mRNA, study of the miR-191/425 cluster also found very few proteins with 2-fold changes in total abundance (Di Leva et al., 2013). Taken together with the present results, this suggests that the modified metabolic properties of cancerous MCF-7 cells may be mainly based on perturbed spatial distribution of proteins and opens the possibility that transformation and tumorigenicity may also be strongly influenced by perturbed spatial distribution of proteins. Refocusing on the dominant mechanism of cellular response to estradiol may have strong implications for development of therapeutic compounds.

Much recent work on the role of oestrogen in breast cancer has focussed on the relative importance of ER-dependent activities versus direct genotoxic effects of oestrogen metabolites, with both seemingly relevant (Yue et al., 2013). Chromatin organization is highly linked to cellular state and to subcellular distribution of proteins and recent work has shown strong epigenetic changes in the chromatin landscape related to oestrogen response and resistance to endocrine therapy (Magnani et al., 2013). In short, both of the presently most discussed mechanisms for involvement of oestrogen in breast cancer could be influenced by major perturbations in subcellular protein spatial organization. Whether highly perturbed spatial distributions are a by-product or represent a facilitator for transformation/tumorigenicity remains to be investigated. An intriguing observation is that cells may be transformed by perturbations in nucleo-cytoplasmic shuttling of nuclear hormone receptors and other proteins (Bonamy and Allison, 2006, Bonamy et al., 2005, Mavinakere et al., 2012).

The proteins involved in the metabolic pathways have been found to be relatively changed after 24 h exposure of MCF-7 to various conditions mimicking the biological perturbations, E2 exposure and hypoxia (Drabovich et al., 2012), these results are consistent with the current findings. Furthermore, novel localizations of both ERα and β within the mitochondria of MCF-7 were significantly increased after E2 treatment and the possible explanation was related to ER-mediated genomic transcription of mitochondria (Chen et al., 2004). Perinuclear location, dynamic structure, and ability to produce the reactive oxygen species (ROS) are all unique observations related to the possible role of mitochondria in growth signalling in response to the external biological perturbations (Felty and Roy, 2005).

4.2 Part-II: Spatial dynamics in response to tamoxifen-stimulated breast cancer cell line (MCF-7)

The response of MCF-7 cells to the tamoxifen treatment shows significant changes in subcellular abundance rather than in their total abundance. In the following part, we discuss three main topics: 1) extensive redistribution of the subcellular abundance as a consequence of 4OHT; 2) the relevance of moonlighting proteins in this proteomics study; and 3) the most relevant pathways associated to agonistic and antagonistic response of Tamoxifen in MCF-7.

4.2.1 Redistribution of subcellular proteins and moonlighting proteins

From the large MaxQuant dataset, we selected an overall response list of proteins (270-TAM) and a more reliable response (97-TAM) for which more significant changes actually occurred in response to treatment (see Material and Method Section). Within the 97 proteins, it was possible to observe three major grouping of proteins that differently responded to 4-OHT: a) Proteins with exclusive changes in total abundance without redistribution in the nucleus/cytoplasm. They represent 20% and give a low contribution to the cellular response; b) Proteins with abundance changes only in one of two compartments (nucleus or cytoplasm); c) Proteins with significant abundance changes in both compartments (nucleus/cytoplasm) with any change in total abundance (20%). Whether the (a) group is equally important for the large scale studies, we are more interested in (b) and (c) groups, representing the majority (70%) of proteins responsive to 4-OHT. Based on the latest studies, the extensive spatio-temporal redistribution of subcellular proteins is an evidence of cellular response to various stimuli (Jung et al., 2013). Extensive changes by quantitative proteomics were also observed for hundreds of proteins, significantly changing in abundance (Zhou et al., 2012) as well as in the phosphorylation level (Oyama et al., 2011), that

adaptively response to the long term treatment of the MCF-7 cell line. In this study, the massive changes of subcellular proteins have allowed to figure out numerous pathways involved in 4-OHT response of MCF-7, some of which explain the agonistic role of drug while others point to the antagonistic role. This dual behaviour observed by us demonstrates that in a complex system like cell the “real” response to 4-OHT follows more complicated ways than those imagined and those recorded with monitoring single proteins. Thus, the study of pathways or metabolic processes of the most significantly changed proteins by quantitative proteomics is undisputedly of relevant importance in revealing molecular basis of any disease.

4.2.2 Multiple locations of subcellular proteins and moonlighting proteins

The cellular compartmentalization, the highly specialization of organelle functions and particularly the changes in subcellular localization of each protein seem to support the existence of an evolutionary retargeting (Gabaldón and Pittis, 2015). As already mentioned, large scale studies are revealing that organellar proteomes not only differ from cell type but also dynamically change as a result of a massive trafficking of subcellular proteins in response to perturbations (Radulovic et al., 2016). The targeting of the same protein to multiple locations is the evidence of a strong and intertwined communication between organelles within which different targeting signals can be differently activated. The cross-communication ensuring a checked cellular response to external environment determines protein dynamic fluxes versus specific locations for spatial partitioning of major cellular functions.

In the dynamic studies, the isolation of “permanent resident” proteins by highly purified subcellular organelles, that should be more representative possible of the fractionated compartment, has been surpassed by the existence of numerous “moonlighting” proteins that escape to crystallized concept of one protein → one compartment → one function. Actually, the finding of hundreds of moonlighting proteins brings forth the importance of cellular function at the proteome level and the need to deal with them by subcellular proteomics rather than by genomic/transcriptomic approaches. A recent mass spectrometry review has pointed out the limitations of fractionation process based on the assumption that each organelle cannot be completely separated from the rest of cell (Pinto et al., 2016). The isolation of mitochondria or other organelle can cause the loss of membrane proteins stripped by fractionation. Even the nucleus, rather than as a shiny ball, it is depicted as highly complex “reticulum” (Malhas et al., 2011) containing large numbers of previously unsuspected proteins associated with the nuclear envelope (Talamas and Capelson, 2015). In the present study, within the (b) group, some proteins (25%) have shown only changes in cytoplasm abundance without any significant change in total or nuclear abundance as a response of 4-OHT stimulation. Within this group, ALDOA, an interesting protein well-known for its glycolytic role, has revealed to perform numerous moonlighting activities in both cytoplasm and nuclear compartments (Lincet and Icard, 2015), besides being involved in tumorigenesis (Chang et al., 2015, Du et al., 2014). The main functions, absolved in cytoplasm and nucleus, have been summarized in Figure 4-1.

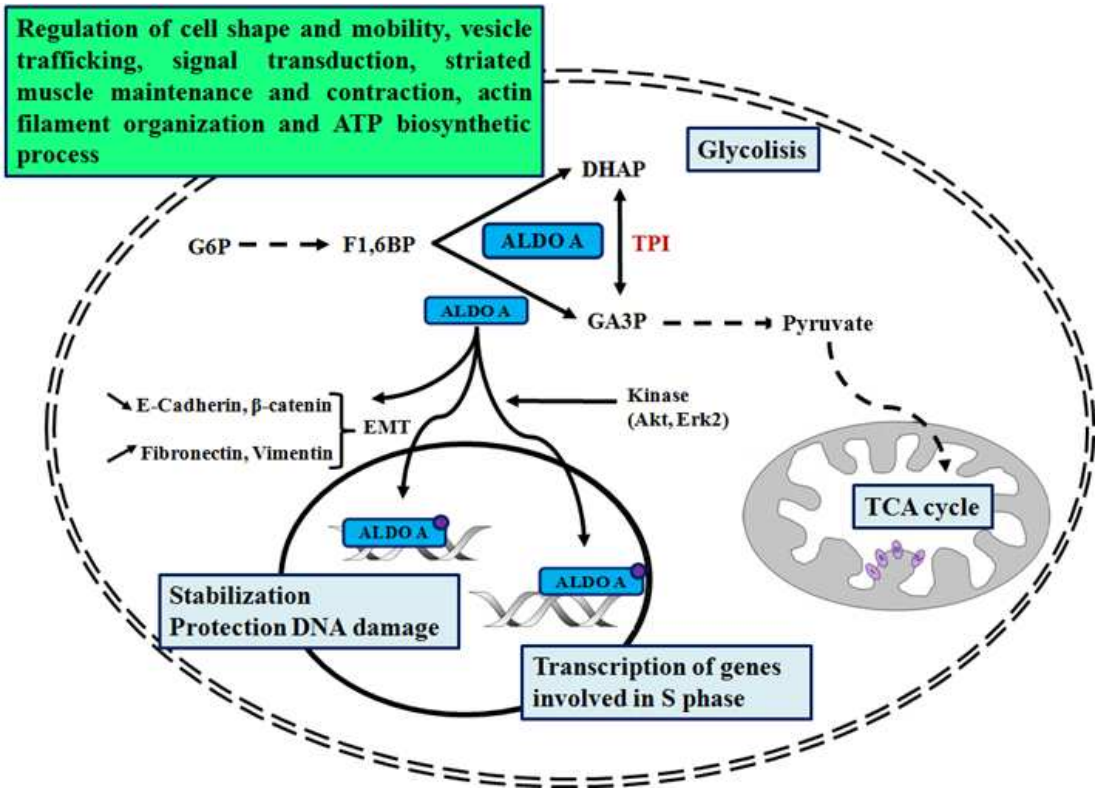

Figure 4-1: Schematic representation of non-glycolytic functions of aldolase

The upregulation of ALDOA, as found in our study, has been demonstrated to promote epithelial-mesenchymal transition (EMT) and cell migration by inducing an expression decrease of epithelial markers, E-cadherin and β-catenin, with a concomitant increase of Fibronectin and Vimentin, both events favouring tumorigenicity (Du et al., 2014). The ALDOA phosphorylation of by Akt or Erk 2 kinases triggers the nuclear translocation of aldolase enzyme, which contributes to regulate the transcription of some genes of cell cycle progression, to protect DNA in response to the damage and to stabilise some transcripts particularly with AT-rich DNA sequences (Lincet and Icard, 2015). Other non-glycolytic functions for ALDOA are related to cell mobility, signal transduction, vesicle trafficking, etc., as listed in Figure 4-1.

Distinct from the known mitochondrial role in energy generating process, some proteins of oxidative phosphorylation, like MT-CO2, shown to bind directly to cytochrome c, have been demonstrated to regulate apoptosis (Acehan et al., 2002, Kulms and Schwarz, 2002). A small fraction of cytochrome c, more weakly attached to inner membrane of mitochondria, is presumably more available for compartmental shuttling within cell. Its redistribution from mitochondria to cytosol occurs in response to pro-apoptotic stimuli activating, through the interaction with Apaf-1, caspase cascade events that lead to apoptosis (Acehan et al., 2002, Kulms and Schwarz, 2002). Then, a cytochorme accumulation in nucleus compartment triggers massive translocation of acetylated histone H2A from nucleus to cytoplasm with irreversible consequence on chromatin condensation (Nur-E-Kamal et al., 2004).

The cytoplasm cytochrome can further block calcium-dependent inhibition of IP3 receptor on the endoplasmic reticulum (ER) and increase the calcium release from ER that in turn activates cytochrome c release (Boehning et al., 2003). In addition, the depletion or altered expression of some of OXPHOS proteins (MT-CO2, COX I, III) has been also implicated in tumorigenic transformation (Abril et al., 2008, Chatterjee et al., 2011).

Another moonlighter, downregulated in our cytoplasm and nucleus fractions, is CRYAB, a potential biomarker of several tumours included in triple-negative breast cancer (TNBC) (Malin et al., 2014, Tsang et al., 2012). Whether CRYAB has been found as a major structural protein in ocular lens for transparency maintenance, in non-lenticular tissues, it functions as cytoprotective molecular chaperone capable to prevent non-specific protein interactions under particular cellular stress. It specifically binds and corrects intracellular misfolded/unfolded proteins such as vascular endothelial growth factor (VEGF), promoting angiogenesis in metastatic event (Chen et al., 2014, Ruan et al., 2011). An anti-apoptotic function has been attributed to this protein by inhibiting the autoproteolytic cleavage of caspase3 (Kamradt et al., 2001, Kamradt et al., 2002), or by directly interacting with the pro-apoptotic Bax and Bcl-xs (Mao et al., 2004), in response to diverse stimuli. Moreover, in response to heat-stress, CRYAB translocated from cytoplasm to nucleus and complexed to F-actin for regulating cytoskeletal stability and dynamics (Singh et al., 2007) but also it shuttles to mitochondria where inhibits cytochrome c release into cytosol during MI by binding to VDAC1 channel under cellular stress (Chis et al., 2012).

Some discrepancies between the GO annotation and the present subcellular locations confirm further the underestimation of subcellular annotations related to the GO CC database. The high dispersion of proteins over multiple locations as recently reported in large scale proteomics papers (Qattan et al. 2010, 2012 and Pinto 2014) suggests that the real spatial distribution of cellular functions is much more complicated than that annotated in current GO CC. In the present study, for more than 60% of proteins (all 97 dataset), there is at least one location omitted in GO annotation. While for some proteins the additional subcellular location found is not well documented, for others it is. For example, the finding of LDHA in nuclear fraction is in agreement with hypothesis that some cytoplasmic metabolic enzymes translocate into nucleus for moonlighting transcription functions under stress condition. LDHA would seem to translocate to nucleus for taking part to OCA-S transcriptional coactivator complex and regulate indirectly the S phase-specific H2B transcription (Zheng et al., 2003) but also directly functioning as metabolic/redox sensors (He et al., 2013). The nuclear upregulation of LDHA has been attributed to the transcriptional and translational regulation by HIF-1α in cancer cells (Koukourakis et al., 2005, Miao et al., 2013, Semenza, 2013). Further example is the translocation of ALDOA to nucleus in response to stimulus (Figure 4-1).

Within the (c) group, an additional nuclear location has been found also for MT-CO2, DES, HBB, DCD, mainly GO annotated in cytoplasm and/or in extracellular region (Table 3-9). For other proteins annotated with a single location, *e.g.* MYL3 (Cytosol), FUBP1 (Nucleus), LYAR (Nucleus) CALML5 (extracellular vesicular exosome), a subcellular redistribution between nucleus and cytoplasm have been found following the 4-OHTam treatment (Table 3-9).

For example, LYAR, a zinc finger protein, more frequently found in the nucleolus for promoting cell growth by preventing nucleolin self-cleavage (Wang et al., 2012), has been also associated to cytoplasmic ribosomes in human cancer cells (Yonezawa et al., 2014). From the cytoplasmic compartment, LYAR protein dissociates from the cytoplasmic 60S ribosomial subunit for shuttling rapidly to the nucleolus for absolving nuclear functions. The abnormal expression of these ribosome-interacting proteins has been associated to the deregulation in growth and viability of malignant neoplasms (Stumpf and Ruggero, 2011).

Studies entirely referred to GO-database suffer from the limitation that less functions and locations than those actually explorable are considered, leaving just a small space to the investigation of the changes induced from cellular response to stimuli. In this contest, the finding of new locations for subcellular proteins should be a lighthouse for further studies.

4.3.3 Possible implication in cancer and/or cancer resistance

Tamoxifen and its active metabolite, 4-OHT, are known as selective ER modulators (SERM) that are not pure ER antagonist (anti- oestrogenic) in all tissues; rather 4-OHT has been observed as ER antagonist in the treatment of breast cancer (Osborne 1998, Riggs and Hartmann 2003). The efficacy of this treatment was limited by the development of resistance in nearly 30 % of ER-positive breast cancers whom they were responding to the initial tamoxifen (SERM) treatment that interrupted the breast tumour growth for a while (Jiang et al., 2013). Commencing the growth of breast cancer tumours, despite the presence of 4-OHT and ER expression (Lewis and Jordan, 2005), linked the resistance to the modulation of response due to the agonistic (oestrogenic) activity of tamoxifen (Dorssers et al., 2001).

However, about tamoxifen resistance, there are several mechanisms suggested to attribute to the acquired resistance and they have been reviewed in details (Chang, 2012, Dixon, 2014). In the wild type MCF-7 used in this study, there were agonist–antagonist properties representing the inducible changes following 4-OHT treatment. An appreciable number of proteins showing up- or down-regulation is involved in regulation of many cellular mechanisms that are involved in metabolic, reduction/oxidation cycling process, signal transduction, cell cycle, cross-talk between signalling pathways, maintenance of cytoskeleton, adhesion, progression, and apoptosis processes. In the following discussion, we address some of the proteome changes that contribute to the modulation of carcinogenesis regarding loss or gain of functions with emphasis on those mediating cancer development as an agonistic activity of 4-OHT. However, in the beginning, this discussion might shed some light on some of the results that are supporting the antagonistic activity (tumour suppression), to flavour the complexity which is an innate characteristic of cancer. For example, 4-OHT demonstrated an antagonistic effect and was able significantly to

reduce the expression of OAT ($\downarrow S_n$), Ornithine aminotransferase (OAT) (Figure 3-18A). In addition to its known key role in mitochondrial arginine synthesis, a novel role for OAT was revealed as to participate in control of the mitosis of cells (Wang et al., 1995). It has been reported that, instead of tubulin, OAT is the cellular target for AB-5, an alkaloid drug that block cancer cell division through binding to OAT (Wang et al., 2007). Androgens can modulate OAT expression, and therefore, modulate the severity of cancer (Jariwala et al., 2007). In U87MG-AAV-decorin cells that show slower cell proliferation, OAT was observed significantly reduced in response to decorin (Ma et al., 2014). Results from the current study demonstrate that there is a significant reduction of OAT and localization to the nuclear fraction, suggesting that the compartmental distribution of OAT is important as much as the level of expression for the mitotic role. Furthermore, 4-OHT could have paradoxical actions inside the cells that need further investigation.

It has been known for many decades that normal and cancer cells are different in many aspects including metabolism. It is observed that nearly all cancers express aerobic glycolysis, suggesting that cancer may be primarily a metabolic disease. Many metabolic alterations are associated with the increased biomass of cancer cells to replace the normal energetic source of mitochondrial oxidative phosphorylation with aerobic glycolysis, glutaminolysis or fatty acid synthesis that are abnormally increased to meet cell proliferation (Munoz-Pinedo et al., 2012, Vander Heiden, 2013, Warburg et al., 1927). These observations have been reported independently from mitochondrial malfunctioning in many tumours (Vander Heiden et al., 2009, Ward and Thompson, 2012).

Although the exact biochemical and/or molecular mechanism behind the “Warburg effect” or aerobic glycolysis in the presence of oxygen is not completely elucidated due to complexity (Woo et al., 2015), lactate fermentation in the cytosol is widely accepted as an alternative source for ATP production in cancer cells and replacing the oxidative phosphorylation of pyruvate in mitochondria as in normal cells (Christofk et al., 2008, Kim and Dang, 2006). Moreover, an increased rate of lactate production has been associated with the aggressiveness of cancer, which is the more metastatic and drug-resistant cancers, the higher lactic acid level is produced (Lu et al., 2002, Semenza, 2009).

The findings of the present study indicate that appreciable number of proteins are major regulatory proteins in the metabolic pathways. Proteins involved in glycolysis are upregulated while those involved in citric acid cycle and oxidative phosphorylation are aberrantly downregulated as these proteins were overrepresented in pathways analysis (Table 3-5Table 3-7, andTable 3-8 and Figure 3-18A). Some proteins were showing substantial variations in the subcellular locations (C and N) with or without modifications in the total abundance (Figure 3-18A) including MTCO2 (↑Sc, ↑S_n), LDHA (↑S_n), TKT (↑S_c, ↑S_t), IDH1 (↑S_c), and ALDOA (↑S_c). There is exponential growth of papers that point a link between alteration in glucose metabolism and the acquired resistance to chemotherapeutic drugs such as doxorubicin, cytosine arabinoside, taxol, cisplatin, and vincristine (Clarke et al., 2009, Lu et al., 2008, Lyon et al., 1988, Pelicano et al., 2006, Woo et al., 2015, Xu et al., 2005). Furthermore, as mentioned in the previous section, many of these proteins may have moonlighting functions that are distinctive from their metabolic roles, for example ALDOA found to have different roles, apart from its glycolytic activity, such as signal transductions (Ishida et al., 2005, Orosz et al., 1988), vesicle trafficking and transport of materials from site to site (Lundmark and Carlsson, 2004), and increased rate of cell motility (Jewett and Sibley, 2003). Therefore, its non-catalytic role in cancer transformation has been

investigated using RNAi in Ras-transformed NIH-3T3 cells; the authors observed consequences of ALDOA knockdown in cell proliferation rather than glycolytic flux/ATP level; the cell proliferation was restored by expression of exogenous ALDOA (Lew and Tolan, 2012).

However, the number of studies that have demonstrated a link between abnormal glycolytic metabolism and the development of tamoxifen resistance is still minimal in comparison with other drugs that are used in cancer treatment (Woo et al., 2015).

The rationale behind identifying the metabolic alterations that promote carcinogenesis and/or resistance to the treatment is to understand and validate the cellular pathways interaction and contribution to malignancy. Although the mechanisms of either developing or resisting treatment in relations to the altered metabolic pathway remains to be elucidated, there is a plethora of evidence, provided by many studies, supporting the link between oncoproteins and glycolysis (Ganapathy-Kanniappan and Geschwind, 2013) and glutaminolysis (DeBerardinis and Cheng, 2010), to regulate the cellular metabolism and provide the energy and new cellular components to the highly demanding proliferative cancer cells. Furthermore, glycolysis has been attributed to the treatment resistance in cervical cancer cells through two isoforms, pyruvate dehydrogenase kinases (PDK) (PDK1 and PDK3) (Lu et al., 2008), and accumulation of lactate in colon cancer cells (Fanciulli et al., 2000). However, inhibition of PDK has induced apoptosis and inhibited the cell growth, in many types of cancer, by restoration of glucose oxidation and oxidative phosphorylation (Bonnet et al., 2007).

Glycolytic intermediates are essential fuels to the pentose phosphate pathway (PPP), in animals, to maintain the production of NADPH reducing power and 5-carbon sugar (ribose-5-phosphate) that are required for lipid and nucleic acid synthesis (Horecker, 2002).

Also, NADPH serves as an electron donor that maintain the cellular level of the reduced form of a tripeptide antioxidant glutathione (GSH); chemotherapy resistance in cancer has been linked to the cellular level of GSH and related enzymes that are contributing to the cell survival through the activated antioxidant dynamic cascade (Backos et al., 2012, Estrela et al., 2006). Isocitrate dehydrogenase 1 (NADP+, soluble) (IDH1) is the cytoplasmic enzyme that serves a significant role in cytoplasmic NADPH production and found to be upregulated in the cytoplasmic fraction in our study. IDH1 has been reported as one of five critical components of GSH pathway and contributed to the development of chemoresistance in breast cancer (Wang et al., 2015). From general response proteomics data obtained in this study (TAM-270), no conflict was observed with the published studies where glutathione synthetase (GSS) was highly expressed (St = 5.244) in the total lysate (Supplementary Table 7).

The expression of glycolytic intermediate, transketolase (TKT1) a key enzyme in PPP, has been found of particular importance in sustaining the cancer cells viable while inhibition of TKT has reduced the growth, glucose consumption, and lactate production in HCT116 colon carcinoma cells, moreover, the stress-induced apoptosis was commenced in the TKT1 knocked down cells (Xu et al., 2009). The catalytic activity of TKT was upregulated (↑Sc, ↑St) in response to 4-OHT.

Several mechanisms have been suggested to explain the utilization of cancer cells to aerobic glycolysis for ATP generation. In general, alterations in proteins that are essential to glycolysis or truncating TCA cycle by the mitochondria, are the two most important themes that can accumulate lactate and enhance the use of lactate fermentation as an alternative source of energy.

Several glycolytic enzymes like glucose transporters (GLUTs), hexokinase, pyruvate kinase, lactate dehydrogenase A (LDHA) and monocarboxylate transporter (MCT) are oncogenes and hypoxia-inducible factor (HIF) induced expressional, promoting glycolytic flux in cancer cells. On the other side, citric acid cycle is truncated due to frequent mutations in mitochondrial DNA (mtDNA), dysfunctional tumour suppressor genes, and the most important one is the reduced level of respiratory substrates (Ju et al., 2014, Levine and Puzio-Kuter, 2010, Simon, 2006, Zhang et al., 2015). In consistency with these findings, for central metabolic pathways, glycolysis and TCA, the induced level expression of glycolytic enzymes lactate dehydrogenase A (LDHA) and isocitrate dehydrogenase 1 (IDH1) as high SILAC ratios were determined in nuclear and cytoplasmic fractions, respectively. Table 3-8 shows that both respiratory electron transport and TCA were the top ranked down-regulated pathways. Moreover, identification of nuclear DE LDHA in the proteomics analysis generated from this work is consist out with nuclear localization/synthesis of LDHA that was shown in the rat's liver and the in the nucleus of several cell lines (Cattaneo et al., 1985, Kuehl, 1967).

Furthermore, we observed that 4-OHT may exert agonistic activity via enhancing the protective mechanism of cancer cells. The treatment of wild type MCF-7 with 4-OHT has induced the change in a total abundance (St) with no subcellular distribution of a key protein involved in oxidative stress control, thioredoxin reductase 1 (TXNRD1). Increased expression of TXRND1 is associated with some essential functions that are contributing to the hallmarks of cancers, including enhanced proliferation and avoiding apoptosis, and self-sustaining of blood supplies (angiogenesis).

For these key hallmarks, TXRND1 is essentially activated to maintain the cellular redox homeostasis, turn on the DNA synthesis via activating ribonucleotide reductase, deactivating ASK1 (apoptosis signal-regulating kinase 1) and activating HIF-1 and VEGF (Cadenas et al., 2010, Nishiyama et al., 1999). In contrast, thioredoxin-interacting protein (TXNIP) is an apoptosis-inducing protein that is known to bind the reduced TXRND1. Using MCF-7 cells, the influence of oncogenic ERBB2 on the level of expression of these proteins was investigated, it was demonstrated as an immediate increase of TXNRD1 and decrease in TXNIP (Cadenas et al., 2010).

It has been reported that oestrogens through sequential events taken place in nuclear, mitochondria, and plasma membrane, play a fundamental role in regulating the mitochondrial biogenesis (Klinge, 2008). Ivanova et al. (2013) have found that both active metabolites of oestrogen and tamoxifen, E2 and 4-OHT, cause efficient transcription initiation of nuclear-encoded nuclear respiratory factor 1 (NRF-1) by binding, respectively, to the classical ERs, ERα and ERβ in MCF-7 cells. Subsequently, NRF acts as a transcriptional activator that upregulates the transcription of nuclear-encoded mitochondrial genes, and nuclear-encoded components of OXPHOS, e.g., cytochrome c family of proteins (Cyclooxygenases) (Fong et al., 2007, Fong et al., 2010).

Recently, MT-CO2 was remarkably increased (>20 fold), in hTERT-GFP(+) MCF-7 Cells; this result reveals a reflection to be a powerful mechanism behind mitochondrial biogenesis (Lamb et al., 2015). Interestingly, in this project, the significant data sets have shown increased expression of MTCO2 in the subcellular compartments, ($\uparrow S_c$, $\uparrow S_n$), only.

Adenylate cyclase-activating G-protein coupled receptor signalling pathway and G-protein beta/gamma-subunit complex binding are among the top ranked GO terms that were enriched in the nuclear fraction for biological processes and molecular functions, respectively (Table 3-6), furthermore, applying the restrictive measures of identification and SILAC on the significance data set (97-TAM) has introduced no difference in the enrichment analysis (Table 3-7). Figure 3-19, shows that Guanine nucleotide-binding protein subunits GNAI2 (Gα), GNAQ (Gqα), GNAS (Gs-α), GNB1(Gβ1), and GNA13 (Gα) were overrepresented in Pathways of cancer pathway, moreover, in the nuclear fraction the Circadian entrainment pathway was a top ranked pathway as it was enriched with the upregulation of these proteins (Figure 3-18C and Table 3-5). These findings imply the importance of the heterotrimeric G-proteins in transducing the non-genomic and genomic (transcriptional) signalling in response to the clinical relevant dose (I μM) 4-OHT (Castoria et al., 2009). Although the active tamoxifen metabolite, 4-OHT, is known as a selective modulator for ER (SERM), 4-OHT, in breast cancer cells, acts as agonist on a member of the 7-transmembrane G protein-coupled receptor (GPCR) family that is now recognized as a novel ER and also known as G-protein coupled receptor 30 (GPR30) (Fitts et al., 2011), and G protein-coupled receptor 30/G protein-coupled oestrogen receptor-1(GPR30/GPER-1) (Prossnitz et al., 2008, Wei et al., 2012).

G-protein coupled receptors (GPCRs) are cell surface receptors; they have wide spectrum of functions in the context of physiological and pathophysiological processes. From tumour formation to the spread of cancer cells, ligand-dependent GPCRs, e.g. SDF-1, thrombin, LPA, S1P, and endothelin, found to have pivotal roles in many forms of tumours including prostate and breast cancer (Lappano and Maggiolini, 2012). The downstream signalling cascades are transduced through G-Alpha12 (GNA12) and G-Alpha13 (GNA13) subunits constituting the subfamily of heterotrimeric G-Proteins.

Indeed, invasion and metastasis have been attributed to GNA proteins in many cancer types (Kelly et al., 2007, Malchinkhuu et al., 2008). Some finding reported in (Rasheed et al., 2015) suggested that GNA13 is highly upregulated in the aggressive form of breast cancer cells, moreover, restoration of GNA13 activity has been shown to enhance the progression and invasion characteristics of prostate cancer cells (Rasheed et al., 2013).

Our findings reported here that under 4-OHT stimulation GNA13 was highly expressed in the nuclear fraction with an appreciable change in the cytoplasmic sample while GNA12 and GNAQ were upregulated exclusively to the nuclear fraction (Figure 5B). In addition to the localization of 7TMR to the plasma membrane, subcellular localization of GPR30 was reported to localize as bound to endoplasmic reticulum (Revankar et al., 2005), with possible localization in Golgi (Sakamoto et al., 2007). Furthermore, shuttling of GRP30 nucleus and cytoplasm was suggested (Wang et al., 2008).

The ligand binding to the most described ERs (termed ERα and ERβ) initiates a sequence of events that result in genomic (transcriptional) and non-genomic signalling processes; GPR30 has been found to be expressed in 50% of cancer patients and could induce the non-genomic mediated tumour progression through mitogen-activated protein kinase (MAPK) even when ERs are absent or blocked (Prossnitz and Maggiolini, 2009, Wang et al., 2010). The time frame for these two responses is not the same, the genomic response is slower than non-genomic and lasts hours to days while the later lasts seconds to minutes. The rapid (non-genomic) oestrogen response transfers the signals/information to the subsequent effectors in the cascade that include second messengers (Ca2+, cAMP, and NO), and kinase activation (e.g. PI 3-kinase, Akt, and MAPK) (Prossnitz et al., 2008). The discoveries of these two receptors has complicated the interpretation of their actions and functions; their localizations in the cytosol and/or nucleus justifying the slow response, genomic actions (transcriptional), on the other hand, the non- genomic actions (rapid) that involve pathways and signalling transactions was linked to the existence of membrane-associated ERs that are structurally distinguished from the classical ERs (Govind and Thampan, 2003, Mizukami, 2010). A number of studies have demonstrated that tamoxifen and its metabolites have a profound effect on breast cancer proliferation through GPR30 implying the role of upregulation of this protein in the acquired resistance to targeted tamoxifen treatment in breast cancer patients (Ariazi et al., 2010, Pandey et al., 2009, Vivacqua et al., 2009). Furthermore, one of the suggested mechanism that induce the tamoxifen resistance is to activate the epidermal growth factor receptor (EGFR). An expression of GPR30 in 50% of ER + breast cancer patients (Wang et al., 2010), which happen together with the overexpression of EGFR and acquired resistance, suggests that Gβγ subunit protein of GPR30 induces the GPR30/EGFR signalling cascade (Mo et al., 2013).

The downstream ligand-activated GPR30 signalling involves activation of SRC-like tyrosine kinase and metalloproteinases leading to activate the HB-EFG (heparan-bound) which, in turn, activates the EGFR signalling pathway. Subsequently, the cells are commencing growth in response to the phosphorylated Erk1/2 (Filardo et al., 2000, Mo et al., 2013).

Non-genomic actions of oestrogen occurr rapidly and are accompanied with intercompartmental ions flux and flux of other molecules across the plasma membrane (extracellular to intracellular), (Saint-Criq et al., 2012). Several proteins were related to solute transporters were DE (Supplement tables 5&6) in response to 4-OHT, of these are SLC1A5, SLC25A24, SLC25A4, SLC3A2, and SLC7A5. Alanine, serine, cysteine-preferring transporter 2 (ASCT2; SLC1A5) and SLC3A2 were upregulated in the ($\uparrow S_c$) and ($\uparrow S_c, \uparrow S_n$), respectively. They play a role in mediating the amino acids transport particularly glutamine (Kanai and Hediger, 2004, Kekuda et al., 1996).

Glutamate pool is critical for normal and abnormal cells; the demand is exponentially increased in the cancer cells from transformation through proliferation and metastasis stages, to compensate the needs for detoxification and metabolism that is needed for high rate proliferated cancer cells (DeBerardinis et al., 2007). Furthermore, mTORC1 is the master regulator signalling for growth and protein biosynthesis (Duran et al., 2012, Wullschleger et al., 2006). It also needs a level of glutamic acid to be maintained to sustain its functions (DeBerardinis et al., 2007). Some studies have found a link between oncogenes and glutamate metabolism by linking the deregulation of c-Myc gene to the upregulation of glutamate metabolism (Dang et al., 2006, Little et al., 1983). SLC1A5 was found to be a direct target for c-MYC gene, supporting the increase in the glutamic influx (Dang, 2010). Another study was shown that autophagy was induced in relation to the inhibition of glutamine-dependent activation of mTORC1, that was shown to be initiated via inhibition of

SLC7A5/SLC3A2 (Esslinger et al., 2005). Combining the in vitro and in vivo approaches of gene expressions, (van Geldermalsen et al., 2015) have investigated the role of SLC1A5 (ASCT2) in breast cancer triple negative cell lines (TN) and patients. They have shown in the cell line that targeted knockdown of ASCT2, alone, was enough to inhibit rapidly in vitro growth and reduce the xenografted cells, suggesting the dynamic regulation of ASCT2 by MYC- and ATF4-driven transcriptional in triple negative breast cancer cells. Furthermore, mRNA measurement was highly expressed in both cell line (TN) and patient samples.

Our study identified several proteins involved in cell growth and apoptotic process. A general response set enrichment analysis (270-TAM) reveals that of the 40 proteins involved in the cellular growth function, 27.5% representing 11 proteins were significantly changed in the three sample types (CNT), and the major changes were associated with the subcellular compartments and involved eight proteins.

For number of DE proteins involved in the apoptotic process, out of 32 proteins (Table 3-6), there were 24 proteins DE in the subcellular compartments (75%), two proteins were DE in all three sample types (S100A8 and A100A9), the rest were changed in the total abundances only (Figure 3-22A and B). Some of these proteins are known to promote tumorigenesis and progression but their changes in response to tamoxifen treatment were favouring a selective action rather than pure agonist or antagonist mode of action, furthermore, roles of some of these proteins in relation to tamoxifen resistance is yet to be revealed. For example, YWHAE (tyrosine 3-monooxygenase/tryptophan 5-monooxygenase activation protein, epsilon) is one of seven isoforms constituting 14-3-3 protein family (β, γ, ε, ζ, η, σ, and τ) that are expressed in all eukaryotic cells (Aitken, 2006) and via interacting with phospho-serine or phospho-threonine motifs, they are involved in wide ranges of cellular functions, including those related to metabolic, survival, and signal transduction, and transcriptional activities. In relation to tumorigenesis, they found to play both roles as tumour suppressor (14-3-3σ, SFN) and oncogene that contributes to the malignancy transformation (14-3-3ζ, YWHAZ) (Hermeking, 2003, Morrison, 2009). We found that 14-3-3ζ (YWHAE) expression was up-regulated in the cytoplasmic fraction ($\uparrow S_c$) with no significant changes in S_n or S_t. Various forms of cancers, including breast cancer, have shown increased level of expression of YWHAE implying its role in inhibiting the cell detachment-induced apoptosis (Anoikis) via activation of TGF-β/Smads (Transforming growth factor-β) leading to anchorage-independent growth in anoikic cells and promoting the metastasis of the tumour cells (Li et al., 2008, Lu et al., 2009, Neal et al., 2009). Moreover, the nucleo-cytoplasmic distribution of 14-3-3 proteins is of a profound importance to control the cell cycle and prevent apoptosis, Brunet et al. (2002) have shown that the majority of these proteins, upon ligand activation, are relocalized to the cytoplasm and home to the nucleus in the absence of ligand binding.

Anchorage-independent manifestation, in the present work, was observed as the decreased expression of proteins that are components of tight junctions that stabilize the tissue/cell seal such as DSP, DES, DSG1, and DSC1 (Al-Jassar et al., 2013, Waschke, 2008), in the subcellular compartments ($\downarrow S_c$, $\downarrow S_n$). In the absence of changes in total abundance, the distribution calculations (S_n/S_c) show that these proteins are redistributed in the cytoplasm ($N \rightarrow C$) or vice versa (Table 3-9). Therefore, tamoxifen seems to exert its "antagonistic" effects releasing anchorage-independent cells that appear to undergo "agonistic" effects enhancing their proliferation individually (anoikis cells) via upregulated YWHAE and downstream effectors; however, this needs further investigations. Interestingly, the cross-talk between pathways as depicted in Figure 3-19 demonstrates the overlap between ECM-receptor pathway and Pathways in cancer pathway (focal adhesion). This was observed as an impact of protein distribution to the subcellular compartment rather than overlapping between the DE genes/proteins. Recently, Sun et al. (2015), using the Rank Product method to identify DE genes in five sets of breast cancer gene expression data, have identified the lists of overlapping proteins and constructed crosstalk analysis of pathways. They concluded that the greatest degree overlapping was observed between ECM and focal adhesion pathway, furthermore, Pathways in cancer was the main pathway in breast cancer showing the crosstalk between different pathways. We found that proteins enriched ECM (CLO1A2, COL6A2, COL1A1, and COL6A3) (Figure 3-20A), were significantly reduced in the total lysate fraction while two more components related to this pathway were observed as significantly decreased in the nuclear sub-compartment (COL6A1 and ITGA3) as shown (Figure 3-20B).

Cross-talk between pathways is a phenomenon that has been addressed as suggestive mechanisms of tamoxifen related resistance in breast cancer (Dixon, 2014), moreover, a group of researchers has determined the changes in metabolic pathways and ceoss-talk phenomenon were observed in 17β-Estradiol treated breast cancer cells at 3 timepoints (12h, 24h, and 34h), the most remarkable finding of this study was that the changes were fundamentally related to Pathways in cancer, Focal adhesion, and Chemokine signalling pathways (Huan et al., 2014).

In the current project, 4-OHT induced significant changes in expression of the SET nuclear oncogene; the upregulated SET protein was relocalized to the cytoplasm. This protein, among other, has been found to have overexpression in MCF-7 resistant form to paclitaxel increasing multidrug resistance (MDR) (Chen et al., 2014a), and has been previously shown to relocalize from nucleus to cytoplasm following inhibition of DNA replication origin activation checkpoint kinase in CDC7-depleted fibroblasts (Mulvey et al., 2013). Additionally, exposure to genetic insults has caused the nucleocytoplasmic distribution of SET protein in neurons (Qu et al., 2007). In cancer cells, proliferation induction can be achieved via inhibition of the tumour suppressor genes, SET known as a potent inhibitor of the tumour suppressor proteins phosphatase 2A (PP2A) and Nm23-H1 (Fan et al., 2003). Truncating the antagonistic effects of PP2A on AKT and ERK phosphorylation was suggested as a role that SET may play to enhance the resistance to chemotherapy (Christensen et al., 2011).

The multifunctional ANXA1 is well known protein that contributes to variety of functions within the cells that determine differential, proliferative, or apoptotic fates of the cells (Lim and Pervaiz, 2007, Mussunoor and Murray, 2008). Moreover, the spatiotemporal distribution of annexins grounds for their regulation to the signal transductions (Monastyrskaya et al., 2009). It has been indicated that subcellular localization of ANXA1 is an essential detriment for the role that this protein may play in all stages of cancer development. In contrast to the normal epithelial cells where ANXA1 was mainly localized in the cytoplasm, the transitional cells carcinomas (TCC) was shown that ANXA1 was redistributed primarily to the nucleus, suggesting a role in mediating the transition and differentiation of cancer cells (Cui et al., 2007). Furthermore, ANXA1 expression found to be context dependent and differs from cancer type to another implying its role in cancer progression as a tumour suppressor and/or promoter (Guo et al., 2013). In a study carried out on the poor response of breast cancer patients to neoadjuvant chemotherapy, ANXA1 was downregulated and was associated with poor pathological response (Chuthapisith et al., 2009). However, the mechanism is not completely elucidated.

Chapter 5 Conclusions

The high degree of spatial/functional inhomogeneity of cells and the need for efficient subcellular communication means that the study of dynamic spatial distribution of subcellular proteins is of fundamental importance for the improvement of the understanding of cellular processes underlying human disease. Indeed, this remarkable phenomenon occurs in any kind of cell: roughly half of all subcellular proteins are known to translocate into another compartments to reach their functional location (Chacinska et al., 2009), while most of the ~1,000 different 'resident' proteins contained in mitochondria are imported from the cytosol to exert their functional role (Schmidt et al., 2010). Moreover, numerous mis-localised proteins have been associated with human diseases as diverse as Alzheimer's or various types of cancer and aberrant localisation of proteins has been shown to contribute to the pathogenesis of many human diseases (Hung and Link, 2011).

It is becoming more apparent that relying on global genomics information is a valuable asset to formulate a hypothesis, identify recognisable tissue signatures, and seek correlations to medical conditions, but the functional states of cells are beyond the scope of genomics alone. The more focussed approach of proteomics is complementary to genomics and can define the functional products (proteins) of the deregulated genes in space and time, which increases our understanding of the underlying biological processes (Lam et al., 2014, Scott and Pawson, 2009).

Recent advances in the characterisation of the subcellular location of proteins now indicate that dynamic trafficking of multitudinous proteins over many subcellular locations is a central mechanism in cellular function. There is now an urgent need for global characterisation of the dynamic subcellular partitioning of proteins for many cell types and functional contexts.

The main conclusions of this work are now summarised as follows:

1. Numerous existing evidence suggests that the subcellular location of proteins is being as much important as the change in total protein abundance in cellular response to environmental cues, cell cycle stages, hormonal stimulation, oxidative stress, among others.

2. Healthy and diseased states can be further characterised and distinguished by developing appropriate model systems allowing us to follow the dispersion of functional systems over multiple subcellular locations and include the dynamic redistribution of proteins. This would need more integration of the large scale technologies including genomics, transcriptomics, metabolomics and proteomics.

3. This concept of cellular functions that are revealed via the subcellular spatial razor method, may contribute to an advance in effective medical diagnostics and safe therapeutics.

4. In adopting practical and suitable biological modelling systems, the dynamicity of highly complex systems such as cells can be systematically investigated at different scales.

5. The goals of studying largescale changes in protein abundances and modifications of changes in subcellular compartments have become feasible, owing to the maturity of MS-based proteomics into state of art technologies.

6. There is also a need for improved databases that explicitly tie together function/location as pair relationships for individual proteins; at present, databases such as GO obscure crucial information by neglecting this.

7. Discrete functional roles, and dual or multiple roles of proteins that are disseminated to multiple subcellular locations are thought to play a role in modulating cellular response to stimulation, treatment or insults. Therefore, ‘moonlighting’ phenomena are more visible at proteome level, than through genome or transcriptome approaches.

8. Proteins are the terminal players involved in highly complex processes that are connected via multiple networks linking hierarchical anatomical system entities and formulating the function or dysfunction of an organism. Thus, the subcellular spatial distribution of proteins is dynamic; a change in cellular state is a central mechanism of cellular functions.

9. Change in subcellular localisation and abundance in response to biological perturbations was the dominant response of MCF-7 cells exposed to oestrogen and antioestrogen (tamoxifen). The nuclear-cytoplasmic trafficking of proteins is a major response to hormonal stimulation, rather than changes in total abundances.

10. Distribution of sub-proteome changes in subsystems of MCF-7 cancer cells appear to be essential for tumour survival and/or resistance to treatment that to adapt metabolism, oxidative phosphorylation, signalling transduction, cell adhesion, cross talk between pathways, cell growth, cell cycle and non-apoptotic proteins that are spatially distributed to enhance the progression of cancer cells.

11. Tamoxifen resistance is correlated to numerous mechanisms that are involved in changes in order and magnitude of a large number of proteins, elucidating complexity and heterogeneity of cancer cells. Most of the subcellular changes associated with tamoxifen stimulation in this project were of upregulation of proteins known to enhance tumour proliferation rather than suppression, therefore, an agonist or partial agonistic effects of the drug could be predicted in light of the subcellular localisation of proteins and/or moonlighting roles of localised/redistributed proteins.

Chapter 6 Future directions

Elucidating the exact mechanisms underlying the proliferative actions of hormonal exposure, particularly E2, and overcoming the failure of the endocrine-targeted therapy (ETT) to prevent the relapse of the disease in (HR+ve) positive breast cancers, will remain extremely challenging. However, the new high performance technologies are helping to gain better insight using modelling systems without jeopardising the dynamics of the integral cellular parts.

In this project, the spatial distribution of proteins between subcellular compartments and their possible functions involved in cancer formation and progression following biological perturbations, mainly E2 and 4-OHT, was investigated. The conclusions were reached using stimulated MCF-7 and were consistent to those previously reported in this laboratory (Baqader et al., 2014, Mulvey et al., 2013, Pinto et al., 2016, Qattan et al., 2012, Radulovic et al., 2016), and using different stimuli and/or cell lines demonstrates that the spatial-temporal dynamics of the subcellular proteomes appears to be an essential cellular control of major cell processes such as metabolism, oxidative phosphorylation, signalling transduction, cell cycle and cell growth, to name a few.

Carcinogenesis is a multistep process and involves many biological alterations that are accumulated over time due to specific and nonspecific causes and effects. The complexity of neoplasm prompted the need to develop methods for subcellular proteomic analysis to obtain an in-depth understanding of the molecular basis of cancer.

In breast cancer, cell growth can be mediated by genomic and non-genomic pathways, therefore, in the rapid (non-genomic) response numerous cross talked pathways, different forms of receptors, and activated protein kinases are involved and eventually lead to enhanced transcriptional activities and tumour survival and progression. For example, in response to tamoxifen treatment we have shown that the upregulated G proteins (GNA12, 13, GNAS) are significantly redistributed in the subcellular compartments. Moreover, they are significantly impacted in suggested cancer pathways. They are constituting subunits of GPCR, particularly GRP30, which is a new form of ERs that can modulate non-oestrogenic pathways by attenuating a cyclic adenosine pathway (cAMP), activating ERK1 and ERK2, and PIP3/AKT pathways (see discussion). Additionally, SET oncoprotein was upregulated in nuclear compartment, indicating that multiple cellular inhibition, such as protein phosphatase 2A (PP2A), and activation, such as AKT signalling, are likely to take place as a consequence to the potent actions of SET.

Future studies will need to gain more understanding of cellular signalling networks. Thus, an extension of the current subcellular fractionation model, designing a suitable experiment to involve other selective oestrogenic down regulators (SERDs) and a pure ER antagonist ICI 182,780 for quantitative phosphoproteomic analysis and a spatial razor model for interpretation would help to highlight many aspects related to signalling in cancer cells and interaction with ER receptors that are far from elucidation.

Recently the effort was made to address the total changes of phosphorylation in a phosphoproteome study of tamoxifen stimulated wild type MCF-7 and tamoxifen resistant MCF-7 cell lines. Although this is a valuable approach, no attempt was made to study the dynamics of sub cellular distribution (Wu et all, 2015).

Comparing phosphoproteomics dynamics in response to SERM (Tamoxifen), SERD (Fulvestrant), oestrogen, and pure antagonist ICI 182,780 would generate a massive number of phosphoproteins that change in abundance, or in subcellular localisation that needs to be integrated with publicly available data on breast cancer and ETT clinical trials. Therefore, using an advanced knowledge management software package would offer a graphical, interactive and dynamic map of breast cancer and ETTacquired chemoresistance based on connecting the obtained research data with patient clinical information. BioXM™ Knowledge Management Environment (Blake et al., 2011, Cano et al., 2014, Losko et al., 2006, Suh et al., 2013) can be used to create an interactive, semantically integrated map of breast cancer and targeted therapy resistance in which pre-existing knowledge on protein-protein interactions, subcellular localisation, gene expression, pathway activation, protein modification, drugs and drug treatments and clinical data and trials will be integrated with experimental data obtained in phosphoproteomics.

Cell line models are not ideal biological representatives in all forms of resistance, as seen in clinical patients. For example, aromatase inhibitors target the peripheral tissues and inhibit the oestrogen production via enzymatic conversion of androgens by aromatase (Dixon, 2014, Miller and O'Neill, 1987). It would be interesting to feed the xenograft with diets of heavy amino acids instead of the light (SILAC in vivo) which would give rise, after one generation, to a spike-in standard model organism that can be used for further analysis of tissues or body fluids (Krüger et al., 2008, Sury et al., 2010). This would allow the investigation of the peripheral conversion of progestogens into active metabolites (E2) by aromatase, and therefore, ER-induced cellular proliferation, aromatase inhibition and suppression of ER, and ultimately, the acquired resistance to tamoxifen. Furthermore, this method may also be used as a long term future approach and may also be extended to involve other forms of ETT.

In terms of mass spectrometry-driven proteomics, the future direction is pointing towards the development of DIA (data independent acquisition) (Bruderer et al., 2015) in mass spectrometric experiments, thus increasing the number of observed proteins. However this approach needs to be balanced against an increase in false positive results. Bioinformatic analyses are expected to evolve in ‘Big Data’ systemic analyses, which in turn can revolutionise cellular biology.

References

ABDOLZADE-BAVIL, A., HAYES, S., GORETZKI, L., KROGER, M., ANDERS, J. & HENDRIKS, R. 2004. Convenient and versatile subcellular extraction procedure, that facilitates classical protein expression profiling and functional protein analysis. *Proteomics,* 4**,** 1397-405.

ABRIL, J., DE HEREDIA, M. L., GONZALEZ, L., CLERIES, R., NADAL, M., CONDOM, E., AGUILO, F., GOMEZ-ZAERA, M. & NUNES, V. 2008. Altered expression of 12S/MT-RNR1, MT-CO2/COX2, and MT-ATP6 mitochondrial genes in prostate cancer. *Prostate,* 68**,** 1086-96.

ACEHAN, D., JIANG, X., MORGAN, D. G., HEUSER, J. E., WANG, X. & AKEY, C. W. 2002. Three-dimensional structure of the apoptosome: implications for assembly, procaspase-9 binding, and activation. *Mol Cell,* 9**,** 423-32.

ACKERMANN, B. L. & BERNA, M. J. 2007. Coupling immunoaffinity techniques with MS for quantitative analysis of low-abundance protein biomarkers. *Expert Rev Proteomics,* 4**,** 175-86.

AEBERSOLD, R. & MANN, M. 2003. Mass spectrometry-based proteomics. *Nature,* 422**,** 198-207.

AITKEN, A. 2006. 14-3-3 proteins: a historic overview. *Semin Cancer Biol,* 16**,** 162-72.

AL-JASSAR, C., BIKKER, H., OVERDUIN, M. & CHIDGEY, M. 2013. Mechanistic Basis of Desmosome-Targeted Diseases. *Journal of Molecular Biology,* 425**,** 4006-4022.

ALARID, E. T. 2006. Lives and Times of Nuclear Receptors. *Molecular Endocrinology,* 20**,** 1972-1981.

ALARID, E. T., BAKOPOULOS, N. & SOLODIN, N. 1999. Proteasome-Mediated Proteolysis of Estrogen Receptor: A Novel Component in Autologous Down-Regulation. *Molecular Endocrinology,* 13**,** 1522-1534.

ALBREKTSEN, G., HEUCH, I., HANSEN, S. & KVALE, G. 2005. Breast cancer risk by age at birth, time since birth and time intervals between births: exploring interaction effects. *Br J Cancer,* 92**,** 167-75.

ALEXA, A., RAHNENFUHRER, J. & LENGAUER, T. 2006. Improved scoring of functional groups from gene expression data by decorrelating GO graph structure. *Bioinformatics,* 22**,** 1600-7.

ALI, S. & COOMBES, R. C. 2002. Endocrine-responsive breast cancer and strategies for combating resistance. *Nat Rev Cancer,* 2**,** 101-112.

ALLISON, K. H. 2012. Molecular Pathology of Breast Cancer: What a Pathologist Needs to Know. *American Journal of Clinical Pathology,* 138**,** 770-780.

AMERICAN CANCER SOCIETY. 2016. Available: http://lrweb.beds.ac.uk/guides/a-guide-to-referencing/citing-e-sources [Accessed 03/09 2015].

ANDERSEN, J. S., LAM, Y. W., LEUNG, A. K., ONG, S. E., LYON, C. E., LAMOND, A. I. & MANN, M. 2005. Nucleolar proteome dynamics. *Nature,* 433**,** 77-83.

ANDERSEN, J. S., LYON, C. E., FOX, A. H., LEUNG, A. K., LAM, Y. W., STEEN, H., MANN, M. & LAMOND, A. I. 2002. Directed proteomic analysis of the human nucleolus. *Curr Biol,* 12**,** 1-11.

ANDERSEN, J. S. & MANN, M. 2006. Organellar proteomics: turning inventories into insights. *EMBO Rep,* 7**,** 874-9.

ANDERSON, L. & SEILHAMER, J. 1997. A comparison of selected mRNA and protein abundances in human liver. *Electrophoresis,* 18**,** 533-7.

ANDERSON, N. L. & ANDERSON, N. G. 2002. The human plasma proteome: history, character, and diagnostic prospects. *Mol Cell Proteomics,* 1**,** 845-67.

ANDERSON, N. L. & ANDERSON, N. G. 2002. The Human Plasma Proteome: History, Character, and Diagnostic Prospects. *Molecular & Cellular Proteomics,* 1**,** 845-867.

ANDREY, L. 1989. Chaos in cancer. *Med Hypotheses,* 28**,** 143-4.

ANGELOPOULOS, N., BARBOUNIS, V., LIVADAS, S., KALTSAS, D. & TOLIS, G. 2004. Effects of estrogen deprivation due to breast cancer treatment. *Endocrine-Related Cancer,* 11**,** 523-535.

ARIAZI, E. A., BRAILOIU, E., YERRUM, S., SHUPP, H. A., SLIFKER, M. J., CUNLIFFE, H. E., BLACK, M. A., DONATO, A. L., ARTERBURN, J. B., OPREA, T. I., PROSSNITZ, E. R., DUN, N. J. & JORDAN, V. C. 2010. The G protein-coupled receptor GPR30 inhibits proliferation of estrogen receptor-positive breast cancer cells. *Cancer Res,* 70**,** 1184-94.

ASHBURNER, M., BALL, C. A., BLAKE, J. A., BOTSTEIN, D., BUTLER, H., CHERRY, J. M., DAVIS, A. P., DOLINSKI, K., DWIGHT, S. S., EPPIG, J. T., HARRIS, M. A., HILL, D. P., ISSEL-TARVER, L., KASARSKIS, A., LEWIS, S., MATESE, J. C., RICHARDSON, J. E., RINGWALD, M., RUBIN, G. M. & SHERLOCK, G. 2000. Gene ontology: tool for the unification of biology. The Gene Ontology Consortium. *Nat Genet,* 25**,** 25-9.

ASHER, G., BERCOVICH, Z., TSVETKOV, P., SHAUL, Y. & KAHANA, C. 2005. 20S proteasomal degradation of ornithine decarboxylase is regulated by NQO1. *Mol Cell,* 17**,** 645-55.

AZAM, S., JOUVET, N., JILANI, A., VONGSAMPHANH, R., YANG, X., YANG, S. & RAMOTAR, D. 2008. Human glyceraldehyde-3-phosphate dehydrogenase plays a direct role in reactivating oxidized forms of the DNA repair enzyme APE1. *J Biol Chem,* 283**,** 30632-41.

BACKOS, D. S., FRANKLIN, C. C. & REIGAN, P. 2012. The role of glutathione in brain tumor drug resistance. *Biochem Pharmacol,* 83**,** 1005-12.

BANG, Y. J., VAN CUTSEM, E., FEYEREISLOVA, A., CHUNG, H. C., SHEN, L., SAWAKI, A., LORDICK, F., OHTSU, A., OMURO, Y., SATOH, T., APRILE, G., KULIKOV, E., HILL, J., LEHLE, M., RÜSCHOFF, J. & KANG, Y. K. 2010. Trastuzumab in combination with chemotherapy versus chemotherapy alone for treatment of HER2-positive advanced gastric or gastro-oesophageal junction cancer (ToGA): A phase 3, open-label, randomised controlled trial. *The Lancet,* 376**,** 687-697.

BAQADER, N. O., RADULOVIC, M., CRAWFORD, M., STOEBER, K. & GODOVAC-ZIMMERMANN, J. 2014. Nuclear Cytoplasmic Trafficking of Proteins is a Major Response of Human Fibroblasts to Oxidative Stress. *Journal of Proteome Research,* 13**,** 4398-4423.

BAQADER, N. O., RADULOVIC, M., CRAWFORD, M., STOEBER, K. & GODOVAC-ZIMMERMANN, J. 2014. Nuclear cytoplasmic trafficking of proteins is a major response of human fibroblasts to oxidative stress. *J Proteome Res,* 13**,** 4398-423.

BATEMAN, N. W., SUN, M., HOOD, B. L., FLINT, M. S. & CONRADS, T. P. 2010. Defining central themes in breast cancer biology by differential proteomics: conserved regulation of cell spreading and focal adhesion kinase. *J Proteome Res,* 9**,** 5311-24.

BENJAMINI, Y. & HOCHBERG, Y. 1995. Controlling the False Discovery Rate: A Practical and Powerful Approach to Multiple Testing. *Journal of the Royal Statistical Society. Series B (Methodological),* 57**,** 289-300.

BERNSTEIN, L. 2002. Epidemiology of Endocrine-Related Risk Factors for Breast Cancer. *Journal of Mammary Gland Biology and Neoplasia,* 7**,** 3-15.

BERNSTEIN, L., DEPUE, R. H., ROSS, R. K., JUDD, H. L., PIKE, M. C. & HENDERSON, B. E. 1986. Higher maternal levels of free estradiol in first compared to second pregnancy: early gestational differences. *J Natl Cancer Inst,* 76**,** 1035-9.

BJORNSTROM, L. & SJOBERG, M. 2005. Mechanisms of estrogen receptor signaling: convergence of genomic and nongenomic actions on target genes. *Mol Endocrinol,* 19**,** 833-42.

BLAKE, P. M., DECKER, D. A., GLENNON, T. M., LIANG, Y. M., LOSKO, S., NAVIN, N. & SUH, K. S. 2011. Toward an integrated knowledge environment to support modern oncology. *Cancer J,* 17**,** 257-63.

BOCK, G., STEINLEIN, P. & HUBER, L. A. 1997. Cell biologists sort things out: Analysis and purification of intracellular organelles by flow cytometry. *Trends Cell Biol,* 7**,** 499-503.

BOEHNING, D., PATTERSON, R. L., SEDAGHAT, L., GLEBOVA, N. O., KUROSAKI, T. & SNYDER, S. H. 2003. Cytochrome c binds to inositol (1,4,5) trisphosphate receptors, amplifying calcium-dependent apoptosis. *Nat Cell Biol,* 5**,** 1051-61.

BOISVERT, F.-M., LAM, Y. W., LAMONT, D. & LAMOND, A. I. 2010. A Quantitative Proteomics Analysis of Subcellular Proteome Localization and Changes Induced by DNA Damage. *Molecular & Cellular Proteomics,* 9**,** 457-470.

BOLT, M. J., STOSSI, F., NEWBERG, J. Y., ORJALO, A., JOHANSSON, H. E. & MANCINI, M. A. 2013. Coactivators enable glucocorticoid receptor recruitment to fine-tune estrogen receptor transcriptional responses. *Nucleic Acids Res,* 41**,** 4036-48.

BONAMY, G. M. & ALLISON, L. A. 2006. Oncogenic conversion of the thyroid hormone receptor by altered nuclear transport. *Nucl Recept Signal,* 4**,** e008.

BONAMY, G. M., GUIOCHON-MANTEL, A. & ALLISON, L. A. 2005. Cancer promoted by the oncoprotein v-ErbA may be due to subcellular mislocalization of nuclear receptors. *Mol Endocrinol,* 19**,** 1213-30.

BONNET, S., ARCHER, S. L., ALLALUNIS-TURNER, J., HAROMY, A., BEAULIEU, C., THOMPSON, R., LEE, C. T., LOPASCHUK, G. D., PUTTAGUNTA, L., BONNET, S., HARRY, G., HASHIMOTO, K., PORTER, C. J., ANDRADE, M. A., THEBAUD, B. & MICHELAKIS, E. D. 2007. A mitochondria-K+ channel axis is suppressed in cancer and its normalization promotes apoptosis and inhibits cancer growth. *Cancer Cell,* 11**,** 37-51.

BOYD, Z. S., WU, Q. J., O'BRIEN, C., SPOERKE, J., SAVAGE, H., FIELDER, P. J., AMLER, L., YAN, Y. & LACKNER, M. R. 2008. Proteomic analysis of breast cancer molecular subtypes and biomarkers of response to targeted kinase inhibitors using reverse-phase protein microarrays. *Mol Cancer Ther,* 7**,** 3695-706.

BRAFFORD, P. & HERLYN, M. 2005. Gene expression profiling of melanoma cells – searching the haystack. *Journal of Translational Medicine,* 3**,** 2-2.

BREUER, E. K. & MURPH, M. M. 2011. The Role of Proteomics in the Diagnosis and Treatment of Women's Cancers: Current Trends in Technology and Future Opportunities. *Int J Proteomics,* 2011.

BREUER, K., FOROUSHANI, A. K., LAIRD, M. R., CHEN, C., SRIBNAIA, A., LO, R., WINSOR, G. L., HANCOCK, R. E., BRINKMAN, F. S. & LYNN, D. J. 2013. InnateDB: systems biology of innate immunity and beyond--recent updates and continuing curation. *Nucleic Acids Res,* 41**,** D1228-33.

BROOKS, J. D. 2012. Translational genomics: the challenge of developing cancer biomarkers. *Genome Res,* 22**,** 183-7.

BROWN, M. & SHARP, P. A. 1990. Human estrogen receptor forms multiple protein-DNA complexes. *J Biol Chem,* 265**,** 11238-43.

BRUDERER, R., BERNHARDT, O. M., GANDHI, T., MILADINOVIĆ, S. M., CHENG, L.-Y., MESSNER, S., EHRENBERGER, T., ZANOTELLI, V., BUTSCHEID, Y., ESCHER, C., VITEK, O., RINNER, O. & REITER, L. 2015. Extending the Limits of Quantitative Proteome Profiling with Data-

Independent Acquisition and Application to Acetaminophen-Treated Three-Dimensional Liver Microtissues. *Molecular & Cellular Proteomics,* 14**,** 1400-1410.

BRUNET, A., KANAI, F., STEHN, J., XU, J., SARBASSOVA, D., FRANGIONI, J. V., DALAL, S. N., DECAPRIO, J. A., GREENBERG, M. E. & YAFFE, M. B. 2002. 14-3-3 transits to the nucleus and participates in dynamic nucleocytoplasmic transport. *J Cell Biol,* 156**,** 817-28.

BRUNNER, N., BOYSEN, B., JIRUS, S., SKAAR, T. C., HOLST-HANSEN, C., LIPPMAN, J., FRANDSEN, T., SPANG-THOMSEN, M., FUQUA, S. A. & CLARKE, R. 1997. MCF7/LCC9: an antiestrogen-resistant MCF-7 variant in which acquired resistance to the steroidal antiestrogen ICI 182,780 confers an early cross-resistance to the nonsteroidal antiestrogen tamoxifen. *Cancer Res,* 57**,** 3486-93.

BUZDAR, A. U. 2005. Aromatase inhibitors: Changing the face of endocrine therapy for breast cancer. *Breast Disease,* 24**,** 107-117.

CADENAS, C., FRANCKENSTEIN, D., SCHMIDT, M., GEHRMANN, M., HERMES, M., GEPPERT, B., SCHORMANN, W., MACCOUX, L. J., SCHUG, M., SCHUMANN, A., WILHELM, C., FREIS, E., ICKSTADT, K., RAHNENFUHRER, J., BAUMBACH, J. I., SICKMANN, A. & HENGSTLER, J. G. 2010. Role of thioredoxin reductase 1 and thioredoxin interacting protein in prognosis of breast cancer. *Breast Cancer Res,* 12**,** R44.

CALIN, G. A., VASILESCU, C., NEGRINI, M. & BARBANTI-BRODANO, G. 2003. Genetic chaos and antichaos in human cancers. *Med Hypotheses,* 60**,** 258-62.

CAMPBELL, M. R., KARACA, M., ADAMSKI, K. N., CHORLEY, B. N., WANG, X. & BELL, D. A. 2013. Novel Hematopoietic Target Genes in the NRF2-Mediated Transcriptional Pathway. *Oxidative Medicine and Cellular Longevity,* 2013**,** 12.

CANO, I., TÉNYI, Á., SCHUELLER, C., WOLFF, M., HUERTAS MIGUELÁÑEZ, M. M., GOMEZ-CABRERO, D., ANTCZAK, P., ROCA, J., CASCANTE, M., FALCIANI, F. & MAIER, D. 2014. The COPD Knowledge Base: enabling data analysis and computational simulation in translational COPD research. *Journal of Translational Medicine,* 12**,** 1-9.

CASTORIA, G., MIGLIACCIO, A. & AURICCHIO, F. 2009. Signaling-dependent nuclear export of estradiol receptor controls cell cycle progression in breast cancer cells. *Mol Cell Endocrinol,* 308**,** 26-31.

CASTORIA, G., MIGLIACCIO, A. & AURICCHIO, F. 2009. Signaling-dependent nuclear export of estradiol receptor controls cell cycle progression in breast cancer cells. *Molecular and Cellular Endocrinology,* 308**,** 26-31.

CATTANEO, A., BIOCCA, S., CORVAJA, N. & CALISSANO, P. 1985. Nuclear localization of a lactic dehydrogenase with single-stranded DNA-binding properties. *Experimental Cell Research,* 161**,** 130-140.

CELIS, J. E., KRUHOFFER, M., GROMOVA, I., FREDERIKSEN, C., OSTERGAARD, M., THYKJAER, T., GROMOV, P., YU, J., PALSDOTTIR, H., MAGNUSSON, N. & ORNTOFT, T. F. 2000. Gene expression profiling: monitoring transcription and translation products using DNA microarrays and proteomics. *FEBS Lett,* 480**,** 2-16.

CENTERS FOR DISEASE CONTROL AND PREVENTION. 2015. *Statistics for Different Kinds of Cancer* [Online]. Available: http://www.cdc.gov/cancer/dcpc/data/types.htm [Accessed 01/02 2016].

CHACINSKA, A., KOEHLER, C. M., MILENKOVIC, D., LITHGOW, T. & PFANNER, N. 2009. Importing mitochondrial proteins: machineries and mechanisms. *Cell,* 138**,** 628-44.

CHAFFER, C. L. & WEINBERG, R. A. 2011. A Perspective on Cancer Cell Metastasis. *Science,* 331**,** 1559-1564.

CHAN, C. M., MARTIN, L. A., JOHNSTON, S. R., ALI, S. & DOWSETT, M. 2002. Molecular changes associated with the acquisition of oestrogen hypersensitivity in MCF-7 breast cancer cells on long-term oestrogen deprivation. *J Steroid Biochem Mol Biol,* 81**,** 333-41.

CHANG, M. 2012. Tamoxifen Resistance in Breast Cancer. *Biomolecules & Therapeutics,* 20**,** 256-267.

CHANG, Y.-C., JAN, Y.-H., SU, C.-Y. & HSIAO, M. 2015. Non-glycolytic Function of Aldolase A Promotes Lung Cancer Metastasis through Down-regulation of PLD2 Enzyme to Activate PLD1. *The FASEB Journal,* 29.

CHATTERJEE, A., DASGUPTA, S. & SIDRANSKY, D. 2011. Mitochondrial subversion in cancer. *Cancer Prev Res (Phila),* 4**,** 638-54.

CHEN, E. I. & YATES, J. R., 3RD 2007. Cancer proteomics by quantitative shotgun proteomics. *Mol Oncol,* 1**,** 144-59.

CHEN, J. Q., CAMMARATA, P. R., BAINES, C. P. & YAGER, J. D. 2009. Regulation of mitochondrial respiratory chain biogenesis by estrogens/estrogen receptors and physiological, pathological and pharmacological implications. *Biochim Biophys Acta,* 1793**,** 1540-70.

CHEN, J. Q., DELANNOY, M., COOKE, C. & YAGER, J. D. 2004. Mitochondrial localization of ERalpha and ERbeta in human MCF7 cells. *Am J Physiol Endocrinol Metab,* 286**,** E1011-22.

CHEN, Z., RUAN, Q., HAN, S., XI, L., JIANG, W., JIANG, H., OSTROV, D. A. & CAI, J. 2014. Discovery of structure-based small molecular inhibitor of alphaB-crystallin against basal-like/triple-negative breast cancer development in vitro and in vivo. *Breast Cancer Res Treat,* 145**,** 45-59.

CHIS, R., SHARMA, P., BOUSETTE, N., MIYAKE, T., WILSON, A., BACKX, P. H. & GRAMOLINI, A. O. 2012. alpha-Crystallin B prevents apoptosis after H2O2 exposure in mouse neonatal cardiomyocytes. *Am J Physiol Heart Circ Physiol,* 303**,** H967-78.

CHRISTOFK, H. R., VANDER HEIDEN, M. G., HARRIS, M. H., RAMANATHAN, A., GERSZTEN, R. E., WEI, R., FLEMING, M. D., SCHREIBER, S. L. & CANTLEY, L. C. 2008. The M2 splice isoform of pyruvate kinase is important for cancer metabolism and tumour growth. *Nature,* 452**,** 230-3.

CHU, H. Y. & HOPPER, A. K. 2013. Genome-wide investigation of the role of the tRNA nuclear-cytoplasmic trafficking pathway in regulation of the yeast Saccharomyces cerevisiae transcriptome and proteome. *Mol Cell Biol,* 33**,** 4241-54.

CICATIELLO, L., SICA, V., BRESCIANI, F. & WEISZ, A. 1993. Identification of a specific pattern of "immediate-early" gene activation induced by estrogen during mitogenic stimulation of rat uterine cells. *Receptor,* 3**,** 17-30.

CLARKE, R., DICKSON, R. B. & BRÜNNER, N. 1990. The process of malignant progression in human breast cancer. *Annals of Oncology,* 1**,** 401-407.

CLARKE, R., SHAJAHAN, A. N., RIGGINS, R. B., CHO, Y., CRAWFORD, A., XUAN, J., WANG, Y., ZWART, A., NEHRA, R. & LIU, M. C. 2009. Gene network signaling in hormone responsiveness modifies apoptosis and autophagy in breast cancer cells. *J Steroid Biochem Mol Biol,* 114**,** 8-20.

COLDITZ, G. A. 1998. Relationship between estrogen levels, use of hormone replacement therapy, and breast cancer. *J Natl Cancer Inst,* 90**,** 814-23.

COLDITZ, G. A. & ROSNER, B. 2000. Cumulative risk of breast cancer to age 70 years according to risk factor status: data from the Nurses' Health Study. *Am J Epidemiol,* 152**,** 950-64.

COLLEONI, M., GELBER, S., COATES, A. S., CASTIGLIONE-GERTSCH, M., GELBER, R. D., PRICE, K., RUDENSTAM, C. M., LINDTNER, J., COLLINS, J., THÜRLIMANN, B., HOLMBERG, S. B., CORTES-FUNES, H., SIMONCINI, E., MURRAY, E., FEY, M. & GOLDHIRSCH, A. 2001. Influence of endocrine-related factors on response to perioperative chemotherapy for patients with node-negative breast cancer. *Journal of Clinical Oncology,* 19**,** 4141-4149.

COLLER, H. A. 2014. Is cancer a metabolic disease? *Am J Pathol,* 184**,** 4-17.

COLOMBO, S. L., PALACIOS-CALLENDER, M., FRAKICH, N., CARCAMO, S., KOVACS, I., TUDZAROVA, S. & MONCADA, S. 2011. Molecular basis for the differential use of glucose and glutamine in cell proliferation as revealed by synchronized HeLa cells. *Proc Natl Acad Sci U S A,* 108**,** 21069-74.

CONESA, C. & ACKER, J. 2010. Sub1/PC4 a chromatin associated protein with multiple functions in transcription. *RNA Biol,* 7**,** 287-90.

COX, J. & MANN, M. 2008. MaxQuant enables high peptide identification rates, individualized p.p.b.-range mass accuracies and proteome-wide protein quantification. *Nat Biotech,* 26**,** 1367-1372.

COX, J. & MANN, M. 2011. Quantitative, High-Resolution Proteomics for Data-Driven Systems Biology. *Annual Review of Biochemistry,* 80**,** 273-299.

COX, J. & MANN, M. 2011. Quantitative, high-resolution proteomics for data-driven systems biology. *Annu Rev Biochem,* 80**,** 273-99.

COX, J., MATIC, I., HILGER, M., NAGARAJ, N., SELBACH, M., OLSEN, J. V. & MANN, M. 2009. A practical guide to the MaxQuant computational platform for SILAC-based quantitative proteomics. *Nat Protoc,* 4**,** 698-705.

CROFT, D., O'KELLY, G., WU, G., HAW, R., GILLESPIE, M., MATTHEWS, L., CAUDY, M., GARAPATI, P., GOPINATH, G., JASSAL, B., JUPE, S., KALATSKAYA, I., MAHAJAN, S., MAY, B., NDEGWA, N., SCHMIDT,

E., SHAMOVSKY, V., YUNG, C., BIRNEY, E., HERMJAKOB, H., D'EUSTACHIO, P. & STEIN, L. 2011. Reactome: a database of reactions, pathways and biological processes. *Nucleic Acids Res,* 39**,** D691-7.

CUI, J., SHEN, Y. & LI, R. 2013. Estrogen synthesis and signaling pathways during aging: from periphery to brain. *Trends Mol Med,* 19**,** 197-209.

DANG, C. V. 2010. Rethinking the Warburg effect with Myc micromanaging glutamine metabolism. *Cancer Res,* 70**,** 859-62.

DANG, C. V., O'DONNELL, K. A., ZELLER, K. I., NGUYEN, T., OSTHUS, R. C. & LI, F. 2006. The c-Myc target gene network. *Semin Cancer Biol,* 16**,** 253-64.

DANIEL, V. C., MARCHIONNI, L., HIERMAN, J. S., RHODES, J. T., DEVEREUX, W. L., RUDIN, C. M., YUNG, R., PARMIGIANI, G., DORSCH, M., PEACOCK, C. D. & WATKINS, D. N. 2009. A primary xenograft model of small-cell lung cancer reveals irreversible changes in gene expression imposed by culture in vitro. *Cancer Res,* 69**,** 3364-73.

DAS, C., HIZUME, K., BATTA, K., KUMAR, B. R., GADAD, S. S., GANGULY, S., LORAIN, S., VERREAULT, A., SADHALE, P. P., TAKEYASU, K. & KUNDU, T. K. 2006. Transcriptional coactivator PC4, a chromatin-associated protein, induces chromatin condensation. *Mol Cell Biol,* 26**,** 8303-15.

DAVIES, C., GODWIN, J., GRAY, R., CLARKE, M., CUTTER, D., DARBY, S., MCGALE, P., PAN, H. C., TAYLOR, C., WANG, Y. C., DOWSETT, M., INGLE, J. & PETO, R. 2011. Relevance of breast cancer hormone receptors and other factors to the efficacy of adjuvant tamoxifen: patient-level meta-analysis of randomised trials. *Lancet,* 378**,** 771-84.

DAVIES, C., PAN, H., GODWIN, J., GRAY, R., ARRIAGADA, R., RAINA, V., ABRAHAM, M., ALENCAR, V. H. M., BADRAN, A., BONFILL, X., BRADBURY, J., CLARKE, M., COLLINS, R., DAVIS, S. R., DELMESTRI, A., FORBES, J. F., HADDAD, P., HOU, M.-F., INBAR, M., KHALED, H., KIELANOWSKA, J., KWAN, W.-H., MATHEW, B. S., MÜLLER, B., NICOLUCCI, A., PERALTA, O., PERNAS, F., PETRUZELKA, L., PIENKOWSKI, T., RAJAN, B., RUBACH, M. T., TORT, S., URRÚTIA, G., VALENTINI, M., WANG, Y., PETO, R. & FOR THE ADJUVANT TAMOXIFEN: LONGER AGAINST SHORTER COLLABORATIVE, G. 2013. Long-term effects of continuing adjuvant tamoxifen to 10 years versus stopping at 5 years after diagnosis of oestrogen

receptor-positive breast cancer: ATLAS, a randomised trial. *Lancet,* 381**,** 805-816.

DE ARAUJO, M. E., HUBER, L. A. & STASYK, T. 2008. Isolation of endocitic organelles by density gradient centrifugation. *Methods Mol Biol,* 424**,** 317-31.

DEBERARDINIS, R. J. & CHENG, T. 2010. Q's next: the diverse functions of glutamine in metabolism, cell biology and cancer. *Oncogene,* 29**,** 313-24.

DEBERARDINIS, R. J., MANCUSO, A., DAIKHIN, E., NISSIM, I., YUDKOFF, M., WEHRLI, S. & THOMPSON, C. B. 2007. Beyond aerobic glycolysis: transformed cells can engage in glutamine metabolism that exceeds the requirement for protein and nucleotide synthesis. *Proc Natl Acad Sci U S A,* 104**,** 19345-50.

DELLA TORRE, S., MITRO, N., FONTANA, R., GOMARASCHI, M., FAVARI, E., RECORDATI, C., LOLLI, F., QUAGLIARINI, F., MEDA, C., OHLSSON, C., CRESTANI, M., UHLENHAUT, NINA H., CALABRESI, L. & MAGGI, A. 2016. An Essential Role for Liver ERα in Coupling Hepatic Metabolism to the Reproductive Cycle. *Cell Reports,* 15**,** 360-371.

DI LEVA, G., PIOVAN, C., GASPARINI, P., NGANKEU, A., TACCIOLI, C., BRISKIN, D., CHEUNG, D. G., BOLON, B., ANDERLUCCI, L., ALDER, H., NUOVO, G., LI, M., IORIO, M. V., GALASSO, M., SANTHANAM, R., MARCUCCI, G., PERROTTI, D., POWELL, K. A., BRATASZ, A., GAROFALO, M., NEPHEW, K. P. & CROCE, C. M. 2013. Estrogen mediated-activation of miR-191/425 cluster modulates tumorigenicity of breast cancer cells depending on estrogen receptor status. *PLoS Genet,* 9**,** e1003311.

DIXON, J. M. 2014. Endocrine Resistance in Breast Cancer. *New Journal of Science,* 2014**,** 27.

DOMON, B. & AEBERSOLD, R. 2006. Mass Spectrometry and Protein Analysis. *Science,* 312**,** 212-217.

DOPIE, J., SKARP, K.-P., KAISA RAJAKYLÄ, E., TANHUANPÄÄ, K. & VARTIAINEN, M. K. 2012. Active maintenance of nuclear actin by importin 9 supports transcription. *Proceedings of the National Academy of Sciences.*

DORSSERS, L. C., VAN DER FLIER, S., BRINKMAN, A., VAN AGTHOVEN, T., VELDSCHOLTE, J., BERNS, E. M., KLIJN, J. G., BEEX, L. V. &

FOEKENS, J. A. 2001. Tamoxifen resistance in breast cancer: elucidating mechanisms. *Drugs,* 61**,** 1721-33.

DRABOVICH, A. P., PAVLOU, M. P., DIMITROMANOLAKIS, A. & DIAMANDIS, E. P. 2012. Quantitative analysis of energy metabolic pathways in MCF-7 breast cancer cells by selected reaction monitoring assay. *Mol Cell Proteomics,* 11**,** 422-34.

DRAGHICI, S., KHATRI, P., TARCA, A. L., AMIN, K., DONE, A., VOICHITA, C., GEORGESCU, C. & ROMERO, R. 2007. A systems biology approach for pathway level analysis. *Genome Res,* 17**,** 1537-45.

DRISSI, R., DUBOIS, M. L. & BOISVERT, F. M. 2013. Proteomics methods for subcellular proteome analysis. *Febs j,* 280**,** 5626-34.

DU, S., GUAN, Z., HAO, L., SONG, Y., WANG, L., GONG, L., LIU, L., QI, X., HOU, Z. & SHAO, S. 2014. Fructose-Bisphosphate Aldolase A Is a Potential Metastasis-Associated Marker of Lung Squamous Cell Carcinoma and Promotes Lung Cell Tumorigenesis and Migration. *PLoS ONE,* 9**,** e85804.

DUMITRESCU, R. G. 2012. DNA methylation and histone modifications in breast cancer. *Methods Mol Biol,* 863**,** 35-45.

DUNKLEY, T. P., WATSON, R., GRIFFIN, J. L., DUPREE, P. & LILLEY, K. S. 2004. Localization of organelle proteins by isotope tagging (LOPIT). *Mol Cell Proteomics,* 3**,** 1128-34.

DURAN, R. V., OPPLIGER, W., ROBITAILLE, A. M., HEISERICH, L., SKENDAJ, R., GOTTLIEB, E. & HALL, M. N. 2012. Glutaminolysis activates Rag-mTORC1 signaling. *Mol Cell,* 47**,** 349-58.

DZIJAK, R., YILDIRIM, S., KAHLE, M., NOVAK, P., HNILICOVA, J., VENIT, T. & HOZAK, P. 2012. Specific nuclear localizing sequence directs two myosin isoforms to the cell nucleus in calmodulin-sensitive manner. *PLoS One,* 7**,** e30529.

ECHEVERRIA, P. C. & PICARD, D. 2010. Molecular chaperones, essential partners of steroid hormone receptors for activity and mobility. *Biochim Biophys Acta,* 1803**,** 641-9.

ECKERSALL, D. & WHITFIELD, P. D. 2011. *Methods in Animal Proteomics*, Wiley.

ELBI, C., WALKER, D. A., ROMERO, G., SULLIVAN, W. P., TOFT, D. O., HAGER, G. L. & DEFRANCO, D. B. 2004. Molecular chaperones function as steroid receptor nuclear mobility factors. *Proc Natl Acad Sci U S A,* 101**,** 2876-81.

ELIUK, S. & MAKAROV, A. 2015. Evolution of Orbitrap Mass Spectrometry Instrumentation. *Annu Rev Anal Chem (Palo Alto Calif),* 8**,** 61-80.

ELLSWORTH, R. E., DECEWICZ, D. J., SHRIVER, C. D. & ELLSWORTH, D. L. 2010. Breast Cancer in the Personal Genomics Era. *Current Genomics,* 11**,** 146-161.

ENCYCLOPÆDIA BRITANNICA ONLINE. 2016. *Cancer* [Online]. Available: http://www.britannica.com/science/cancer-disease [Accessed 25/02 2016].

ENGER, S. M., ROSS, R. K., HENDERSON, B. & BERNSTEIN, L. 1997. Breastfeeding history, pregnancy experience and risk of breast cancer. *Br J Cancer,* 76**,** 118-23.

ENGER, S. M., ROSS, R. K., PAGANINI-HILL, A. & BERNSTEIN, L. 1998. Breastfeeding experience and breast cancer risk among postmenopausal women. *Cancer Epidemiol Biomarkers Prev,* 7**,** 365-9.

EROLES, P., BOSCH, A., ALEJANDRO PÉREZ-FIDALGO, J. & LLUCH, A. 2012. Molecular biology in breast cancer: Intrinsic subtypes and signaling pathways. *Cancer Treatment Reviews,* 38**,** 698-707.

ESSLINGER, C. S., CYBULSKI, K. A. & RHODERICK, J. F. 2005. Ngamma-aryl glutamine analogues as probes of the ASCT2 neutral amino acid transporter binding site. *Bioorg Med Chem,* 13**,** 1111-8.

ESTRELA, J. M., ORTEGA, A. & OBRADOR, E. 2006. Glutathione in cancer biology and therapy. *Crit Rev Clin Lab Sci,* 43**,** 143-81.

FAN, P. W. & BOLTON, J. L. 2001. Bioactivation of tamoxifen to metabolite E quinone methide: reaction with glutathione and DNA. *Drug Metab Dispos,* 29**,** 891-6.

FANCIULLI, M., BRUNO, T., GIOVANNELLI, A., GENTILE, F. P., DI PADOVA, M., RUBIU, O. & FLORIDI, A. 2000. Energy metabolism of human LoVo colon carcinoma cells: correlation to drug resistance and influence of lonidamine. *Clin Cancer Res,* 6**,** 1590-7.

FELTY, Q. & ROY, D. 2005. Estrogen, mitochondria, and growth of cancer and non-cancer cells. *J Carcinog,* 4**,** 1.

FELTY, Q. & ROY, D. 2005. Estrogen, mitochondria, and growth of cancer and non-cancer cells. *Journal of Carcinogenesis,* 4**,** 1-1.

FENN, J. B., MANN, M., MENG, C. K., WONG, S. F. & WHITEHOUSE, C. M. 1989. Electrospray ionization for mass spectrometry of large biomolecules. *Science,* 246**,** 64-71.

FERLAY, J., SOERJOMATARAM, I., DIKSHIT, R., ESER, S., MATHERS, C., REBELO, M., PARKIN, D. M., FORMAN, D. & BRAY, F. 2015. Cancer incidence and mortality worldwide: sources, methods and major patterns in GLOBOCAN 2012. *Int J Cancer,* 136**,** E359-86.

FILARDO, E. J., QUINN, J. A., BLAND, K. I. & FRACKELTON, A. R., JR. 2000. Estrogen-induced activation of Erk-1 and Erk-2 requires the G protein-coupled receptor homolog, GPR30, and occurs via trans-activation of the epidermal growth factor receptor through release of HB-EGF. *Mol Endocrinol,* 14**,** 1649-60.

FITTS, J. M., KLEIN, R. M. & POWERS, C. A. 2011. Tamoxifen Regulation of Bone Growth and Endocrine Function in the Ovariectomized Rat: Discrimination of Responses Involving Estrogen Receptor α/Estrogen Receptor β, G Protein-Coupled Estrogen Receptor, or Estrogen-Related Receptor γ Using Fulvestrant (ICI 182780). *Journal of Pharmacology and Experimental Therapeutics,* 338**,** 246-254.

FONG, C. J., BURGOON, L. D., WILLIAMS, K. J., FORGACS, A. L. & ZACHAREWSKI, T. R. 2007. Comparative temporal and dose-dependent morphological and transcriptional uterine effects elicited by tamoxifen and ethynylestradiol in immature, ovariectomized mice. *BMC Genomics,* 8**,** 151.

FONG, C. J., BURGOON, L. D., WILLIAMS, K. J., JONES, A. D., FORGACS, A. L. & ZACHAREWSKI, T. R. 2010. Effects of tamoxifen and ethynylestradiol cotreatment on uterine gene expression in immature, ovariectomized mice. *J Mol Endocrinol,* 45**,** 161-73.

FOSS, E. J., RADULOVIC, D., SHAFFER, S. A., GOODLETT, D. R., KRUGLYAK, L. & BEDALOV, A. 2011. Genetic variation shapes protein networks mainly through non-transcriptional mechanisms. *PLoS Biol,* 9**,** e1001144.

FOULDS, L. 1958. The natural history of cancer. *J Chronic Dis,* 8**,** 2-37.

FRASOR, J., DANES, J. M., KOMM, B., CHANG, K. C., LYTTLE, C. R. & KATZENELLENBOGEN, B. S. 2003. Profiling of estrogen up- and down-regulated gene expression in human breast cancer cells: insights into gene networks and pathways underlying estrogenic control of proliferation and cell phenotype. *Endocrinology,* 144**,** 4562-74.

FUQUA, S. A. 1994. Estrogen receptor mutagenesis and hormone resistance. *Cancer,* 74**,** 1026-9.

GABALDÓN, T. & PITTIS, A. A. 2015. Origin and evolution of metabolic sub-cellular compartmentalization in eukaryotes. *Biochimie,* 119**,** 262-268.

GANAPATHY-KANNIAPPAN, S. & GESCHWIND, J. F. 2013. Tumor glycolysis as a target for cancer therapy: progress and prospects. *Mol Cancer,* 12**,** 152.

GANNON, L. M., COTTER, M. B. & QUINN, C. M. 2013. The classification of invasive carcinoma of the breast. *Expert Review of Anticancer Therapy,* 13**,** 941-954.

GARRAWAY, LEVI A. & LANDER, ERIC S. 2013. Lessons from the Cancer Genome. *Cell,* 153**,** 17-37.

GAUTHIER, D. J. & LAZURE, C. 2008. Complementary methods to assist subcellular fractionation in organellar proteomics. *Expert Rev Proteomics,* 5**,** 603-17.

GENE ONTOLOGY CONSORTIUM 2001. Creating the gene ontology resource: design and implementation. *Genome Res,* 11**,** 1425-33.

GIRAULT, I., BIECHE, I. & LIDEREAU, R. 2006. Role of estrogen receptor alpha transcriptional coregulators in tamoxifen resistance in breast cancer. *Maturitas,* 54**,** 342-51.

GIRAULT, I., LEREBOURS, F., AMARIR, S., TOZLU, S., TUBIANA-HULIN, M., LIDEREAU, R. & BIECHE, I. 2003. Expression analysis of estrogen receptor alpha coregulators in breast carcinoma: evidence that NCOR1 expression is predictive of the response to tamoxifen. *Clin Cancer Res,* 9**,** 1259-66.

GLISH, G. L. & BURINSKY, D. J. 2008. Hybrid Mass Spectrometers for Tandem Mass Spectrometry. *Journal of the American Society for Mass Spectrometry,* 19**,** 161-172.

GOSS, P. E., INGLE, J. N., MARTINO, S., ROBERT, N. J., MUSS, H. B., PICCART, M. J., CASTIGLIONE, M., TU, D., SHEPHERD, L. E., PRITCHARD, K. I., LIVINGSTON, R. B., DAVIDSON, N. E., NORTON, L., PEREZ, E. A., ABRAMS, J. S., CAMERON, D. A., PALMER, M. J. & PATER, J. L. 2005. Randomized trial of letrozole following tamoxifen as extended adjuvant therapy in receptor-positive breast cancer: updated findings from NCIC CTG MA.17. *J Natl Cancer Inst,* 97**,** 1262-71.

GOTTARDIS, M. M. & JORDAN, V. C. 1988. Development of tamoxifen-stimulated growth of MCF-7 tumors in athymic mice after long-term antiestrogen administration. *Cancer Res,* 48**,** 5183-7.

GOVIND, A. P. & THAMPAN, R. V. 2003. Membrane associated estrogen receptors and related proteins: localization at the plasma membrane and the endoplasmic reticulum. *Mol Cell Biochem,* 253**,** 233-40.

GRADISHAR, W. J. 2010. Adjuvant endocrine therapy for early breast cancer: the story so far. *Cancer Invest,* 28**,** 433-42.

GRIZZI, F. & CHIRIVA-INTERNATI, M. 2006. Cancer: looking for simplicity and finding complexity. *Cancer Cell International,* 6**,** 1-7.

GYGI, S. P., RIST, B., GERBER, S. A., TURECEK, F., GELB, M. H. & AEBERSOLD, R. 1999. Quantitative analysis of complex protein mixtures using isotope-coded affinity tags. *Nat Biotechnol,* 17**,** 994-9.

HADDOW, A., WATKINSON, J. M., PATERSON, E. & KOLLER, P. C. 1944. Influence of Synthetic Oestrogens on Advanced Malignant Disease. *British Medical Journal,* 2**,** 393-398.

HALL, S. L., HESTER, S., GRIFFIN, J. L., LILLEY, K. S. & JACKSON, A. P. 2009. The organelle proteome of the DT40 lymphocyte cell line. *Mol Cell Proteomics,* 8**,** 1295-305.

HAMELERS, I., VAN SCHAIK, R., SUSSENBACH, J. & STEENBERGH, P. 2003. 17beta-Estradiol responsiveness of MCF-7 laboratory strains is dependent on an autocrine signal activating the IGF type I receptor. *Cancer Cell International,* 3**,** 10.

HANAHAN, D. & WEINBERG, R. A. 2000. The hallmarks of cancer. *Cell,* 100**,** 57-70.

HANAHAN, D. & WEINBERG, R. A. 2011. Hallmarks of cancer: the next generation. *Cell,* 144**,** 646-74.

HARA, M. R. & SNYDER, S. H. 2006. Nitric oxide-GAPDH-Siah: a novel cell death cascade. *Cell Mol Neurobiol,* 26**,** 527-38.

HARVEY, B. 2009. Novel aspects of oestrogen actions. *The Journal of Physiology,* 587**,** 5017-5017.

HE, H., LEE, M. C., ZHENG, L. L., ZHENG, L. & LUO, Y. 2012. Integration of the Metabolic/Redox State, Histone Gene Switching, DNA Replication and S-phase Progression by Moonlighting Metabolic Enzymes. *Biosci Rep*.

HE, H., LEE, M. C., ZHENG, L. L., ZHENG, L. & LUO, Y. 2013. Integration of the metabolic/redox state, histone gene switching, DNA replication and S-phase progression by moonlighting metabolic enzymes. *Biosci Rep,* 33**,** e00018.

HELDRING, N., PIKE, A., ANDERSSON, S., MATTHEWS, J., CHENG, G., HARTMAN, J., TUJAGUE, M., STRÖM, A., TREUTER, E., WARNER, M. & GUSTAFSSON, J.-Å. 2007. Estrogen Receptors: How Do They Signal and What Are Their Targets. *Physiological Reviews,* 87**,** 905-931.

HELDRING, N., PIKE, A., ANDERSSON, S., MATTHEWS, J., CHENG, G., HARTMAN, J., TUJAGUE, M., STROM, A., TREUTER, E., WARNER, M. & GUSTAFSSON, J. A. 2007. Estrogen receptors: how do they signal and what are their targets. *Physiol Rev,* 87**,** 905-31.

HEMMINKI, A. & HEMMINKI, K. 2005. The Genetic Basis of Cancer. *In:* CURIEL, D. & DOUGLAS, J. (eds.) *Cancer Gene Therapy.* Humana Press.

HENDERSON, B. E. & BERNSTEIN, L. 1991. The international variation in breast cancer rates: an epidemiological assessment. *Breast Cancer Res Treat,* 18 Suppl 1**,** S11-7.

HENKE, R. M., DASTIDAR, R. G., SHAH, A., CADINU, D., YAO, X., HOODA, J. & ZHANG, L. 2011. Hypoxia elicits broad and systematic changes in protein subcellular localization. *American Journal of Physiology-Cell Physiology,* 301**,** C913-C928.

HERMEKING, H. 2003. The 14-3-3 cancer connection. *Nat Rev Cancer,* 3**,** 931-43.

HESKETH, R. 2013. *Introduction to Cancer Biology,* NEW YORK, Cambridge University Press.

HIRD, S. J., LAU, B. P. Y., SCHUHMACHER, R. & KRSKA, R. 2014. Liquid chromatography-mass spectrometry for the determination of chemical contaminants in food. *TrAC Trends in Analytical Chemistry,* 59**,** 59-72.

HODGES, L. C., COOK, J. D., LOBENHOFER, E. K., LI, L., BENNETT, L., BUSHEL, P. R., ALDAZ, C. M., AFSHARI, C. A. & WALKER, C. L. 2003. Tamoxifen Functions As a Molecular Agonist Inducing Cell Cycle-Associated Genes in Breast Cancer Cells1 1 National Institute of Environmental Health Sciences (ES98263 and ES07784) and the Women's American Legion Auxiliary Fellowship.2 2 IMAGE clones were annotated according to the official gene names from the Human Gene Nomenclature Committee, when available. The official gene names for cyclin D1, cyclin A2, and fra-1 are CCND1, CCNA2, and FOSL1, respectively. *Molecular Cancer Research,* 1**,** 300-311.

HOLLIDAY, D. L. & SPEIRS, V. 2011. Choosing the right cell line for breast cancer research. *Breast Cancer Res,* 13**,** 215.

HORECKER, B. L. 2002. The pentose phosphate pathway. *J Biol Chem,* 277**,** 47965-71.

HOU, N., HONG, S., WANG, W., OLOPADE, O. I., DIGNAM, J. J. & HUO, D. 2013. Hormone Replacement Therapy and Breast Cancer: Heterogeneous Risks by Race, Weight, and Breast Density. *Journal of the National Cancer Institute,* 105**,** 1365-1372.

HU, Z. Z., KAGAN, B. L., ARIAZI, E. A., ROSENTHAL, D. S., ZHANG, L. H., LI, J. V., HUANG, H. Z., WU, C., JORDAN, V. C., RIEGEL, A. T. & WELLSTEIN, A. 2011. Proteomic Analysis of Pathways Involved in Estrogen-Induced Growth and Apoptosis of Breast Cancer Cells. *Plos One,* 6.

HUAN, J., WANG, L., XING, L., QIN, X., FENG, L., PAN, X. & ZHU, L. 2014. Insights into significant pathways and gene interaction networks underlying breast cancer cell line MCF-7 treated with 17β-Estradiol (E2). *Gene,* 533**,** 346-355.

HUGHES, P., MARSHALL, D., REID, Y., PARKES, H. & GELBER, C. 2007. The costs of using unauthenticated, over-passaged cell lines: how much more data do we need? *Biotechniques,* 43**,** 575, 577-8, 581-2 passim.

HUNG, M. C. & LINK, W. 2011. Protein localization in disease and therapy. *J Cell Sci,* 124**,** 3381-92.

HYDER, S. M., NAWAZ, Z., CHIAPPETTA, C., YOKOYAMA, K. & STANCEL, G. M. 1995. The protooncogene c-jun contains an unusual estrogen-inducible enhancer within the coding sequence. *J Biol Chem,* 270**,** 8506-13.

IDEKER, T. & KROGAN, N. J. 2012. *Differential network biology*.

INTERNATIONAL AGENCY FOR RESEARCH ON CANCER. 2016. *Estimated Incidence, Mortality and Prevalence Worldwide in 2012* [Online]. Available: http://globocan.iarc.fr/Pages/fact_sheets_cancer.aspx [Accessed 01/02 2016].

IORNS, E., TURNER, N. C., ELLIOTT, R., SYED, N., GARRONE, O., GASCO, M., TUTT, A. N., CROOK, T., LORD, C. J. & ASHWORTH, A. 2008. Identification of CDK10 as an important determinant of resistance to endocrine therapy for breast cancer. *Cancer Cell,* 13**,** 91-104.

ISHIDA, A., TADA, Y., NIMURA, T., SUEYOSHI, N., KATOH, T., TAKEUCHI, M., FUJISAWA, H., TANIGUCHI, T. & KAMESHITA, I. 2005. Identification of major Ca(2+)/calmodulin-dependent protein kinase phosphatase-binding proteins in brain: biochemical analysis of the interaction. *Arch Biochem Biophys,* 435**,** 134-46.

IVANOVA, M. M., RADDE, B. N., SON, J., MEHTA, F. F., CHUNG, S.-H. & KLINGE, C. M. 2013. Estradiol and tamoxifen regulate NRF-1 and mitochondrial function in mouse mammary gland and uterus. *Journal of molecular endocrinology,* 51**,** 233-246.

JAIYESIMI, I. A., BUZDAR, A. U., DECKER, D. A. & HORTOBAGYI, G. N. 1995. Use of tamoxifen for breast cancer: twenty-eight years later. *J Clin Oncol,* 13**,** 513-29.

JARIWALA, U., PRESCOTT, J., JIA, L., BARSKI, A., PREGIZER, S., COGAN, J. P., ARASHEBEN, A., TILLEY, W. D., SCHER, H. I., GERALD, W. L., BUCHANAN, G., COETZEE, G. A. & FRENKEL, B. 2007. Identification of novel androgen receptor target genes in prostate cancer. *Mol Cancer,* 6**,** 39.

JEFFERY, C. J. 2009. Moonlighting proteins--an update. *Mol Biosyst,* 5**,** 345-50.

JEMAL, A., BRAY, F., CENTER, M. M., FERLAY, J., WARD, E. & FORMAN, D. 2011. Global cancer statistics. *CA Cancer J Clin,* 61**,** 69-90.

JEMAL, A., SIEGEL, R., XU, J. & WARD, E. 2010. Cancer statistics, 2010. *CA Cancer J Clin,* 60**,** 277-300.

JEWETT, T. J. & SIBLEY, L. D. 2003. Aldolase forms a bridge between cell surface adhesins and the actin cytoskeleton in apicomplexan parasites. *Mol Cell,* 11**,** 885-94.

JIANG, Q., ZHENG, S. & WANG, G. 2013. Development of new estrogen receptor-targeting therapeutic agents for tamoxifen-resistant breast cancer. *Future medicinal chemistry,* 5**,** 10.4155/fmc.13.63.

JIANG, S. Y., LANGAN-FAHEY, S. M., STELLA, A. L., MCCAGUE, R. & JORDAN, V. C. 1992. Point mutation of estrogen receptor (ER) in the ligand-binding domain changes the pharmacology of antiestrogens in ER-negative breast cancer cells stably expressing complementary DNAs for ER. *Mol Endocrinol,* 6**,** 2167-74.

JOE, I. & RAMIREZ, V. D. 2001. Binding of estrogen and progesterone-BSA conjugates to glyceraldehyde-3-phosphate dehydrogenase (GAPDH) and the effects of the free steroids on GAPDH enzyme activity: physiological implications. *Steroids,* 66**,** 529-38.

JORDAN, V. C. 2003. Tamoxifen: a most unlikely pioneering medicine. *Nat Rev Drug Discov,* 2**,** 205-213.

JU, Y. S., ALEXANDROV, L. B., GERSTUNG, M., MARTINCORENA, I., NIK-ZAINAL, S., RAMAKRISHNA, M., DAVIES, H. R., PAPAEMMANUIL, E., GUNDEM, G., SHLIEN, A., BOLLI, N., BEHJATI, S., TARPEY, P. S., NANGALIA, J., MASSIE, C. E., BUTLER, A. P., TEAGUE, J. W., VASSILIOU, G. S., GREEN, A. R., DU, M. Q., UNNIKRISHNAN, A., PIMANDA, J. E., TEH, B. T., MUNSHI, N., GREAVES, M., VYAS, P., EL-NAGGAR, A. K., SANTARIUS, T., COLLINS, V. P., GRUNDY, R., TAYLOR, J. A., HAYES, D. N., MALKIN, D., FOSTER, C. S., WARREN, A. Y., WHITAKER, H. C., BREWER, D., EELES, R., COOPER, C., NEAL, D., VISAKORPI, T., ISAACS, W. B., BOVA, G. S., FLANAGAN, A. M., FUTREAL, P. A., LYNCH, A. G., CHINNERY, P. F., MCDERMOTT, U., STRATTON, M. R. & CAMPBELL, P. J. 2014. Origins and functional consequences of somatic mitochondrial DNA mutations in human cancer. *Elife,* 3.

JUNG, S., SMITH, J. J., VON HALLER, P. D., DILWORTH, D. J., SITKO, K. A., MILLER, L. R., SALEEM, R. A., GOODLETT, D. R. & AITCHISON, J. D. 2013. Global Analysis of Condition-specific Subcellular Protein Distribution and Abundance. *Molecular & Cellular Proteomics,* 12**,** 1421-1435.

KAMPA, M., PELEKANOU, V., NOTAS, G., STATHOPOULOS, E. N. & CASTANAS, E. 2013. The estrogen receptor: two or more molecules, multiple variants, diverse localizations, signaling and functions. Are we undergoing a paradigm-shift as regards their significance in breast cancer? *Hormones (Athens),* 12**,** 69-85.

KAMRADT, M. C., CHEN, F. & CRYNS, V. L. 2001. The small heat shock protein alpha B-crystallin negatively regulates cytochrome c- and caspase-8-dependent activation of caspase-3 by inhibiting its autoproteolytic maturation. *J Biol Chem,* 276**,** 16059-63.

KAMRADT, M. C., CHEN, F., SAM, S. & CRYNS, V. L. 2002. The small heat shock protein alpha B-crystallin negatively regulates apoptosis during myogenic differentiation by inhibiting caspase-3 activation. *J Biol Chem,* 277**,** 38731-6.

KANAI, Y. & HEDIGER, M. A. 2004. The glutamate/neutral amino acid transporter family SLC1: molecular, physiological and pharmacological aspects. *Pflugers Arch,* 447**,** 469-79.

KANEHISA, M. & GOTO, S. 2000. KEGG: Kyoto Encyclopedia of Genes and Genomes. *Nucleic Acids Research,* 28**,** 27-30.

KANEHISA, M., GOTO, S., FURUMICHI, M., TANABE, M. & HIRAKAWA, M. 2010. KEGG for representation and analysis of molecular networks involving diseases and drugs. *Nucleic Acids Res,* 38**,** D355-60.

KANEHISA, M., GOTO, S., KAWASHIMA, S. & NAKAYA, A. 2002. The KEGG databases at GenomeNet. *Nucleic Acids Res,* 30**,** 42-6.

KANEHISA, M., GOTO, S., SATO, Y., FURUMICHI, M. & TANABE, M. 2012. KEGG for integration and interpretation of large-scale molecular data sets. *Nucleic Acids Res,* 40**,** D109-14.

KANEHISA, M., GOTO, S., SATO, Y., KAWASHIMA, M., FURUMICHI, M. & TANABE, M. 2014. Data, information, knowledge and principle: back to metabolism in KEGG. *Nucleic Acids Res,* 42**,** D199-205.

KARIHTALA, P., MANTYNIEMI, A., KANG, S. W., KINNULA, V. L. & SOINI, Y. 2003. Peroxiredoxins in breast carcinoma. *Clin Cancer Res,* 9**,** 3418-24.

KAZMA, R., BABRON, M. C., GABORIEAU, V., GENIN, E., BRENNAN, P., HUNG, R. J., MCLAUGHLIN, J. R., KROKAN, H. E., ELVESTAD, M. B.,

SKORPEN, F., ANDERSSEN, E., VOODER, T., VALK, K., METSPALU, A., FIELD, J. K., LATHROP, M., SARASIN, A. & BENHAMOU, S. 2012. Lung cancer and DNA repair genes: multilevel association analysis from the International Lung Cancer Consortium. *Carcinogenesis,* 33**,** 1059-64.

KEKUDA, R., PRASAD, P. D., FEI, Y. J., TORRES-ZAMORANO, V., SINHA, S., YANG-FENG, T. L., LEIBACH, F. H. & GANAPATHY, V. 1996. Cloning of the sodium-dependent, broad-scope, neutral amino acid transporter Bo from a human placental choriocarcinoma cell line. *J Biol Chem,* 271**,** 18657-61.

KELLY, P., CASEY, P. J. & MEIGS, T. E. 2007. Biologic functions of the G12 subfamily of heterotrimeric g proteins: growth, migration, and metastasis. *Biochemistry,* 46**,** 6677-87.

KEY, T. J., APPLEBY, P. N., REEVES, G. K., RODDAM, A. W., HELZLSOUER, K. J., ALBERG, A. J., ROLLISON, D. E., DORGAN, J. F., BRINTON, L. A., OVERVAD, K., KAAKS, R., TRICHOPOULOU, A., CLAVEL-CHAPELON, F., PANICO, S., DUELL, E. J., PEETERS, P. H., RINALDI, S., FENTIMAN, I. S., DOWSETT, M., MANJER, J., LENNER, P., HALLMANS, G., BAGLIETTO, L., ENGLISH, D. R., GILES, G. G., HOPPER, J. L., SEVERI, G., MORRIS, H. A., HANKINSON, S. E., TWOROGER, S. S., KOENIG, K., ZELENIUCH-JACQUOTTE, A., ARSLAN, A. A., TONIOLO, P., SHORE, R. E., KROGH, V., MICHELI, A., BERRINO, F., BARRETT-CONNOR, E., LAUGHLIN, G. A., KABUTO, M., AKIBA, S., STEVENS, R. G., NERIISHI, K., LAND, C. E., CAULEY, J. A., LUI, L. Y., CUMMINGS, S. R., GUNTER, M. J., ROHAN, T. E. & STRICKLER, H. D. 2011. Circulating sex hormones and breast cancer risk factors in postmenopausal women: reanalysis of 13 studies. *Br J Cancer,* 105**,** 709-22.

KHOLODENKO, B. N. 2006. Cell-signalling dynamics in time and space. *Nat Rev Mol Cell Biol,* 7**,** 165-76.

KIJIMA, I., ITOH, T. & CHEN, S. 2005. Growth inhibition of estrogen receptor-positive and aromatase-positive human breast cancer cells in monolayer and spheroid cultures by letrozole, anastrozole, and tamoxifen. *J Steroid Biochem Mol Biol,* 97**,** 360-8.

KIM, J. W. & DANG, C. V. 2006. Cancer's molecular sweet tooth and the Warburg effect. *Cancer Res,* 66**,** 8927-30.

KIM, K. H. & BENDER, J. R. 2009. Membrane-initiated actions of estrogen on the endothelium. *Mol Cell Endocrinol,* 308**,** 3-8.

KITANO, H. 2002. Systems biology: a brief overview. *Science,* 295**,** 1662-4.

KITTANEH, M., MONTERO, A. J. & GLÜCK, S. 2013. Molecular Profiling for Breast Cancer: A Comprehensive Review. *Biomarkers in Cancer,* 5**,** 61-70.

KLINGE, C. M. 2000. Estrogen receptor interaction with co-activators and co-repressors. *Steroids,* 65**,** 227-51.

KLINGE, C. M. 2008. Estrogenic control of mitochondrial function and biogenesis. *J Cell Biochem,* 105**,** 1342-51.

KLINGE, C. M. 2012. miRNAs and estrogen action. *Trends Endocrinol Metab,* 23**,** 223-33.

KOCANOVA, S., MAZAHERI, M., CAZE-SUBRA, S. & BYSTRICKY, K. 2010. Ligands specify estrogen receptor alpha nuclear localization and degradation. *BMC Cell Biology,* 11**,** 1-13.

KOUKOURAKIS, M. I., GIATROMANOLAKI, A., SIMOPOULOS, C., POLYCHRONIDIS, A. & SIVRIDIS, E. 2005. Lactate dehydrogenase 5 (LDH5) relates to up-regulated hypoxia inducible factor pathway and metastasis in colorectal cancer. *Clin Exp Metastasis,* 22**,** 25-30.

KOULMAN, A., WOFFENDIN, G., NARAYANA, V. K., WELCHMAN, H., CRONE, C. & VOLMER, D. A. 2009. High-resolution extracted ion chromatography, a new tool for metabolomics and lipidomics using a second-generation orbitrap mass spectrometer. *Rapid Commun Mass Spectrom,* 23**,** 1411-8.

KREGE, J. H., HODGIN, J. B., COUSE, J. F., ENMARK, E., WARNER, M., MAHLER, J. F., SAR, M., KORACH, K. S., GUSTAFSSON, J.-Å. & SMITHIES, O. 1998. Generation and reproductive phenotypes of mice lacking estrogen receptor β. *Proceedings of the National Academy of Sciences,* 95**,** 15677-15682.

KRÜGER, M., MOSER, M., USSAR, S., THIEVESSEN, I., LUBER, C. A., FORNER, F., SCHMIDT, S., ZANIVAN, S., FÄSSLER, R. & MANN, M. 2008. SILAC Mouse for Quantitative Proteomics Uncovers Kindlin-3 as an Essential Factor for Red Blood Cell Function. *Cell,* 134**,** 353-364.

KRYSTON, T. B., GEORGIEV, A. B., PISSIS, P. & GEORGAKILAS, A. G. 2011. Role of oxidative stress and DNA damage in human carcinogenesis. *Mutat Res,* 711**,** 193-201.

KUEHL, L. 1967. Evidence for Nuclear Synthesis of Lactic Dehydrogenase in Rat Liver. *Journal of Biological Chemistry,* 242**,** 2199-2206.

KUIPER, G. G., CARLSSON, B., GRANDIEN, K., ENMARK, E., HAGGBLAD, J., NILSSON, S. & GUSTAFSSON, J. A. 1997. Comparison of the ligand binding specificity and transcript tissue distribution of estrogen receptors alpha and beta. *Endocrinology,* 138**,** 863-70.

KUIPER, G. G., ENMARK, E., PELTO-HUIKKO, M., NILSSON, S. & GUSTAFSSON, J. A. 1996. Cloning of a novel receptor expressed in rat prostate and ovary. *Proceedings of the National Academy of Sciences,* 93**,** 5925-5930.

KULMS, D. & SCHWARZ, T. 2002. Independent contribution of three different pathways to ultraviolet-B-induced apoptosis. *Biochem Pharmacol,* 64**,** 837-41.

KUMAR, V. & CHAMBON, P. 1988. The estrogen receptor binds tightly to its responsive element as a ligand-induced homodimer. *Cell,* 55**,** 145-56.

KUMLE, M., WEIDERPASS, E., BRAATEN, T., PERSSON, I., ADAMI, H.-O. & LUND, E. 2002. Use of Oral Contraceptives and Breast Cancer Risk: The Norwegian-Swedish Women's Lifestyle and Health Cohort Study. *Cancer Epidemiology Biomarkers & Prevention,* 11**,** 1375-1381.

LAM, S. W., JIMENEZ, C. R. & BOVEN, E. 2014. Breast cancer classification by proteomic technologies: Current state of knowledge. *Cancer Treatment Reviews,* 40**,** 129-138.

LAMAS, B., NACHAT-KAPPES, R., GONCALVES-MENDES, N., MISHELLANY, F., ROSSARY, A., VASSON, M. P. & FARGES, M. C. 2013. Dietary fat without body weight gain increases in vivo MCF-7 human breast cancer cell growth and decreases natural killer cell cytotoxicity. *Mol Carcinog*.

LAMB, R., OZSVARI, B., BONUCCELLI, G., SMITH, D. L., PESTELL, R. G., MARTINEZ-OUTSCHOORN, U. E., CLARKE, R. B., SOTGIA, F. & LISANTI, M. P. 2015. Dissecting tumor metabolic heterogeneity: Telomerase and large cell size metabolically define a sub-population of stem-like, mitochondrial-rich, cancer cells. *Oncotarget,* 6**,** 21892-21905.

LAMOND, A. I., UHLEN, M., HORNING, S., MAKAROV, A., ROBINSON, C. V., SERRANO, L., HARTL, F. U., BAUMEISTER, W., WERENSKIOLD,

A. K., ANDERSEN, J. S., VORM, O., LINIAL, M., AEBERSOLD, R. & MANN, M. 2012. Advancing Cell Biology Through Proteomics in Space and Time (PROSPECTS). *Molecular & Cellular Proteomics,* 11.

LAPPANO, R. & MAGGIOLINI, M. 2012. GPCRs and cancer. *Acta Pharmacol Sin,* 33**,** 351-62.

LARIONOV, A. A. & MILLER, W. R. 2009. Challenges in defining predictive markers for response to endocrine therapy in breast cancer. *Future Oncol,* 5**,** 1415-28.

LARONGA, C. & DRAKE, R. R. 2007. Proteomic approach to breast cancer. *Cancer Control,* 14**,** 360-8.

LE ROMANCER, M., POULARD, C., COHEN, P., SENTIS, S., RENOIR, J. M. & CORBO, L. 2011. Cracking the estrogen receptor's posttranslational code in breast tumors. *Endocr Rev,* 32**,** 597-622.

LEE, J., KIM, H. K., HAN, Y. M. & KIM, J. 2008. Pyruvate kinase isozyme type M2 (PKM2) interacts and cooperates with Oct-4 in regulating transcription. *Int J Biochem Cell Biol,* 40**,** 1043-54.

LEE, Y. H., TAN, H. T. & CHUNG, M. C. 2010. Subcellular fractionation methods and strategies for proteomics. *Proteomics,* 10**,** 3935-56.

LEUNG, E., KIM, J. E., ASKARIAN-AMIRI, M., FINLAY, G. J. & BAGULEY, B. C. 2014. Evidence for the Existence of Triple-Negative Variants in the MCF-7 Breast Cancer Cell Population. *BioMed Research International,* 2014**,** 7.

LEVINE, A. J. & PUZIO-KUTER, A. M. 2010. The control of the metabolic switch in cancers by oncogenes and tumor suppressor genes. *Science,* 330**,** 1340-4.

LEW, C. R. & TOLAN, D. R. 2012. Targeting of Several Glycolytic Enzymes Using RNA Interference Reveals Aldolase Affects Cancer Cell Proliferation through a Non-glycolytic Mechanism. *The Journal of Biological Chemistry,* 287**,** 42554-42563.

LEWIS, J. S. & JORDAN, V. C. 2005. Selective estrogen receptor modulators (SERMs): Mechanisms of anticarcinogenesis and drug resistance. *Mutation Research/Fundamental and Molecular Mechanisms of Mutagenesis,* 591**,** 247-263.

LI, Z., ZHAO, J., DU, Y., PARK, H. R., SUN, S. Y., BERNAL-MIZRACHI, L., AITKEN, A., KHURI, F. R. & FU, H. 2008. Down-regulation of 14-3-3zeta suppresses anchorage-independent growth of lung cancer cells through anoikis activation. *Proc Natl Acad Sci U S A,* 105**,** 162-7.

LINCET, H. & ICARD, P. 2015. How do glycolytic enzymes favour cancer cell proliferation by nonmetabolic functions? *Oncogene,* 34**,** 3751-9.

LIST, H. J., LAURITSEN, K. J., REITER, R., POWERS, C., WELLSTEIN, A. & RIEGEL, A. T. 2001. Ribozyme targeting demonstrates that the nuclear receptor coactivator AIB1 is a rate-limiting factor for estrogen-dependent growth of human MCF-7 breast cancer cells. *J Biol Chem,* 276**,** 23763-8.

LITTLE, C. D., NAU, M. M., CARNEY, D. N., GAZDAR, A. F. & MINNA, J. D. 1983. Amplification and expression of the c-myc oncogene in human lung cancer cell lines. *Nature,* 306**,** 194-6.

LIU, X., LUO, M. & WU, K. 2012. Epigenetic interplay of histone modifications and DNA methylation mediated by HDA6. *Plant Signal Behav,* 7**,** 633-5.

LOMBARDI, M., CASTORIA, G., MIGLIACCIO, A., BARONE, M. V., DI STASIO, R., CIOCIOLA, A., BOTTERO, D., YAMAGUCHI, H., APPELLA, E. & AURICCHIO, F. 2008. Hormone-dependent nuclear export of estradiol receptor and DNA synthesis in breast cancer cells. *J Cell Biol,* 182**,** 327-40.

LONARD, D. M., NAWAZ, Z., SMITH, C. L. & O'MALLEY, B. W. 2000. The 26S proteasome is required for estrogen receptor-alpha and coactivator turnover and for efficient estrogen receptor-alpha transactivation. *Mol Cell,* 5**,** 939-48.

LONG, X. & NEPHEW, K. P. 2006. Fulvestrant (ICI 182,780)-dependent interacting proteins mediate immobilization and degradation of estrogen receptor-α. *Journal of Biological Chemistry,* 281**,** 9607-9615.

LOSKO, S., WENGER, K., KALUS, W., RAMGE, A., WIEHLER, J. & HEUMANN, K. 2006. Knowledge networks of biological and medical data: an exhaustive and flexible solution to model life science domains. *Proceedings of the Third international conference on Data Integration in the Life Sciences.* Hinxton, UK: Springer-Verlag.

LU, C. W., LIN, S. C., CHEN, K. F., LAI, Y. Y. & TSAI, S. J. 2008. Induction of pyruvate dehydrogenase kinase-3 by hypoxia-inducible factor-1 promotes metabolic switch and drug resistance. *J Biol Chem,* 283**,** 28106-14.

LU, H., FORBES, R. A. & VERMA, A. 2002. Hypoxia-inducible factor 1 activation by aerobic glycolysis implicates the Warburg effect in carcinogenesis. *J Biol Chem,* 277**,** 23111-5.

LU, J., GUO, H., TREEKITKARNMONGKOL, W., LI, P., ZHANG, J., SHI, B., LING, C., ZHOU, X., CHEN, T., CHIAO, P. J., FENG, X., SEEWALDT, V. L., MULLER, W. J., SAHIN, A., HUNG, M. C. & YU, D. 2009. 14-3-3zeta Cooperates with ErbB2 to promote ductal carcinoma in situ progression to invasive breast cancer by inducing epithelial-mesenchymal transition. *Cancer Cell,* 16**,** 195-207.

LUBAHN, D. B., MOYER, J. S., GOLDING, T. S., COUSE, J. F., KORACH, K. S. & SMITHIES, O. 1993. Alteration of reproductive function but not prenatal sexual development after insertional disruption of the mouse estrogen receptor gene. *Proceedings of the National Academy of Sciences,* 90**,** 11162-11166.

LUNDMARK, R. & CARLSSON, S. R. 2004. Regulated membrane recruitment of dynamin-2 mediated by sorting nexin 9. *J Biol Chem,* 279**,** 42694-702.

LUO, W. & SEMENZA, G. L. 2011. Pyruvate kinase M2 regulates glucose metabolism by functioning as a coactivator for hypoxia-inducible factor 1 in cancer cells. *Oncotarget,* 2**,** 551-6.

LYKKESFELDT, A. E., LARSEN, J. K., CHRISTENSEN, I. J. & BRIAND, P. 1984. Effects of the antioestrogen tamoxifen on the cell cycle kinetics of the human breast cancer cell line, MCF-7. *British Journal of Cancer,* 49**,** 717-722.

LYNCH, T. J., BELL, D. W., SORDELLA, R., GURUBHAGAVATULA, S., OKIMOTO, R. A., BRANNIGAN, B. W., HARRIS, P. L., HASERLAT, S. M., SUPKO, J. G., HALUSKA, F. G., LOUIS, D. N., CHRISTIANI, D. C., SETTLEMAN, J. & HABER, D. A. 2004. Activating Mutations in the Epidermal Growth Factor Receptor Underlying Responsiveness of Non–Small-Cell Lung Cancer to Gefitinib. *New England Journal of Medicine,* 350**,** 2129-2139.

LYNN, D. J., WINSOR, G. L., CHAN, C., RICHARD, N., LAIRD, M. R., BARSKY, A., GARDY, J. L., ROCHE, F. M., CHAN, T. H., SHAH, N., LO, R., NASEER, M., QUE, J., YAU, M., ACAB, M., TULPAN, D., WHITESIDE, M. D., CHIKATAMARLA, A., MAH, B., MUNZNER, T., HOKAMP, K., HANCOCK, R. E. & BRINKMAN, F. S. 2008. InnateDB: facilitating systems-level analyses of the mammalian innate immune response. *Mol Syst Biol,* 4**,** 218.

LYON, R. C., COHEN, J. S., FAUSTINO, P. J., MEGNIN, F. & MYERS, C. E. 1988. Glucose metabolism in drug-sensitive and drug-resistant human breast cancer cells monitored by magnetic resonance spectroscopy. *Cancer Res,* 48**,** 870-7.

MA, H.-I., HUENG, D.-Y., SHUI, H.-A., HAN, J.-M., WANG, C.-H., LAI, Y.-H., CHENG, S.-Y., XIAO, X., CHEN, M.-T. & YANG, Y.-P. 2014. Intratumoral Decorin Gene Delivery by AAV Vector Inhibits Brain Glioblastomas and Prolongs Survival of Animals by Inducing Cell Differentiation. *International Journal of Molecular Sciences,* 15**,** 4393-4414.

MACCONAILL, L. E. & GARRAWAY, L. A. 2010. Clinical implications of the cancer genome. *J Clin Oncol,* 28**,** 5219-28.

MACMAHON, B., COLE, P., LIN, T. M., LOWE, C. R., MIRRA, A. P., RAVNIHAR, B., SALBER, E. J., VALAORAS, V. G. & YUASA, S. 1970. Age at first birth and breast cancer risk. *Bull World Health Organ,* 43**,** 209-21.

MADAK-ERDOGAN, Z., KIESER, K. J., KIM, S. H., KOMM, B., KATZENELLENBOGEN, J. A. & KATZENELLENBOGEN, B. S. 2008. Nuclear and Extranuclear Pathway Inputs in the Regulation of Global Gene Expression by Estrogen Receptors. *Molecular Endocrinology,* 22**,** 2116-2127.

MAGNANI, L., STOECK, A., ZHANG, X., LANCZKY, A., MIRABELLA, A. C., WANG, T. L., GYORFFY, B. & LUPIEN, M. 2013. Genome-wide reprogramming of the chromatin landscape underlies endocrine therapy resistance in breast cancer. *Proc Natl Acad Sci U S A,* 110**,** E1490-9.

MAKAROV, A., DENISOV, E., KHOLOMEEV, A., BALSCHUN, W., LANGE, O., STRUPAT, K. & HORNING, S. 2006. Performance evaluation of a hybrid linear ion trap/orbitrap mass spectrometer. *Anal Chem,* 78**,** 2113-20.

MALCHINKHUU, E., SATO, K., MAEHAMA, T., MOGI, C., TOMURA, H., ISHIUCHI, S., YOSHIMOTO, Y., KUROSE, H. & OKAJIMA, F. 2008. S1P(2) receptors mediate inhibition of glioma cell migration through Rho signaling pathways independent of PTEN. *Biochem Biophys Res Commun,* 366**,** 963-8.

MALHAS, A., GOULBOURNE, C. & VAUX, D. J. 2011. The nucleoplasmic reticulum: form and function. *Trends Cell Biol,* 21**,** 362-73.

MALIK, S., GUERMAH, M. & ROEDER, R. G. 1998. A dynamic model for PC4 coactivator function in RNA polymerase II transcription. *Proc Natl Acad Sci U S A,* 95**,** 2192-7.

MALIN, D., STREKALOVA, E., PETROVIC, V., DEAL, A. M., AL AHMAD, A., ADAMO, B., MILLER, C. R., UGOLKOV, A., LIVASY, C., FRITCHIE, K., HAMILTON, E., BLACKWELL, K., GERADTS, J., EWEND, M., CAREY, L., SHUSTA, E. V., ANDERS, C. K. & CRYNS, V. L. 2014. alphaB-crystallin: a novel regulator of breast cancer metastasis to the brain. *Clin Cancer Res,* 20**,** 56-67.

MAO, Y. W., LIU, J. P., XIANG, H. & LI, D. W. 2004. Human alphaA- and alphaB-crystallins bind to Bax and Bcl-X(S) to sequester their translocation during staurosporine-induced apoptosis. *Cell Death Differ,* 11**,** 512-26.

MARINO, M., GALLUZZO, P. & ASCENZI, P. 2006. Estrogen signaling multiple pathways to impact gene transcription. *Curr Genomics,* 7**,** 497-508.

MARTY, M., COGNETTI, F., MARANINCHI, D., SNYDER, R., MAURIAC, L., TUBIANA-HULIN, M., CHAN, S., GRIMES, D., ANTÓN, A., LLUCH, A., KENNEDY, J., O'BYRNE, K., CONTE, P., GREEN, M., WARD, C., MAYNE, K. & EXTRA, J.-M. 2005. Randomized Phase II Trial of the Efficacy and Safety of Trastuzumab Combined With Docetaxel in Patients With Human Epidermal Growth Factor Receptor 2–Positive Metastatic Breast Cancer Administered As First-Line Treatment: The M77001 Study Group. *Journal of Clinical Oncology,* 23**,** 4265-4274.

MAVINAKERE, M. S., POWERS, J. M., SUBRAMANIAN, K. S., ROGGERO, V. R. & ALLISON, L. A. 2012. Multiple novel signals mediate thyroid hormone receptor nuclear import and export. *Journal of Biological Chemistry,* 287**,** 31280-31297.

MCDONNELL, D. P., CONNOR, C. E., WIJAYARATNE, A., CHANG, C. Y. & NORRIS, J. D. 2002. Definition of the molecular and cellular mechanisms underlying the tissue-selective agonist/antagonist activities of selective estrogen receptor modulators. *Recent Prog Horm Res,* 57**,** 295-316.

MCNALLY, J. G., MULLER, W. G., WALKER, D., WOLFORD, R. & HAGER, G. L. 2000. The glucocorticoid receptor: rapid exchange with regulatory sites in living cells. *Science,* 287**,** 1262-5.

MEIER-ABT, F. & BENTIRES-ALJ, M. 2013. How pregnancy at early age protects against breast cancer. *Trends in molecular medicine*.

MEIJER, D., VAN AGTHOVEN, T., BOSMA, P. T., NOOTER, K. & DORSSERS, L. C. 2006. Functional screen for genes responsible for tamoxifen resistance in human breast cancer cells. *Mol Cancer Res,* 4**,** 379-86.

MIAO, P., SHENG, S., SUN, X., LIU, J. & HUANG, G. 2013. Lactate dehydrogenase A in cancer: a promising target for diagnosis and therapy. *IUBMB Life,* 65**,** 904-10.

MICHALSKI, A., COX, J. & MANN, M. 2011. More than 100,000 Detectable Peptide Species Elute in Single Shotgun Proteomics Runs but the Majority is Inaccessible to Data-Dependent LC−MS/MS. *Journal of Proteome Research,* 10**,** 1785-1793.

MICHOR, F., IWASA, Y. & NOWAK, M. A. 2004. Dynamics of cancer progression. *Nat Rev Cancer,* 4**,** 197-205.

MILACIC, M., HAW, R., ROTHFELS, K., WU, G., CROFT, D., HERMJAKOB, H., #039, EUSTACHIO, P. & STEIN, L. 2012. Annotating Cancer Variants and Anti-Cancer Therapeutics in Reactome. *Cancers,* 4**,** 1180-1211.

MILLER, W. R. & O'NEILL, J. 1987. The importance of local synthesis of estrogen within the breast. *Steroids,* 50**,** 537-48.

MIZUKAMI, Y. 2010. In vivo functions of GPR30/GPER-1, a membrane receptor for estrogen: from discovery to functions in vivo. *Endocr J,* 57**,** 101-7.

MO, Z., LIU, M., YANG, F., LUO, H., LI, Z., TU, G. & YANG, G. 2013. GPR30 as an initiator of tamoxifen resistance in hormone-dependent breast cancer. *Breast Cancer Res,* 15**,** R114.

MOORE, J. W., KEY, T. J., BULBROOK, R. D., CLARK, G. M., ALLEN, D. S., WANG, D. Y. & PIKE, M. C. 1987. Sex hormone binding globulin and risk factors for breast cancer in a population of normal women who had never used exogenous sex hormones. *Br J Cancer,* 56**,** 661-6.

MORRISON, D. K. 2009. The 14-3-3 proteins: integrators of diverse signaling cues that impact cell fate and cancer development. *Trends Cell Biol,* 19**,** 16-23.

MULVEY, C. M., TUDZAROVA, S., CRAWFORD, M., WILLIAMS, G. H., STOEBER, K. & GODOVAC-ZIMMERMANN, J. 2013. Subcellular Proteomics Reveals a Role for Nucleo-cytoplasmic Trafficking at the DNA Replication Origin Activation Checkpoint. *Journal of Proteome Research,* 12**,** 1436-1453.

MULVEY, C. M., TUDZAROVA, S., CRAWFORD, M., WILLIAMS, G. H., STOEBER, K. & GODOVAC-ZIMMERMANN, J. 2013. Subcellular proteomics reveals a role for nucleo-cytoplasmic trafficking at the DNA replication origin activation checkpoint. *J Proteome Res,* 12**,** 1436-53.

MUNOZ-PINEDO, C., EL MJIYAD, N. & RICCI, J. E. 2012. Cancer metabolism: current perspectives and future directions. *Cell Death and Dis,* 3**,** e248.

MURPHY, M. P. 2009. How mitochondria produce reactive oxygen species. *Biochem J,* 417**,** 1-13.

MYERS, E., HILL, A. D., KELLY, G., MCDERMOTT, E. W., O'HIGGINS, N. J., BUGGY, Y. & YOUNG, L. S. 2005. Associations and interactions between Ets-1 and Ets-2 and coregulatory proteins, SRC-1, AIB1, and NCoR in breast cancer. *Clin Cancer Res,* 11**,** 2111-22.

NASSA, G., TARALLO, R., GUZZI, P. H., FERRARO, L., CIRILLO, F., RAVO, M., NOLA, E., BAUMANN, M., NYMAN, T. A., CANNATARO, M., AMBROSINO, C. & WEISZ, A. 2011. Comparative analysis of nuclear estrogen receptor alpha and beta interactomes in breast cancer cells. *Mol Biosyst,* 7**,** 667-76.

NEAL, C. L., YAO, J., YANG, W., ZHOU, X., NGUYEN, N. T., LU, J., DANES, C. G., GUO, H., LAN, K. H., ENSOR, J., HITTELMAN, W., HUNG, M. C. & YU, D. 2009. 14-3-3zeta overexpression defines high risk for breast cancer recurrence and promotes cancer cell survival. *Cancer Res,* 69**,** 3425-32.

NELSON, H. D., ZAKHER, B., CANTOR, A., FU, R., GRIFFIN, J., O'MEARA, E. S., BUIST, D. S. M., KERLIKOWSKE, K., VAN RAVESTEYN, N. T., TRENTHAM-DIETZ, A., MANDELBLATT, J. & MIGLIORETTI, D. 2012. Risk Factors for Breast Cancer for Women Age 40 to 49: A Systematic Review and Meta-analysis. *Annals of internal medicine,* 156**,** 635-648.

NEVE, R. M., CHIN, K., FRIDLYAND, J., YEH, J., BAEHNER, F. L., FEVR, T., CLARK, L., BAYANI, N., COPPE, J. P., TONG, F., SPEED, T., SPELLMAN, P. T., DEVRIES, S., LAPUK, A., WANG, N. J., KUO, W. L., STILWELL, J. L., PINKEL, D., ALBERTSON, D. G., WALDMAN, F. M., MCCORMICK, F., DICKSON, R. B., JOHNSON, M. D., LIPPMAN, M., ETHIER, S., GAZDAR, A. & GRAY, J. W. 2006. A collection of breast cancer cell lines for the study of functionally distinct cancer subtypes. *Cancer Cell,* 10**,** 515-27.

NIK-ZAINAL, S., VAN LOO, P., WEDGE, D. C., ALEXANDROV, L. B., GREENMAN, C. D., LAU, K. W., RAINE, K., JONES, D., MARSHALL, J.,

RAMAKRISHNA, M., SHLIEN, A., COOKE, S. L., HINTON, J., MENZIES, A., STEBBINGS, L. A., LEROY, C., JIA, M., RANCE, R., MUDIE, L. J., GAMBLE, S. J., STEPHENS, P. J., MCLAREN, S., TARPEY, P. S., PAPAEMMANUIL, E., DAVIES, H. R., VARELA, I., MCBRIDE, D. J., BIGNELL, G. R., LEUNG, K., BUTLER, A. P., TEAGUE, J. W., MARTIN, S., JONSSON, G., MARIANI, O., BOYAULT, S., MIRON, P., FATIMA, A., LANGEROD, A., APARICIO, S. A., TUTT, A., SIEUWERTS, A. M., BORG, A., THOMAS, G., SALOMON, A. V., RICHARDSON, A. L., BORRESEN-DALE, A. L., FUTREAL, P. A., STRATTON, M. R. & CAMPBELL, P. J. 2012. The life history of 21 breast cancers. *Cell,* 149**,** 994-1007.

NILSSON, S., MAKELA, S., TREUTER, E., TUJAGUE, M., THOMSEN, J., ANDERSSON, G., ENMARK, E., PETTERSSON, K., WARNER, M. & GUSTAFSSON, J. A. 2001. Mechanisms of estrogen action. *Physiol Rev,* 81**,** 1535-65.

NIRMALA, P. B. & THAMPAN, R. V. 1995. Ubiquitination of the rat uterine estrogen receptor: dependence on estradiol. *Biochem Biophys Res Commun,* 213**,** 24-31.

NISHIYAMA, A., MATSUI, M., IWATA, S., HIROTA, K., MASUTANI, H., NAKAMURA, H., TAKAGI, Y., SONO, H., GON, Y. & YODOI, J. 1999. Identification of thioredoxin-binding protein-2/vitamin D(3) up-regulated protein 1 as a negative regulator of thioredoxin function and expression. *J Biol Chem,* 274**,** 21645-50.

NISHIZUKA, S., CHARBONEAU, L., YOUNG, L., MAJOR, S., REINHOLD, W. C., WALTHAM, M., KOUROS-MEHR, H., BUSSEY, K. J., LEE, J. K., ESPINA, V., MUNSON, P. J., PETRICOIN, E., 3RD, LIOTTA, L. A. & WEINSTEIN, J. N. 2003. Proteomic profiling of the NCI-60 cancer cell lines using new high-density reverse-phase lysate microarrays. *Proc Natl Acad Sci U S A,* 100**,** 14229-34.

NOBLE, D. 2002. Modeling the heart--from genes to cells to the whole organ. *Science,* 295**,** 1678-82.

NONCLERCQ, D., JOURNE, F., LAIOS, I., CHABOTEAUX, C., TOILLON, R. A., LECLERCQ, G. & LAURENT, G. 2007. Effect of nuclear export inhibition on estrogen receptor regulation in breast cancer cells. *J Mol Endocrinol,* 39**,** 105-18.

NUR-E-KAMAL, A., GROSS, S. R., PAN, Z., BALKLAVA, Z., MA, J. & LIU, L. F. 2004. Nuclear Translocation of Cytochrome c during Apoptosis. *Journal of Biological Chemistry,* 279**,** 24911-24914.

O'REGAN, R. M., OSIPO, C., ARIAZI, E., LEE, E. S., MEEKE, K., MORRIS, C., BERTUCCI, A., SARKER, M. A., GRIGG, R. & JORDAN, V. C. 2006. Development and therapeutic options for the treatment of raloxifene-stimulated breast cancer in athymic mice. *Clin Cancer Res,* 12**,** 2255-63.

ONG, S.-E., BLAGOEV, B., KRATCHMAROVA, I., KRISTENSEN, D. B., STEEN, H., PANDEY, A. & MANN, M. 2002. Stable Isotope Labeling by Amino Acids in Cell Culture, SILAC, as a Simple and Accurate Approach to Expression Proteomics. *Molecular & Cellular Proteomics,* 1**,** 376-386.

ONG, S. E. 2012. The expanding field of SILAC. *Anal Bioanal Chem,* 404**,** 967-76.

OROSZ, F., CHRISTOVA, T. Y. & OVADI, J. 1988. Modulation of phosphofructokinase action by macromolecular interactions. Quantitative analysis of the phosphofructokinase-aldolase-calmodulin system. *Biochim Biophys Acta,* 957**,** 293-300.

OSBORNE , C. K. 1998. Tamoxifen in the Treatment of Breast Cancer. *New England Journal of Medicine,* 339**,** 1609-1618.

OSBORNE, C. K., BARDOU, V., HOPP, T. A., CHAMNESS, G. C., HILSENBECK, S. G., FUQUA, S. A., WONG, J., ALLRED, D. C., CLARK, G. M. & SCHIFF, R. 2003. Role of the estrogen receptor coactivator AIB1 (SRC-3) and HER-2/neu in tamoxifen resistance in breast cancer. *J Natl Cancer Inst,* 95**,** 353-61.

OYAMA, M., NAGASHIMA, T., SUZUKI, T., KOZUKA-HATA, H., YUMOTO, N., SHIRAISHI, Y., IKEDA, K., KUROKI, Y., GOTOH, N., ISHIDA, T., INOUE, S., KITANO, H. & OKADA-HATAKEYAMA, M. 2011. Integrated Quantitative Analysis of the Phosphoproteome and Transcriptome in Tamoxifen-resistant Breast Cancer. *Journal of Biological Chemistry,* 286**,** 818-829.

PANDEY, D. P., LAPPANO, R., ALBANITO, L., MADEO, A., MAGGIOLINI, M. & PICARD, D. 2009. Estrogenic GPR30 signalling induces proliferation and migration of breast cancer cells through CTGF. *Embo j,* 28**,** 523-32.

PAO, W., MILLER, V., ZAKOWSKI, M., DOHERTY, J., POLITI, K., SARKARIA, I., SINGH, B., HEELAN, R., RUSCH, V., FULTON, L.,

MARDIS, E., KUPFER, D., WILSON, R., KRIS, M. & VARMUS, H. 2004. EGF receptor gene mutations are common in lung cancers from “never smokers” and are associated with sensitivity of tumors to gefitinib and erlotinib. *Proceedings of the National Academy of Sciences of the United States of America,* 101**,** 13306-13311.

PARL, F. F. 2000. Estrogen Receptor. *Estrogens, Estrogen Receptor and Breast Cancer.* Amsterdam: IOS Press.

PATEL, A. P., TIROSH, I., TROMBETTA, J. J., SHALEK, A. K., GILLESPIE, S. M., WAKIMOTO, H., CAHILL, D. P., NAHED, B. V., CURRY, W. T., MARTUZA, R. L., LOUIS, D. N., ROZENBLATT-ROSEN, O., SUVÀ, M. L., REGEV, A. & BERNSTEIN, B. E. 2014. Single-cell RNA-seq highlights intratumoral heterogeneity in primary glioblastoma. *Science (New York, N.Y.),* 344**,** 1396-1401.

PATHAK, D. N., PONGRACZ, K. & BODELL, W. J. 1996. Activation of 4-hydroxytamoxifen and the tamoxifen derivative metabolite E by uterine peroxidase to form DNA adducts: comparison with DNA adducts formed in the uterus of Sprague-Dawley rats treated with tamoxifen. *Carcinogenesis,* 17**,** 1785-90.

PAVLOU, M. P., DIMITROMANOLAKIS, A. & DIAMANDIS, E. P. 2013. Coupling proteomics and transcriptomics in the quest of subtype-specific proteins in breast cancer. *Proteomics,* 13**,** 1083-95.

PELICANO, H., CAREW, J. S., MCQUEEN, T. J., ANDREEFF, M., PLUNKETT, W., KEATING, M. J. & HUANG, P. 2006. Targeting Hsp90 by 17-AAG in leukemia cells: mechanisms for synergistic and antagonistic drug combinations with arsenic trioxide and Ara-C. *Leukemia,* 20**,** 610-9.

PENNEY, R. B. & ROY, D. 2013. Thioredoxin-mediated redox regulation of resistance to endocrine therapy in breast cancer. *Biochim Biophys Acta,* 1836**,** 60-79.

PEROU, C. M., JEFFREY, S. S., VAN DE RIJN, M., REES, C. A., EISEN, M. B., ROSS, D. T., PERGAMENSCHIKOV, A., WILLIAMS, C. F., ZHU, S. X., LEE, J. C., LASHKARI, D., SHALON, D., BROWN, P. O. & BOTSTEIN, D. 1999. Distinctive gene expression patterns in human mammary epithelial cells and breast cancers. *Proc Natl Acad Sci U S A,* 96**,** 9212-7.

PEROU, C. M., SORLIE, T., EISEN, M. B., VAN DE RIJN, M., JEFFREY, S. S., REES, C. A., POLLACK, J. R., ROSS, D. T., JOHNSEN, H., AKSLEN, L. A., FLUGE, O., PERGAMENSCHIKOV, A., WILLIAMS, C., ZHU, S. X.,

LONNING, P. E., BORRESEN-DALE, A. L., BROWN, P. O. & BOTSTEIN, D. 2000. Molecular portraits of human breast tumours. *Nature,* 406**,** 747-52.

PHAM, T. & ICHIKAWA, K. 2013. Spatial chaos and complexity in the intracellular space of cancer and normal cells. *Theoretical Biology and Medical Modelling,* 10**,** 62.

PICCART-GEBHART, M. J., PROCTER, M., LEYLAND-JONES, B., GOLDHIRSCH, A., UNTCH, M., SMITH, I., GIANNI, L., BASELGA, J., BELL, R., JACKISCH, C., CAMERON, D., DOWSETT, M., BARRIOS, C. H., STEGER, G., HUANG, C.-S., ANDERSSON, M., INBAR, M., LICHINITSER, M., LÁNG, I., NITZ, U., IWATA, H., THOMSSEN, C., LOHRISCH, C., SUTER, T. M., RÜSCHOFF, J., SÜTŐ, T., GREATOREX, V., WARD, C., STRAEHLE, C., MCFADDEN, E., DOLCI, M. S. & GELBER, R. D. 2005. Trastuzumab after Adjuvant Chemotherapy in HER2-Positive Breast Cancer. *New England Journal of Medicine,* 353**,** 1659-1672.

PINTO, G., ALHAIEK, A. A., AMADI, S., QATTAN, A. T., CRAWFORD, M., RADULOVIC, M. & GODOVAC-ZIMMERMANN, J. 2014. Systematic nucleo-cytoplasmic trafficking of proteins following exposure of MCF7 breast cancer cells to estradiol. *J Proteome Res,* 13**,** 1112-27.

PINTO, G., ALHAIEK, A. A. & GODOVAC-ZIMMERMANN, J. 2015. Proteomics reveals the importance of the dynamic redistribution of the subcellular location of proteins in breast cancer cells. *Expert Rev Proteomics,* 12**,** 61-74.

PINTO, G., ALHAIEK, A. A. M., AMADI, S., QATTAN, A., CRAWFORD, M., RADULOVIC, M. & GODOVAC-ZIMMERMANN, J. 2014. Systematic Nucleo-Cytoplasmic Trafficking of Proteins Following Exposure of MCF7 Breast Cancer Cells to Estradiol. *Journal of Proteome Research*.

PINTO, G., ALHAIEK, A. A. M., AMADI, S., QATTAN, A. T., CRAWFORD, M., RADULOVIC, M. & GODOVAC-ZIMMERMANN, J. 2014. Systematic Nucleo-Cytoplasmic Trafficking of Proteins Following Exposure of MCF7 Breast Cancer Cells to Estradiol. *Journal of Proteome Research,* 13**,** 1112-1127.

PINTO, G., RADULOVIC, M. & GODOVAC-ZIMMERMANN, J. 2016. Spatial perspectives in the redox code-Mass spectrometric proteomics studies of moonlighting proteins. *Mass Spectrom Rev*.

PRAT, A., PARKER, J., KARGINOVA, O., FAN, C., LIVASY, C., HERSCHKOWITZ, J., HE, X. & PEROU, C. 2010. Phenotypic and

molecular characterization of the claudin-low intrinsic subtype of breast cancer. *Breast cancer research,* 12**,** R68.

PROSSNITZ, E. R., ARTERBURN, J. B., SMITH, H. O., OPREA, T. I., SKLAR, L. A. & HATHAWAY, H. J. 2008. Estrogen signaling through the transmembrane G protein-coupled receptor GPR30. *Annu Rev Physiol,* 70**,** 165-90.

PROSSNITZ, E. R. & MAGGIOLINI, M. 2009. Mechanisms of estrogen signaling and gene expression via GPR30. *Mol Cell Endocrinol,* 308**,** 32-8.

PUGH, T. J., MOROZOVA, O., ATTIYEH, E. F., ASGHARZADEH, S., WEI, J. S., AUCLAIR, D., CARTER, S. L., CIBULSKIS, K., HANNA, M., KIEZUN, A., KIM, J., LAWRENCE, M. S., LICHENSTEIN, L., MCKENNA, A., PEDAMALLU, C. S., RAMOS, A. H., SHEFLER, E., SIVACHENKO, A., SOUGNEZ, C., STEWART, C., ALLY, A., BIROL, I., CHIU, R., CORBETT, R. D., HIRST, M., JACKMAN, S. D., KAMOH, B., KHODABAKSHI, A. H., KRZYWINSKI, M., LO, A., MOORE, R. A., MUNGALL, K. L., QIAN, J., TAM, A., THIESSEN, N., ZHAO, Y., COLE, K. A., DIAMOND, M., DISKIN, S. J., MOSSE, Y. P., WOOD, A. C., JI, L., SPOSTO, R., BADGETT, T., LONDON, W. B., MOYER, Y., GASTIER-FOSTER, J. M., SMITH, M. A., GUIDRY AUVIL, J. M., GERHARD, D. S., HOGARTY, M. D., JONES, S. J., LANDER, E. S., GABRIEL, S. B., GETZ, G., SEEGER, R. C., KHAN, J., MARRA, M. A., MEYERSON, M. & MARIS, J. M. 2013. The genetic landscape of high-risk neuroblastoma. *Nat Genet,* 45**,** 279-84.

QATTAN, A. T., MULVEY, C., CRAWFORD, M., NATALE, D. A. & GODOVAC-ZIMMERMANN, J. 2010. Quantitative organelle proteomics of MCF-7 breast cancer cells reveals multiple subcellular locations for proteins in cellular functional processes. *J Proteome Res,* 9**,** 495-508.

QATTAN, A. T., RADULOVIC, M., CRAWFORD, M. & GODOVAC-ZIMMERMANN, J. 2012. Spatial distribution of cellular function: the partitioning of proteins between mitochondria and the nucleus in MCF7 breast cancer cells. *J Proteome Res,* 11**,** 6080-101.

QATTAN, A. T., RADULOVIC, M., CRAWFORD, M. & GODOVAC-ZIMMERMANN, J. 2012. Spatial Distribution of Cellular Function: The Partitioning of Proteins between Mitochondria and the Nucleus in MCF7 Breast Cancer Cells. *Journal of Proteome Research,* 11**,** 6080-6101.

RADULOVIC, M., BAQADER, N. O., STOEBER, K. & GODOVAC-ZIMMERMANN, J. 2016. Spatial Cross-Talk Between Oxidative Stress and DNA Replication in Human Fibroblasts. *J Proteome Res*.

RAMSBY, M. L., MAKOWSKI, G. S. & KHAIRALLAH, E. A. 1994. Differential detergent fractionation of isolated hepatocytes: biochemical, immunochemical and two-dimensional gel electrophoresis characterization of cytoskeletal and noncytoskeletal compartments. *Electrophoresis,* 15**,** 265-77.

RASHEED, S. A., TEO, C. R., BEILLARD, E. J., VOORHOEVE, P. M. & CASEY, P. J. 2013. MicroRNA-182 and microRNA-200a control G-protein subunit alpha-13 (GNA13) expression and cell invasion synergistically in prostate cancer cells. *J Biol Chem,* 288**,** 7986-95.

RASHEED, S. A., TEO, C. R., BEILLARD, E. J., VOORHOEVE, P. M., ZHOU, W., GHOSH, S. & CASEY, P. J. 2015. MicroRNA-31 controls G protein alpha-13 (GNA13) expression and cell invasion in breast cancer cells. *Mol Cancer,* 14**,** 67.

REID, G., HUBNER, M. R., METIVIER, R., BRAND, H., DENGER, S., MANU, D., BEAUDOUIN, J., ELLENBERG, J. & GANNON, F. 2003. Cyclic, proteasome-mediated turnover of unliganded and liganded ERalpha on responsive promoters is an integral feature of estrogen signaling. *Mol Cell,* 11**,** 695-707.

RENOIR, J. M. 2012. Estradiol receptors in breast cancer cells: associated co-factors as targets for new therapeutic approaches. *Steroids,* 77**,** 1249-61.

REVANKAR, C. M., CIMINO, D. F., SKLAR, L. A., ARTERBURN, J. B. & PROSSNITZ, E. R. 2005. A Transmembrane Intracellular Estrogen Receptor Mediates Rapid Cell Signaling. *Science,* 307**,** 1625-1630.

RIGGS , B. L. & HARTMANN , L. C. 2003. Selective Estrogen-Receptor Modulators — Mechanisms of Action and Application to Clinical Practice. *New England Journal of Medicine,* 348**,** 618-629.

RING, A. & DOWSETT, M. 2004. Mechanisms of tamoxifen resistance. *Endocr Relat Cancer,* 11**,** 643-58.

RIVENZON-SEGAL, D., BOLDIN-ADAMSKY, S., SEGER, D., SEGER, R. & DEGANI, H. 2003. Glycolysis and glucose transporter 1 as markers of response to hormonal therapy in breast cancer. *Int J Cancer,* 107**,** 177-82.

ROSS, P. L., HUANG, Y. N., MARCHESE, J. N., WILLIAMSON, B., PARKER, K., HATTAN, S., KHAINOVSKI, N., PILLAI, S., DEY, S., DANIELS, S., PURKAYASTHA, S., JUHASZ, P., MARTIN, S., BARTLET-JONES, M., HE, F., JACOBSON, A. & PAPPIN, D. J. 2004. Multiplexed Protein Quantitation in Saccharomyces cerevisiae Using Amine-reactive Isobaric Tagging Reagents. *Molecular & Cellular Proteomics,* 3**,** 1154-1169.

RUAN, Q., HAN, S., JIANG, W. G., BOULTON, M. E., CHEN, Z. J., LAW, B. K. & CAI, J. 2011. alphaB-crystallin, an effector of unfolded protein response, confers anti-VEGF resistance to breast cancer via maintenance of intracrine VEGF in endothelial cells. *Mol Cancer Res,* 9**,** 1632-43.

RUFF, M., GANGLOFF, M., MARIE WURTZ, J. & MORAS, D. 2000. Estrogen receptor transcription and transactivation Structure-function relationship in DNA- and ligand-binding domains of estrogen receptors. *Breast Cancer Research,* 2**,** 1-7.

SADOWSKI, P. G., DUNKLEY, T. P., SHADFORTH, I. P., DUPREE, P., BESSANT, C., GRIFFIN, J. L. & LILLEY, K. S. 2006. Quantitative proteomic approach to study subcellular localization of membrane proteins. *Nat Protoc,* 1**,** 1778-89.

SAINT-CRIQ, V., RAPETTI-MAUSS, R., YUSEF, Y. R. & HARVEY, B. J. 2012. Estrogen regulation of epithelial ion transport: Implications in health and disease. *Steroids,* 77**,** 918-23.

SAKAMOTO, H., MATSUDA, K., HOSOKAWA, K., NISHI, M., MORRIS, J. F., PROSSNITZ, E. R. & KAWATA, M. 2007. Expression of G protein-coupled receptor-30, a G protein-coupled membrane estrogen receptor, in oxytocin neurons of the rat paraventricular and supraoptic nuclei. *Endocrinology,* 148**,** 5842-50.

SCHIFF, R., MASSARWEH, S. A., SHOU, J., BHARWANI, L., ARPINO, G., RIMAWI, M. & OSBORNE, C. K. 2005. Advanced concepts in estrogen receptor biology and breast cancer endocrine resistance: implicated role of growth factor signaling and estrogen receptor coregulators. *Cancer Chemother Pharmacol,* 56 Suppl 1**,** 10-20.

SCHMIDT, O., PFANNER, N. & MEISINGER, C. 2010. Mitochondrial protein import: from proteomics to functional mechanisms. *Nat Rev Mol Cell Biol,* 11**,** 655-667.

SCOTT, J. D. & PAWSON, T. 2009. Cell Signaling in Space and Time: Where Proteins Come Together and When They're Apart. *Science,* 326**,** 1220-1224.

SEMENZA, G. L. 2009. Regulation of cancer cell metabolism by hypoxia-inducible factor 1. *Semin Cancer Biol,* 19**,** 12-6.

SEMENZA, G. L. 2013. HIF-1 mediates metabolic responses to intratumoral hypoxia and oncogenic mutations. *J Clin Invest,* 123**,** 3664-71.

SEO, M. J., LIU, X., CHANG, M. & PARK, J. H. 2012. GATA-binding protein 1 is a novel transcription regulator of peroxiredoxin 5 in human breast cancer cells. *Int J Oncol,* 40**,** 655-64.

SHARMA, D., BLUM, J., YANG, X., BEAULIEU, N., MACLEOD, A. R. & DAVIDSON, N. E. 2005. Release of methyl CpG binding proteins and histone deacetylase 1 from the Estrogen receptor alpha (ER) promoter upon reactivation in ER-negative human breast cancer cells. *Mol Endocrinol,* 19**,** 1740-51.

SHAULIAN, E. & KARIN, M. 2002. AP-1 as a regulator of cell life and death. *Nat Cell Biol,* 4**,** E131-6.

SHAW, R. J. & CANTLEY, L. C. 2012. Decoding key nodes in the metabolism of cancer cells: sugar & spice and all things nice. *F1000 Biol Rep,* 4**,** 2.

SHEVCHENKO, A., TOMAS, H., HAVLIS, J., OLSEN, J. V. & MANN, M. 2006. In-gel digestion for mass spectrometric characterization of proteins and proteomes. *Nat Protoc,* 1**,** 2856-60.

SHIAU, A. K., BARSTAD, D., LORIA, P. M., CHENG, L., KUSHNER, P. J., AGARD, D. A. & GREENE, G. L. 1998. The structural basis of estrogen receptor/coactivator recognition and the antagonism of this interaction by tamoxifen. *Cell,* 95**,** 927-937.

SIEGEL, D., KEPA, J. K. & ROSS, D. 2012. NAD(P)H:quinone oxidoreductase 1 (NQO1) localizes to the mitotic spindle in human cells. *PLoS One,* 7**,** e44861.

SILVA, E., KABIL, A. & KORTENKAMP, A. 2010. Cross-talk between non-genomic and genomic signalling pathways — Distinct effect profiles of environmental estrogens. *Toxicology and Applied Pharmacology,* 245**,** 160-170.

SIMON, M. C. 2006. Coming up for air: HIF-1 and mitochondrial oxygen consumption. *Cell Metab,* 3**,** 150-1.

SINGH, B. N., RAO, K. S., RAMAKRISHNA, T., RANGARAJ, N. & RAO, C. M. 2007. Association of αB-Crystallin, a Small Heat Shock Protein, with Actin: Role in Modulating Actin Filament Dynamics in Vivo. *Journal of Molecular Biology,* 366**,** 756-767.

SIROVER, M. A. 2012. Subcellular dynamics of multifunctional protein regulation: mechanisms of GAPDH intracellular translocation. *J Cell Biochem,* 113**,** 2193-200.

SMITH, P. K., KROHN, R. I., HERMANSON, G. T., MALLIA, A. K., GARTNER, F. H., PROVENZANO, M. D., FUJIMOTO, E. K., GOEKE, N. M., OLSON, B. J. & KLENK, D. C. 1985. Measurement of protein using bicinchoninic acid. *Anal Biochem,* 150**,** 76-85.

SOROKIN, A. V., KIM, E. R. & OVCHINNIKOV, L. P. 2007. Nucleocytoplasmic transport of proteins. *Biochemistry (Mosc),* 72**,** 1439-57.

STEPHENSON, G. D. & ROSE, D. P. 2003. Breast Cancer and Obesity: An Update. *Nutrition and Cancer,* 45**,** 1-16.

STOSSI, F., MADAK-ERDOGAN, Z. & KATZENELLENBOGEN, B. S. 2009. Estrogen receptor alpha represses transcription of early target genes via p300 and CtBP1. *Mol Cell Biol,* 29**,** 1749-59.

STUMPF, C. R. & RUGGERO, D. 2011. The cancerous translation apparatus. *Curr Opin Genet Dev,* 21**,** 474-83.

SUH, K. S., SAROJINI, S., YOUSSIF, M., NALLEY, K., MILINOVIKJ, N., ELLOUMI, F., RUSSELL, S., PECORA, A., SCHECTER, E. & GOY, A. 2013. Tissue Banking, Bioinformatics, and Electronic Medical Records: The Front-End Requirements for Personalized Medicine. *Journal of Oncology,* 2013**,** 368751.

SUN, Y., YUAN, K. A. I., ZHANG, P., MA, R., ZHANG, Q.-W. & TIAN, X.-S. 2015. Crosstalk analysis of pathways in breast cancer using a network model based on overlapping differentially expressed genes. *Experimental and Therapeutic Medicine,* 10**,** 743-748.

SURY, M. D., CHEN, J.-X. X. & SELBACH, M. 2010. The SILAC fly allows for accurate protein quantification in vivo. *Molecular & Cellular Proteomics*.

SZATHMÁRY, E., JORDÁN, F. & PÁL, C. 2001. Can Genes Explain Biological Complexity? *Science,* 292**,** 1315-1316.

TAKATALO, M. S., KOUVONEN, P., CORTHALS, G., NYMAN, T. A. & RONNHOLM, R. H. 2006. Identification of new Golgi complex specific proteins by direct organelle proteomic analysis. *Proteomics,* 6**,** 3502-8.

TALAMAS, J. A. & CAPELSON, M. 2015. Nuclear envelope and genome interactions in cell fate. *Frontiers in Genetics,* 6**,** 95.

TANAKA, K. 2003. The Origin of Macromolecule Ionization by Laser Irradiation (Nobel Lecture). *Angewandte Chemie International Edition,* 42**,** 3860-3870.

TARCA, A. L., DRAGHICI, S., KHATRI, P., HASSAN, S. S., MITTAL, P., KIM, J. S., KIM, C. J., KUSANOVIC, J. P. & ROMERO, R. 2009. A novel signaling pathway impact analysis. *Bioinformatics,* 25**,** 75-82.

TAYLOR, K. J., SIMS, A. H., LIANG, L., FARATIAN, D., MUIR, M., WALKER, G., KUSKE, B., DIXON, J. M., CAMERON, D. A., HARRISON, D. J. & LANGDON, S. P. 2010. Dynamic changes in gene expression in vivo predict prognosis of tamoxifen-treated patients with breast cancer. *Breast Cancer Res,* 12**,** R39.

TENG, J., WANG, Z.-Y., JARRARD, D. F. & BJORLING, D. E. 2008. Roles of estrogen receptor α and β in modulating urothelial cell proliferation. *Endocrine-related cancer,* 15**,** 351-364.

THE CANCER GENOME ATLAS RESEARCH, N. 2008. Comprehensive genomic characterization defines human glioblastoma genes and core pathways. *Nature,* 455**,** 1061-1068.

THE CANCER GENOME ATLAS RESEARCH, N. 2011. Integrated Genomic Analyses of Ovarian Carcinoma. *Nature,* 474**,** 609-615.

THOMAS, C. & GUSTAFSSON, J.-Å. 2011. The different roles of ER subtypes in cancer biology and therapy. *Nat Rev Cancer,* 11**,** 597-608.

THOMPSON, M. E. 2010. BRCA1 16 years later: nuclear import and export processes. *Febs j,* 277**,** 3072-8.

TIEN, J. C.-Y. & XU, J. 2012. Steroid Receptor Coactivator-3 as a Potential Molecular Target for Cancer Therapy. *Expert opinion on therapeutic targets,* 16**,** 1085-1096.

TORA, L., WHITE, J., BROU, C., TASSET, D., WEBSTER, N., SCHEER, E. & CHAMBON, P. 1989. The human estrogen receptor has two independent nonacidic transcriptional activation functions. *Cell,* 59**,** 477-87.

TRISTAN, C., SHAHANI, N., SEDLAK, T. W. & SAWA, A. 2011. The diverse functions of GAPDH: views from different subcellular compartments. *Cell Signal,* 23**,** 317-23.

TSANG, J. Y., LAI, M. W., WONG, K. H., CHAN, S. K., LAM, C. C., TSANG, A. K., YU, A. M., TAN, P. H. & TSE, G. M. 2012. alphaB-crystallin is a useful marker for triple negative and basal breast cancers. *Histopathology,* 61**,** 378-86.

VALENTINA CONTRÒ, J. R. B. P. P. 2015. Sex steroid hormone receptors, their ligands, and nuclear and non-nuclear pathways. *AIMS Molecular Science,* 2**,** 294-310.

VAN AGTHOVEN, T., GODINHO, M. F. E., WULFKUHLE, J. D., PETRICOIN, E. F. & DORSSERS, L. C. J. 2012. Protein pathway activation mapping reveals molecular networks associated with antiestrogen resistance in breast cancer cell lines. *International Journal of Cancer,* 131**,** 1998-2007.

VAN CUTSEM, E., KÖHNE, C.-H., LÁNG, I., FOLPRECHT, G., NOWACKI, M. P., CASCINU, S., SHCHEPOTIN, I., MAUREL, J., CUNNINGHAM, D., TEJPAR, S., SCHLICHTING, M., ZUBEL, A., CELIK, I., ROUGIER, P. & CIARDIELLO, F. 2011. Cetuximab Plus Irinotecan, Fluorouracil, and Leucovorin As First-Line Treatment for Metastatic Colorectal Cancer: Updated Analysis of Overall Survival According to Tumor KRAS and BRAF Mutation Status. *Journal of Clinical Oncology,* 29**,** 2011-2019.

VAN GELDERMALSEN, M., WANG, Q., NAGARAJAH, R., MARSHALL, A. D., THOENG, A., GAO, D., RITCHIE, W., FENG, Y., BAILEY, C. G., DENG, N., HARVEY, K., BEITH, J. M., SELINGER, C. I., O'TOOLE, S. A., RASKO, J. E. J. & HOLST, J. 2015. ASCT2/SLC1A5 controls glutamine uptake and tumour growth in triple-negative basal-like breast cancer. *Oncogene*.

VANDER HEIDEN, M. G. 2013. Exploiting tumor metabolism: challenges for clinical translation. *The Journal of Clinical Investigation,* 123**,** 3648-3651.

VANDER HEIDEN, M. G., CANTLEY, L. C. & THOMPSON, C. B. 2009. Understanding the Warburg effect: the metabolic requirements of cell proliferation. *Science,* 324**,** 1029-33.

VANDER HEIDEN, M. G., CANTLEY, L. C. & THOMPSON, C. B. 2009. Understanding the Warburg Effect: The Metabolic Requirements of Cell Proliferation. *Science,* 324**,** 1029-1033.

VANDER HEIDEN, M. G., LOCASALE, J. W., SWANSON, K. D., SHARFI, H., HEFFRON, G. J., AMADOR-NOGUEZ, D., CHRISTOFK, H. R., WAGNER, G., RABINOWITZ, J. D., ASARA, J. M. & CANTLEY, L. C. 2010. Evidence for an alternative glycolytic pathway in rapidly proliferating cells. *Science,* 329**,** 1492-9.

VERHAAK, R. G. W., HOADLEY, K. A., PURDOM, E., WANG, V., QI, Y., WILKERSON, M. D., MILLER, C. R., DING, L., GOLUB, T., MESIROV, J. P., ALEXE, G., LAWRENCE, M., O'KELLY, M., TAMAYO, P., WEIR, B. A., GABRIE, S., WINCKLER, W., GUPTA, S., JAKKULA, L., FEILER, H. S., HODGSON, J. G., JAMES, C. D., SARKARIA, J. N., BRENNAN, C., KAHN, A., SPELLMAN, P. T., WILSON, R. K., SPEED, T. P., GRAY, J. W., MEYERSON, M., GETZ, G., PEROU, C. M., HAYES, D. N. & THE CANCER GENOME ATLAS RESEARCH, N. 2010. An integrated genomic analysis identifies clinically relevant subtypes of glioblastoma characterized by abnormalities in PDGFRA, IDH1, EGFR and NF1. *Cancer cell,* 17**,** 98.

VIC, P., VIGNON, F., DEROCQ, D. & ROCHEFORT, H. 1982. Effect of estradiol on the ultrastructure of the MCF7 human breast cancer cells in culture. *Cancer Res,* 42**,** 667-73.

VIVACQUA, A., LAPPANO, R., DE MARCO, P., SISCI, D., AQUILA, S., DE AMICIS, F., FUQUA, S. A., ANDO, S. & MAGGIOLINI, M. 2009. G protein-coupled receptor 30 expression is up-regulated by EGF and TGF alpha in estrogen receptor alpha-positive cancer cells. *Mol Endocrinol,* 23**,** 1815-26.

VOGELSTEIN, B. & KINZLER, K. W. 1993. The multistep nature of cancer. *Trends Genet,* 9**,** 138-41.

VOGELSTEIN, B. & KINZLER, K. W. 2004. Cancer genes and the pathways they control. *Nat Med,* 10**,** 789-99.

WAKELING, A. E. 2000. Similarities and distinctions in the mode of action of different classes of antioestrogens. *Endocr Relat Cancer,* 7**,** 17-28.

WALTHER, T. C. & MANN, M. 2010. Mass spectrometry–based proteomics in cell biology. *The Journal of Cell Biology,* 190**,** 491-500.

WANG, C., PROSSNITZ, E. R. & ROY, S. K. 2008. G Protein-Coupled Receptor 30 Expression Is Required for Estrogen Stimulation of Primordial Follicle Formation in the Hamster Ovary. *Endocrinology,* 149**,** 4452-4461.

WANG, D., HU, L., ZHANG, G., ZHANG, L. & CHEN, C. 2010. G protein-coupled receptor 30 in tumor development. *Endocrine,* 38**,** 29-37.

WANG, G., FULKERSON, C. M., MALEK, R., GHASSEMIFAR, S., SNYDER, P. W. & MENDRYSA, S. M. 2012. Mutations in Lyar and p53 are synergistically lethal in female mice. *Birth Defects Res A Clin Mol Teratol,* 94**,** 729-37.

WANG, G., SHANG, L., BURGETT, A. W., HARRAN, P. G. & WANG, X. 2007. Diazonamide toxins reveal an unexpected function for ornithine delta-amino transferase in mitotic cell division. *Proc Natl Acad Sci U S A,* 104**,** 2068-73.

WANG, T., LAWLER, A. M., STEEL, G., SIPILA, I., MILAM, A. H. & VALLE, D. 1995. Mice lacking ornithine-delta-aminotransferase have paradoxical neonatal hypoornithinaemia and retinal degeneration. *Nat Genet,* 11**,** 185-90.

WANG, Z., LIANG, S., LIAN, X., LIU, L., ZHAO, S., XUAN, Q., GUO, L., LIU, H., YANG, Y., DONG, T., LIU, Y., LIU, Z. & ZHANG, Q. 2015. Identification of proteins responsible for adriamycin resistance in breast cancer cells using proteomics analysis. *Scientific Reports,* 5**,** 9301.

WARBURG, O., WIND, F. & NEGELEIN, E. 1927. THE METABOLISM OF TUMORS IN THE BODY. *J Gen Physiol,* 8**,** 519-30.

WARD, P. S. & THOMPSON, C. B. 2012. Metabolic reprogramming: a cancer hallmark even warburg did not anticipate. *Cancer Cell,* 21**,** 297-308.

WASCHKE, J. 2008. The desmosome and pemphigus. *Histochemistry and Cell Biology,* 130**,** 21-54.

WASINGER, V. C., CORDWELL, S. J., CERPA-POLJAK, A., YAN, J. X., GOOLEY, A. A., WILKINS, M. R., DUNCAN, M. W., HARRIS, R., WILLIAMS, K. L. & HUMPHERY-SMITH, I. 1995. Progress with gene-product mapping of the Mollicutes: Mycoplasma genitalium. *Electrophoresis,* 16**,** 1090-4.

WASINGER, V. C., ZENG, M. & YAU, Y. 2013. Current Status and Advances in Quantitative Proteomic Mass Spectrometry. *International Journal of Proteomics,* 2013**,** 12.

WEBB, P., NGUYEN, P., SHINSAKO, J., ANDERSON, C., FENG, W., NGUYEN, M. P., CHEN, D., HUANG, S. M., SUBRAMANIAN, S., MCKINERNEY, E., KATZENELLENBOGEN, B. S., STALLCUP, M. R. & KUSHNER, P. J. 1998. Estrogen receptor activation function 1 works by binding p160 coactivator proteins. *Mol Endocrinol,* 12**,** 1605-18.

WEI, Y., ZHANG, Z., LIAO, H., WU, L., WU, X., ZHOU, D., XI, X., ZHU, Y. & FENG, Y. 2012. Nuclear estrogen receptor-mediated Notch signaling and GPR30-mediated PI3K/AKT signaling in the regulation of endometrial cancer cell proliferation. *Oncol Rep,* 27**,** 504-10.

WIESE, S., GRONEMEYER, T., OFMAN, R., KUNZE, M., GROU, C. P., ALMEIDA, J. A., EISENACHER, M., STEPHAN, C., HAYEN, H., SCHOLLENBERGER, L., KOROSEC, T., WATERHAM, H. R., SCHLIEBS, W., ERDMANN, R., BERGER, J., MEYER, H. E., JUST, W., AZEVEDO, J. E., WANDERS, R. J. & WARSCHEID, B. 2007. Proteomics characterization of mouse kidney peroxisomes by tandem mass spectrometry and protein correlation profiling. *Mol Cell Proteomics,* 6**,** 2045-57.

WIJAYARATNE, A. L. & MCDONNELL, D. P. 2001. The human estrogen receptor-alpha is a ubiquitinated protein whose stability is affected differentially by agonists, antagonists, and selective estrogen receptor modulators. *J Biol Chem,* 276**,** 35684-92.

WILDING, J. L. & BODMER, W. F. 2014. Cancer Cell Lines for Drug Discovery and Development. *Cancer Research,* 74**,** 2377-2384.

WILKINS, M. R., SANCHEZ, J. C., GOOLEY, A. A., APPEL, R. D., HUMPHERY-SMITH, I., HOCHSTRASSER, D. F. & WILLIAMS, K. L. 1996. Progress with proteome projects: why all proteins expressed by a genome should be identified and how to do it. *Biotechnol Genet Eng Rev,* 13**,** 19-50.

WOO, Y. M., SHIN, Y., LEE, E. J., LEE, S., JEONG, S. H., KONG, H. K., PARK, E. Y., KIM, H. K., HAN, J., CHANG, M. & PARK, J.-H. 2015. Inhibition of Aerobic Glycolysis Represses Akt/mTOR/HIF-1α Axis and Restores Tamoxifen Sensitivity in Antiestrogen-Resistant Breast Cancer Cells. *PLoS ONE,* 10**,** e0132285.

WULLSCHLEGER, S., LOEWITH, R. & HALL, M. N. 2006. TOR signaling in growth and metabolism. *Cell,* 124**,** 471-84.

XU, R. H., PELICANO, H., ZHOU, Y., CAREW, J. S., FENG, L., BHALLA, K. N., KEATING, M. J. & HUANG, P. 2005. Inhibition of glycolysis in cancer

cells: a novel strategy to overcome drug resistance associated with mitochondrial respiratory defect and hypoxia. *Cancer Res,* 65**,** 613-21.

XU, X., ZUR HAUSEN, A., COY, J. F. & LOCHELT, M. 2009. Transketolase-like protein 1 (TKTL1) is required for rapid cell growth and full viability of human tumor cells. *Int J Cancer,* 124**,** 1330-7.

YALCIN, A., CLEM, B. F., SIMMONS, A., LANE, A., NELSON, K., CLEM, A. L., BROCK, E., SIOW, D., WATTENBERG, B., TELANG, S. & CHESNEY, J. 2009. Nuclear targeting of 6-phosphofructo-2-kinase (PFKFB3) increases proliferation via cyclin-dependent kinases. *J Biol Chem,* 284**,** 24223-32.

YANG, W., XIA, Y., JI, H., ZHENG, Y., LIANG, J., HUANG, W., GAO, X., ALDAPE, K. & LU, Z. 2011. Nuclear PKM2 regulates beta-catenin transactivation upon EGFR activation. *Nature,* 480**,** 118-22.

YEH, W. L., SHIODA, K., COSER, K. R., RIVIZZIGNO, D., MCSWEENEY, K. R. & SHIODA, T. 2013. Fulvestrant-induced cell death and proteasomal degradation of estrogen receptor alpha protein in MCF-7 cells require the CSK c-Src tyrosine kinase. *PLoS One,* 8**,** e60889.

YONEZAWA, K., SUGIHARA, Y., OSHIMA, K., MATSUDA, T. & NADANO, D. 2014. Lyar, a cell growth-regulating zinc finger protein, was identified to be associated with cytoplasmic ribosomes in male germ and cancer cells. *Mol Cell Biochem,* 395**,** 221-9.

YUE, W., WANG, J. P., LI, Y., FAN, P., LIU, G., ZHANG, N., CONAWAY, M., WANG, H., KORACH, K. S., BOCCHINFUSO, W. & SANTEN, R. 2010. Effects of estrogen on breast cancer development: Role of estrogen receptor independent mechanisms. *Int J Cancer,* 127**,** 1748-57.

YUE, W., YAGER, J. D., WANG, J. P., JUPE, E. R. & SANTEN, R. J. 2013. Estrogen receptor-dependent and independent mechanisms of breast cancer carcinogenesis. *Steroids,* 78**,** 161-70.

ZAJCHOWSKI, D. A., KAUSER, K., ZHU, D., WEBSTER, L., ABERLE, S., WHITE, F. A., 3RD, LIU, H. L., HUMM, R., MACROBBIE, J., PONTE, P., HEGELE-HARTUNG, C., KNAUTHE, R., FRITZEMEIER, K. H., VERGONA, R. & RUBANYI, G. M. 2000. Identification of selective estrogen receptor modulators by their gene expression fingerprints. *J Biol Chem,* 275**,** 15885-94.

ZHANG, W., ZHANG, S.-L., HU, X. & TAM, K. Y. 2015. Targeting Tumor Metabolism for Cancer Treatment: Is Pyruvate Dehydrogenase Kinases (PDKs) a Viable Anticancer Target? *International Journal of Biological Sciences,* 11**,** 1390-1400.

ZHENG, L., ROEDER, R. G. & LUO, Y. 2003. S phase activation of the histone H2B promoter by OCA-S, a coactivator complex that contains GAPDH as a key component. *Cell,* 114**,** 255-66.

ZHOU, C., ZHONG, Q., RHODES, L. V., TOWNLEY, I., BRATTON, M. R., ZHANG, Q., MARTIN, E. C., ELLIOTT, S., COLLINS-BUROW, B. M., BUROW, M. E. & WANG, G. 2012. Proteomic analysis of acquired tamoxifen resistance in MCF-7 cells reveals expression signatures associated with enhanced migration. *Breast Cancer Res,* 14**,** R45.

ZHOU, Q., ATADJA, P. & DAVIDSON, N. E. 2007. Histone deacetylase inhibitor LBH589 reactivates silenced estrogen receptor alpha (ER) gene expression without loss of DNA hypermethylation. *Cancer Biol Ther,* 6**,** 64-9.

ZHU, Q., JIN, L., CASERO, R. A., DAVIDSON, N. E. & HUANG, Y. 2012. Role of ornithine decarboxylase in regulation of estrogen receptor alpha expression and growth in human breast cancer cells. *Breast Cancer Res Treat,* 136**,** 57-66.

ZISCHKA, H., BRAUN, R. J., MARANTIDIS, E. P., BURINGER, D., BORNHOVD, C., HAUCK, S. M., DEMMER, O., GLOECKNER, C. J., REICHERT, A. S., MADEO, F. & UEFFING, M. 2006. Differential analysis of Saccharomyces cerevisiae mitochondria by free flow electrophoresis. *Mol Cell Proteomics,* 5**,** 2185-200.